GEOLOGICA ULTRAIECTINA

Mededelingen van de Faculteit Geowetenschappen
Universiteit Utrecht

No.276

TEX_{86} paleothermometry: proxy validation and application in marine sediments

Carme Huguet

ISBN: 978-90-5744-141-7

TEX_{86} paleothermometry: proxy validation and application in marine sediments

TEX_{86} paleothermometer: proxy validatie en toepassing op mariene sedimenten

(met een samenvatting in het Nederlands)

TEX_{86} paleotermometre: validació i aplicació de la proxi en sediments marins

(amb un sumari en Català)

Proefschrift

ter verkrijging van de graad van doctor aan de Universiteit Utrecht op gezag van de rector magnificus, prof. dr. W. H. Gispen, ingevolge het besluit van het college voor promoties in het openbaar te verdedigen op maandag 17 september des middags 12.45 uur

door

Carme Huguet

geboren op 11 oktober 1976 te Barcelona, Spanje

Promotor: Prof. Dr. Ir. J. S. Sinnighe Damsté
Co-promotor: Dr. Ir. S. Schouten

This work has been financially supported by the Research Council for Earth and Life Sciences of the Netherlands Organisation for Scientific Research (NWO-ALW) and the Royal Netherlands Institute for Sea Research (NIOZ), Texel, The Netherlands.

Bressol de tots els blaus

El meu amic el mar
té la calma d'un déu adormit,
quan la meva nau busca recer
a l'illa del seu pit.

El meu amic el mar
té el coratge d'un déu exaltat,
i quan s'omple d'aire el meu velam
seguim un joc incert.

I, tanmateix, potser
el gep de l'onada acabarà
amb tot el meu somni desitjós
d'anar a aquell port d'atzars.

El meu amic el mar
és l'immens bressol de tots els blaus,
i en el seu va-i-vé de so i color
aprenc el poc que tinc.

És per això que mai
no em podré allunyar del seu batec,
i fidel viuré amarinat
fins acabar el vent.

Lluís Llach

A la meva mare

A la meva familia

A la Neus

Table of contents

Chapter 1
Introduction

1.1 Climate change

The Earth's surface temperature has risen by 0.76±0.2°C from 1850 to 2005 with a stronger and accentuated warming trend in the past two decades [*IPCC*, 2007, http://www.ipcc.ch]. As the CO_2 concentration rose from a pre-industrial value of about 280 parts per million by volume (ppmv) to 379 ppmv in 2005 A.D. [*IPCC*, 2007, http://www.ipcc.ch], the question arises whether most of the warming is attributable to increased concentrations of greenhouse gases caused by human activities. It is now clear that greenhouse gas forcing is becoming the dominant, though not the only process driving the warming trend [*IPCC*, 2007, http://www.ipcc.ch]. To understand the extent of the anthropogenic impact on climate, we must have accurate climatic records that can help establish the natural climatic change. The understanding of natural climate change and anthropogenic impact can help to build and test models to predict future climate trends.

Climate on earth is defined as the long-term average of weather patterns including e.g. temperature, humidity, and seasonal changes and is ultimately controlled by solar energy and its interaction with the atmosphere. However, the atmosphere and the ocean are interdependent systems and the two are linked through complex feedback loops. For example, ocean currents are related to atmospheric wind patterns and higher air temperatures will influence sea surface temperatures (SST). Conversely, the oceans have an important role in climate, for example, though heat storage and redistribution through circulation patterns [*Thurman and Trujillo* 1999] as well as controlling the water cycle and precipitation patterns [*Henderson,* 2002]. Thus, SST is an important variable in the earth's climate system and can be linked to all the climatic processes. Determination of past SST is therefore of primary importance for the reconstruction of natural climatic changes, modeling of climate and reconstruction of ocean circulation. The best way to determine SST is to have instrumental records; however, these are usually regional and relatively short, covering at best the last two centuries. These short records do not allow the precise description of long-term SST changes or the accurate evaluation of the anthropologic impact on climate. To do that we need to

extend the climate records beyond the time scale of instrumental records when there was no anthropological impact. This can be achieved by modeling or assessed with temperature proxies. While mathematical models can be very useful, they still need long climatic records to validate them and increase their reliability and thus are also dependant on proxy data. For these reasons, accurate proxy records are essential to understand and predict future climate trends.

1.2 Reconstruction of past sea surface temperatures

Several geochemical proxies for SST reconstruction have been proposed since the 1950s, and they can generally be divided between proxies based in inorganic (calcite and opal shells and skeletons) and organic remains (lipid biomarkers) (Table 1). Some of the inorganic proxies use species composition to estimate past temperature (Table 1). A using sedimented species assemblage to estimate past temperatures, calibrated through modern assemblage composition, is a common technique and can be used to determine temperature at different depths depending on the group of species chosen (Fig. 1). One of the best known examples of the use of species assemblages are the CLIMAP maps [*Climap* 1981]. There are five basic temperature proxies based on assemblage composition: the Imbrie and Kipp method [*Imbrie and Kipp* 1971], the modern analog technique [*Hutson,* 1977], the modern analog technique with a similarity index [*Pflaumann et al.,* 1996], the revised analog method [*Waelbroeck et al.,* 1998] and the artificial neural networks [*Malmgren and Nordlund,* 1997]. However, all these methods have problems related to depth habitat and seasonality of the individual species, selective dissolution and lack of modern analogs (Table 1). All this techniques rely on a constant assemblage composition being associated to a single parameter and the lack of adaptative evolution of the species composing a particular assemblage. This kind of proxies range in accuracy between ±0.4 and ±2.7 (Table 1).

One of the most commonly used inorganic proxies takes advantage of the temperature dependant fractionation process of oxygen that takes place in calcite and opal producing organisms. Species of foraminifera, corals and molluscs build their shells using carbonates (CO_3^{-2}) and calcium (Ca^{+2}) (Fig. 1), while diatoms build their shells from silica and water (Fig. 1).

	Proxy	Basic assumptions	Empirical relationship	Accuracy	Pitfalls	References
Inorganic Fossil Remains	IKM (Imbrie and Kipp Method)	1)assemblage composition determined by one parameter	Statistical treatment of downcore changes in the fauna and flora assemblage composition.	±1-1.6 ºC	a) More than one parameter may determine the assemblage composition	[*Imbrie and Kipp* 1971]
	MAT (Modern Analog Technique)	2)No evolutionary adaptation		±0.7-2.7ºC	b) Uncertainty about seasonality and depth habitat	[*Hutson* 1977]
	SIMMAX (MAT with a similarity index)	3) The assemblage is not affected by post depositional processes		±0.95ºC		[*Pflaumann et al.* 1996]
	RAM (Revised Analog Method)			±0.4-1.9ºC	c) When downcore assemblages do not exist in the reference data	[*Waelbroeck et al.* 1998]
	Artificial neural networks	Depending on input	Fuzzy logic	±0.7-1.8ºC	d) Selective dissolution	[*Malmgren and Nordlund* 1997]
	$\delta^{18}O$ (calcite)	1) The difference between $\delta_{calcite/opal}$ and δ_{water} decreases with increasing temperature (thermodynamic equilibrium)	T (ºC)=a+b(δ_c-δ_w)+c(δ_c-δ_w) where δ_w=*f*(S, ice-volume)	±1ºC	a) δ_w (ice effect) and regional δ_w-S relationship is unknown b) There are vital effects ($[CO_3^{2-}]$, photosynthesis, respiration, crusting) c) Diagenesis	[*Urey* 1947]
	$\delta^{18}O$ (opal)		T (ºC)=A-4.1 (δ_c-δ_w) where A depends on the conditions of treatment of the unstable oxygen	unknown	*Additionally for opal:* d) Species separation not possible, (i.e no control on species effect) e) Oxygen exchange during dehydratation	[*Epstein et al.*1953]
	Mg/Ca	Mg and Sr levels incorporated into biogenic calcite are controlled by a temperature dependant physiological process	T=a·10 $^{(b\cdot[mg/Ca])}$	±1ºC	a) Vital effects b) Dissolution c) Residence time of Mg 13 Myr d) Effect of carbonate ion concentration	[*Chave* 1954]
	Sr/Ca		T=a·[Sr/Ca]	±1ºC	*Additionally for Sr:* d) Growth rate artefact (i. e. slower rates are associated with higher [Sr/Ca] e) The residence time of Sr is 2.5 Myr	[*Beck et al.* 1992]
Organic Fossil Remains	$U^{K'}_{37}$ (Alkenone unsaturation ratio)	Unknown temperature dependent biochemical process	T= ($U^{K'}_{37}$+a)/b where $U^{K'}_{37}$=[$C_{37:2}$]/[$C_{37:2}$+$C_{37:3}$]	±0.7-1.6ºC	a) Mechanism unknown b) Uncertainty about species composition c) Seasonality and depth habitat of species d) Preferential degradation of one of the isomers	[*Brassell et al.* 1986b]
	TEX_{86}(TetraEther index of GDGTs with 86 carbons)	Although distributed throughout the water column they reflect sea surface temperature	T=(TEX_{86}-0.28)/0.015 where TEX_{86}=(GDGT 2+GDGT 3+GDGT 4')/(GDGT 1+ GDGT 2+GDGT 3+GDGT 4')	±0.7-1.2ºC	a) Variable seasonality and depth habitat of species b) Uncertainty about species c) Riverine terrestrial input may bias TEX_{86} results	[*Schouten et al.* 2002]

The numbers indicate the number of cyclopentanyl moieties

Table 1. Summary of the main sea surface temperature proxies

In both cases, O^{18} is preferentially taken up instead of the lighter ^{16}O during the shell building process, but the proportion of O^{18} versus O^{16} varies depending on water temperature [*Urey,* 1947; *Epstein et al.,* 1953]. The ratio between ^{18}O and ^{16}O, expressed as $\delta^{18}O$, translates into temperature though an empirical relationship (Table 1). The use of $\delta^{18}O$ for SST reconstruction is complicated by several uncertainties related to the formation and preservation of shells as well as the carbonate ion concentration, and the $\delta^{18}O$ and salinity of the original seawater [e.g. *Spero et al.,* 1997; *Wefer et al.,* 1999; *Lea,* 2003]. Dissolution of shells become especially important when the $\delta^{18}O_{opal}$ is considered as opal is more prone to dissolution. Moreover there are vital effects related to the metabolic reactions performed by the organisms during shell formation (Table 1). Despite these caveats, this isotopic technique has errors of only ±1ºC and is one of the most widely used SST proxies.

One of the more recent inorganic proxies uses an element ratio rather than an isotope one. Usually the composition of most calcareous shells approximates that of the minerals calcite and aragonite. However, in almost all shells there is a substantial substitution of Ca by the element Mg which seems to be a temperature dependant process and thus the Mg/Ca ratio can be used to estimate temperature [*Elderfield and Ganssen,* 2000] (Table 1, Fig. 1). While the Mg/Ca ratio is less dependent on the composition of the original sea water, other factors like the carbonate ion concentration, species-dependent vital effects and shell dissolution as well as the residence time of Mg and Ca over geological time scales are still an issue [*Wefer et al.,* 1999; *Lea,* 2003] (Table 1). The Sr/Ca ratio, which is also measured in calcite (Fig. 1), is based on the same principle as the Mg/Ca ratio and it has been used in coral skeletons to reconstruct SST [*Beck et al.,* 1992]. Similar to the Mg/Ca ratio, the Sr/Ca ratio is not only affected by dissolution but also by differences in growth rate. Moreover, the residence time of Sr is only 2.5 Myr, thus limiting the application of this proxy to Quaternary climate reconstructions as on longer time scales there is a lack of knowledge about the amount of Sr in sea water [*Henderson,* 2002] (Table 1).

The first proxy based on organic remains was proposed in 1986 by *Brassell et al.* [1986a]. This proxy uses the ratio of $C_{37:2}$ and $C_{37:3}$ long-chain unsaturated ketones synthesized by haptophyte algae to define the $U^{K'}_{37}$ index (Table 1) [*Brassell et al.,* 1986b]. Haptophyte algae are light dependant which means they must live in the upper part of the water column and thus there is usually a good correlation between $U^{K'}_{37}$ and SST (Table 1;

[*Brassell et al.,* 1986a]). The $U_{37}^{K'}$ index is often considered more robust than the inorganic proxies discussed above, as the values are not directly controlled by sea-water chemistry and, hence, assumptions concerning this are not required. Furthermore, global surveys of surface sediments and water column particulate organic matter reveal a strong and consistent correlation between the $U_{37}^{K'}$ and SST (reviewed by *Herbert*, [2003]). However, the biochemical function of alkenones is still unknown and the $U_{37}^{K'}$ may be affected by changes in the species composition through time, nutrient utilization [*Prahl et al.,* 2005] and also by oxic degradation [*Hoefs et al.,* 1998; *Gong and Hollander,* 1999]. In addition, the $U_{37}^{K'}$ may be affected by seasonality and depth habitat changes of the haptophytes. Alkenones are mainly produced by *Emiliana huxleyi* but in certain areas there are also contributions of *Gyphyrocapsa oceanica* thus creating uncertainties about species variability which could affect the $U_{37}^{K'}$ ratio [*Herbert,* 2003]. None the less the $U_{37}^{K'}$ is one of the most accurate proxies to date with an estimated accuracy of ±0.7ºC and is been used in numerous paleocenographic studies [*Herbert,* 2003].

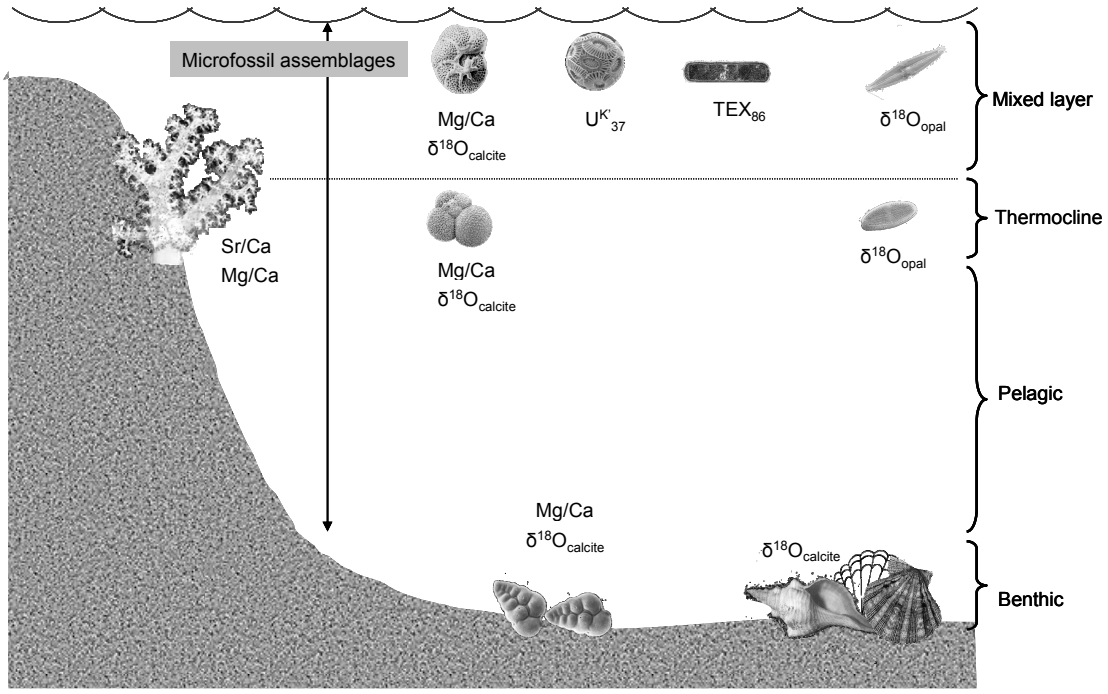

Figure 1. Schematic drawing showing the organisms from which sea surface temperature proxies are derived as well as their standard depth distribution.

In 2002, a second proxy based on organic remains was proposed by *Schouten et al.* [2002]. This proxy, the TEX_{86}, is based on the distribution of glycerol dialkyl glycerol tetraethers (GDGTs), membrane lipids of the marine Crenarchaeota Group I (Table 1), a group of micro-organisms belonging to the domain of Archaea and occurring ubiquitously in the ocean. Crenarchaeota biosynthesize isoprenoid GDGTs with a varying number of cyclopentyl moieties which has been found to change according to temperature [*Schouten et al.,* 2002; *Wuchter et al.,* 2004]. Although Crenarchaeota are distributed throughout the water column, TEX_{86} values of particulate organic matter, sediment traps and sediment core tops are better correlated with SST (depths <100m) than with the temperature of deeper water [*Wuchter et al.,* 2006b] (Fig. 1). However, as is the case with the other temperature proxies, the TEX_{86} proxy may be affected by seasonality and depth habitat changes of the Crenarchaeota as well as species variability through time (Table 1, and see below).

1.3 Biology and ecology of Crenarchaeota

Archaea were originally grouped within the extremophilic bacteria but genetic work by [*Woese et al.,* 1990] revealed that the Archaea form a separate domain of life (Fig. 2). Archaea synthesise unique membrane lipids that, coupled with their unique gene composition, sets them apart as a third domain of life [*Woese et al.,* 1990]. While Archaea are prokaryotes like Bacteria, they have similar replication and expression systems as the Eukarya, suggesting that they were the ancestors of both those groups and thus positions them at the base of the evolution tree [*Woese et al.,* 1990]. Archaea are further subdivided into three phyla, the Crenarchaeota, including marine Group I, the Euryarchaeota [*Woese et al.,* 1990] and the Korarchaeota [*Barns et al.,* 1996] (Fig. 2).

Marine Crenarchaeota Group I (Fig. 2) have been found in a wide variety of aquatic environments like marine settings [*Murray et al.,* 1998; *Murray et al.,* 1999b; *Teira et al.,* 2004; *Herndl et al.,* 2005], large lakes [*MacGregor et al.,* 1997; *Powers et al.,* 2005] and rivers [*Herfort et al.,* 2006; *Kim et al.,* 2006]. Crenarchaeota are distributed throughout the water column [*Massana et al.,* 1998; *Murray et al.,* 1999b; *Massana et al.,* 2000; *Karner et al.,* 2001; *Wells et al.,* 2006] though the highest abundances are usually noted in the upper hundred meters both in the Pacific [*Karner et al.,* 2001], the Atlantic [*Herndl et al.,* 2005] and

in the Black Sea [*Coolen et al.,* 2007]. However, there are known exceptions for the Santa Barbara Basin [*Murray et al.,* 1999a], and the Arabian Sea [*Sinninghe Damsté et al.,* 2002a].

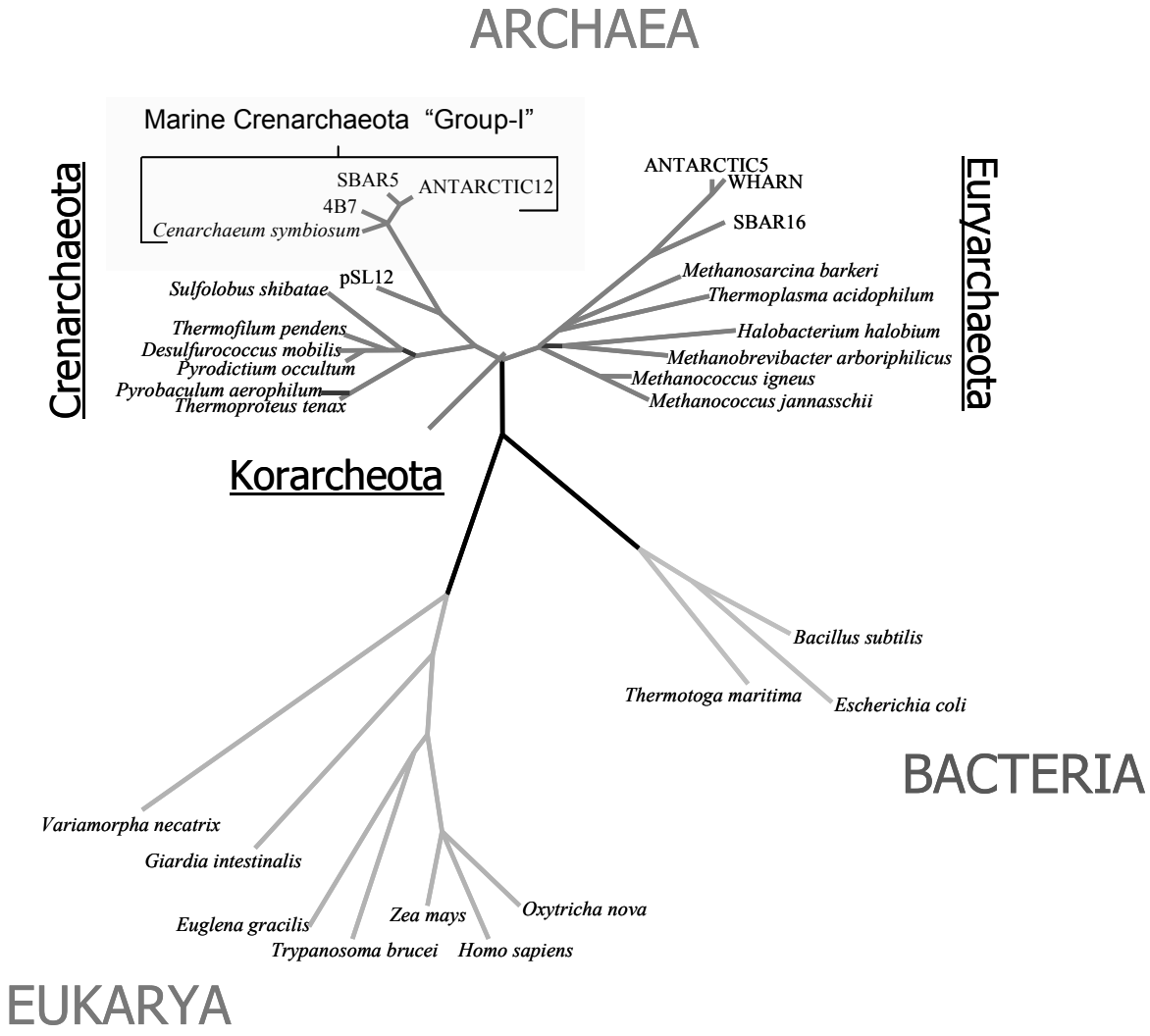

Figure 2. Tree of life based on rDNA showing the three main Domains of life. Archaea are further subdivided into three kingdoms, the Crenarchaeota, including marine Group I, the Euryarchaeota [*Woese et al.,* 1990] and the Korarchaeota [*Barns et al.,* 1996]. The Group I Crenarchaeota has been highlighted.

Crenarchaeotal abundance may also vary with season. High abundances have been reported in winter in the North Sea [*Wuchter et al.,* 2005], the Santa Barbara Basin [*Murray et al.,* 1999a] and the Pacific Ocean [*Karner et al.,* 2001]. Supposedly, in these environments Crenarchaeota thrive in winter as then they do not need to compete for ammonia with phytoplankton (see below). However, in other areas the seasonality might be different; for example, in the Antarctic Ocean Crenarchaeota bloom in spring [*Massana et al.,* 1998; *Murray et al.,* 1999b].

Crenarchaeota have been suggested to be chemoautotrophs [*Hoefs et al.,* 1997], but the physiology of the marine Crenarchaeota is still largely unknown, although recently significant progress has been made. Crenarchaeota have been reported to take up dissolved amino acids [*Ouverney and Fuhrman,* 2000; *Teira et al.,* 2006] and recent evidence has shown that part of them are chemoautotrophic nitrifiers [*Könneke et al.,* 2005; *Wuchter et al.,* 2006a]. They reportedly take up NH_4 and, thus, are linked to the nitrogen cycle. However, the Crenarchaeota are a diverse group with a ubiquitous distribution [*DeLong et al.,* 1994] and potentially they may have a wide range of physiologies and ecological niches.

1.4. Membrane lipids of Crenarchaeota

Living cells have a cytoplasmatic membrane that functions as a barrier between the cytoplasm and the environment [*van de Vossenberg et al.,* 1998]. Cell membranes are also essential to control the exchange between the cell and the surrounding environment. Most cell membranes of Bacteria and Eukarya are formed by fatty acyl chains ester bound to glycerol with a polar head group. These phospholipids are organised in a bi-layer structure with the polar head-groups oriented towards the aqueous phase and the hydrophobic carbon chains position in the middle [*van de Vossenberg et al.,* 1998] (Fig. 3).

The cell membranes of Archaea on the other hand, are unique and different from the bi-layered cytoplasmatic membranes of Bacteria and Eukarya [*Woese et al.,* 1990]. Archaeal membrane lipids are composed of saturated isoprene chains of different length which are ether bound to glycerols and with a polar head group [*Gliozzi et al.,* 2002]. A large number of Archaea also synthesize tetraether membrane lipids which span the whole width of the membrane and form a mono-layer [*de Rosa,* 1996] (Fig. 3).

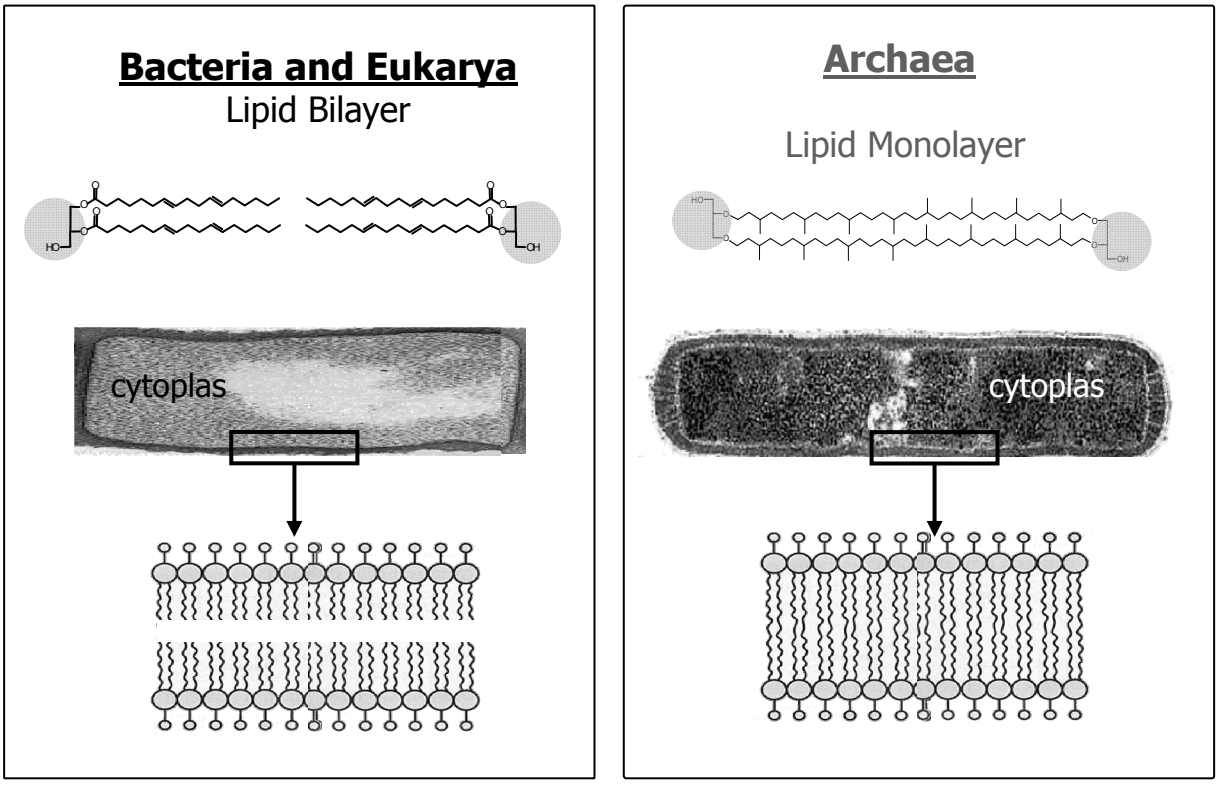

Figure 3. Membrane structure and lipids of Bacteria, Eukarya and Archaea.

Liposomes composed of archaeal tetraether lipids are more stable than bi-layer lipid ones and have extremely low proton permeability [*van de Vossenberg et al.,* 1998] which is thought to enable archaea to survive in extreme environmental conditions such as low pH, or high temperatures [*Gliozzi et al.,* 2002].

Remarkably, marine Crenarchaeota Group I also biosynthesize different types of GDGTs (Fig. 4a) despite that they do not live under extreme conditions. Their GDGTs contain 0 to 3 cyclopentane moieties (GDGT 0-3; Fig. 4a) and crenarchaeol (GDGT 4; [*Schouten et al.,* 2000a; *Sinninghe Damsté et al.,* 2002b]) which, in addition to 4 cyclopentane moieties, has a cyclohexane moiety. Crenarchaeol (GDGT 4) is though to be a biomarker for the non-thermophilic Crenarchaeota [*Sinninghe Damsté et al.,* 2002b]. The unique presence of a cyclohexane moiety in non thermophilic Crenarchaeota compared to hyperthermophilic Crenarchaeota is thought to be the result of an adaptation of the latter group to relatively cold sea temperatures. To cope with the relatively lower temperatures in the ocean, a key step in the evolution of group I Crenarchaeota was the formation of the cyclohexane moiety which

created a three-dimensional structure that reduces the packaging of the membrane in cold conditions [*Sinninghe Damsté et al.,* 2002b]. This structural change still allows the exchange of products between the cytoplasm and the surrounding water while maintaining the integrity of the membrane. Crenarchaeota also biosynthesize small quantities of the crenarchaeol regio-isomer GDGT 4' (Fig.4a).

A

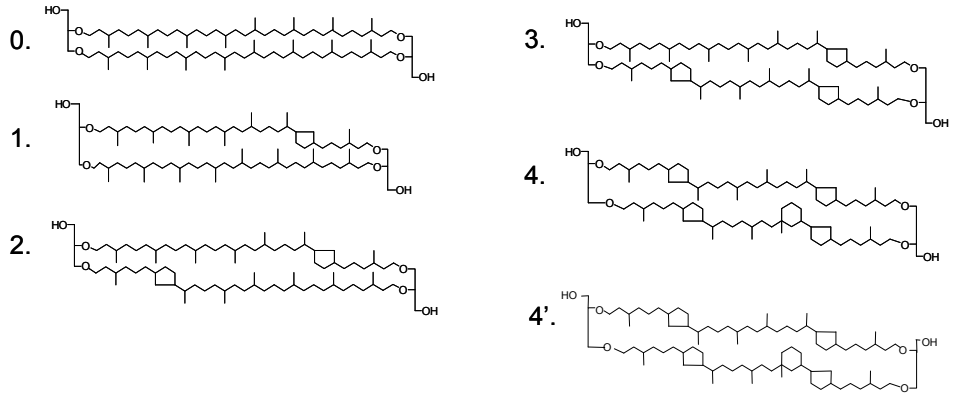

B

$$TEX_{86} = \frac{GDGT\,2 + GDGT\,3 + GDGT\,4'}{GDGT\,1 + GDGT\,2 + GDGT\,3 + GDGT\,4'}$$

C

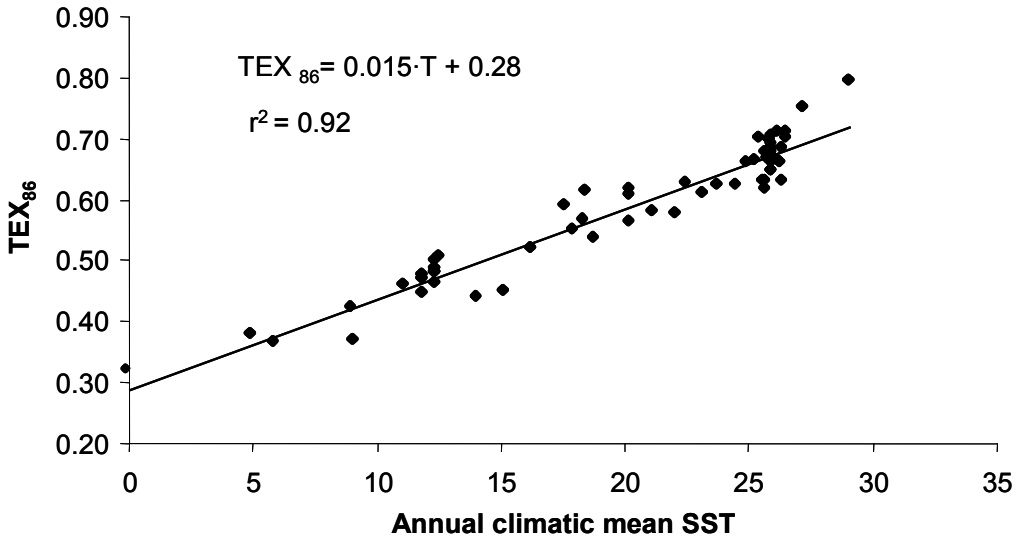

Figure 4. Definition of the TEX_{86} proxy; a) GDGT lipids used in the TEX_{86}, b) the definition of the TEX_{86} ratio and c) empirical correlation between TEX_{86} values of core tops and annual mean SST [from *Schouten et al.* 2002]

Recently, it has also become clear that GDGTs such as those occurring in marine Crenarchaeota are present in lacustrine [*Schouten et al.,* 2000b; *Powers et al.,* 2004] and riverine environments [*Herfort et al.,* 2006]. Some of these crenarchaeotal GDGTs have also been found in terrestrial organic matter albeit in much lower abundances [*Hopmans et al.,* 2004; *Weijers et al.,* 2004].

1.5. Membrane lipids of Crenarchaeota as a new temperature proxy

Crenarchaeotal GDGTs are characterized by the presence of cyclopentane moieties. Previous culture studies of hyperthermophilic Archaea had already indicated that the relative number of cyclopentane moieties of GDGT membrane lipids changed with growth temperature [*Gliozzi et al.,* 1983; *Sugai et al.,* 2004], i.e. there is an increasing number of cyclopentane moieties with increasing temperature. This increase in the number of moieties is thought to provide a better packing of the membrane at higher temperatures [*Gliozzi et al.,* 2002].

This temperature adaptation has also been detected in the GDGTs of non-thermophilic Crenarchaeota and forms the basis for a new temperature proxy proposed by *Schouten et al*. in 2002. This proxy, the TEX_{86}, is based on the distribution of GDGTs (Fig. 4; Table 1); with increasing number of cyclopentane moieties in the GDGTs, the TEX_{86} ratio also increases. This ratio was determined for a range of marine core top sediments and found to correlate well with annual mean SST [*Schouten et al.,* 2002] (Fig. 4c). However, this is merely an empirical correlation and there was no direct prove for a functional relationship between temperature and TEX_{86}. The observed correlation was confirmed by *Wuchter et al.* [2004] using a Crenarchaeota enrichment culture which was incubated under different temperatures. Their results showed that TEX_{86} is linearly correlated with temperature and that changes in salinity and nutrients do not substantially affect the TEX_{86} [*Wuchter et al.,* 2004]. A subsequent study of particulate organic matter (POM) from different marine settings revealed that the TEX_{86} correlates well with surface water temperatures (depths <100m) and that the signal in the deeper water layers and surface sediments is primarily derived from these surface waters [*Wuchter et al*., 2005].

The apparent paradox of a SST origin of the TEX_{86} signal whereas Crenarchaeota also occur at much larger depths was explained by the GDGTs transport mechanism to the sediment floor, i.e. through consumption and re-packaging which mostly takes place in the active food web in the upper part of the water column [*Wuchter et al.,* 2006b].

The diagenetic stability of the TEX_{86} proxy was also tested. To do this, a number of sediment samples deposited at the same time in oxic and anoxic settings in the Arabian sea were compared, and this indicated that the TEX_{86} proxy seems to be unaffected by water redox conditions [*Schouten et al.,* 2004]. Artificial maturation of the GDGTs showed a clear effect on TEX_{86}-derived temperatures at higher maturity levels [*Schouten et al.,* 2004].

These initial results clearly showed that the TEX_{86} is a potentially useful SST proxy. However, further validation of the TEX_{86} proxy is clearly needed. For example, the analytical reproducibility of TEX_{86} analysis was initially reported to be as high as 2ºC [*Schouten et al.,* 2002]. In addition, this proxy had not been compared to either instrumental records or other SST proxies and was, until recently, not used in paleocanographic studies. Thus, further research is necessary to validate the TEX_{86} as a SST proxy and understand its use and limitations.

1.6. Scope and framework of the thesis

The main objective of this thesis was to improve, validate and apply the TEX_{86} proxy. The thesis is divided in three parts:

I. Analytical aspects of measuring the TEX_{86}
II. Transport mechanisms and influence of diagenesis on the TEX_{86} signal
III. Application and validation of the TEX_{86} proxy

Part I covers the analytical aspects and consists of **Chapters 2** and **3**. **Chapter 2** deals with the analytical aspects related to the work-up procedures and the methods to determine the TEX_{86}. Extraction using Soxhlet, ultrasonic, and accelerated high pressure extraction techniques did not give a significant bias in TEX_{86}. The same was true when two different HPLC/APCI-MS set-ups were used to determine the TEX_{86}. However, comparison of TEX_{86}

analysis using Single Ion Mode (SIM) and mass scanning detection, respectively, revealed that SIM is up to 2 orders of magnitude more sensitive.

The detection limit of the GDGTs was also established and shown to be 0.05 ng GDGTs injected on-column. At higher levels the TEX_{86} could be analyzed with a reproducibility of 0.3ºC.

Chapter 3 focuses on the testing of a synthetic internal standard (C_{46} GDGT) to improve the accuracy of absolute GDGT abundance measurements. Initially, GDGT abundances were determined with an external standard curve but the introduction of an internal standard greatly improved the accuracy and reproducibility of the abundance measurements, reducing the standard deviation from 43% with the external standard curve to only 5% with the internal standard. Thus, the new internal standard technique will greatly improve the accuracy of GDGT abundance measurements, enlarging the potential of GDGTs in (paleo)ecological studies and enabling the detection of degradation patterns in studies such as the one in Chapter 6.

Part II of the thesis deals with the transport of the signal from the water column to the sediment and the effect of GDGT degradation on the TEX_{86} signal. The origin and transport of the signal was covered in **Chapter 4**, where different transport mechanisms and possible degradation of GDGTs through incorporation in the food web was investigated by analyzing GDGTs in stomachs and intestines of crustacean decapods. Results from this study suggested that both passive (by sinking particles) and active (by organism migration) transport mechanism can explain, at least in part, the transport of GDGTs from surface waters to the sediment. GDGTs were found in most decapods' guts, suggesting they are taken up by decapods and that they are transported to the sediment by their faecal pellets. Furthermore, pigment analysis of the stomach content confirmed that the fresh GDGT signal can be transported by massive falls of organic matter after peaks in surface production. GDGT abundances are significantly lower in intestines, but TEX_{86}-derived temperatures are not significantly different between stomachs and intestines (<1°C), suggesting that TEX_{86} values are not altered during gut transit.

In **Chapter 5** a two year sediment trap series was analyzed to understand the factors that control the production and transport of the TEX_{86} signal in the Santa Barbara Basin (SBB). Highest fluxes of crenarchaeotal lipids in the water column were found in May-June

1996 and from October 1996 to January 1997, and in general showed a good correlation with mass fluxes.

TEX_{86} reconstructed temperatures from the sediment trap series ranged from 8-11°C and were usually substantially lower than sea surface temperatures (SST), indicating that, unlike in previous studies, the TEX_{86} corresponds to sub-surface temperatures, likely between 100-150 m. TEX_{86} temperature variations observed in trap samples were not coupled to changes in SST or deep-water temperatures and only to some degree with crenarchaeotal lipid fluxes. This suggests that a complex combination of different depth origins and seasonal growth periods of Crenarchaeota contributed to the variations in TEX_{86} signal during the annual cycle. We also analyzed a high resolution record for the last 150 years from this basin which confirmed the sub-surface origin of the TEX_{86} signal in this particular setting. This result highlights the importance of performing calibration studies using sediment traps and core tops before applying the TEX_{86} temperature proxy in a given study area.

In **Chapter 6** the effect of oxic degradation on the TEX_{86} and Branched versus Isoprenoid Tetraether index (BIT) [*Hopmans et al.,* 2004], was evaluated by analyzing turbidite sediments from the Madeira Abyssal Plain (MAP). Concentrations of GDGTs were reduced by one or two orders of magnitude in the oxidized turbidite parts, suggesting substantial degradation of GDGTs. This was also the case for long-chain alkenones and to a lesser extent for organic carbon. Upon oxidation large shifts in the BIT and TEX_{86} occurred which can be explained by a strong relative increase in soil-derived GDGTs compared to the marine-derived GDGTs. This selective preservation of soil-derived lipids which are chemically nearly identical to that of their marine counterpart strongly suggests that the mineral matrix to which soil organic matter is attached enhanced its preservation. The results show that care has to be taken when analyzing TEX_{86} in sediments which have been exposed to oxygen for a long time.

Part III includes **Chapters 7, 8 and 9** and deals with the application of the TEX_{86} in different settings. With a similar time span as the SBB study in Chapter 5 we analyzed two cores in the Drammensfjord, Norway in **Chapter 7**. While some of the signal could be coming from the chemocline our results suggest that TEX_{86} indicates surface (upper 25m) temperatures. Moreover, TEX_{86} temperature patterns seem to follow variations in the historical record of averaged spring to fall Oslo air temperature relatively closely suggesting

the signal is produced during this period. Therefore, TEX_{86} temperature records of fjord sediment cores can potentially be a useful tool in reconstructing past variations of coastal climates.

Chapter 8 describes the behavior of the TEX_{86} and $U^{K'}_{37}$ during the last glacial-interglacial transition in two cores in the Arabian Sea. $U^{K'}_{37}$ and TEX_{86} SST records from two sites in the Arabian Sea revealed different temperature variations over the last 23 Kyr for each proxy. TEX_{86} SST records were similar at the two study sites over the last glacial-interglacial cycle and were in phase with temperature changes recorded in Antarctica ice core records. This suggests that the TEX_{86} records of SST in the area are mainly controlled by the southern hemisphere climate dynamics during the SW monsoon. $U^{K'}_{37}$ SST records from the same cores are different in magnitude of change and differ also in phase, and are partly in phase with northern hemisphere climate dynamics during the NE monsoon. This is likely due to different growing seasons of the biomarker source organisms, and to a change in the upwelling dynamics and monsoon strengths between the LGM and the Holocene.

Finally, in **Chapter 9**, TEX_{86} was applied to a sediment core spanning the Marine Isotope Stadials (MIS) 6 and 7 in the Western Mediterranean. A recent study in the Alboran Sea (Western Mediterranean, core ODP-977A) revealed that alkenone records not only show temperature trends similar to $\delta^{18}O$ records of *G. bulloides*, but also stadial-interstadial temperature changes during the penultimate climate cycle (from 244 to 130 cal. ky BP). To independently confirm these abrupt changes we have applied the TEX_{86} proxy to reconstruct SST using the same sediment core and compared it with the previously published $U^{K'}_{37}$ and $\delta^{18}O$ records. The TEX_{86} indicates similar stadial-interstadial changes as detected with the $U^{K'}_{37}$, thus providing independent evidence for rapid temperature changes. However, the two proxies behave differently during glacial marine isotopic stage (MIS-6) and interglacial MIS-7. During MIS-7 there is very good correspondence in absolute SST estimates between the two proxies, but in MIS-6 the TEX_{86} showed much larger temperature changes compared to the $U^{K'}_{37}$. We hypothesize that this may be caused by changes in the season in which the haptophytes and Crenarchaeota are blooming and/or variations in the depth habitat of Crenarchaeota. As the climate forcing differs between glacials and interglacials, a change in

seasonal patterns and/or depth habitat can be expected which could have a strong and differential effect on the TEX_{86} and $U^{k'}_{37}$ proxies.

In summary, the analytical work shown here has greatly improved the analysis of TEX_{86} as well as the determination of absolute abundances of GDGTs. Some of the possible transport mechanisms for GDGTs were confirmed and gut passage degradation of GDGTs was found to have no effect on the TEX_{86} signal. However, the degradation of GDGTs after long term exposure to oxygen was found to affect the TEX_{86} and caution should be exerted when the sediment cores are known to have been exposed to oxygen for long periods of time. Finally, the use of TEX_{86} as a paleo-proxy was validated by a number of down core applications and found to work in most of the study areas. This shows that TEX_{86} is a useful SST proxy which can provide complementary information to other SST proxies.

References

Barns, S. M., C. F. Delwiche, J. D. Palmer, and N. R. Pace (1996), Perspectives on archaeal diversity, thermophily and monophyly from environmental rRNA sequences, *Proc. Natl. Acd. Sci. USA*, *93*, 9188-9193.

Beck, J. W., R. L. Edwards, E. Ito, F. W. Taylor, J. Recy, F. Rougerie, P. Joannot, and C. Henin (1992), Sea-Surface Temperature from Coral Skeletal Strontium Calcium Ratios, *Science*, *257*, 644-647.

Brassell, S. C., R. G. Brereton, G. Eglinton, J. Grimalt, G. Liebezeit, I. T. Marlowe, U. Pflaumann, and M. Sarnthein (1986a), Palaeoclimatic signals recognized by chemometric treatment of molecular stratigraphic data, *Org. Geochem.*, *10*, 649-660.

Brassell, S. C., G. Eglinton, I. T. Marlowe, U. Pflaumann, and M. Sarnthein (1986b), Molecular stratigraphy: A new tool for climatic assessment, *Nature*, *320*, 129-133.

Chave, K. E. (1954), Aspects of the Biochemistry of magnesium. 1. Calcareous marine organisms. *J. Geol.,* 62, 266-283.

CLIMAP-Project Members (1981) Seasonal reconstruction of earth's Surface at the last Glacial Maximum. *Geol. Soc. Amer. Map and Chart Series* MC-36.

Coolen, M. J., B. Abbas, J. van Bleiswijk, E.C. Hopmans, M.M.M.Kuypers, S. G. Wakeham and J. S. Sinninghe Damsté (2007), Putative ammonia-oxidizing Crenarchaeota in suboxic waters of the Black Sea: a basin-wide ecological study using 16S ribosomal and functional genes and membrane lipids, *Envir. Microbiol.,* doi:10.1111/j.1462-2920.2006.01227

de Rosa, M. (1996), Archaeal lipids: structural features and supramolecular organization, *Thin Solid Films*, *284-285*, 13-17.

DeLong, E. F., K. Y. Wu, B. B. Prézelin, and R. V. M. Jovine (1994), High abundance of Archaea in Antarctic marine picoplankton, *Nature*, *371*, 695-697.

Elderfield, H. and G. Ganssen (2000), Past temperature and $d^{18}O$ of surface ocean waters inferred from foraminiferal Mg/Ca ratios, *Nature*, *405*, 442-445.

Epstein, S., E., Buchsbaum R., Lowenstam H. A., Urey H. C. (1953), Revised carbonate-water isotopic temperature scale. *Bull. Geol. Soc. Amer. 64*:1315-1325.

Gliozzi, A., G. Paoli, M. de Rosa, and A. Gambacorta (1983), Effect of isoprenoid cyclization on the transition temperature of lipids in thermophilic archaebacteria., *Biochim. Biophys. Acta*, *735*, 234-242.

Gliozzi, A., A. Relini, and P. L. G. Chong (2002), Structure and permeability properties of biomimetic membranes of bolaform archaeal tetraether lipids, *J. Membrane Sci.*, *206*, 131-147.

Gong, C. and D. J. Hollander (1999), Evidence for differential degradation of alkenones under contrasting bottom water oxygen conditions: Implications for paleotemperature reconstruction, *Geochim. Cosmochim. Acta*, *63*, 405-411.

Henderson, G. M. (2002), New oceanic proxies for paleoclimate, *Earth. Planet. Sci. Lett.*, *203*, 1-13.

Herbert, T. D., Alkenone Paleotemperature Determinations, in *The Ocean and Marine Geochemistry VOL. 6 Treatise on Geochemistry*, edited by H. D. Holland and Turekian.K.K., pp. 365-390, Elsevier-Pergamon, Oxford, 2003.

Herfort, L., S. Schouten, J. P. Boon, M. Woltering, M. Baas, J. W. H. Weijers, and J. S. Sinninghe Damsté (2006), Characterization of transport and deposition of terrestrial organic matter in the southern North Sea using the BIT index, *Limnology and Oceanography*, *51*, 2196-2205.

Herndl, G. J., T. Reinthaler, E. Teira, H. van Aken, C. Veth, A. Pernthaler, and J. Pernthaler (2005), Contribution of Archaea to total prokaryotic production in the deep Atlantic Ocean, *Appl. Environ. Microbiol.*, *71*, 2303-2309.

Hoefs, M. J. L., S. Schouten, J. W. deLeeuw, L. L. King, S. G. Wakeham, and J. S. Sinninghe Damsté (1997), Ether lipids of planktonic archaea in the marine water column, *Appl. Environ. Microbiol.*, *63*, 3090-3095.

Hoefs, M. J. L., G. J. M. Versteegh, W. I. C. Rijpstra, J. W. de Leeuw, and J. S. Sinninghe Damsté (1998), Postdepositional oxic degradation of alkenones: Implications for the measurement of palaeo sea surface temperatures, *Paleoceanography*, *13*, 42-49.

Hopmans, E. C., J. W. H. Weijers, E. Schefuss, L. Herfort, J. S. Sinninghe Damsté, and S. Schouten (2004), A novel proxy for terrestrial organic matter in sediments based on branched and isoprenoid tetraether lipids, *Earth and Planetary Science Letters*, *224*, 107-116.

Hutson, W. H. (1977), Transfer-Functions Under No-Analog Conditions - Experiments with Indian-Ocean Planktonic Foraminifera, *Quaternary Research*, *8*, 355-367.

Imbrie, J. Kipp, N. G. A new micropaleontological method for quantitative paleoclimatology: Application to a Late Pleistocene Caribean core. In: *The Late Cenozoic Glacial Ages* Turekian, K. (ed). Yale Univ. Press, New Haven, Conn, pp71-181, 1971.

Karner, M. B., E. F. DeLong, and D. M. Karl (2001), Archaeal dominance in the mesopelagic zone of the Pacific Ocean, *Nature*, *409*, 507-510.

Kim, J.-H., S. Schouten, R. Buscail, W. Ludwig, J. Bonnin, J. S. Sinninghe Damsté, and F. Bourrin (2006), Origin and distribution of terrestrial organic matter in the NW Mediterranean (Gulf of Lions): Exploring the newly developed BIT index, *Geochem.Geophy.Geosy.*, *7*, 1-20.

Könneke, M., A. E. Bernhard, J. R. de la Torre, C. B. Walker, J. B. Waterbury, and D. A. Stahl (2005), Isolation of an autotrophic ammonia-oxidizing marine archaeon, *Nature*, *437*, 543-546.

Lea, D. W., Elemental and Isotopic proxies of Past Ocean temperatures, in *The Ocean and Marine Geochemistry VOL. 6 Treatise on Geochemistry*, edited by H. D. Holland and Turekian.K.K., pp. 365-390, Elsevier-Pergamon, Oxford, 2003.

MacGregor, B. J., D. P. Moser, E. W. Alm, K. H. Nealson, and D. A. Stahl (1997), Crenarchaeota in Lake Michigan sediment, *Appl. Environ. Microbiol.*, *63*, 1178-1181.

Malmgren, B. A. and U. Nordlund (1997), Application of artificial neural networks to paleoceanographic data, *Palaeogeography Palaeoclimatology Palaeoecology*, *136*, 359-373.

Massana, R., E. F. DeLong, and C. Pedrós-Alió (2000), A few cosmopolitan phylotypes dominate planktonic archaeal assemblages in widely different oceanic provinces, *Appl. Environ. Microbiol.*, *66*, 1777-1787.

Massana, R., L. T. Taylor, A. E. Murray, K. Y. Wu, W. H. Jeffrey, and E. F. DeLong (1998), Vertical distribution and temporal variation of marine planktonic archaea in the Gerlache Strait, Antarctica, during early spring, *Limnol.Oceanogr.*, *43*, 607-617.

Murray, A. E., A. Blakis, R. Massana, S. Strawzewski, U. Passow, A. Alldredge, and E. F. DeLong (1999a), A time series assessment of planktonic archaeal variability in the Santa Barbara Channel, *Aquat. Microb. Ecol.*, *20*, 129-145.

Murray, A. E., C. M. Preston, R. Massana, L. T. Taylor, A. Blakis, K. Wu, and E. F. DeLong (1998), Seasonal and spatial variability of bacterial and archaeal assemblages in the coastal waters near Anvers Island, Antarctica, *Appl. Environ. Microbiol.*, *64*, 2585-2595.

Murray, A. E., K. Y. Wu, C. L. Moyer, D. M. Karl, and E. F. DeLong (1999b), Evidence for circumpolar distribution of planktonic Archaea in the Southern Ocean, *Aquat.Microb.Ecol.*, *18*, 263-273.

Ouverney, C. C. and J. A. Fuhrman (2000), Marine planktonic Archaea take up amino acids, *Appl. Environ. Microbiol.*, *66*, 4829-4833.

Pflaumann, U., J. Duprat, C. Pujol, and L. D. Labeyrie (1996), SIMMAX: A modern analog technique to deduce Atlantic sea surface temperatures from planktonic foraminifera in deep-sea sediments, *Paleoceanography*, *11*, 15-35.

Powers, L. A., T. C. Johnson, J. P. Werne, I. S. Castañeda, E. Hopmans, J. S. Sinninghe Damsté, and S. Schouten (2005), Large temperature variability in the southern African tropics since the Last Glacial Maximum, *Geophys. Res. Lett.*, *32*, doi:L08706-10.1029/2004GL022014.

Powers, L. A., J. P. Werne, T. C. Johnson, E. C. Hopmans, J. S. Sinninghe Damsté, and S. Schouten (2004), Crenarchaeotal membrane lipids in lake sediments: A new paleotemperature proxy for continental paleoclimate reconstruction?, *Geology*, *32*, 613-616.

Prahl, F. G., B. N. Popp, D. M. Karl, and M. A. Sparrow (2005), Ecology and biogeochemistry of alkenone production at Station ALOHA, *Deep-Sea Res. I*, *52*, 699-719.

Schouten, S., M. J. L. Hoefs, and J. S. . Sinninghe Damsté (2000a), A molecular and stable carbon isotopic study of lipids in late Quaternary sediments from the Arabian Sea, *Organic Geochemistry*, *31*, 509-521.

Schouten, S., E. C. Hopmans, R. D. Pancost, and J. S. Sinninghe Damsté (2000b), Widespread occurrence of structurally diverse tetraether membrane lipids: Evidence for the ubiquitous presence of low-temperature relatives of hyperthermophiles, *Proc. Natl. Acd. Sci. USA*, *97*, 14421-14426.

Schouten, S., E. C. Hopmans, E. Schefuss, and J. S. Sinninghe Damsté (2002), Distributional variations in marine crenarchaeotal membrane lipids: a new tool for reconstructing ancient sea water temperatures?, *Earth and Planetary Science Letters*, *204*, 265-274.

Schouten, S., E. C. Hopmans, and J. S. Sinninghe Damsté (2004), The effect of maturity and depositional redox conditions on archaeal tetraether lipid paleothermometry., *Organic Geochemistry*, *35*, 567-571.

Sinninghe Damsté, J. S., W. I. C. Rijpstra, E. C. Hopmans, F. G. Prahl, S. G. Wakeham, and S. Schouten (2002a), Distribution of Membarne Lipids of Planktonic *Creanarchaeota* in the Arabian Sea., *Appl. Environ. Microbiol.*, *68*, 2997-3022.

Sinninghe Damsté, J. S., S. Schouten, E. C. Hopmans, A. C. T. van Duin, and J. A. J. Geenevasen (2002b), Crenarchaeol: the characteristic core glycerol dibiphytanyl glycerol tetraether membrane lipid of cosmopolitan pelagic crenarchaeota, *J. Lipid Res.*, *43*, 1641-1651.

Spero, H. J., J. Bijma, D. W. Lea, and B. E. Bemis (1997), Effect of seawater carbonate concentration on foraminiferal carbon and oxygen isotopes, *Nature*, *390*, 497-500.

Sugai, A., I. Uda, Y. H. Itoh, and T. Itoh (2004), The core lipid composition of the 17 strains of hyperthermophilic Archaea, *Thermococcales*, *Journal of Oleo Science*, *53*, 41-44.

Teira, E., T. Reinthaler, A. Pernthaler, J. Pernthaler, and G. J. Herndl (2004), Combining catalyzed reporter deposition-fluorescence in situ hybridization and microautoradiography to detect substrate utilization by bacteria and archaea in the deep ocean, *Appl. Environ. Microbiol.*, *70*, 4411-4414.

Teira, E., H. van Aken, C. Veth, and G. J. Herndl (2006), Archaeal uptake of enantiomeric amino acids in the meso and bathypelagic waters of the North Atlantic, *Limnol. Oceanogr.*, *51*, 60-69.

Thurman, H, V. and A. Trujillo Air Sea interaction, in *Essentials of oceanography, 6th ed*. Macmillan Publishing company, a division of Macmillan, Inc. pp171-204, 1999.

Urey, H. C. (1947), The thermodynamic properties of isotopic substances, *Journal of the Chemical Society*, 562-581.

van de Vossenberg, J. L. C. M., A. J. M. Driessen, and W. N. Konings (1998), The essence of being extremophilic: the role of the unique archaeal membrane lipids., *Extremophiles*, *2*, 163-170.

Waelbroeck, C., L. Labeyrie, J. C. Duplessy, J. Guiot, M. Labracherie, H. Leclaire, and J. Duprat (1998), Improving past sea surface temperature estimates based on planktonic fossil faunas, *Paleoceanography*, *13*, 272-283.

Wefer, G., W. H. Berger, J. Bijma, and G. Fisher, Clues to ocean history: a brief overview of proxies, in *The use of proxies in palaeoceanography: Examples from the South Atlantic*, edited by G. Fisher and G. Wefer, pp. 1-68, Springer-verlag, Berlin, 1999.

Weijers, J. W. H., S. Schouten, M. van der Linden, B. Van Geel, and J. S. Sinninghe Damsté (2004), Water table related variations in the abundance of intact archaeal membrane lipids in a Swedish peat bog, *Fems Microbiology Letters*, *239*, 51-56.

Wells, L. E., M. Cordray, S. Bowerman, L. A. Miller, W. F. Vincent, and J. W. Deming (2006), Archaea in particle-rich waters of the Beaufort Shelf and Franklin Bay, Canadian Arctic: Clues to an allochthonous origin?, *Limnol. Oceanogr.*, *51*, 47-59.

Woese, C. R., O. Kandler, and M. L. Wheels (1990), Towards a natural system of organisms: proposal for the domains Archaea, Bacteria, and Eucarya, *Proc. Natl.Acd. Sci. USA*, *87*, 4576-4579.

Wuchter, C., B. Abbas, M. J. L. Coolen, L. Herfort, J. van Bleijswijk, P. Timmers, M. Strous, E. Teira, G. J. Herndl, J. J. Middelburg, S. Schouten, and J. S. Sinninghe Damsté (2006a), Archaeal nitrification in the ocean, *PNAS*, *103*, 12317-12322.

Wuchter, C., S. Schouten, M. J. L. Coolen, and J. S. Sinninghe Damsté (2004), Temperature-dependent variation in the distribution of tetraether membrane lipids of marine Crenarchaeota: Implications for TEX_{86} paleothermometry, *Paleoceanography*, *19,* doi:10.1029/2004PA001041.

Wuchter, C., S. Schouten, S. G. Wakeham, and J. S. Sinninghe Damsté (2005), Temporal and spatial variation in tetraether membrane lipids of marine Crenarchaeota in particulate organic matter: Implications for TEX_{86} paleothermometry, *Paleoceanography*, *20,* doi:10.1029/2004PA001110.

Wuchter, C., S. Schouten, S. G. Wakeham, and J. S. Sinninghe Damsté (2006b), Archaeal tetraether membrane lipid fluxes in the northeastern Pacific and the Arabian Sea: Implications for TEX_{86} paleothermometry, *Paleoceanography*, *21*, doi:PA4208-1-PA4208-9.

Chapter 2

Improved analytical methodology for TEX_{86} paleothermometry by high performance liquid chromatography/atmospheric pressure chemical ionization-mass spectrometry

Stefan Schouten, Carme Huguet, Ellen C. Hopmans, Michiel V.M. Kienhuis

and Jaap S. Sinninghe Damsté

Published in *Analytical Chemistry* **79**, 2940-2944(2007)

Abstract

The TEX_{86} is a recently proposed paleothermometer through which ancient sea water temperatures of up to 120 My ago can be reconstructed. It is based on the relative distribution of glycerol dibiphytanyl glycerol tetraethers as measured by high performance liquid chromatography/atmospheric pressure chemical ionization-mass spectrometry (HPLC/APCI-MS). The aim of this study was to examine and improve several analytical aspects in the determination of this important proxy in environmental matrices. Comparison of TEX_{86} analysis using Single Ion Mode (SIM) and mass scanning (*m/z* 950 to 1450) detection, respectively, revealed that SIM is up to 2 orders of magnitude more sensitive and that the TEX_{86} can be determined with a reproducibility of ±0.004 or ±0.3°C using this method. Comparison of TEX_{86} values obtained with two different HPLC/APCI-MS set-ups revealed no significant differences. In addition, analysis of TEX_{86} of extracts obtained by Soxhlet, ultrasonic, and accelerated high pressure extraction techniques also showed no significant differences between the methods. Our results suggest that TEX_{86} analysis by HPLC/APCI-MS is robust and can be determined with analytical errors comparable to those of other temperature proxies.

2.1. Introduction

Reconstruction of temperatures of ancient oceans is of crucial importance in understanding past climate changes and generally relies on the chemical analysis of ancient sediments. Several of these chemical temperature proxies are currently used to reconstruct past sea water temperatures and they can be broadly subdivided into proxies based on inorganic or organic fossil remains. Inorganic temperature proxies include, for example, $\delta^{18}O$ and Mg/Ca ratios of foraminifera and transfer functions of foraminiferal assemblages, [e.g. *Lea,* 2003]. The $U_{37}^{K'}$ ratio based on the relative distribution of di- and tri-unsaturated long-chain C_{37} alkenones derived from haptophyte algae was, until recently, the only proxy based on organic fossil remains. Originally proposed as a temperature proxy by *Brassell et al*.[1986] based on sediment core studies, it was later validated by temperature controlled culture studies of the haptophyte *Emiliania huxleyi* [*Prahl and Wakeham,* 1987]. The $U_{37}^{K'}$ is typically measured by determining the relative concentrations of long-chain alkenones using gas chromatography (GC) and a flame ionization detector and an analytical precision of ±0.2°C can be achieved [*Herbert,* 2003]. The analytical sensitivity can be further improved by using GC chemical ionization mass spectrometry [*Rosell-Melé et al.,* 1995] though this potentially also introduces analytical biases in determining this ratio [*Chaler et al.,* 2000].

Recently, a second organic sea water temperature proxy based on archaeal glycerol dibiphytanyl glycerol tetraether (GDGT) lipids, the $TEX_{86,}$ was proposed [*Schouten et al.,* 2002]. These lipids are biosynthesized by marine Crenarchaeota which are ubiquitous in marine environments, occur throughout the water column and are one of the dominant prokaryotic groups in today's oceans [*Karner et al.,* 2001]. Marine Crenarchaeota biosynthesize different types of GDGTs, i.e. GDGTs containing 0 to 3 cyclopentyl moieties (GDGT 0-3; see structures in Fig. 1) and crenarchaeol which, in addition to 4 cyclopentyl moieties, has a cyclohexyl moiety (GDGT 4)[*Schouten et al.,* 2002; *Sinninghe Damsté et al.,* 2002]. Finally, they also biosynthesize small quantities of a crenarchaeol regio-isomer (GDGT 4'). A study of marine surface sediments showed that higher sea surface temperatures result in an increase in the relative amounts of GDGTs with two or more cyclopentyl moieties [*Schouten et al.,* 2002]. Thus, measuring the relative amounts of GDGTs present in sediments allows determination of the temperature at which the Crenarchaeota were living when they produced their membranes.

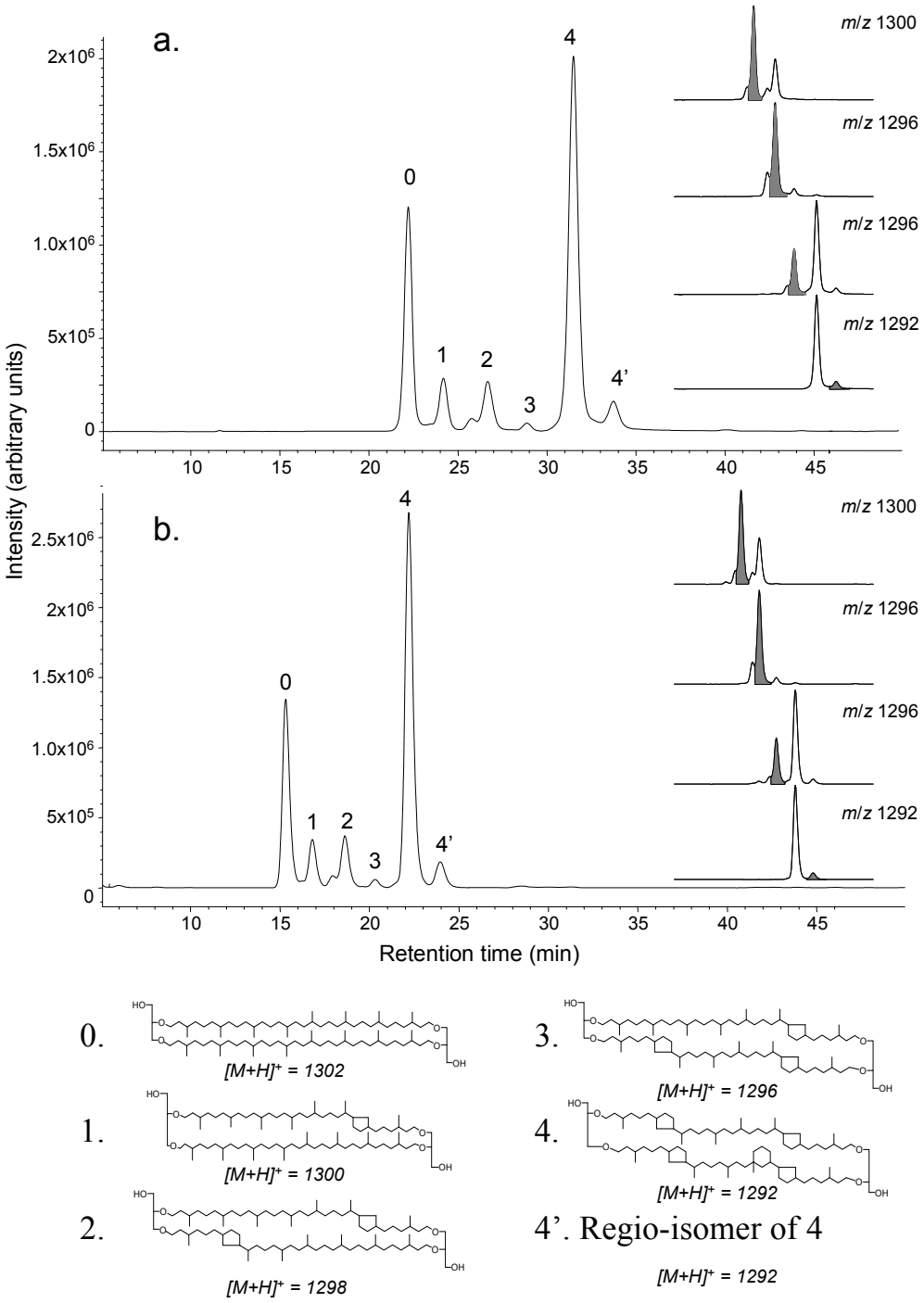

Figure 1. Base peak chromatogram of GDGTs eluting on (a) an Econosphere Amino column (4.6 x 250 mm, 5 μm) at 1 ml.min^{-1} flow rate and (b) a Prevail Cyano column (2.1 x 150 mm, 3 μm) at 0.2 ml.min^{-1}. Inserts show mass chromatograms and integrated peak area's of the four GDGTs used in the determination of the TEX_{86}.

The TEX_{86} ratio was proposed as a means to quantify the relative abundance of GDGTs (see also Fig. 1):

$$TEX_{86} = \frac{[GDGT\ 2] + [GDGT\ 3] + [GDGT\ 4']}{[GDGT\ 1] + [GDGT\ 2] + [GDGT\ 3] + [GDGT\ 4']} \quad [1]$$

TEX_{86} was calibrated using over 40 sediment core-tops obtained from 15 different locations with the following resulting equation:

$$TEX_{86} = 0.015 \times T + 0.28 \qquad r^2 = 0.92 \quad [2]$$

This equation allows the conversion of the calculated TEX_{86} values into SSTs (see for details *Schouten et al.* [2002]).

This initial work has been followed by other studies which investigate the validity of the TEX_{86} as a SST proxy. For example, mesocosm experiments confirmed that marine Crenarchaeota change their membrane composition with growth temperature [*Sinninghe Damsté et al.,* 2002] and a survey of particulate organic matter showed that TEX_{86} values correlated well with in situ temperature at depths <100m [*Wuchter et al.,* 2005]. Furthermore, sediment trap studies revealed that the TEX_{86} in sinking particulate matter in the Arabian Sea corresponds well with satellite-derived SST measurements [*Wuchter et al.,* 2006]. Application of the TEX_{86} proxy in the reconstruction of glacial to Holocene SST in the Arabian Sea showed that several features in the TEX_{86}-SST record corresponded with well known global climatic temperature changes [*Huguet et al.,* 2006b].

Although these studies have now shown that the TEX_{86} proxy is capable of reconstructing past SST, a number of issues still have to be resolved. The analytical uncertainty associated with determining TEX_{86} from environmental matrices such as sediments is one of the most important issues. The measurement of the relative amounts of GDGTs requires the use of high performance liquid chromatography/atmospheric pressure chemical ionization-mass spectrometry (HPLC/APCI-MS) [*Hopmans et al.,* 2000], a technique not commonly used in the fields of organic geochemistry, paleoceanography and paleoclimatology.

Schouten et al., [2002] reported that the reproducibility in quantification of the TEX_{86} was 0.022 or 2°C using HPLC/APCI-MS which is substantially less than that for alkenones (0.2ºC) and they suggested that this required improvement. Here we report on a number of analytical experiments designed to improve the reproducibility and to explore the limitations of TEX_{86} analysis in sediments.

2.2. Experimental section

2.2.1. Sediment extraction

Sediments (1-3 g dry mass) were taken at selected intervals from the NIOP 905 sediment core from the Arabian Sea [*Huguet et al.,* 2006b] and were freeze-dried and homogenized by mortar and pestle. The freeze-dried sediments were extracted by ultrasonication with methanol, methanol/dichloromethane (DCM) (1:1; v/v) and finally with DCM. The supernatants were collected and after evaporation of the solvents, the extracts were dried over a sodium sulfate column. An aliquot of the total lipid extract was fractionated into apolar and polar fractions using a small column with activated aluminum oxide and using hexane/DCM (9:1; v/v) and DCM/methanol (1:1; v/v) as eluents, respectively. Aliquots of the polar fractions were pooled into one large polar fraction for the analytical experiments described below. The resulting pooled polar fraction was condensed by rotary evaporation, dried further under a stream of nitrogen, dissolved in hexane/isopropanol (99:1; v/v), and filtered using a PTFE 0.4 μm filter prior to injection in the HPLC/MS.

Approximately 700 g of sediment of a box core taken from Drammensfjord [*Smittenberg et al.,* 2005] were freeze-dried and homogenized. To test the effect of extraction techniques the Drammensfjord sediment was extracted using three different methods: (1) by Soxhlet extraction with DCM/methanol (7:1; v/v) for 24 h, (2) by ultrasonic extraction using solvents of decreasing polarity, i.e. methanol (3 times), a DCM/methanol mixture (1:1; v/v, 3 times), and finally DCM (3 times) and (3) by accelerated solvent extraction (ASE, Dionex™) [*Richter et al.,* 1996] using a mixture of dichloromethane (DCM) and methanol (MeOH) (9:1, v/v) at 100°C and $7.6 \cdot 10^6$ Pa. The extracts were then separated by column chromatography and prepared for HPLC/MS analysis as described above.

2.2.2. HPLC/MS analysis

Most analyses were performed using an Agilent (Palo-Alto, CA, USA) 1100 series LC/MSD SL equipped with an auto-injector and Chemstation chromatography manager software. For comparison of HPLC/APCI-MS set ups, a range of sediment extracts with different TEX_{86} values were also analyzed by an Agilent 1100 HPLC coupled to a TSQ Quantum Ultra EM triple quadrupole mass spectrometer (Thermo Inc., San Jose, CA, USA) equipped with an Ion Max source with APCI probe. Separation was achieved on a Prevail Cyano column (2.1 x 150 mm, 3 μm; Alltech, Deerfield, IL, USA), maintained at 30°C. For comparison with the original separation method of Hopmans et al.[*Hopmans et al.,* 2000] we also used an Econosphere Amino column (4.6 x 250 mm, 5 μm; Alltech). Injection volumes varied from 1 to 20 μl. GDGTs were eluted isocratically with 99% A and 1% B for 5 min, followed by a linear gradient to 1.8% B in 45 min, where A = hexane and B = isopropanol. Flow rate was 0.2 ml/min for the Cyano column and 1 ml/min for the Amino column. After each analysis the column was cleaned by back-flushing hexane/propanol (90:10; v/v).

Detection was achieved using positive ion APCI of the eluent. Conditions for the Agilent 1100 APCI-MS were as follows: nebulizer pressure 60 psi, vaporizer temperature 400°C, drying gas (N_2) flow 6 l/min and temperature 200°C, capillary voltage -3 kV, corona 5 μA (~ 3.2 kV). Conditions for the TSQ Quantum Ultra positive ion APCI-MS were as follows: vaporizer temperature 375°C, discharge current 2.0 μA, sheath gas (N_2) pressure 20 (arbitrary units), auxiliary gas (N_2) pressure 4 (arbitrary units), and capillary temperature 280°C. The conditions for GDGT analysis were optimized by injection or infusion of cholesterol or by a GDGT-0 standard.

To study the effect of scanning mode vs. SIM on the TEX_{86}, GDGTs were detected with SIM of their protonated molecules $[M+H]^+$ (dwell time = 234 ms) and by mass scanning from *m/z* 950-1450 on the Agilent 1100 HPLC/MS. In addition, GDGTs were detected by SIM on the TSQ Quantum Ultra triple quadrupole MS to investigate the influence of a different brand of mass spectrometer on TEX_{86} measurements. In this case the triple quadrupole MS was utilized as a single quadrupole MS, using the third quadrupole only. GDGTs were quantified by integration of the peak areas using Excalibur software. TEX_{86} values were calculated according to equation [1]. Absolute amounts of GDGTs injected on column were determined by using external standard curves of a crenarchaeol standard [*Huguet et al.,* 2006a].

2.3. Results and discussion

2.3.1. Separation of GDGTs

The original method to separate and analyze GDGT isomers by HPLC/MS involved the use of a 25 cm x 4.6mm Amino column and 5 μm particle size and using a solvent flow rate of 1 ml/min [*Hopmans et al.* 2000]. To improve speed of analysis and reduce the amount of solvent used, i.e. reducing flow rate which also improves ionization chamber stability, we tested a Cyano column with reduced column width (2.1 cm) and length (15 cm) and smaller particle size (3 μm) and reduced flow rate of 0.2 ml/min. Injection of an identical amount of polar fraction of the sediment extract from the Arabian Sea using similar MS conditions shows that the reduced column width, particle size and flow rate yielded slightly reduced peak widths at halve height (for crenarchaeol 0.64 min versus 0.49 min for Amino and Cyano columns, respectively) and thus also slightly higher peak heights (Fig 1), mainly because the GDGTs eluted much faster (25 min versus 35 min). Furthermore, separation between crenarchaeol (GDGT-4) and its regio-isomer was substantially improved (see inserts in Fig 1), an important point considering that the regio-isomer is used in the determination of the TEX_{86} index (see introduction). Nevertheless, TEX_{86} under these two different column conditions was nearly identical, i.e. 0.658 and 0.653 for the Amino column and Cyano column, respectively. These new column conditions, thus, substantially speed up the time of analysis for TEX_{86} determinations and resulted in a 5-fold reduction of the amount of solvents needed.

2.3.2. Mass spectrometry techniques

The original study proposing the TEX_{86} as an SST proxy used mass scanning from *m/z* 950 to 1450 to detect, identify and quantify the GDGTs required for TEX_{86} calculations [*Schouten et al.,* 2002]. Although this technique is suitable for the detection and identification of GDGTs, i.e. through the presence of their characteristic $[M+H]^+$-18 and $[M+H]^+$-74 ions [*Hopmans et al.,* 2000], it is less suitable for quantification due to the relatively low signal-to-noise-ratio compared to, for example, Single Ion Monitoring (SIM) or Selected Reaction Monitoring techniques. Indeed, the reproducibility reported in the study by *Schouten et al.,* [2002] using mass scanning was not very high (±0.022 or ±2°C based on duplicate analysis of various sediment samples) and required further improvement. Ions from co-eluting molecules interfering with the $[M+H]^+$ ions of GDGTs were rarely encountered using our LC separation

technique and therefore we decided to use SIM to quantify the relative GDGT abundances needed for the TEX_{86} (Fig. 1).

The reproducibility of the SIM-MS detection technique was tested by analyzing two different sediments for the five TEX_{86} GDGT isomers (Fig. 1). One sediment is from a Norwegian fjord, Drammensfjord [*Smittenberg et al.,* 2005] characterized by relatively low annual mean sea surface temperatures (SST) of ca. 8°C whilst the other sediment is from the Arabian Sea [*Huguet et al.,* 2006b] with an annual mean SST of ca. 26°C. HLPC/MS analysis showed that, in agreement with the above water temperatures, the TEX_{86} value of the Drammensfjord sediment was lower, 0.42, than that of the Arabian Sea sediment, 0.66. The reproducibility of TEX_{86} using SIM-MS detection for the Drammensfjord was 0.0043 (1σ s.d, n=6) and for the Arabian Sea 0.0035 (1σ s.d., n=6) with total GDGT amounts injected on-column ranging from 4 to 1000 ng. Using equation [2] this translates to a reproducibility of ca. 0.3°C for TEX_{86} analysis using SIM, at least for sediments with TEX_{86} values ranging from 0.4 to 0.7 or 8 to 28°C. The reproducibility for samples with TEX_{86} values >0.7 is expected to be similar or even better due to the relatively high amounts of the different GDGTs used for determination of the TEX_{86}, whilst for samples with TEX_{86} values <0.4 potentially poorer reproducibilities may be expected. The improved reproducibility using SIM is a substantial improvement, by nearly one order of magnitude, from that using mass scanning previously reported [*Schouten et al.* 2002].

We then compared the sensitivity of the SIM mode to that of the mass scanning mode. When the amount of polar fractions injected on column was decreased in several steps from 20 μg down to 0.2 ng, or from 990 to 0.02 ng total GDGTs depending on the sediment analyzed, detection of peaks in the mass scanning mode quickly became difficult, as expected. Some of the less abundant GDGTs used in the TEX_{86} (GDGT 2, 3 and 4'; Fig 1) became non detectable in mass scanning mode when the amount of extract injected on column was reduced to 4 ng GDGTs inject on column in case of the Drammensfjord or 0.1 ng in case of the Arabian Sea (Fig. 2). This difference in sensitivity between the extracts is caused by the relatively lower abundance of GDGTs 1, 2, 3 and 4' compared to GDGT 0 and 4 in the Drammensfjord extract. However, at these concentrations, the TEX_{86} could still be easily determined by SIM. In fact, analysis by SIM yielded, within analytical uncertainty, identical TEX_{86} values compared to those at high (>100 ng) concentrations down to 0.05 ng of GDGTs

injected on column in case of the Arabian Sea though with decreasing reproducibility (Fig. 2). Thus, SIM yields reproducible TEX_{86} values at two orders (Arabian Sea) and one order (Drammensfjord) of magnitude lower concentrations than the scanning mode. At the lowest amounts of injected GDGTs where peaks could still be detected with SIM, TEX_{86} values start to significantly deviate from those at higher concentrations suggesting that care has to be taken when analyzing TEX_{86} close to the limit of detection of the GDGTs.

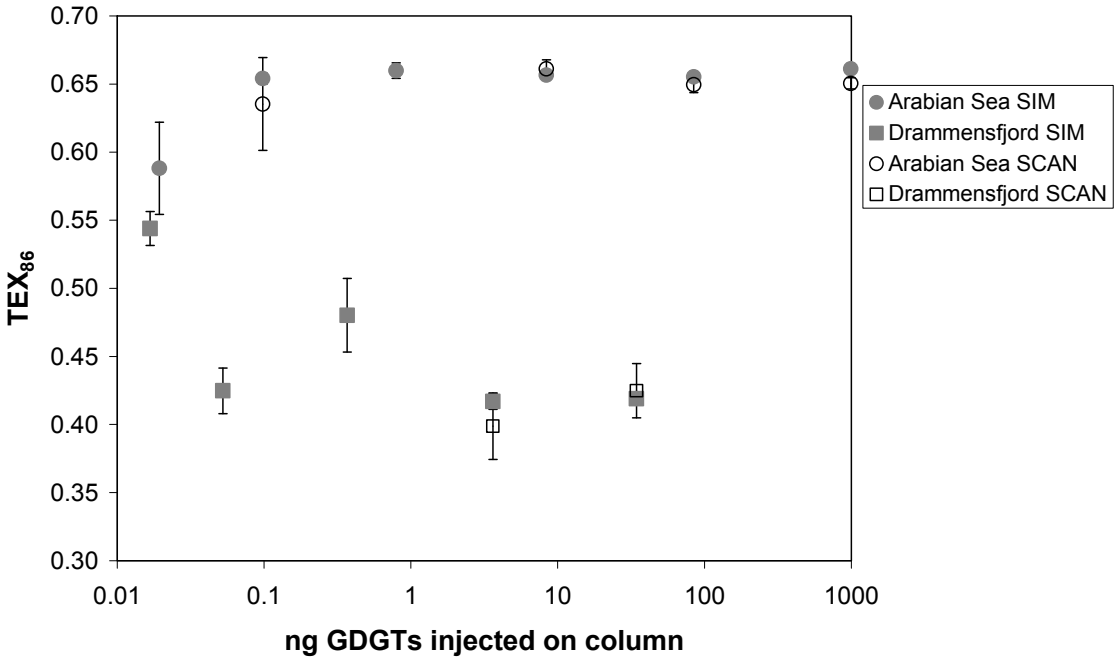

Figure 2. TEX_{86} values as a function of total amount of GDGTs injected on column and using different mass spectrometry techniques (scanning and SIM) as analysed on an Agilent 1100 MSD SL HPLC/APCI-MS. The polar fractions are derived from pooled polar fractions of sediments from the NIOP905 core of the Arabian Sea and from extract of a composite sediment of the Drammensfjord, respectively. Error bars indicate ± 1σ standard deviation of triplicate measurements.

2.3.3. Comparison of mass spectrometers

A selected set of sediment extracts, with a range of TEX_{86} values, were analyzed by HPLC/APCI/MS in SIM mode using two different mass spectrometers, i.e. the Agilent 1100 MSD SL and the Thermo Inc. TSQ Quantum Ultra Triple Quadrupole MS.

The resulting TEX_{86} values from single analysis of similar quantities of GDGTs injected on column are cross plotted in Fig. 3 which shows that the TEX_{86} values are close to the 1:1 correlation line, suggesting little systematic instrumental biases. Thus, it seems that the TEX_{86} is not strongly dependent on APCI interface design and mass spectrometer. However, it should be noted that this method was only tested in SIM mode on a quadrupole mass spectrometer and it is unknown if the use of other mass spectrometry techniques such as ion trap mass spectrometers causes deviations. Recently, *Escala et al.,* [2007] reported the analysis of TEX_{86} with an HPLC/APCI/ion trap-MS and a reproducibility of 0.012 or 0.8°C suggesting that this index can be determined on different types of instruments.

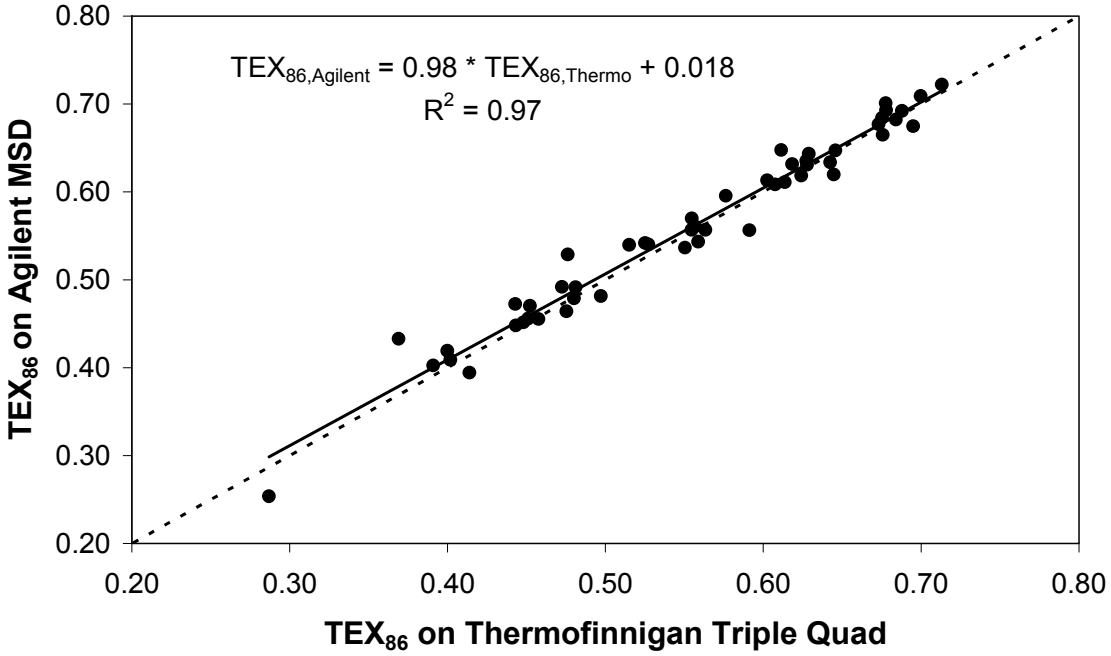

Figure 3. Cross plot of TEX_{86} values determined using the TSQ Quantum Ultra (Thermo Inc.) and an Agilent 1100 MSD HPLC/APCI-MS. Dashed line indicates the 1:1 line.

2.3.4. Effect of extraction techniques

We also investigated whether the use of different extraction techniques could potentially bias the TEX_{86}. Sediment from Drammensfjord was extracted in triplicate using ultrasonic extraction, Soxhlet extraction and accelerated solvent extraction at high pressure and temperature.

The results show that the TEX_{86} values obtained through the different techniques are identical within error (Fig. 4). The average error is 0.010 or 0.7°C which is twice as high as that of the analytical reproducibility (see above). However, this error now also includes errors due to different extraction techniques and the work up procedure (e.g. column chromatography, filtration) of the extracts. Thus, it seems that only relatively minor errors are introduced due to the work up procedures and that all these different extraction techniques can be used. Importantly, this includes accelerated solvent extraction which allows rapid extraction (<30 min.) in a highly automated fashion [*Richter et al.,* 1996] and therefore a high throughput of samples, an important prerequisite for high resolution paleoceanographic studies [*Forster et al.,* 2007].

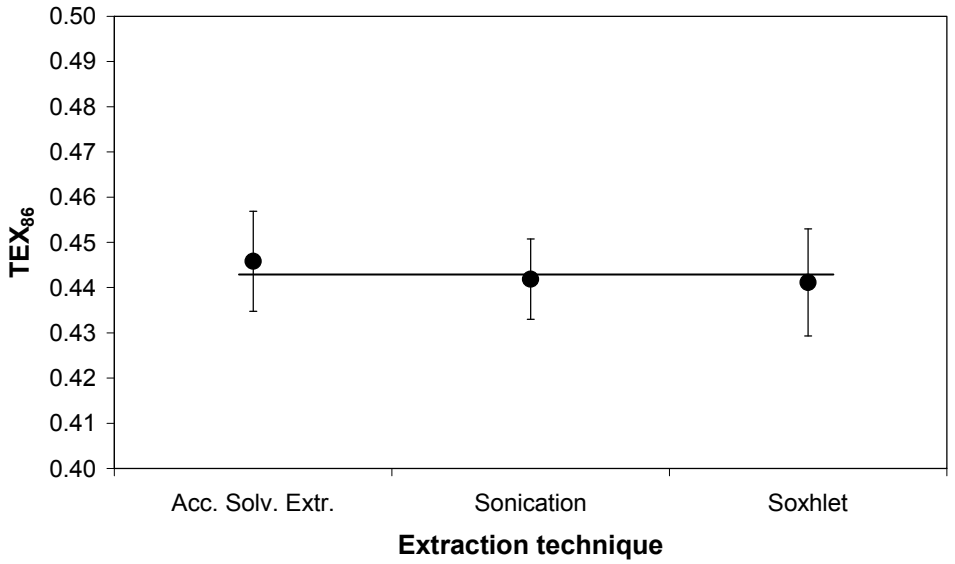

Figure 4. TEX_{86} values of composite sediment of Drammensfjord extracted using ultrasonic, Soxhlet and accelerated solvent extraction techniques. Error bars indicate ±1σ standard deviation of triplicate extractions and triplicate analysis. Line represents the average TEX_{86} of all the experiments.

2.4. Conclusions

Our results show that TEX_{86} is not biased by extraction techniques and that different HPLC/APCI-MS set ups can be used. We substantially decreased the time of analysis of TEX_{86} compared to previous methods by using a smaller LC column and reduced flow rates. We also show that SIM is an improved technique for TEX_{86} analysis compared to the originally used mass scanning technique and gives a reproducibility in TEX_{86} determination of ca. ±0.004 or ca. ±0.3°C.

Acknowledgements

Sediments for this study were provided by Rienk Smittenberg and Tjeerd van Weering. We thank two anonymous reviewers for useful comments. This study was supported by NWO-ALW (Equipment grant 843.03.001 and project grant 152911)

References

Brassell, S. C., G. Eglinton, I. T. Marlowe, U. Pflaumann, and M. Sarnthein (1986), Molecular stratigraphy: A new tool for climatic assessment, *Nature*, *320*, 129-133.

Chaler, R., J. O. Grimalt, C. Pelejero, and E. Calvo (2000), Sensitivity effects in $U^{k'}_{37}$ paleotemperature estimation by chemical ionization mass spectrometry, *Anal. Chem.*, *72*, 5892-5897.

Escala, M., A. Rosell-Melé, and P. Masque (2007), Rapid screening of glycerol dialkyl glycerol tetraethers in continental Eurasia samples using HPLC/APCI-ion trap mass spectrometry, *Org. Geochem.*, *38*, 161-164.

Forster, A., S. Schouten, K. Moriya, P. A. Wilson, and J. S. Sinninghe Damsté (2007), Tropical warming and intermittent cooling during the Cenomanian/Turonian oceanic anoxic event 2: Sea surface temperature records from the equatorial Atlantic, *Paleoceanography*, *22*, doi: PA1219-1-PA1219-14.

Herbert, T. D., Alkenone Paleotemperature Determinations, in *The Ocean and Marine Geochemistry VOL. 6 Treatise on Geochemistry*, edited by H. D. Holland and Turekian.K.K., pp. 365-390, Elsevier-Pergamon, Oxford, 2003.

Hopmans, E. C., S. Schouten, R. D. Pancost, M. T. J. Van der Meer, and J. S. Sinninghe Damsté (2000), Analysis of intact tetraether lipids in archaeal cell material and sediments by high performance liquid chromatography/atmospheric pressure chemical ionization mass spectrometry, *Rap. Comm. Mass Spectrom.*, *14*, 585-589.

Huguet, C., E. C. Hopmans, W. Febo-Ayala, D. H. Thompson, J. S. Sinninghe Damsté, and S. Schouten (2006a), An improved method to determine the absolute abundance of glycerol dibiphytanyl glycerol tetraether lipids, *Org. Geochem.*, *37*, 1036-1041.

Huguet, C., J. H. Kim, J. S. Sinninghe Damsté, and S. Schouten (2006b), Reconstruction of sea surface temperature variations in the Arabian Sea over the last 23 kyr using organic proxies (TEX_{86} and $U^{K'}_{37}$), *Paleoceanography*, *21,* doi:10.1029/2005PA001215.

Karner, M. B., E. F. DeLong, and D. M. Karl (2001), Archaeal dominance in the mesopelagic zone of the Pacific Ocean, *Nature*, *409*, 507-510.

Lea, D. W., Elemental and Isotopic proxies of Past Ocean temperatures, in *The Ocean and Marine Geochemistry VOL. 6 Treatise on Geochemistry*, edited by H. D. Holland and Turekian.K.K., pp. 365-390, Elsevier-Pergamon, Oxford, 2003.

Prahl, F. G. and S. G. Wakeham (1987), Calibration of unsaturation patterns in long-chain ketone compositions for paleotemperature assessment., *Nature*, *330*, 367-369.

Richter, B. E., B. A. Jones, J. L. Ezzell, N. L. Porter, N. Avdalovic, and C. Pohl (1996), Accelerated solvent extraction: A technique for sample preparation, *Anal. Chem.*, *68*, 1033-1039.

Rosell-Melé, A., J. F. Carter, A. T. Parry, and G. Eglinton (1995), Determination of the $U^{K'}_{37}$ index in geological samples, *Anal. Chem.*, *67*, 1283-1289.

Schouten, S., E. C. Hopmans, E. Schefuss, and J. S. Sinninghe Damsté (2002), Distributional variations in marine crenarchaeotal membrane lipids: a new tool for reconstructing ancient sea water temperatures?, *Earth Plan. Scie. Let.s*, *204*, 265-274.

Sinninghe Damsté, J. S., S. Schouten, E. C. Hopmans, A. C. T. van Duin, and J. A. J. Geenevasen (2002), Crenarchaeol: the characteristic core glycerol dibiphytanyl glycerol tetraether membrane lipid of cosmopolitan pelagic crenarchaeota, *J. Lipid Res.*, *43*, 1641-1651.

Smittenberg, R. H., M. Baas, M. J. Green, E. C. Hopmans, S. Schouten, and J. S. Sinninghe Damsté (2005), Pre- and post-industrial environmental changes as revealed by the biogeochemical sedimentary record of Drammensfjord, Norway, *Mar.Geol.*, *214*, 177-200.

Wuchter, C., S. Schouten, S. G. Wakeham, and J. S. Sinninghe Damsté (2005), Temporal and spatial variation in tetraether membrane lipids of marine Crenarchaeota in particulate organic matter: Implications for TEX86 paleothermometry, *Paleoceanography*, *20*, doi:10.1029/2004PA001110

Wuchter, C., S. Schouten, S. G. Wakeham, and J. S. Sinninghe Damsté (2006), Archaeal tetraether membrane lipid fluxes in the northeastern Pacific and the Arabian Sea: Implications for TEX86 paleothermometry, *Paleoceanography*, *21*, doi: PA4208-1-PA4208-9.

Chapter 3

An improved method to determine the absolute abundance of glycerol dibiphytanyl glycerol tetraether lipids

Carme Huguet, Ellen C. Hopmans, Wilma Febo-Ayala, David H. Thompson, Jaap S. Sinninghe Damsté and Stefan Schouten

Published in *Organic Geochemistry,* **37**, 1036-1041 (2006)

Abstract

Isoprenoid glycerol dialkyl glycerol tetraethers (GDGTs) are specific membrane lipids derived from archaea, one of the three domains of life. These lipids can be used as biomarkers in paleo-ecological studies. GDGTs can be analyzed by high performance liquid chromatography (HPLC)/mass spectrometry (MS). To quantify GDGTs, external standard curves were run monthly on the HPLC/MS. However, external standard curves represented a snapshot and do not adjust for changes during storage, dissolution and manipulation of samples or drifts in HPLC/MS conditions. To measure absolute GDGT abundances more accurately, we tested the use of a newly synthesized C_{46} GDGT as an internal standard. The accuracy in the determination of GDGT concentration improved significantly when using the internal standard (5% standard deviation) compared to that obtained with the monthly external standard curve (43% standard deviation). Thus the new internal standard technique will greatly improve the accuracy of GDGT abundance measurements, enlarging the potential of GDGTs in paleo-ecological studies.

3.1. Introduction

Archaea are prokaryotes which are phylogenetically distinct from bacteria and possess different membrane lipids. While bacterial membranes are generally formed by straight-chain fatty acids ester bound to glycerol, membranes of dominant archaeal groups contain lipids with isoprenoid alkyl chains bound by ether bonds (Fig. 1). Most of the cultured members of the archaeal domain producing isoprenoid glycerol dialkyl glycerol tetraethers (GDGTs) are extremophiles, but recent investigations showed that crenarchaeota, a subgroup of archaea, are ubiquitous and abundant in seawater [*Hoefs et al.*, 1997; *Massana et al.*, 2000; *Karner et al.*, 2001] and lakes [*Powers et al*., 2004]. GDGTs biosynthesized by these crenarchaeota are similar to those of their thermophilic ancestors, except for crenarchaeol, a unique GDGT containing one cyclohexane moiety in addition to the more common cyclopentane moieties [*Sinninghe Damsté et al*., 2002a]. It is thought that the biosynthesis of crenarchaeol is an adaptation to the relatively cold sea water temperatures, compared to thermophilic environments such as hot springs [*Kuypers et al.*, 2002]. For this reason, crenarchaeol (Fig. 1) is a taxonomically-specific biomarker for non-thermophilic crenarchaeota.

Crenarchaeol has been used to study the abundance of crenarchaeota in the Arabian Sea [*Sinninghe Damsté et al.*, 2002b] and the Black Sea [*Wakeham et al.*, 2003]. Results of these studies are in general agreement with those of molecular biological studies which show that crenarchaeota occur throughout the water column [e.g. *Karner et al*., 2001]. GDGTs are separated with high performance liquid chromatography (HPLC) and then identified by mass spectrometry (MS) [*Hopmans et al.*, 2000]. To quantify the GDGTs for the above studies, external standard curves were run, using a GDGT-0 standard (Fig.1) [*Wakeham et al.*, 2003]. However, this technique is likely not very accurate for calculating absolute abundances as it does not account for differences in the extraction, processing, storage of the samples and drifts in MS response. Hence, the changes observed in the relative abundances in depth profiles such as those noted in the Black Sea and the Arabian Sea may be reliable, but the calculated absolute amounts might be less precise. The best way to improve the analytical accuracy in the quantification of GDGTs is to use an internal standard that can be added at the beginning of the extraction process. This internal standard should not occur naturally and needs to be chemically similar to the GDGTs quantified. Here we tested a C_{46} GDGT which was synthesized by *Patwardhan and Thompson* [1999], and compared GDGT absolute abundance

measurements using this new internal standard to those calculated with the external standard curve technique for the same set of samples.

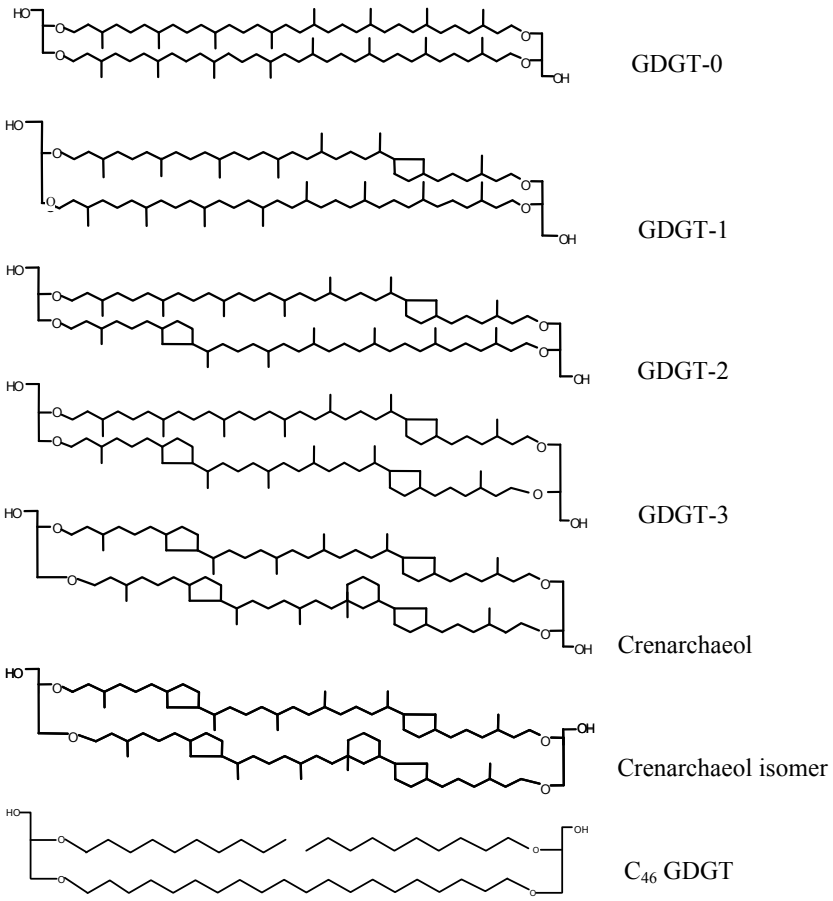

Figure 1. Molecular structures of protonated GDGT molecules and the internal standard, C_{46} GDGT.

3.2. Experimental

As an internal standard we used a GDGT with two glycerol head groups linked by a C_{20} alkyl chain and two C_{10} alkyl chains (Fig. 1) which was synthesized by *Patwardhan and Thompson* [1999]. A mixture of the C_{46} GDGT and crenarchaeol (1:1 w:w) was prepared and analyzed every week over a four month period to determine the relative response factor (RRF). To produce the external standard curves we used crenarchaeol as isolated previously [*Sinninghe Damsté et al.,* 2002b] and injected amounts ranging from 10 to 200 ng.

Both the internal and external standard quantification methods were tested by analyzing GDGTs in a sediment sample from the Drammensfjord (59°40' N 10°23' E). The sediment sample was a composite sample from a core taken in the centre of the Drammensfjord with the RV 'Pelagia' on October 29th, 1999 [*Smittenberg et al.,* 2005]. The core was freeze dried and ground to produce a homogenous sample. The freeze dried sediment sample was extracted using an Accelerated Solvent Extractor 200 (ASE 200, DIONEX) with a mixture of dichloromethane (DCM) and methanol (MeOH) (9:1 vol:vol) at 100°C and $7.6x10^6$ Pa. A solution of the C_{46} GDGT in 99% n-hexane: 1% isopropanol (0.01 mg/ml) was added to the total extract, with a proportion of 750 ng of the C_{46} GDGT for 1 mg of total extract. The total extract was separated using a glass pipette column filled with activated alumina oxide by sequentially eluting with hexane/DCM (9:1 vol:vol) to obtain an apolar fraction and DCM/MeOH (1:1 vol:vol) to obtain a polar fraction. The polar fraction containing the GDGTs was filtered through a 0.45 μm pore size, 4 mm diameter PFTE filter prior to injection. The samples were analyzed by HPLC-atmospheric pressure positive ion chemical ionization mass spectrometry (APCI)-MS by applying conditions slightly modified from *Hopmans et al.* [2000]. Analyses were performed with an HP 1100 Series HPLC/MS equipped with an auto-injector and ChemStation chromatography manager software. Separation was achieved on a Prevail Cyano column (2.1 x 150mm, 3μm; Alltech, Deerfield, Illinois, USA), maintained at 30°C. The GDGTs were first eluted isocratically with (A) hexane and (B) propanol as follows, 99 % A: 1 % B for 5 min, then a linear gradient to 1.8 B in 45 min. Flow rate was 0.2 mL/min. After each analysis the column was cleaned by back flushing hexane/propanol (90:10, vol:vol) at 0.2 mL/min for 10 min. Conditions for APCI/MS were as follows: nebulizer pressure 60 psi, vaporizer temperature 400°C, drying gas (N^2) flow 6 L/min and temperature 200ºC, capillary voltage -3.5kV, corona 5 μA(~3.2kV). Mass spectra of the C_{46} GDGT and crenarchaeol were obtained by scanning at *m/z* 100-1000 and m/z 900-1400 respectively . For the standard curves and GDGT quantification Single Ion Monitoring (SIM) was used instead of mass scanning because SIM improves the signal to noise ratio and thus improves the reproducibility. SIM parameters were set to detect the protonated molecules of the 5 isoprenoid GDGTs (*m/z* 1302, 1300, 1298, 1296, 1292) as well as the protonated molecule of the C_{46} GDGT internal standard (*m/z* 744), with a dwell time of 237 ms per ion.

3.3. Results and discussion

3.3.1 HPLC/MS analysis of the C_{46} GDGT

Analysis of the apolar and polar fraction of the Drammensfjord sample showed that the C_{46} GDGT eluted in the same fraction as the GDGTs, i.e. the polar fraction. The LC retention time of the C_{46} GDGT varied between 22.5 and 23.3 minutes, eluting immediately after crenarchaeol (~21 minutes). The mass spectrum of the C_{46} GDGT shows a predominant protonated molecule ($[M+H]^+$, Fig. 2a). There is a minor fragment due to loss of an OH group (-18 Da) but the most abundant fragment results from the loss of one of the C_{10} chains (-140 Da) and the subsequent loss of an OH group (-158 Da). The second most abundant fragment is the loss of a C_{10} alkyl chain and glycerol group (-232 Da) (Fig. 2a). In comparison, mass spectra of isoprenoid GDGTs are dominated by the $[M+H]^+$ protonated molecule and only show minor fragments due to losses of 18 and 74 Da, which correspond to the loss of an OH and a glycerol group, respectively [*Hopmans et al.* 2000; Fig 2b]. The difference in fragmentation pattern is due to the fact that the C_{46} GDGT is not a macrocyclic compound in contrast to the isoprenoid GDGTs.

3.3.2 Relative response factor

The response factor of both the C_{46} GDGT and crenarchaeol on the HPLC/MS was determined by SIM of both compounds at a range of concentrations (Fig. 3). The response factor of crenarchaeol is much higher than that of the C_{46} GDGT, i.e. 44.8 arbitrary units per ng injected GDGT versus 6.9 arbitrary units per ng injected GDGT. This is likely due to the enhanced fragmentation of the C_{46} GDGT compared to crenarchaeol, which results in a relatively lower abundance of the protonated molecule (Fig. 2). Depending on source conditions and calibration of the MS, differences may occur in the relative fragmentation pattern of the C_{46} GDGT over time. This would affect the response factor as the protonated molecule then represents a changing percentage of the total ion signal over time.

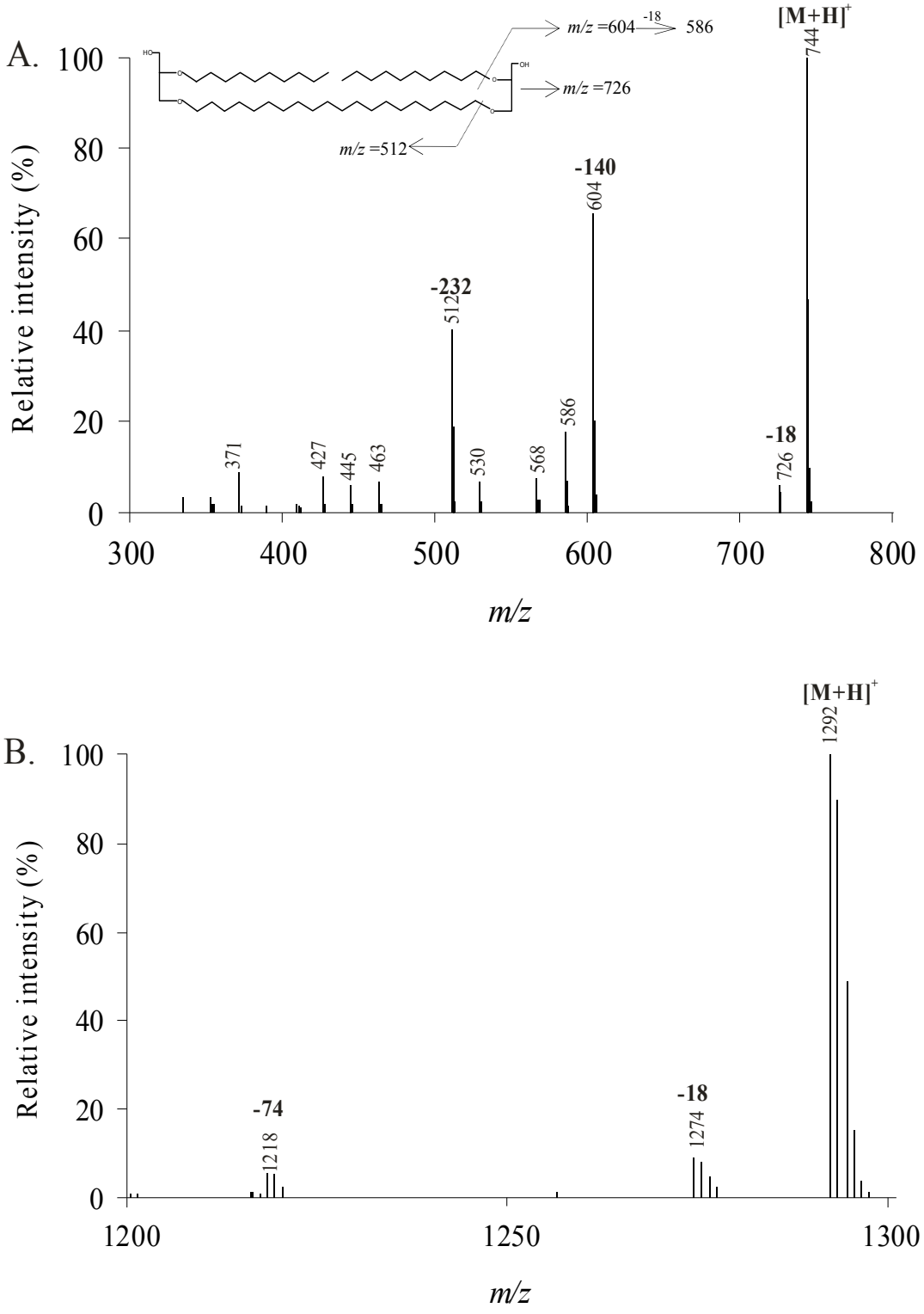

Figure 2. APCI mass spectrum of (A) C_{46} GDGT (*m/z* 744) and (B) crenarchaeol (*m/z* 1292). Mass spectra have been corrected for background.

To assess this, the difference in response factor between the C_{46} GDGT and crenarchaeol was measured over time. For this, a standard mixture of C_{46} GDGT and crenarchaeol (1:1 w:w) was analyzed once every week, over a four month period to determine the relative response factor (RRF). The RRF was calculated as follows:

$$\mathrm{RRF} = \frac{(\text{Area crenarchaeol})}{(\text{Area } C_{46})} \times \frac{(\text{Weight } C_{46})}{(\text{Weight crenarchaeol})} \qquad [1]$$

The RRF changed frequently, with values ranging between 2.9 and 4.8 (Fig. 4). During this study the HPLC/MS conditions regularly changed due to power cuts and re-calibration of the MS (black arrows, Fig. 4). The most marked changes in RRF occurred after the first power cut (Fig. 4a) when the ratio changed from 4.2 to 4.8 and after the MS re-calibrations when RRF values dropped from 4.7 to 3.8 and 3.8 to 2.9 respectively (Fig. 4b and d). Primary reasons for these large changes are changing conditions in the APCI source and loss of mass accuracy due to drifting of the mass axis. The first will change the relative degree of in-source fragmentation of the internal standard and the relative degree of ionization. The latter factor will induce changes in the RRF due to the large mass difference between the internal standard and the GDGTs. This shows that the RRF needs to be determined regularly and in particular after HPLC/MS conditions have changed.

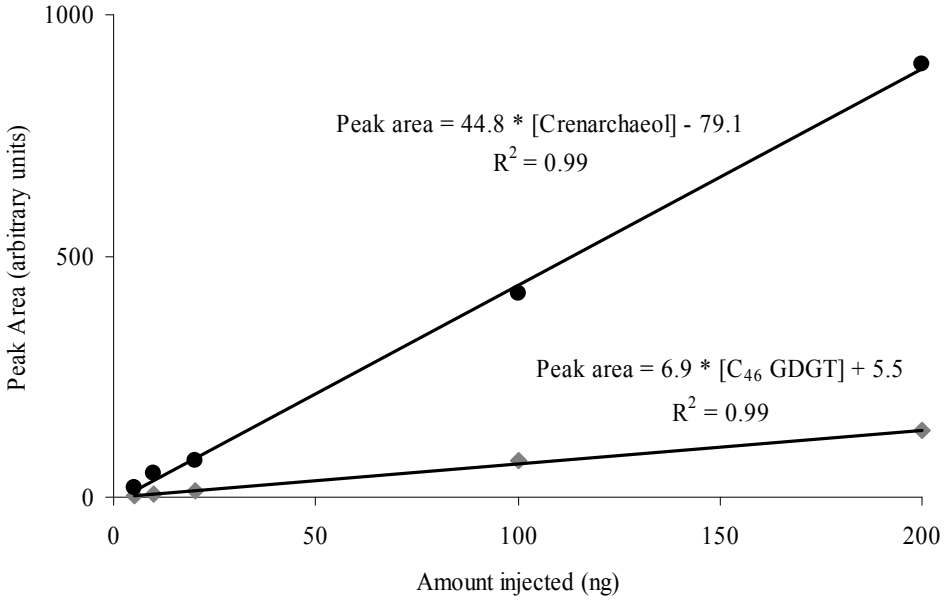

Figure 3. Standard curves of amount injected versus peak area for crenarchaeol and C_{46} GDGT.

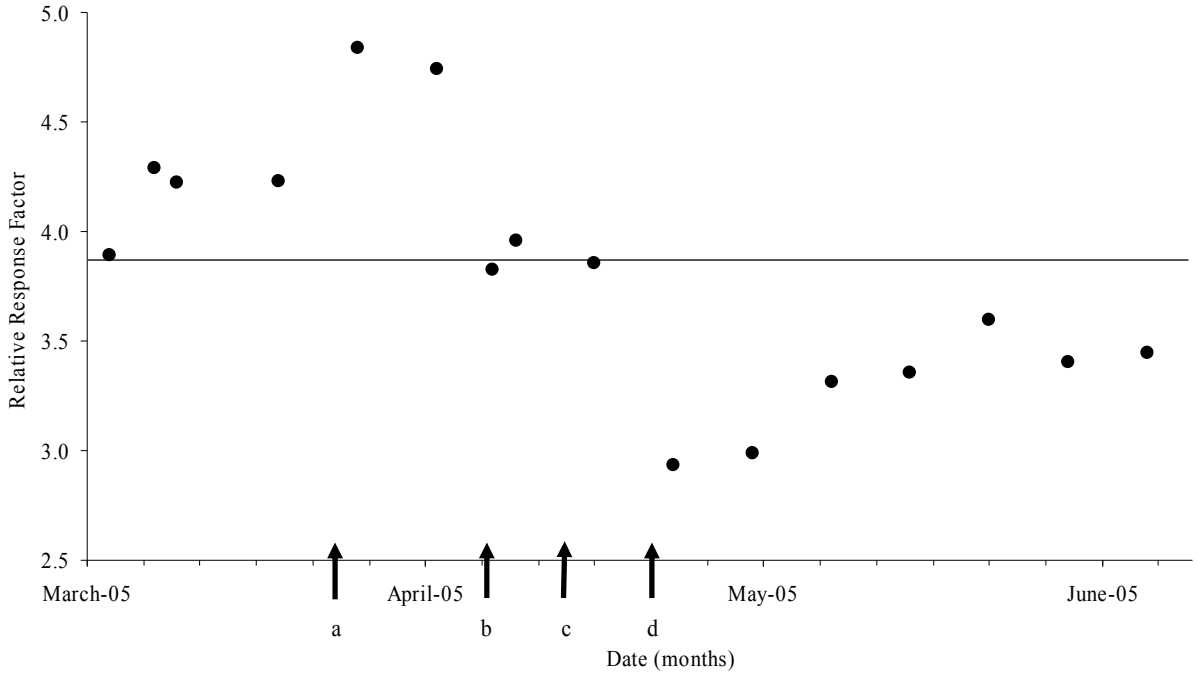

Figure 4. Variation of the relative response factor over time. The average value is indicated by the black line. Black arrows signal changes in the HPLC/MS conditions. (a) power cut, (b) re-tuning, (c) change of parts and air-conditioning restored, (d) MS re-tuning and a power cut.

3.3.3. Quantification of GDGTs using internal and external standards

Over the same period of time that the RRF stability was evaluated, we also measured GDGT abundances in a Drammensfjord sediment sample using both the internal and the external standard. These analyses were performed once every two weeks, directly after determining the RRF value. The external standard curves were determined on a monthly basis and after major alterations in the MS conditions (e.g. MS re-calibration). When calculating the absolute GDGT abundances obtained using either the internal or external standard, similar average GDGT concentrations are obtained for both methods (Fig. 5). However, the relative standard deviation is much higher when using the external standard curves (43%) than with the C_{46} GDGT internal standard (5%). This is likely because the internal standard undergoes the same work up as that of the sedimentary GDGTs. In addition, the internal standard is measured at the same time as the sample, thus reducing errors due to drifts in HPLC/MS conditions that can not be accurately measured with an external standard. Hence, for GDGT

absolute abundance measurements the use of an internal standard will lead to improved accuracy of quantification.

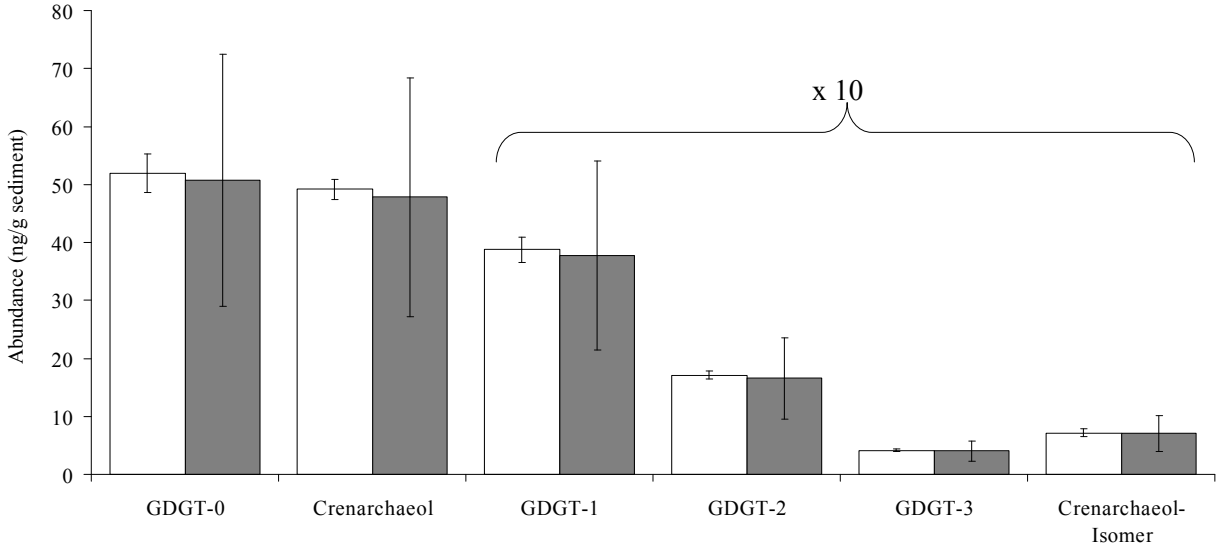

Figure 5. Abundance of GDGT molecules in Drammensfjord sediments, calculated with internal standard (open bars) and external standard (grey bars). Relative standard deviations are shown by the vertical bars. The abundance of GDGT-1, GDGT-2, GDGT-3 and the crenarchaeol isomer are multiplied by 10.

Acknowledgements

Two anonymous reviewers and Dr. Simon George are thanked for constructive comments. This project was supported by NWO-ALW (Project nr. 152911).

References

Hoefs, M. J. L., S. Schouten, J. W. deLeeuw, L. L. King, S. G. Wakeham, and J. S. Sinninghe Damsté (1997), Ether lipids of planktonic archaea in the marine water column, *Appl. Environ. Microbiol.*, *63*, 3090-3095.

Hopmans, E.C., S. Schouten, R.D. Pancost, M.T.J van der Meer, J.S. Sinninghe Damsté, (2000), Analysis of intact GDGT lipids in archaeal cell material and sediments by high performance liquid chromatography/atmospheric pressure chemical ionization mass spectrometry, *Rap. Comm. Mass Spectrom.* 14, 585-589.

Karner, M.B., E.F. DeLong, D.M. Karl, (2001), Archaeal dominance in the mesopelagic zone of the Pacific Ocean, *Nature* 409, 507-510.

Kuypers, M.M.M., P. Blokker, E.C. Hopmans, H. Kinkel, R.D Pancost, S. Schouten, J.S. Sinninghe Damsté,. (2002), Archaeal remains dominate marine organic matter from the early Albian oceanic anoxic event 1b, *Palaeogeography Palaeoclimatology Palaeoecology* 185, 211-234.

Massana, R., DeLong, E.F., Pedrós-Alió, C. (2000), A few cosmopolitan phylotypes dominate planktonic archaeal assemblages in widely different oceanic provinces, *Appl. Environ. Microb. 66*, 1777-1787.

Patwardhan, A.P., D.H. Thompson, (1999), Efficient synthesis of 40-and 48-membered tetraether macrocyclic bisphosphocholines, *Org. Letters* 1, 241-243.

Powers, L. A., J. P. Werne, T. C. Johnson, E. C. Hopmans, J. S. Sinninghe Damsté, and S. Schouten (2004), Crenarchaeotal membrane lipids in lake sediments: A new paleotemperature proxy for continental paleoclimate reconstruction?, *Geology*, *32*, 613-616

Sinninghe Damsté, J. S., S. Schouten, E. C. Hopmans, A. C. T. van Duin, and J. A. J. Geenevasen (2002a), Crenarchaeol: the characteristic core glycerol dibiphytanyl glycerol tetraether membrane lipid of cosmopolitan pelagic crenarchaeota, *J. Lipid Res.*, *43*, 1641-1651.

Sinninghe Damsté, J. S., W. I. C. Rijpstra, E. C. Hopmans, F. G. Prahl, S. G. Wakeham, and S. Schouten (2002b), Distribution of Membarne Lipids of Planktonic *Creanarchaeota* in the Arabian Sea., *Appl. Environ. Microbiol.*, *68*, 2997-3022

Smittenberg, R.H., M. Baas, M.J. Green, E.C. Hopmans, S. Schouten, J. S. Sinninghe Damsté, (2005), Pre- and post-industrial environmental changes as revealed by the biogeochemical sedimentary record of Drammensfjord, Norway, *Mar. Geol.* 214, 177-200.

Wakeham, S.G., C.M Lewis, E.C. Hopmans, S. Schouten, J.S. Sinninghe Damsté, (2003), Archaea mediate anaerobic oxidation of methane in deep euxinic waters of the Black Sea, *Geochim. Cosmochim. Acta* 67, 1359-1374.

Chapter 4

Marine crenarchaeotal membrane lipids in decapods: Implications for the TEX_{86} paleothermometer

Carme Huguet, Joan E. Cartes, Jaap S. Sinninghe Damsté and Stefan Schouten

Published in *Geochemistry Geophysics Geosystems,* **7**, doi:10.1029/2006GC001305 (2006)

Abstract

Pelagic Crenarchaeota produce glycerol dibiphytanyl glycerol tetraethers (GDGTs) as membrane lipids and the GDGT composition changes according to growth temperature. This forms the basis of the TEX_{86} palaeotemperature proxy. This ratio correlates with sea surface temperature (SST) despite the fact that Crenarchaeota are distributed through the water column. Therefore, there must be mechanisms that transport the surface signal to sediments such as repackaging in faecal pellets, marine snow, mass falls after phytoplankton blooms or daily migration. To study GDGT transport, we analyzed stomachs and intestines of Atlantic and Mediterranean decapods as they are one of the major megafaunal groups, are easy to sample and occur in both pelagic and benthic environments. GDGTs were found in most decapods' guts. GDGT abundances are significantly lower in intestines, but TEX_{86}-derived temperatures are not significantly different between stomachs and intestines (<1°C), suggesting that TEX_{86} values are not altered during gut transit. Atlantic decapods show no difference in TEX_{86} values between benthic detritivors and pelagic predators. However, Mediterranean decapods show a substantial difference between macroplankton feeders and bentho-pelagic predators. This is probably related to the freshness of the material consumed. TEX_{86}-derived temperatures in Atlantic decapods are close to the SST around the time of sampling in agreement with stomach content analysis that shows fresh organic matter being ingested. For Mediterranean decapods, TEX_{86} temperatures are significantly higher than SST around the time of sampling. This can be partly attributed to the large variability between decapod specimens and the low amounts of fresh material found in their stomachs.

4.1. Introduction

Sea surface temperature (SST) is one of the most important parameters associated with past climate. Since the 1950s, several temperature proxies have been developed, the most common being $\delta^{18}O$ and Mg/Ca ratios of planktic foraminifera [*Chave,* 1954; *Emiliani,* 1955; *Nurnberg et al.,* 1996] and the $U^{k'}_{37}$ index of long-chain unsaturated ketones synthesized by haptophyte algae [*Brassell et al.,* 1986]. A new SST proxy was recently introduced, the TetraEther indeX of lipids with 86 carbons (TEX_{86}) [*Schouten et al.,* 2002], which may be a useful complimentary palaeotemperature tool. The TEX_{86} proxy is based on temperature-related changes that occur in the composition of archaeal membrane lipids.

Archaea were once thought to be extremophilic bacteria, but genetic studies showed that archaea constitute a different domain of life [*Woese et al.,* 1990]. Furthermore, molecular ecological studies revealed that archaea are ubiquitous and abundant in non-extreme settings such as the marine environment [*Hoefs et al.,* 1997; *Massana et al.,* 2000; *Karner et al.,* 2001]. One archaeal sub-group, the Crenarchaeota, is genetically related to (hyper)thermophilic archaea and has adapted to the relatively cold marine waters [*Kuypers et al.,* 2001]. Archaeal membranes are composed of glycerol dibiphytanyl glycerol tetraethers (GDGTs) [*Sinninghe Damsté et al.,* 2002] and changes in the relative abundance of these lipids allow them to adjust their membrane fluidity as a response to fluctuations in water temperature. The relative abundance of GDGTs is quantified with the TEX_{86} ratio [*Schouten et al.,* 2002]. An empirical correlation between TEX_{86} values of sediment core tops from a wide variety of geographical locations and annual mean SST is used to calibrate the TEX_{86} proxy [*Schouten et al.,* 2002]. Experiments with Crenarchaeota enrichment cultures and particulate organic matter studies have shown that this new proxy is strongly correlated with temperature and is not dependent on salinity or nutrient concentration [*Wuchter et al.,* 2004; 2005]. There is, however, a gap in knowledge that needs to be addressed in order to understand the origin of the TEX_{86} signal. Although several studies have established that Crenarchaeota are distributed throughout the water column [*Murray et al.,* 1999; *Karner et al.,* 2001], TEX_{86} values of particulate organic matter, sediment traps and sediment core tops are better correlated with SST (depth <100 m) than with deeper water temperatures [*Schouten et al.,* 2002; *Wuchter et al.,* 2005; 2006]. Thus, the signal in the deeper water layers and surface sediments seems to be primarily derived from the upper 100 meters of the ocean.

Crenarchaeotal cells are too small (< 1 μm; [*Margot et al*., 2002]) to sink to the sediment after cell death and this would prevent the TEX_{86} signal from reaching the sediment surface. Thus, there have to be mechanisms that allow GDGTs to reach the sediment. Transport of organic matter to the sea floor can be a passive or an active process, though the latter pathway is usually considered to be insignificant. The active pathway requires the vertical migration of surface organisms such as macroplankton, euphausiids or decapods which are located close to the bottom during daylight periods, where they are consumed by benthopelagic and benthic species [e.g. *Cartes*, 1993; *Cartes and Abelló*, 1992]. The passive pathways include the main transport mechanisms such as marine snow, faecal pellets and massive falls of phytoplankton material after surface blooms which are believed to agglomerate water-surface particles and enable them to sink quickly to the bottom of the ocean where they fuel benthic food webs. The formation of particle aggregates is higher in surface waters, where most food webs are active, which could explain why GDGTs produced in the surface of the ocean, carrying a SST TEX_{86} signal, reach the sea floor. Further understanding of the transport mechanisms and deposition of the crenarchaeotal GDGTs is, thus, required to apply this new proxy. Once the GDGTs reach the sediment floor, benthic activity is also likely to have an effect with unknown consequences for the TEX_{86} signal.

To address these issues we investigated the presence of GDGTs in decapod guts. Decapods are a key element of most pelagic food webs. Decapod crustaceans are widely diversified in bathyal marine environments from mid and subtropical latitudes and constitute the most abundant megafaunal group in deep water environments such as the deep Mediterranean Sea [*Cartes and Abelló,* 1992; *Maynou and Cartes,* 2000]. Although they are not the main consumers of plankton in the upper 100 m or the main faecal pellet producers, they are involved at different levels of the food web and can serve as a model system for other organisms such as copepods and microzooplankton. In contrast to copepods they are more easily collected and larger amounts of biomass can be obtained. Pelagic decapods could actively or passively consume lipids and participate in the transport of GDGTs from the surface ocean to the sediment, whilst benthic species potentially could alter the TEX_{86} signal deposited in the sediment. The aim of this study was to assess if Crenarchaeota, and thus their GDGTs, are taken up by decapods and if the TEX_{86} temperature signal may be partly transported or altered through decapod feeding activity. We selected species with different

feeding habits, i.e. trophic resources both associated with bottom sediments (benthos) and/or to the water column (suprabenthos, zooplankton), and from two distinct settings, the oligotrophic Mediterranean Sea and the productive North Atlantic coast in two different seasons. Potential bias of the TEX_{86} ratio due to preferential degradation or differential retention time during passage through the gut system and possible differences caused by diverse decapod feeding strategies were also investigated.

4.2. Material and methods

4.2.1 Study area

Samples were collected from two different areas, (i) the Mediterranean, around the Balearic island (cruise IDEA, 39°N, 2°39'E) at two sites situated northwest and southwest of Mallorca Island in February 2004 and (ii) the North Atlantic coast of Spain (off Gijon) taken 20 km off the north coast of the Iberian Peninsula in April 2004 (ECOMARG03, 44°N, 4°29'W) (Fig. 1). The two sites in the Mediterranean are rarely affected by wind mixing and a strong summer thermocline is often present. Monthly averaged SSTs varied between 28.4°C in August 2003 and 14.3°C in February 2004 around time of sampling (Table 2). The Mediterranean Sea is characterized by an almost constant water temperature of 13°C below 200 m, high salinity (37-39) and very low nutrient concentrations [*Comas et al.,* 1996]. The North Atlantic coast study area, known as Le Danois bank, is a marine mount-shape relief orientated E-W parallel to the northern coast of the Iberian Peninsula coast. SST in this area varied between 24°C in August 2003 and 11.9°C in February 2004 (Table 2), but in contrast to the Mediterranean, temperatures below 200 m in the water column decrease with increasing depth. Conductivity Temperature Depth (CTD) profile data collected in April 2004 during the ECOMARG03 indicated temperatures ~10°C below 30 m depth. The Atlantic has lower salinity values (35.7-35.8) and higher nutrient concentrations than the Mediterranean.

4.2.2. Samples

We selected five decapod species with different feeding strategies and habitats. Two species, *Aristeus antennatus* (Risso, 1816) and *Plesionika martia* (A. Milne-Edwards 1883) were collected at the Mediterranean sites in February 2004. The other three species, *Acanthephyra pelagica* (Risso, 1816), *Munida tenuimana* (Sars, 1872) and *Parapagurus*

pilosimanus (Smith, 1879) were recovered in the North Atlantic (off Gijon) in April 2004 (Fig. 1).

Species	*n*	Time	Location	Sampling depth (m)	Depth interval (m)	Habitat	Diet
Plesionika martia	9	07/02/2004	Mediterranean (39°N, 2°39'E)	675	576-749	Necktobenthic	Macroplankton
Aristeus antennatus	11	07/02/2004	Mediterranean (39°55'N, 2°36'E)	775	576-775	Necktobenthic	Epibenthos-benthos and pelagic prey
Munida tenuimana	12	20/04/2004	Atlantic (44°N, 4°29'W)	1024	540-1024	Benthic	Scavenging-detritivor and pelagic prey Phytoplankton detritus
Parapagurus pilosimanus	11	20/04/2004	Atlantic (44°N, 4°29'W)	1024	820-1024	Benthic	Benthic prey-scavenger Phytoplankton detritus
Acanthephyra pelagica	11	20/04/2004	Atlantic (44°N, 4°29'W)	1024	550-1024	Bathypelagic	Macroplankton predator Megabenthic remains

Table 1. Characteristics of the five species used in the study, including time of sampling, location of fishing habitat, depth of samples, depth interval inhabited by species during the IDEA and ECOMARG surveys and a summary of their main prey (diets). n= number of specimens analyzed.

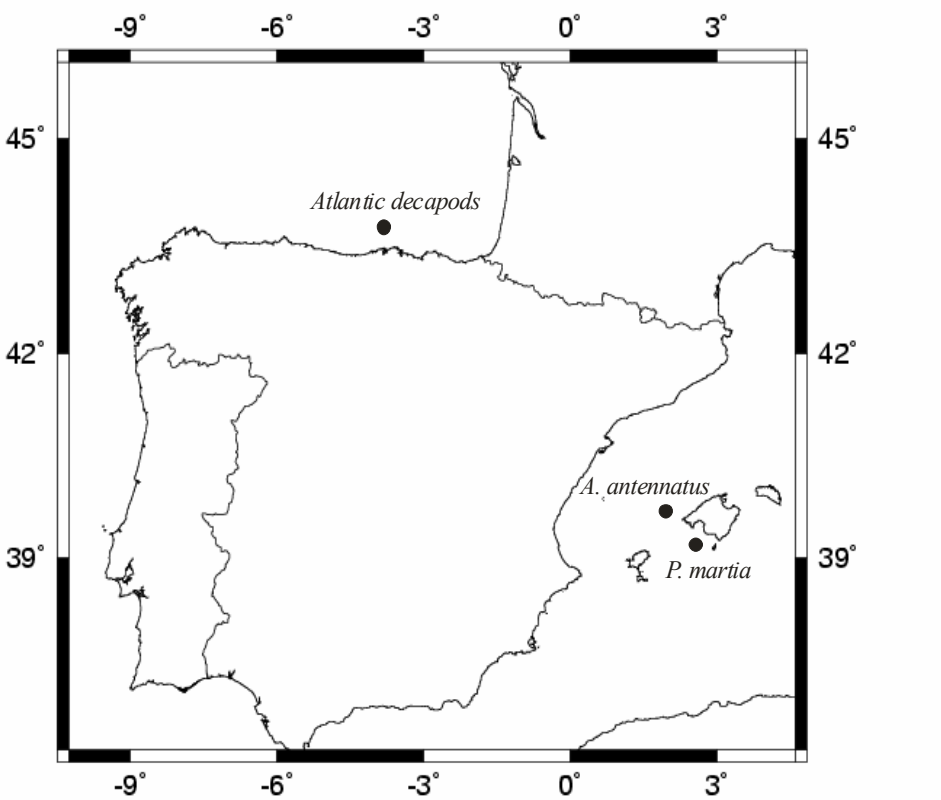

Figure. 1. Map of study area showing sample locations (circles)

Around the Balearic Islands, 11 specimens of *A. antennatus* and 9 specimens of *P. martia* were obtained at 775 and 675 m depth, respectively (Table 1; Fig. 1). Eleven specimens of the bathypelagic shrimp *A. pelagica*, 12 of the squat lobster *M. tenuimana* and 11 of the hermit crab *P. pilosimanus* were collected in the north Atlantic at 1024 m depth (Table 1; Fig. 1). A total of 54 specimens were analyzed and their stomachs and intestines were removed under a stereomicroscope (x10, x40). Once stomachs and intestines were dissected, contents were collected with a spatula or, if they were liquid, pipetted into a tube, and subsequently freeze dried. Livers and gonads of 10 specimens from the Mediterranean were also dissected and portions were freeze dried and analyzed.

4.2.3 GDGT analysis

Freeze-dried stomach and intestine contents, and liver and gonad samples were weighed and extracted by sonication first with methanol, then a mixture (1:1; v/v) of methanol (MeOH) and dichloromethane (DCM) and lastly with pure DCM. After sonication, samples were centrifuged at 3500 rpm to remove particles. The supernatants were collected and after evaporating the solvents, the extracts were dried with a small pipette filled with anhydrous sodium sulphate. For the liver and gonad samples the total lipid extract was divided into apolar and polar fractions using a small column filled with activated alumina and using hexane/DCM (9:1; v/v) and DCM/MeOH (1:1; v/v) as eluents, respectively.

The total extracts (stomachs and intestines) and polar fractions (livers and gonads) were redissolved in hexane/propanol (99:1; v/v) and filtered through 0.45 μm PTFE filters. An HP (Palo Alto, CA, USA) 1100 series LC-MS equipped with an auto-injector and Chemstation chromatography manager software was used to analyse the samples. Separation was attained on a Prevail Cyano column (2.1 x 150 mm, 3 μm; Alltech, Deerfield, Illinois, USA), maintained at 30°C. The GDGTs were eluted using a changing mixture of hexane and propanol. Detection was achieved using atmospheric pressure chemical ionization-mass spectrometry of the eluent [*Hopmans et al.,* 2000]. Single Ion Monitoring (SIM) was used instead of full mass scanning because SIM increases the signal to noise ratio and thus improves reproducibility. SIM was set to scan 5 $[M^+]$ + H ions of the GDGTs with a dwell time of 237 ms for each ion. Concentrations of GDGTs were used to calculate TEX_{86} values using equation [1] [*Schouten et al.* 2002]:

$$TEX_{86} = \frac{(GDGT_2 + GDGT_3 + Crenarchaeol - isomer)}{(GDGT_1 + GDGT_2 + GDGT_3 + Crenarchaeol - isomer)} \quad [1]$$

The numbers refer to the number of cyclopentane moieties in the GDGT molecule; the crenarchaeol-isomer has 4 cyclopentane moieties and a cyclohexane moiety. TEX_{86} temperatures were calculated with the following core top calibration [*Schouten et al.,* 2002]:

$$TEX_{86} = 0.015 \cdot T + 0.28, \text{ with T= temperature (°C)} \quad [2]$$

Absolute GDGT abundances were determined by comparison with an external standard curve obtained with a range between 10 and 200 ng of $GDGT_0$ (GDGT with no cyclopentane moieties).

Month	**Mediterranean**	**SST(°C)**		**Atlantic SST(°C)**
March		14.8		
April		15.2		
May		18.7		15.2
June		23.0		19.2
July		26.5		21.3
August		28.4		24.0
September		26.2		21.6
October		23.2		19.0
November		19.0		15.3
December		16.0		14.0
January		14.7		12.6
February		**14.3**		12.4
March				11.9
April				**12.8**
Annual mean		20.0		16.6
TEX_{86}	*A. antennatus*	17.2 ± 2.2	*A. pelagica*	14.7 ± 2.0
	P. martia	21.9 ± 2.0	*M. tenuimana*	13.9 ± 0.7
			P. pilosimanus	14.5 ± 1.0

Table 2. Mean monthly sea surface temperature data from August 2003 to July 2004, corresponding to sampling sites in the Mediterranean (39°N, 2°E) and Atlantic (44°N, 4°W) from the Advanced Very High Resolution Radiometer (AVHRR) data set at http://podaac.jpl.nasa.gov. Annual mean SST and average stomach and intestine TEX_{86} temperatures for each decapod species are indicated. SST values at the time of sampling for Mediterranean decapods (February) and Atlantic decapods (April) are highlighted in bold.

4.3. Results

4.3.1. GDGTs in decapods

GDGTs were present in most decapod stomachs and intestines from both Atlantic and Mediterranean species (Tables 3 and 4).

Species	Stomach n	Stomach TEX_{86} T (ºC)	Stomach GDGT (µg. g^{-1}gut content)	Intestine n	Intestine TEX_{86} T (ºC)	Intestine GDGT (µg. g^{-1}gut content)
Acanthephyra pelagica	*3*	13.7 ±1.4	10		*nd*	*nd*
	3	14.6 ± 0.7	88	*3*	14.7 ± 0.6	90
	3	15.5 ± 0.9	22	*3*	17.3 ± 1.2	15
	1	12.8	3	*2*	13.9 ± 2.5	5
	2	15.5 ± 0.5	14	*3*	18.8 ± 3.1	4
	3	16.1 ± 0.9	17		*nd*	*nd*
	3	15.3 ± 1.0	13	*3*	16.2 ± 1.5	11
	3	17.3 ± 2.5	20	*3*	15.3 ± 2.0	40
	3	12.9 ± 0.8	6	*3*	15.0 ± 1.2	10
	3	13.6 ± 0.3	95		*nd*	*nd*
	3	12.8 ± 0.6	34	*2*	10.6 ± 0.2	2
	Mean	**14.3**	**29**		**15.2**	**22**
	Error	**1.6**	**32**		**2.5**	**30**
Munida tenuimana	*3*	13.1 ± 0.9	17	*3*	14.3 ± 0.9	16
	3	14.8 ± 1.6	10	*3*	13.2 ± 0.8	20
	3	14.1 ± 0.6	32	*3*	14.6 ± 0.5	29
	3	15.2 ± 0.3	32	*3*	14.2 ± 1.0	30
	2	13.5 ± 0.2	16	*3*	13.6 ± 1.5	20
	3	13.5 ± 0.3	33	*3*	13.2 ± 0.1	30
	3	13.8 ± 0.9	32	*2*	12.7 ± 0.2	25
	2	13.9 ± 0.5	78	*3*	13.7 ± 0.5	16
	3	14.5 ± 0.7	56	*3*	13.7 ± 1.4	24
	2	15.5 ± 0.4	49		*nd*	*nd*
	Mean	**14.2**	**35**		**15.2**	**23**
	Error	**0.8**	**21**		**2.5**	**6**
Parapagurus pilosimanus	*3*	14.7 ± 0.3	37	*1*	16.0	17
	3	15.2 ± 0.7	17	*3*	15.1 ± 1.0	7
	3	12.9 ± 1.0	66	*3*	13.7 ± 1.7	13
	3	15.7 ± 1.4	5	*3*	14.0 ± 0.8	10
	3	15.9 ± 0.6	11	*2*	14.5 ± 0	10
	3	15.0 ± 0.7	49	*2*	12.8 ± 0.1	8
	3	13.3 ± 08	74	*3*	14.5 ± 0.7	14
	3	14.5 ± 0.6	5		*nd*	*nd*
	2	16.1 ± 0.1	16	*2*	13.2 ± 0.7	14
	3	13.7 ± 0.4	49	*3*	14.4 ± 0.2	17
	Mean	**14.7**	**33**		**14.2**	**12**
	Error	**1.1**	**26**		**1.0**	**4**

Table 3. TEX_{86} calculated temperatures and GDGT concentrations for stomachs and intestines in Atlantic decapods. The number of measurements (n) is indicated. The standard deviations of the species-averaged temperatures and concentrations are also shown. Samples with GDGT concentrations below detection limit are labelled as *nd.*

In contrast, analysis of both gonads and livers of decapods did not reveal the presence of GDGTs. The lowest average GDGT concentration (12 ± 3.7 $\mu g \cdot g^{-1}$gut content) was found in *P. pilosimanus* intestines (Table 3; Fig. 2). The stomachs of *A. antennatus* contained the most GDGTs with on average 906 ± 428 $\mu g \cdot g^{-1}$gut (Table 4; Fig. 2). Although average abundances of GDGTs were always higher in stomachs than in intestines (Fig. 2), there were large variations between individual specimens (Table 3 and 4). This resulted in substantial standard deviations for the average GDGT concentrations (Tables 3 and 4).

		Stomach			Intestine	
Species	**n**	**TEX_{86} T (ºC)**	**GDGT ($\mu g. g^{-1}$gut content)**	**n**	**TEX_{86} T (ºC)**	**GDGT ($\mu g. g^{-1}$gut content)**
Aristeus antenatus	*2*	18.3 ± 1.4	1417	*1*	20.7	498
	2	13.2 ± 0.3	540	*1*	14.3	43
	2	18.1 ± 1.0	1416	*2*	18.4 ± 1.0	317
	2	15.5 ± 0.4	603	*2*	17.4 ± 0.2	424
		nd	*nd*	*1*	16.1	75
	2	20.6 ± 0.2	1316	*2*	19.8 ± 1.6	772
		nd	*nd*	*1*	13.4	71
	1	16.8	540	*1*	17.9	270
	2	14.5 ± 0.2	1247	*2*	14.5 ± 1.0	671
	1	18.7	423	*1*	17.4	215
	1	19.2	650	*1*	19.0	1217
	Mean	**17.2**	**906**		**17.2**	**416**
	Error	**2.4**	**428**		**2.4**	**359**
Plesionika martia	*2*	23.5 ± 0.5	1222		*nd*	*nd*
	1	21.9	442		*nd*	*nd*
	2	21.8 ± 0.2	996	*1*	17.8	29
	1	23.2	33	*1*	15.9	1
	2	24.3 ± 0.4	191	*1*	25.7	16
	1	19.5	80		*nd*	*nd*
	1	23.7	10		*nd*	*nd*
	1	21.3	5		*nd*	*nd*
	2	22.7 ± 2	7		*nd*	*nd*
	Mean	**22.4**	**332**		**19.8**	**16**
	Error	**1.5**	**465**		**5.2**	**9**

Table 4. TEX_{86} calculated temperatures and GDGT concentrations for stomachs and intestines in Mediterranean decapods. The number of measurements (n) is indicated. The standard deviations of the measurements are also shown. Samples with GDGT concentrations below detection limit are labelled as *nd.*

However a t-test revealed that intestine concentrations are overall lower than stomach values with a 99.9 % confidence level. *P. martia* showed the largest difference, with an average of 332 ± 465 $\mu g \cdot g^{-1}$gut content in stomachs, but only 16 ± 9 $\mu g \cdot g^{-1}$gut content in intestines (Fig. 2). This difference may be explained because only intestines of three specimens could be analyzed (Table 4) and this may not be representative of the total population. Species in the Mediterranean revealed average GDGT concentrations in stomachs and intestines that were up to 20 times higher than those observed in Atlantic decapods (Table 4; Fig. 2).

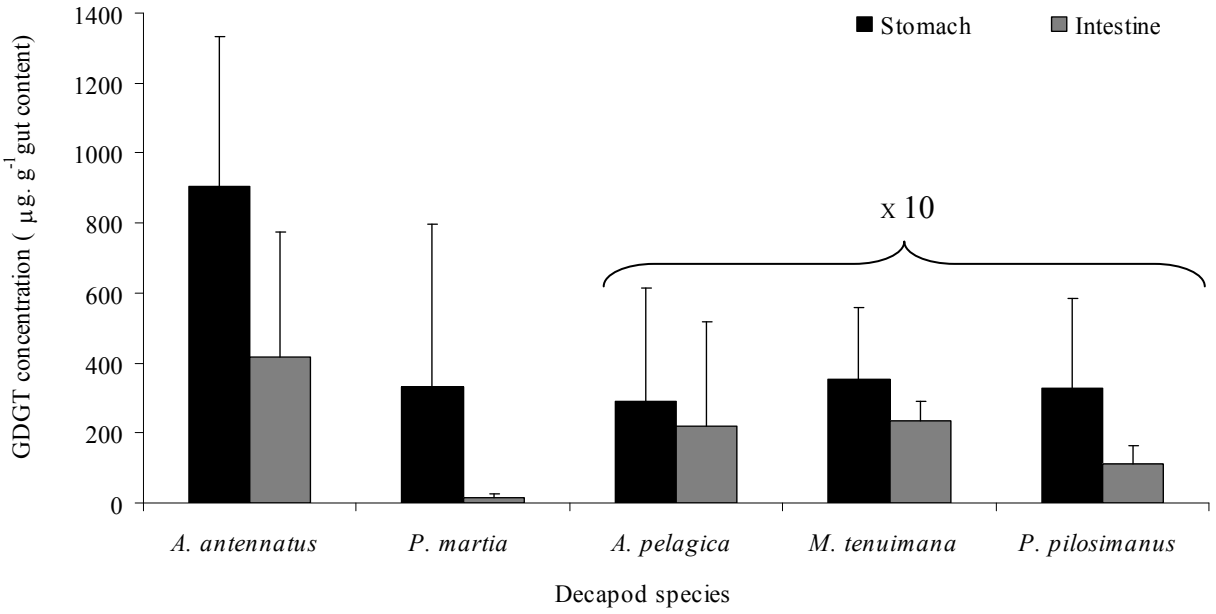

Figure. 2. Average abundance of GDGTs in stomachs (black) and intestines (grey). The abundances in the Atlantic species have been magnified by a factor of 10 to enable a better comparison.

4.3.2. TEX_{86} values

TEX_{86} values for the whole data set ranged from 0.50 to 0.63 and when converted to temperature with equation [2], these values correspond to 14.2 and 22.3°C respectively. Most decapods from the Atlantic coast were measured in triplicate (Table 3), with standard deviations ranging from 0.1 to 2.5°C for TEX_{86}-derived temperatures. Sample amounts from

Mediterranean decapods were smaller, and thus could only be measured at best in duplicate and the standard deviations ranged from 0.2 to 1.6°C (Table 4). For species-averaged TEX_{86}-derived temperature standard deviations ranged from 0.8°C for *M. tenuimana* stomachs to 5.2°C for *P. martia* intestines (Table 3 and 4; Fig. 3).

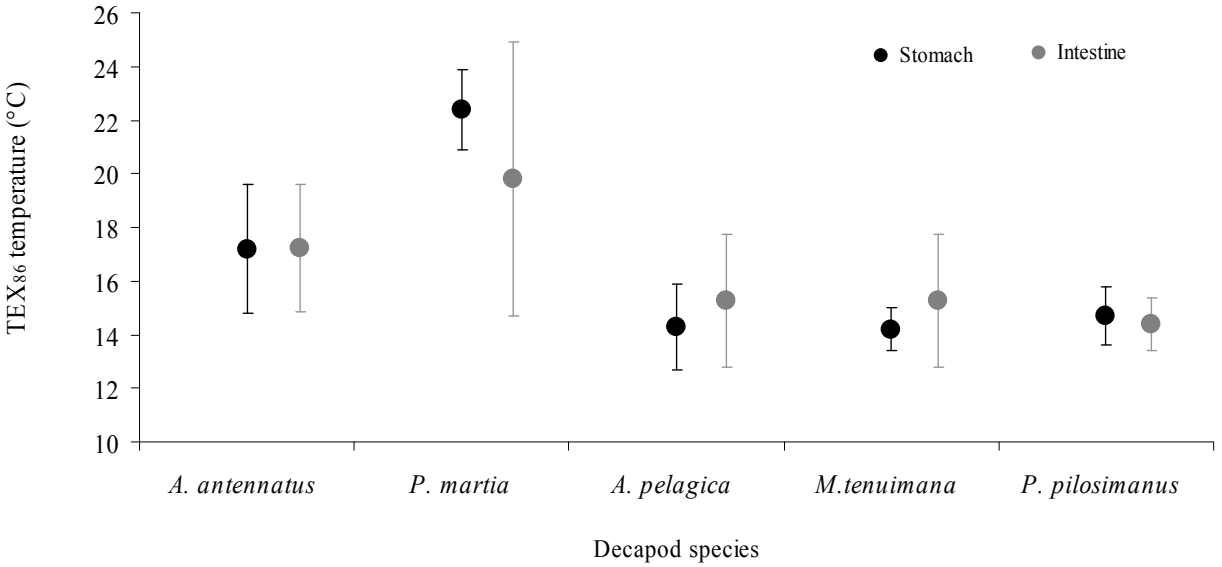

Figure 3. TEX_{86} temperatures calculated from GDGTs present in stomachs (black) and intestines (grey).

TEX_{86}-derived temperatures in Atlantic decapods are all very similar between specimens for all species, suggesting a relatively homogenous distribution over the total population (Table 3). The Atlantic decapods showed identical values for stomach TEX_{86} temperatures of 14.3 ± 1.6°C (*A. pelagica*), 14.2 ± 0.8°C (*M. tenuimana*) and 14.7 ± 1.1°C (*P. pilosimanus*) (Table 3; Fig. 3). TEX_{86}-derived temperatures for the intestine samples were also very similar ranging from 15.2 to 14.3°C (Table 3; Fig. 3). Thus, temperature values calculated with TEX_{86} for stomachs and intestines are not significantly different in Atlantic species (Fig. 3).

TEX_{86}-derived temperatures calculated for Mediterranean decapods showed larger variability between specimens than Atlantic decapods, especially for *A. antennatus* (Table 4). Also, in contrast with Atlantic decapods, there was a significant difference between the two

Mediterranean species, i.e. stomachs of *A. antennatus* have TEX_{86} temperatures of 17.2 ± 2.4°C, whilst stomachs of *P. martia* have TEX_{86} temperatures of 22.4 ± 1.5°C (Table 4 and Fig. 3). However, both stomach and intestines of *A. antennatus* have similar TEX_{86} temperature values of 17.2 ± 2.4°C. For *P. martia* this difference with TEX_{86} temperatures is larger, i.e. 22.4 ± 1.5°C for stomachs and 19.8 ± 5.2°C for intestines. This difference is not significant considering the large standard deviation (Table 4, Fig. 3).

4.4. Discussion

4.4.1. GDGTs in decapod guts

Most stomachs and intestines analyzed in this study contain GDGTs, suggesting that Crenarchaeota may be consumed by decapods. Molecular ecological studies have previously shown the presence of marine archaea in guts of fish [*Van der Maarel et al.,* 1998] and holothurians [*McInerney et al.,* 1995], but in both cases it was not determined whether the marine archaea found in the gut were symbiotic members or had been ingested. Decapod guts are very basic structures compared to those of fish and holothurians, thus in our case the existence of gut symbionts seems unlikely. Moreover, the TEX_{86}-calculated temperatures and stomach content analysis (see below) indicate a surface origin of the GDGT signal while the decapod species were all collected below 500 m (Table 1). Lastly, some specimens did not contain GDGTs, which would contradict the idea of a symbiotic relationship. Thus, it seems likely that GDGTs are taken up in the food web and incorporated in decapod faecal pellets. Even though there is evidence of GDGT consumption by decapods, we can not discern if this is an active or a passive process. But, the scale of the mouth sorting structure of the decapod group does not allow selecting for particles of the size such as those of archaea (<1 μm; [*Margot et al.,* 2002]). Therefore, they must be accidentally ingested during feeding, either dissolved in the water, associated with food particles or already present in guts of prey organisms. Stomach content studies of decapod species showed that detritus, i.e. amorphous organic material, never represented more than 20% of the diet in weight, even in detritivors such as *Parapagurus pilosimanus* (Cartes et al., unpublished results). This further indicates that an active selection of archaea as a food source by decapods is unlikely.

As the study included species with different feeding strategies (Table 1), some of the mechanisms suggested for surface water material transport to the sediments can be assessed. The passive pathway (marine snow, faecal pellets and phytoplankton massive falls) is confirmed by the presence of GDGTs in the guts of benthos feeders or scavengers-detritus feeders such as *A. antennatus*, *M. tenuimana* and *P. pagurus*. The active transport, by organism migration, is suggested by the other two decapod species feeding on migratory macroplankton (Table 1). The presence of GDGTs in decapod guts also suggests that surface organisms such as migrating macroplankton are ingesting GDGTs themselves. Thus, heterotrophic organisms such as the very abundant copepods, which are closely related to the decapods, are likely to play an important role in producing faecal pellets in surface waters that will carry GDGTs to the sediment. In addition, our results show that once the GDGTs are deposited in the sediment benthic reworking of these compounds continues.

4.4.2. TEX_{86} signal preservation

The stomachs and intestines analyzed correspond to separate feeding episodes. However, most bathyal decapods feed continuously through the daily cycle without feeding peaks [*Maynou and Cartes,* 1998]. Thus, the stomach and intestine contents can be considered as a snapshot of the general digestion process, and no major changes in abundance or food source are expected between the two. With only a few exceptions, GDGT abundances in the intestines are consistently lower than in the stomachs in all specimens studied (Tables 3 and 4; Fig. 2) and this difference is statistically significant. The lower intestine abundances and absence of GDGTs in gonad and liver tissues suggest a partial degradation of GDGTs during stomach transit. Alternatively, the residence time for stomach contents might be higher than for intestines. However, this is unlikely as the feeding is a continuous process. Lower intestine than stomach contents can also be explained by a change of food source. However, this is unlikely as very few specimens show a higher intestine than stomach abundance (Table 3 and 4) and benthic species such as *P. pilosimanus* or *M .tenuimana*, that usually cover a small area, also show lower intestine abundances. Thus it seems that a partial degradation is the most likely explanation for the lower intestine abundance of GDGTs. This could be problematic for the TEX_{86} proxy if some of the GDGT isomers were degraded at different rates than others as this would alter the TEX_{86} ratio. However, there is no significant

difference between species averaged TEX_{86} temperatures in stomachs and intestines (Fig. 3). Thus, it seems that all the GDGT molecules are equally affected by degradation. Therefore, the TEX_{86} signal which is taken up by decapods is likely unaffected by passage through the gut and re-packaged in faecal pellets. This suggests that faecal pellets from pelagic species will help transport sea surface temperature signal to the bottom, but also that benthic decapods will not alter sedimentary signal settling or already deposited in the sediment.

4.4.3. Comparison of TEX_{86} with in situ temperatures

4.4.3.1. Atlantic decapods

TEX_{86}-derived temperatures are similar in all the Atlantic decapods. TEX_{86} temperatures are significantly higher than the 10°C deep-water (<30 m) signal recorded by the CTD, so we can assume a surface origin of the GDGT signal. At the time of sampling SST in the study area was 12.8°C, whilst the average TEX_{86} value for the three species is 14.4 ± 1.3°C. Thus, temperatures obtained from decapod guts compare quite well with local SST, being only 1.6ºC higher (Table 2). This relatively small difference may be due to several factors including uncertainties in the calibration of the TEX_{86} with temperature. Indeed, sediment trap studies in the Arabian Sea showed that TEX_{86} values may overestimate surface water temperatures by 1-3°C [*Wuchter et al.* 2006]. Alternatively, the decapods may have ingested GDGTs accumulated over an annual cycle (see below), thereby increasing TEX_{86} values as annual mean SST (16.6°C) is higher than the SST around time of sampling (12.8ºC).

The three Atlantic decapod species studied are known to have different feeding strategies (Table 1), i.e. *M. tenuimana* and *P. pilosimanus* are mainly benthic scavengers while *A pelagica* is a macroplankton predator. However, we could not find any correlation between feeding mode and TEX_{86} temperatures. This is likely because all the Atlantic decapods fed on food from the same origin (i.e. the upper water column) as they were sampled right after a peak in primary production. Even though *A. pelagica* and *M. tenuimana* usually feed on macroplanktonic organisms, with important scavenging activity particularly in the last species (Table 1), this does not seem to be the case in our study. No information is available on the diet of *P. pilosimanus*, but pagurids are often considered as benthic-detritus feeders and scavengers [*Lagardère*, 1977]. However, in our study it seems that the Atlantic decapods' signal is derived from surface waters and is either ingested though macroplankton

predation (*A. pelagica*) or transported down by a flux of phytoplankton detritus and ingested in the benthos (*M. tenuimana* and *P. pilosimanus*). In fact, stable carbon and nitrogen isotope studies showed that marine snow can be the main food source for deep water decapods inhabiting the deep slope around the Balearic Island [*Polunin et al.* 2002]. Indeed, stomach content analysis of *M. tenuimana* and *P. pilosimanus* showed high contents of pigments derived from phytoplankton, suggesting that in this particular case these species fed on fresh phytoplanktonic detritus (Cartes et al., unpublished results). Thus, the transport mechanism of the GDGTs carrying the TEX_{86} signal may be linked to the flux of phytoplankton material after the spring bloom in the sampling area. This confirms one of the passive pathways proposed for quick transport of GDGTs from surface waters to the sediment, and it might be especially important in certain areas such as upwelling regions after periods of high primary production in the photic zone.

4.4.3.2. Mediterranean decapods

TEX_{86} temperatures calculated for stomachs of the Mediterranean decapods studied are significantly different. *A. antennatus* indicates a temperature of ca. 17°C while *P. martia* shows significantly higher values at ca. 22°C. This difference may be partly explained by the slightly different locations where the decapod species were sampled (Fig. 1). This could explain warmer temperatures for *P. martia* as the specimens were obtained in a sheltered coastal area. However, this cannot be the only factor, as this would result in a relatively small temperature difference.

Since Mediterranean temperatures are consistently <13°C below 200 m [*Comas et al.,* 1996] and TEX_{86} values are considerably higher, they must correspond to SST. However, average TEX_{86} temperatures from Mediterranean decapods are also significantly higher than SST around the time of sampling (14.3°C; Table 2). The two Mediterranean species consume different prey (Table 1) and may therefore be showing a signal obtained from distinctive food sources. *A. antennatus* is basically a benthic feeder while *P. martia* has been reported as an active predator of macrozooplankton [*Cartes,* 1993; *Fanelli and Cartes,* 2004]. Thus, the feeding strategy may have affected the TEX_{86} signal in Mediterranean decapods. As SST changes more than 14ºC during the annual cycle (Table 2), the freshness of the organic matter consumed is important. We would expect a pelagic feeder like *P. martia* to ingest GDGTs

present in the guts of surface water macroplankton organisms that migrate down the water column daily, and thus, TEX_{86} signal should be tied to recent SST. Benthic feeders, such as *A. antennatus*, could be ingesting secondary material such as an already packaged GDGT signal from marine snow and faecal pellets from the same or surrounding areas; this would probably result in a dilution of the fresh TEX_{86} signal. Indeed, this could explain why the TEX_{86} derived temperature in *A. antennatus* is an intermediate value between annual mean SST (20.0°C) and SST at the time of sampling. Notably, there is large variability in TEX_{86} temperatures for individual specimens of *A. antennatus* with some values close to the SST around time of sampling and others close to annual mean SST. However, feeding strategy can not explain the large offset between TEX_{86} inferred SST for *P. martia* and SST at the time of sampling as this organism is supposed to feed on migratory macrozooplankton and the variability between specimens is relatively small. For reasons presently unclear, the TEX_{86}-derived temperatures for *P. martia* are closer to annual mean SST, suggesting a diet of older material. In this respect it is interesting to note that, in contrast to Atlantic decapods, stomach contents of both Mediterranean decapod species contained only low abundances of pigments (Cartes et al., unpublished results), suggesting that both decapods did not have fresh phytoplankton material in their diet. This may explain the offset between TEX_{86} temperatures in Mediterranean decapods and that of SST around time of sampling.

4.5. Conclusion

Crenarchaeota lipids have been found both in stomachs and intestines of decapods and are most likely accidentally ingested with water, organic particles or with prey organisms. Despite this uncertainty, we were able to demonstrate both passive and active transport mechanism that can explain, at least in part, the transport of GDGTs from surface waters to the sediment. Even though the GDGTs concentration decreases from stomachs to intestines we did not find evidence of incorporation of GDGTs in liver or gonad tissues of decapods. Most importantly, TEX_{86} values do not show significant differences between stomach and intestines, and thus GDGT composition is not modified during the passage through the guts before it is transported to the sediment in faecal pellets. This holds true for both GDGTs collected from the water column or reworked in benthic settings. Furthermore, we observed that the fresh GDGT signal can be transported by massive falls of organic matter after peaks

in surface production. Different feeding modes were investigated and while no differences in TEX_{86} values were found in the Atlantic site, the Mediterranean decapods showed a significant difference probably related to the freshness of the material consumed. Finally, TEX_{86} calculated with the GDGTs taken up by decapods shows a relatively good correspondence with SST at time of sampling for Atlantic decapods but represents a mix of annual mean SST and SST at time of sampling for Mediterranean decapods. We also suggest that other heterotrophic organisms closely related to decapods, such as the abundant copepods, are likely to play an important role producing faecal pellets that will carry GDGTs from surface waters to the sediment.

Acknowledgements

We would like to thank the members of the research projects ECOMARG (REN2002-00916/MAR) and IDEA (REN2002-00920/MAR), both financed by (CICYT, Ministry of Education and Science, M.E.C., Spain). Dr. Laurent D. Labeyrie and two anonymous reviewers are thanked for constructive comments on earlier drafts of this paper. This project was supported by NWO-ALW (Project nr. 152911).

References

Brassell, S. C., G. Eglinton, I. T. Marlowe, U. Pflaumann, and M. Sarnthein (1986), Molecular stratigraphy: A new tool for climatic assessment, *Nature*, *320*, 129-133.

Cartes, J. E. (1993), Diets of deep-water pandalid shrimps on the Western Mediterranean slope, *Mar. Ecol. Prog. Ser., 96*, 49-61.

Cartes, J. E. and P. Abelló (1992), Comparative feeding-habits of polychelid lobsters in the Western Mediterranean deep-sea communities, *Mar. Ecol. Prog. Ser., 84*, 139-150.

Chave, K. E. (1954), Aspects of the biogeochemistry of magnesium. 1. Calcareous marine organisms, *J. Geol., 62*, 266-283.

Comas, M. C., Zahn, R., and Klaus, A. (1996), *Proceedings of the Ocean Drilling Project, Initial Reports., 161*, 5-13.

Emiliani, C. (1955), Pleistocene temperatures, J. Geol., 63, 538-578.

Fanelli, E. and J. E. Cartes (2004), Feeding habits of pandalid shrimps in the Alboran Sea (SW Mediterranean): influence of biological and environmental factors, *Mar. Ecol. Prog. Ser., 280*, 227-238.

Hoefs, M. J. L., S. Schouten, J. W. de Leeuw, L. L. King, S. G. Wakeham, and J. S. Sinninghe Damsté (1997), Ether lipids of planktonic archaea in the marine water column, Appl. Environ. Microbiol., 63, 3090-3095.

Hopmans, E. C., S. Schouten, R. D. Pancost, M. T. J. Van der Meer, and J. S. Sinninghe Damsté (2000), Analysis of intact tetraether lipids in archaeal cell material and sediments by high performance liquid chromatography/atmospheric pressure chemical ionization mass spectrometry, *Rap. Comm. Mass Spec., 14*, 585-589.

Karner, M. B., E. F. DeLong, and D. M. Karl (2001), Archaeal dominance in the mesopelagic zone of the Pacific Ocean*, Nature, 409*, 507-510.

Kuypers, M., P. Blokker, J. Erbacher, H. Kinkel, R. D. Pancost, S. Schouten, and J. S. Sinninghe Damsté (2001), Massive expansion of marine archaea during a mid-Cretaceous oceanic anoxic event, *Science, 293*, 92-94.

Lagardère, J.P. (1977). Recherches sur la distribution verticale et sur l'alimentation des crustaces decapodes benthiques de la Pente Continentale du Golfe de Gascogne. Analyse des groupements carnicologiques. *Bull. Cent. Etud. Rech. Sci. Biarritz, 11(4)*, 367-440.

Margot, H., C. Acebal, E. Toril, R. Amils, and J. L. Fernandez Puentes (2002), Consistent association of crenarchaeal Archaea with sponges of the genus Axinella, *Mar. Biol., 140*, 739-745.

Massana, R., E. F. DeLong, and C. Pedrós-Alió (2000), A few cosmopolitan phylotypes dominate planktonic archaeal assemblages in widely different oceanic provinces, *Appl. Environ. Microbiol., 66*, 1777-1787.

Maynou, F. and J. E. Cartes (1998), Daily ration estimates and comparative study of food consumption in nine species of deep-water decapod crustaceans of the NW Mediterranean, *Mar. Ecol. Prog. Ser., 171*, 221-231.

Maynou, F. and J. E. Cartes (2000), Community structure of bathyal decapod crustaceans off south-west Balearic Islands (western Mediterranean): seasonality and regional patterns in zonation*, J. Mar. Bio. Ass. UK., 80*, 789-798.

McInerney, J. O., M. Wilkinson, J. W. Patching, T. M. Embley, and R. Powell (1995), Recovery and phylogenetic analysis of novel archaeal rRNA sequences from a deep-sea deposit feeder, *Appl. Environ. Microbiol, 61*, 1646-1648.

Murray, A. E., K. Y. Wu, C. L. Moyer, D. M. Karl, and E. F. DeLong (1999), Evidence for circumpolar distribution of planktonic Archaea in the Southern Ocean, *Aquat. Microb. Ecol., 18*, 263-273.

Nurnberg, D., J. Bijma, and C. Hemleben (1996), Assessing the reliability of magnesium in foraminiferal calcite as a proxy for water mass temperatures, *Geochim. Cosmochim. Acta, 60*, 803-814.

Polunin, N. V. C. (2002), 5th International Conference on Environmental Future: climate change and the future state of the world's aquatic ecosystems, *Environ. Cons., 29*, 1-2.

Schouten, S., E. C. Hopmans, E. Schefuß, and J. S. Sinninghe Damsté (2002), Distributional variations in marine crenarchaeotal membrane lipids: a new tool for reconstructing ancient sea water temperatures?, *Earth Planet. Sci. Lett., 204*, 265-274.

Sinninghe Damsté, J. S., S. Schouten, E. C. Hopmans, A. C. T. van Duin, and J. A. J. Geenevasen (2002), Crenarchaeol: the characteristic core glycerol dibiphytanyl glycerol tetraether membrane lipid of cosmopolitan pelagic crenarchaeota, *J. Lipid Res., 43*, 1641-1651.

Van der Maarel, M. J. E. C., R. R. E. Artz, R. Haanstra, and L. J. Forney (1998), Association of marine archaea with the digestive tracts of two marine fish species, *Appl. Environ. Microbiol., 64*, 2894-2898.

Woese, C. R., O. Kandler, and M. L. Wheels (1990), Towards a natural system of organisms: proposal for the domains Archaea, Bacteria, and Eucarya, *P. Natl. Acad. Sci. USA*, 87, 4576-4579.

Wuchter, C., S. Schouten, M. J. L. Coolen, and J. S. Sinninghe Damsté (2004), Temperature-dependent variation in the distribution of tetraether membrane lipids of marine Crenarchaeota: Implications for TEX_{86} paleothermometry, *Paleoceanography, 19*, doi:10.1029/2004PA001041.

Wuchter C., S. Schouten, S.G. Wakeham and J.S. Sinninghe Damsté (2005) Temporal and spatial variation in tetraether membrane lipids of marine Crenarchaeota in particulate organic matter: Implications for TEX86 paleothermometry, *Paleoceanography, 20*. doi:10.1029/2004PA001110.

Wuchter C., S. Schouten, S. G. Wakeham and J. S. Sinninghe Damsté (2006) Archaeal tetraether membrane lipid fluxes in the northeastern Pacific and Arabian Sea: implications for TEX_{86} paleothermometry, *Paleoceanography, 21*. doi:PA4208-1-PA4208-9.

Chapter 5

A study of the TEX_{86} paleothermometer in the water column and sediments of the Santa Barbara Basin, California

Carme Huguet, Arndt Schimmelmann, Robert Thunell, Lucas J. Lourens, Jaap S. Sinninghe Damsté and Stefan Schouten

Published in *Paleoceanography* doi:10.1029/2006PA001310 (2007)

Abstract

Particulate organic matter collected during a 2-year period, as part of an ongoing sediment trap study, and a high-resolution sediment record from 1850 to 1987 AD from the Santa Barbara Basin were analyzed for TEX_{86}, a temperature proxy based on marine crenarchaeotal membrane lipids. Highest fluxes of crenarchaeotal lipids in the water column were found in May-June 1996 and from October 1996 to January 1997, and in general showed a good correlation with mass fluxes. TEX_{86} reconstructed temperatures from the sediment trap series ranged from 8-11°C and were usually substantially lower than sea surface temperatures (SST), indicating that, unlike in previous studies, the TEX_{86} corresponds to sub-surface temperatures, likely between 100-150 m. TEX_{86} temperature variations observed in trap samples were not coupled to changes in SST or deep-water temperatures and only to some degree with crenarchaeotal lipid fluxes. This suggests that a complex combination of different depth origins and seasonal growth periods of Crenarchaeota contributed to the variations in TEX_{86} signal during the annual cycle. TEX_{86} temperatures in the two sediment cores studied (8-13 °C) were also substantially lower than those of instrumental SST records (14-17.5 °C) confirming that TEX_{86} records a sub-surface temperature signal in the SBB. This result highlights the importance of performing calibration studies using sediment traps and core tops before applying the TEX_{86} temperature proxy in a given study area.

5.1. Introduction

A variety of sea surface temperature (SST) proxies exist for paleoceanographic applications, of which Mg/Ca ratios of planktonic foraminifera and the $U^{K'}_{37}$ index of long chain alkenones are presently the most frequently used. Five years ago, *Schouten et al.* [2002] introduced a new SST proxy, the TEX_{86} based on the relative distribution of glycerol dibiphytanyl glycerol tetraethers (GDGTs), which are membrane lipids produced by non-thermophilic Crenarchaeota. These organisms are ubiquitous and abundant in seawater [*Hoefs et al.,* 1997; *Massana et al.,* 2000; *Karner et al.,* 2001] and large lakes [*Powers et al*., 2005]. Marine Crenarchaeota biosynthesize GDGTs with a varying number of cyclopentyl moieties, and the relative abundance of these moieties changes according to the water temperature [*Wuchter et al*., 2004]. Therefore, by measuring the relative amounts of GDGTs present in sediments, the temperature at which Crenarchaeota were living can be reconstructed. Culture experiments showed that changes in salinity and nutrients do not substantially affect the temperature signal recorded by TEX_{86} [*Wuchter et al*., 2004], the proxy also seems to be unaffected by water redox conditions [*Schouten et al.,* 2004].

Recent evidence has shown that part of the marine Crenarchaeota are nitrifiers [*Wuchter et al.,* 2006a; *Könneke et al.,* 2005] and thus are not depending on light for growth. Indeed, they are distributed throughout the water column though highest abundances are usually noted in the upper few hundred meters both in the Pacific [*Karner et al.,* 2001] and in the Atlantic ocean [*Herndl et al.,* 2005]. In contrast, a study of particulate organic matter (POM) at ten different locations with various oceanographic conditions (i.e. upwelling, stratification) revealed that TEX_{86} correlates well with surface water temperatures (depths <100m) and that the signal in deeper-water layers and surface sediments is primarily derived from these upper 100 meters [*Wuchter et al*., 2005]. This apparent contrast of a surface signal obtained from organisms living within a wide depth range was explained by the GDGTs transport mechanism to the sediment floor, i.e. through consumption and re-packaging which mostly takes place in the active food web in the upper part of the water column [*Wuchter et al.*, 2005; *Huguet et al.,* 2006a].

Laminated sediments from the central Santa Barbara Basin (SBB) represent an important and frequently used archive of climate variability of the California coast [*Schimmelmann and Lange,* 1996; *Biondi et al.,* 1997; *Berger et al.,* 2004]. Sub-sill waters in

the ca. 590 m deep SBB (Fig. 1) have a low oxygen content that enhances preservation of organic matter and prevents bioturbation by macro-benthos. A high export production coupled with high sedimentation rates of several mm per year (before sediment compaction) result in the preservation of light and dark annual varve couplets [*Reimers et al.,* 1990; *Thunell et al.,* 1995] (Fig. 2). Thus, sediment cores of the SBB are excellent for high-resolution paleostudies of the climate and oceanographic conditions in the SBB area which is influenced, at different time-scales, by the El Niño Southern Oscillation (ENSO), the Pacific Decadal Oscillation (PDO), the California Current system, and the upwelling regime related to the North Pacific High as well as local factors [*Weinheimer et al.,* 1999; *Berger et al.,* 2004].

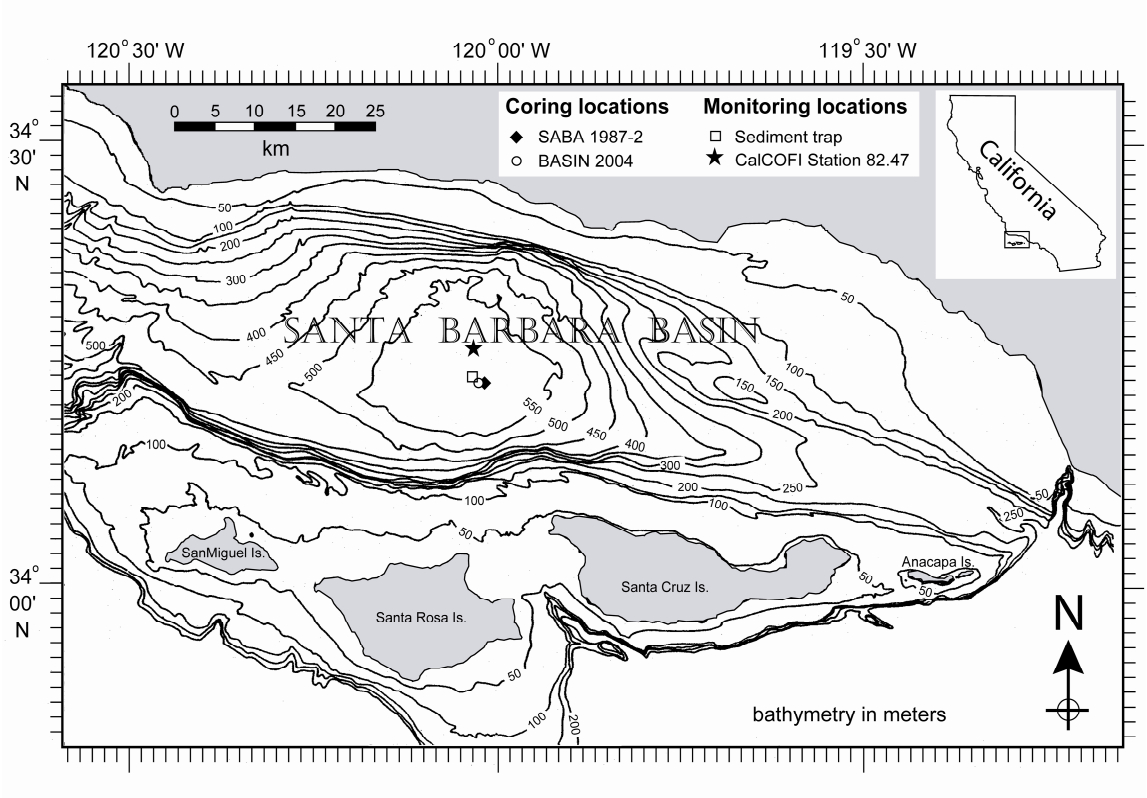

Figure 1. Map of the study area, with indication of sediment sampling locations for SABA 87-2 (34°13.5'N, 120°01.0'W), BASIN 2004 (34°13.41'N, 120°01.53'W) and the location of the sediment trap (34°14'N, 120° 02'W). CalCOFI station 82.47 is located at 34°16'N, 120° 2'W [www.calcofi.org].

A variety of proxies have been used in this area. For example, SST reconstructions using long-chain alkenones revealed occasional warming during 20th century El Niño events [*Kennedy and Brassell,* 1992] although the same proxy was less successful detecting ENSO in older SBB sediments [*Zhao et al.,* 2000] or even during the last century [*Herbert et al.,* 1998]. Similarly, Mg/Ca ratios of planktonic foraminifera did not record the strong increase in surface temperatures during the 1997-1998 El Niño event [*Pak et al.,* 2004]. In contrast, other studies revealed that El Niño events can be recorded by changes in foraminifera assemblages [*Black et al.,* 2001; *Field et al.,* 2006] and that $\delta^{18}O$ of planktonic foraminifera records temperature changes associated with El Niño [*Thunell et al.,* 1999]. Thus, the different proxies used in the SBB seem to yield partially contrasting information. This highlights the importance of a multiproxy approach and the need to understand the response and limitations of a proxy in the SBB area before paleoclimate studies can be performed.

Here we investigated the potential of the TEX_{86} to reconstruct past temperatures in the SBB area by analysing sediment trap material obtained over two annual cycles (1995-1997). In addition, we analysed the TEX_{86} in a high resolution sediment record with annual to tri-annual resolution representing the period from ~1849 to 1987 AD and compared this with an available instrumental temperature record for the SBB.

5.2. Material and Methods

5.2.1. Sample material

5.2.1.1. Sediment trap

An automated sediment trap has been deployed since 1993 in the center of the basin (34º14'N, 120º02'W) (Fig. 1) at ~490 m water depth, ~50 m from the bottom [*Thunell et al.,* 1995; *Thunell*, 1998]. Biweekly to monthly measurements of temperature and salinity down to 100 m depth have been made at the mooring location of the trap sample. For this study we selected 22 samples from the period between December 1995 and December 1997 which were analyzed for GDGT concentration. These samples represent collection periods ranging from 6 to 18 days. Freeze dried and homogenized sub-samples of 50-180 mg were used for this study.

5.2.1.2. Sediment core

Box cores from the depocenter of the SBB were recovered in 1987 during the cruise SABA 87-2 (34°13.5'N, 120°01.0'W), and in 2004 during cruise BASIN 2004 (34°13.41'N, 120°01.53'W, box core 1-MC3) (Fig. 1). Cylindrical sub-cores from box cores were sectioned in layers with approximately annual to tri-annual resolution although the resolution is higher than annual in the upper third section of each core as sediment is less compacted (Fig. 2). The sediment obtained from each section was freeze-dried and stored [*Schimmelmann et al.*, 1990]. BASIN 2004 samples dating from 1917 to 1959 AD were analyzed to cover a sampling hiatus in box core SABA 87-2. A total of 211 samples were analyzed from both cores, covering about 140 years of sedimentation from ca. 1850 to 1987 AD.

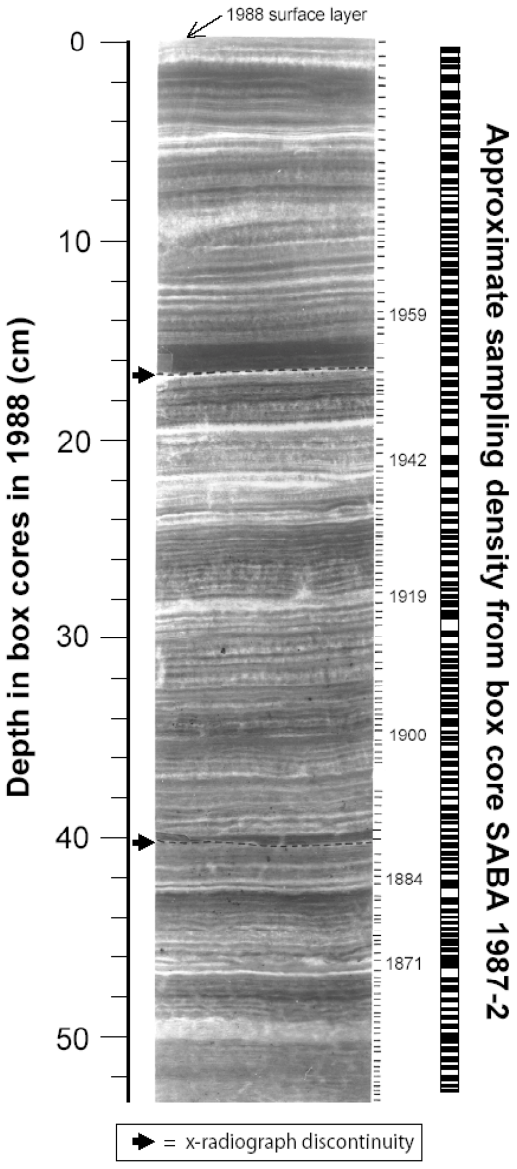

Figure 2. Composite of X-radiograph contact prints showing varves form 1840 to 1988 in the depocenter of the SBB. The black/white pattern indicates the approximate sediment sampling intervals for this study.

Dating of samples was performed by varve counting on sediment X-radiographs that were correlated against high-resolution porosity profiles [*Schimmelmann et al.*, 1990]. Validation of varve-counting for dating in SBB sediment had been independently achieved by 210Pb geochronology, identification of specific diatom assemblages of El Niño events of 1941, 1958 and 1983 AD, and the statistical relationship of varve thickness versus precipitation on land [reviewed by *Schimmelmann and Lange*, 1996; Fig. 2]. The dating uncertainty for individual sediment samples is ~2 years below 1980 AD and about one year for younger sediments [*Schimmelmann et al*., 1990].

5.2.2. TEX_{86} analysis

Freeze-dried samples between 50-180 mg were extracted using an Accelerated Solvent Extractor 200 (ASE 200, DIONEX) with a mixture of dichloromethane (DCM) and methanol (MeOH) (9:1, vol:vol) at 100°C and 7.6 10^6 Pa. A known amount of a C_{46} GDGT was added to the extract of the sediment trap samples as internal standard [*Huguet et al.,* 2006b]. The total extract was then divided into an apolar and a polar fraction, using a glass pipette column filled with activated alumina, and sequential elution with hexane/DCM (9:1 vol:vol) and DCM/MeOH (1:1, vol:vol), respectively. Polar fractions were analyzed for GDGTs according to the procedure described by *Hopmans et al*. [2000]. Analyses were performed in triplicate with an HP 1100 Series Liquid Chromatography-Mass Spectrometer (LC-MS) equipped with an auto-injector and ChemStation chromatography manager software. Separation was achieved on a Prevail Cyano column (2.1 x 150mm, 3µm; Alltech, Deerfield, Illinois, USA), maintained at 30°C. GDGTs were eluted isocratically first with hexane/isopropanol (99:1, vol:vol) for 5 min, then using a linear gradient up to 1.8 % vol of isopropanol over 45 min. Flow rate was 0.2 mL/min. After each analysis the column was cleaned by back flushing hexane/propanol (90:10, vol:vol) at 0.2 mL/min for 10 min. Detection was achieved using atmospheric pressure chemical ionization-mass spectrometry (APCI-MS) of the eluent using the following conditions; nebulizer pressure 4.1 10^5 Pa, vaporizer temperature 400°C, N_2 drying gas flow 6 L/min at 200ºC, capillary voltage -3kV, corona 5 µA (~3.2kV). Single Ion Monitoring (SIM) was used instead of full mass scanning because SIM increases the signal-to-noise-ratio and thus improves reproducibility. SIM was set to scan the five $[M^+]$+H ions of the GDGTs with a dwell time of 237 ms for each ion. Concentrations of GDGTs in the sediment trap samples were calculated based on the added internal standard and the relative response factor of the standard versus crenarchaeol [*Huguet et al.,* 2006b]. Relative abundances of GDGTs were used to calculate TEX_{86} values that relate to temperature in °C according to the following empirical relationship [*Schouten et al.*, 2002]:

$$TEX_{86} = 0.015 \cdot T + 0.28 \qquad [1]$$

This equation results from the correlation of TEX_{86} values from core top sediments with SST (see [*Schouten et al.*, 2002] for details).

An aliquot of an Arabian Sea sediment extract was measured every 10 samples to assess the analytical error. The resulting mean TEX_{86} value for 72 repeat analyses was 0.68 with a standard deviation of ±0.034, corresponding to 26.6 ± 0.5°C according to equation [1].

5.2.3. Time series analysis

Time series analyses were performed on (i) our 1849-1987 AD TEX_{86} record, (ii) the ENSO index Niño 3.4 of *Kaplan et al.* [1998] and *Smith and Reynolds* [2003; 2004], and (iii) the Pacific Decadal Oscillation (PDO) index of *Mantua et al.* [1997] (see http://jisao.washington.edu/pdo/PDO.latest). We also performed a first-order autoregressive (AR1) process to evaluate the influence of climatic red noise on the variability of all the data series. For this purpose we derived spectra directly from the unevenly spaced time series using the REDFIT program [*Schulz and Mudelsee*, 2002]. All time series were analysed with a Welch spectral window and four segments with 50% overlap (n_{50} = 4) [*Schulz and Mudelsee*, 2002].

5.3. Results

5.3.1. Sediment trap

The sediment trap material analyzed covers two annual cycles for the period December 1995 to December 1997. The onset of the 1997-1998 strong El Niño was in March 1997 but the effects only reached the SBB in June 1997 [*Lynn et al*. 1998] and thus our trap series covers both non-El Niño and initial El Niño conditions in the SBB area. The flux of GDGT lipids ranged from 29 μg m^{-2} day^{-1} in November 1997 to 196 μg m^{-2} day^{-1} in November 1996 (Fig. 3a). These GDGT fluxes are similar to those reported for an upwelling station near the Californian coast but higher than those reported for the Arabian Sea (up to 40 μg m^{-2} day^{-1}) [*Wuchter et al.*, 2006b]. During the non-El Niño period, two clear peaks in GDGT fluxes were observed, one in May/June 1996 and the largest between October 1996 and January 1997. During the El Niño period there were no distinct maxima, and GDGT fluxes remained fairly constant oscillating between 25 and 100 μg m^{-2} day^{-1} (Fig. 3a).

TEX_{86}-derived temperatures range from 7.5ºC in November 1996 to 11.4ºC in March 1997 (Fig. 3a). The average flux-weighted TEX_{86} temperature over the time series is 9.6ºC, with average values of 9.3ºC in 1996 and 9.9ºC in 1997, respectively. The average flux-weighted TEX_{86} temperatures were 9.6ºC for the non-El Niño time period (December 1995-

June 1997) and 9.7ºC for the El Niño period (June 1997-December 1997) (Fig 3). Both years follow a similar pattern showing a decrease in temperature in late spring, an increase towards summer, and a second decrease in autumn followed by an increase in winter. Peak TEX_{86} temperatures are found during spring 1996 and 1997, while minima in TEX_{86} temperatures occur during October/November and June/July of both years (Fig. 3a).

5.3.2. Sediment core record

Samples from two partially overlapping sediment cores were analyzed to determine the historical record of TEX_{86}-derived temperatures. The main core analyzed, SABA 87-2 (in black; Fig. 4a), covered the period from 1849 to 1987 AD, but no material was available for the interval 1923 to 1942 AD. We covered this gap with samples from core 1-MC3 from the BASIN 2004 cruise, by analyzing samples dating from 1917 to 1959 AD (in green; Fig. 4a). Overall, TEX_{86} temperatures of the combined cores range between 8.4° C and 13.7°C (Fig 4a). Although the TEX_{86} values in 1-MC 3 are consistently lower than in SABA 87-2, the general trend and interannual variability are similar for the two cores (Fig. 4a). Although with slightly lower temperatures for the BASIN 1-MC3 core, the overlap intervals show good correspondence in terms of temperature ranges and trends (Fig. 4a), especially when the analytical error and the ~ 2 year dating error are taken into account. Average temperatures for the 1942-1959 overlap interval are 10.9°C for SABA 87-2 and 10.4°C for BASIN 1-MC3, a difference which falls within the 0.5°C analytical error for TEX_{86}. For the 1917-1923 AD overlap we also find a 0.5°C difference with average SABA 87-2 and BASIN 1-MC3 values of 10.5°C and 10.0°C, respectively. The interannual variability shows similar trends with most of the differences having overlapping error limits.

5.4. Discussion

5.4.1. Glycerol dibiphytanyl glycerol tetraether fluxes in the SBB

There are two distinct maxima in the GDGT fluxes during the non-El Niño period (Fig. 3a). The first peak at the end of spring coincides with a general increase in sedimentation flux (Fig. 3a) and is associated with upwelling and high phytoplankton productivity in the SBB area in spring [*Thunell et al.,* 1999]. Similar results were reported for a sediment trap study of GDGT fluxes in the Arabian Sea which showed that the highest fluxes in GDGTs are associated with the general increase in fluxes during upwelling [*Wuchter et al.,* 2006b]. This

was attributed to increased primary production and subsequent increased food web turnover leading to enhanced transport of GDGTs to the sediment by settling particles rather than increased production of GDGTs [*Wuchter et al.,* 2005; *Huguet et al.,* 2006a]. A similar explanation can thus be invoked for the first maximum in GDGT fluxes in the SBB. However, this is not the case for the second maximum in GDGT flux observed during winter 1996/1997 as sediment fluxes remained generally low. Reported molecular ecological data revealed that Crenarchaeota in the SBB area occur in higher abundance during winter [*Murray et al.,* 1999], suggesting that the higher flux of GDGTs during the winter months could be a reflection of higher Crenarchaeota production. Alternatively, the second maximum could be caused by a previously reported inshore meander of the California current at this time [*Schwing et al.,* 1997]. This inshore meander caused an unusual increase in chlorophyll concentrations [*Schwing et al.,* 1997] and foraminiferal flux [*Black et al.,* 2001], and may also have substantially increased Crenarchaeota production. Analysis of GDGT fluxes over longer time series should make clear which of these factors played a decisive role.

For the El Niño period there are no distinct maxima in GDGT fluxes during either spring/summer or early winter of 1997, even though there are increases in sediment fluxes at these times (Fig. 3a). This suggests that the El Niño of 1997-1998 strongly reduced Crenarcheaota production during this period. El Niño does not only affect physical parameters such as temperature but also has an impact on nutrient availability and productivity [*Mantua et al.,* 1997; *Chavez et al.,* 2002]. During 1997, temperatures were higher than normal (Fig. 3b) and the upwelling was greatly reduced [*Thunell et al.,* 1999], leading to a reduction in primary production [*Black et al.,* 2001] which usually results in reduced secondary production [*Simpson,* 1992]. Recent evidence suggests that part of the Crenarchaeota are nitrifiers [*Könneke et al.,* 2005; *Wuchter et al.,* 2006a] and use ammonia, produced by decay of phytoplankton and zooplankton, as an energy source. As phytoplankton productivity was greatly reduced during El Niño this could have led to a severe decrease in ammonia availability and thus lower Crenarchaeota productivity.

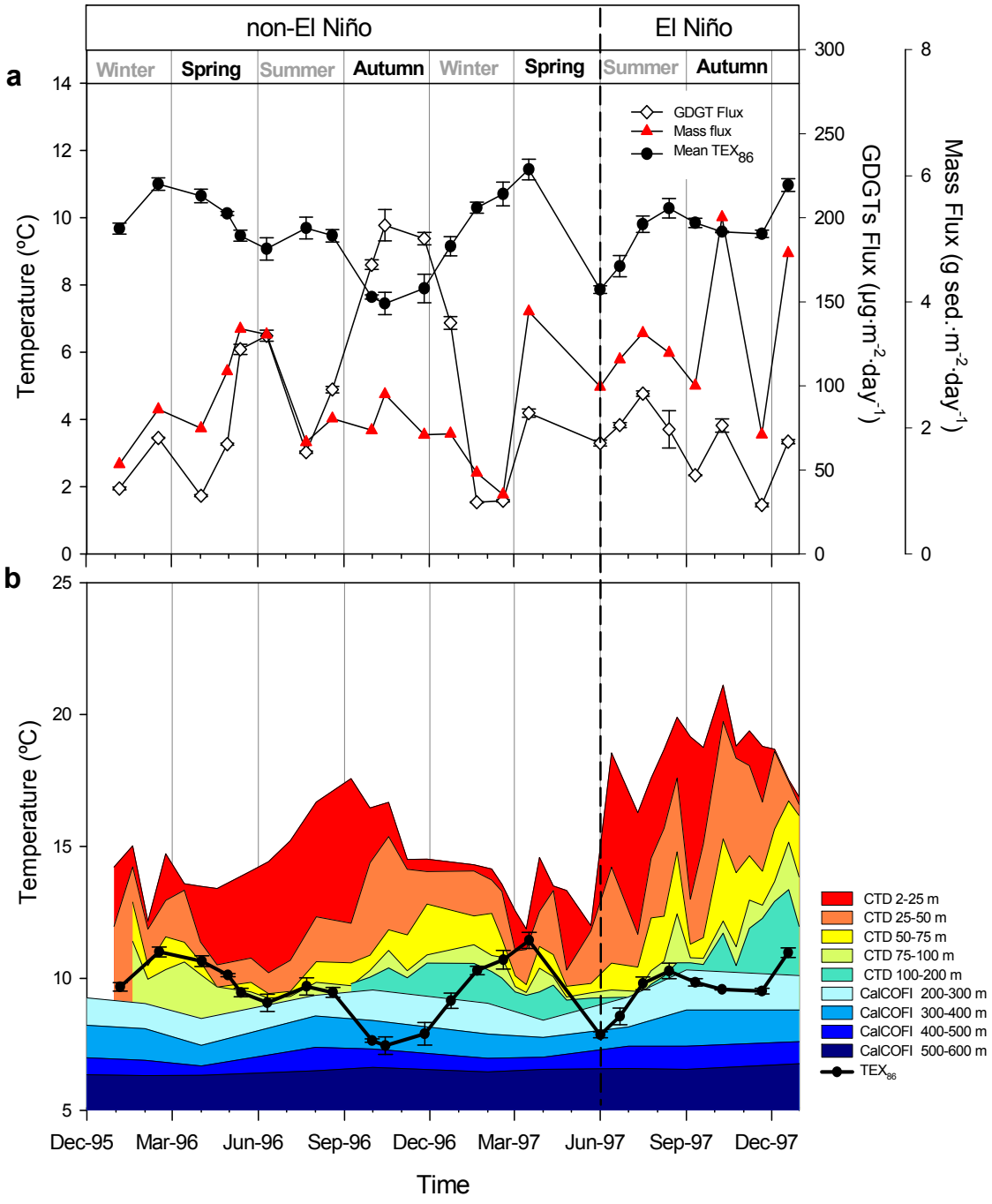

Figure 3. Flux and temperature data for the Santa Barbara Basin between December 1995 and December 1997. (a) Trap sample results for TEX_{86}-derived temperatures (•), GDGT fluxes (◊) and mass fluxes (▲). (b) Comparison of TEX_{86}-derived temperatures (•) with in situ temperatures from 0 to 100 m (CTD data, [*Thunnel,* 1998]) and from 200-500 m (from the California Cooperative Oceanic Fisheries Investigations (CalCOFI, at www.calcofi.org). Error bars indicate analytical error of triplicate measurements.

5.4.2. Origin of the TEX_{86} temperature signal

Comparison of the TEX_{86} temperature signal with instrumental records, obtained by monthly CTD casts (0-100 m) and quarterly shipboard measurements (200-500 m) (Fig. 3b), revealed that the TEX_{86} temperatures, which range from 7.5 to 11.4ºC, are always lower than SST values which range between 12 to 21ºC. TEX_{86}-derived temperatures seem, in general, to correspond better to temperatures below 75 m, suggesting that in the SBB area TEX_{86} represents a sub-surface temperature signal, rather than SST (Fig. 3b). This is in contrast to previous sediment trap results from the Arabian Sea where TEX_{86} temperatures were slightly higher than in-situ surface temperatures [*Wuchter et al.,* 2006b]. Molecular ecological studies in the Santa Barbara Channel have shown that Crenarchaeota are most abundant below 75 m depth [*Murray et al.,* 1999] and a depth profile of GDGT concentrations in the water column of the Santa Monica Basin (SMB) [*Wuchter et al.,* 2005] also shows the highest abundance of Crenarchaeota lipids between 100-150 m depth. Furthermore, $\Delta^{14}C$ analysis of crenarchaeotal GDGTs in surface sediments of SBB and SMB showed a large ^{14}C-depletion and a lack of bomb-derived ^{14}C, and thus a deep-water origin for the GDGTs was suggested [*Pearson et al.,* 2001]. Hence, several lines of evidence suggest that crenarchaeotal GDGTs in the SBB are mostly derived from waters well below 75 m. TEX_{86}-derived temperatures for the sediment trap samples do not consistently reflect temperature at any particular depth through the annual cycle (Fig. 3b), suggesting that other factors besides deep-water temperature changes must contribute to the changes in TEX_{86} signal. Closer examination of the seasonal variation in TEX_{86} temperatures reveals that, in general, they correspond to temperatures between 100-300 m but that relatively much higher values are found in spring when TEX_{86}-calculated temperatures are only 1-3ºC lower than SST (Fig. 3b). These relatively warm temperatures correspond to times of upwelling and thus lower SSTs. The relatively high TEX_{86} values could be caused by an increase in surface phytoplankton production during upwelling which in turn would have increased the amount of marine snow and fecal-pellet production in the surface during this period. GDGTs present in surface waters would then have been preferentially packaged and associated with sinking particles [*Wuchter et al.*, 2005; *Huguet et al.,* 2006a]. This would increase the relative contribution of the surface (0-100 m) versus deeper-water (below 100 m) signal. However, this should also be reflected in an increased flux in GDGTs which is not the case (Fig. 3a). Alternatively, the deep-water Crenarchaeota could be carried upwards with the upwelled and nutrient-rich waters thereby

experiencing much higher temperatures before dying and sinking to the sediment, although this is not consistent with previously observed Crenarchaeota seasonality, as they are usually more abundant at times of low phytoplankton productivity [*Wuchter et al.* 2005]. However, this is supported by molecular studies in the Santa Barbara Channel which showed that Crenarchaeota were only detected in surface waters during times of upwelling [*Murray et al.,* 1999]. This may also explain why the strong warming of surface waters during El Niño is not reflected in our TEX_{86} record, i.e. the reduced upwelling will have left the Crenarchaeota to thrive in deeper waters and prevented their upward transport to surface waters.

Our results thus suggest that the seasonal variation in TEX_{86} is likely determined by the varying contributions of shallow versus deep-water signals. The behavior of the TEX_{86} proxy is quite different from that of other temperature proxies determined in SBB sediment trap studies. For example, the $U^{K'}_{37}$ [*Hardee and Thunell*, 2006] and planktonic foraminiferal $\delta^{18}O$ [*Thunell et al.,* 1999] signals from SBB sediment trap samples show a good correspondence with SST. Mg/Ca ratios of planktonic foraminifera from sediment traps in the SBB area also show a generally good correspondence with upper water column temperatures although some variation in depth habitat of the foraminifera was noted and the Mg/Ca ratio did not reflect the warming of surface waters during El Niño [e.g. *Pak et al.,* 2004].

5.4.3. Past variation in TEX_{86} temperatures

Our results from the SBB sediment cores show that the TEX_{86} paleothermometer most likely records temperatures below 100 m, as the TEX_{86} temperatures are all well below the COADS instrumental mean annual SST at 31-33º N, 119-121ºW (COADS http://www.ncdc.noaa.gov/oa/climate/coads/) (Fig. 4b), in good agreement with results from our sediment trap study. However, TEX_{86} temperatures do not consistently reflect sub-surface temperatures at a particular depth, as temperatures below the thermocline in the SBB have varied in general by less then 0.5°C over the last 50 years [*Field and Baumgartner,* 2000], while our TEX_{86} temperatures vary by more than 4°C. Thus, it is unlikely that changes in sub-surface temperature alone caused the TEX_{86} variation observed in the sediment cores (Fig. 4). Instead, changes in depth of origin of the GDGT signal and/or changes in seasonality of GDGT production may be responsible for much of the observed variation.

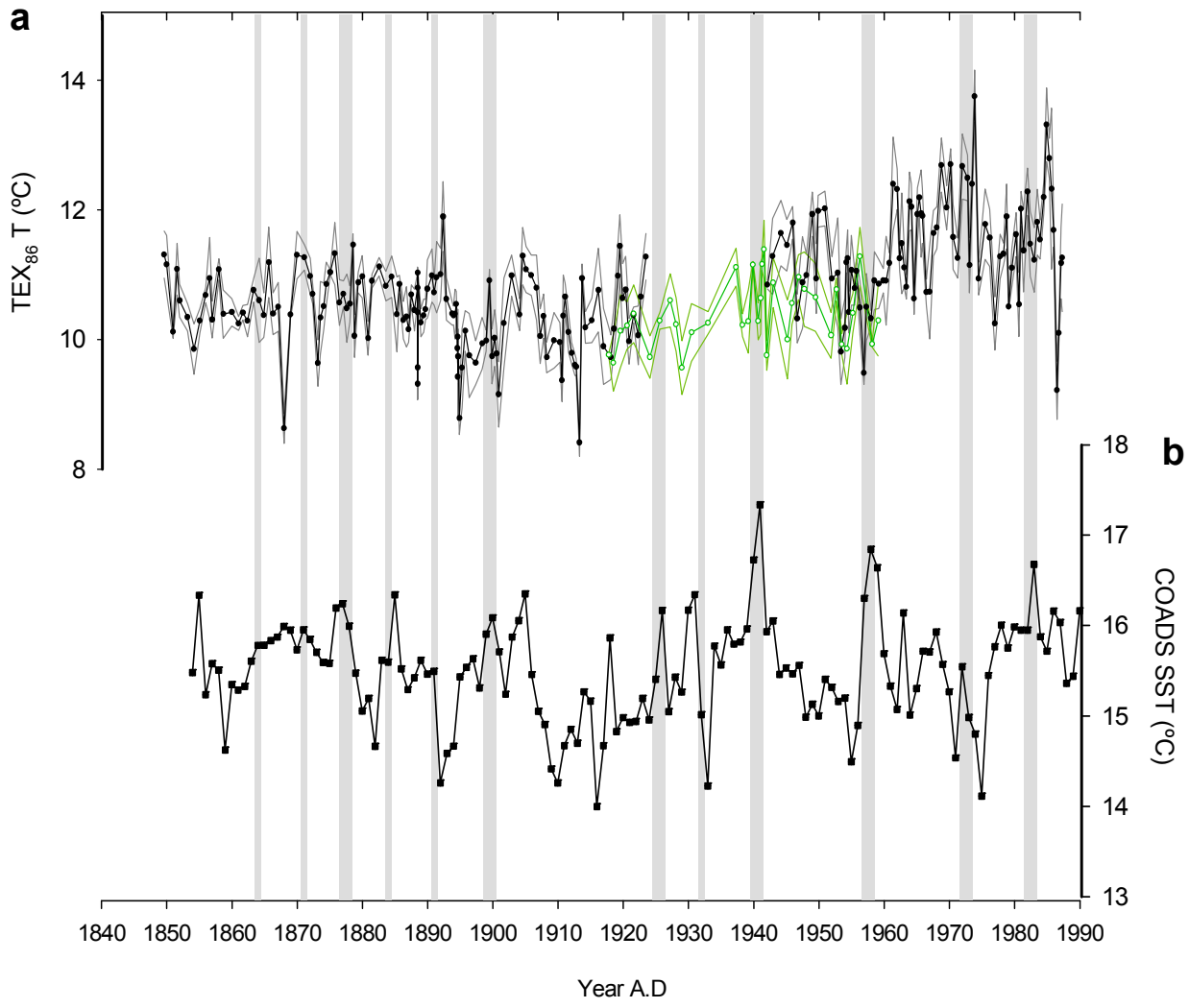

Figure 4. Temperature time series from the Santa Barbara Basin. (a) TEX_{86}-based temperature reconstruction from SABA 87-2 box core sediment (in black with •) and from BASIN 2004 box core sediment (in green with ○); temperatures were calculated using the standard TEX_{86} equation according to *Schouten et al.* [2002], with standard deviation indicated by grey lines. (b) Mean annual SST (31-33º N, 119-121ºW) from the Comprehensive Ocean-Climate Data Set project (COADS; http://www.ncdc.noaa.gov/oa/climate/coads/). Vertical grey bars indicate the timing of historic El Niño events with strengths 4, 5 and 6 according to the compilation by *Quinn* [1999]

The large increase in SST in the SBB during some El Niño events is reflected in a number of temperature proxies preserved in SBB sedimentary records [*Kennedy and Brassell,* 1992; *Field et al.,* 2006]. However, comparison of the TEX_{86} temperature record with SST anomalies caused by El Niño (strengths 4, 5 and 6 according to the compilation by *Quinn* [1999]; indicated by vertical grey bars in Fig. 4) reveals no obvious correlation and generally no elevated TEX_{86} temperatures coinciding with strong El Niño events (Fig. 4a), although El Niño-related SST spikes are apparent in the instrumental SST record (Fig. 4b). This is in agreement with sediment trap data where a strong El Niño warming of surface waters after June 1997 was not recorded by TEX_{86}, i.e. the flux-weighted average TEX_{86} temperature of 9.6ºC for the non-El Niño period was similar to the 9.7ºC for the El Niño period.

We performed frequency analysis to investigate other possible controlling factors in past variations of TEX_{86}-derived temperatures. The results were compared to those from frequency analyses of both ENSO and PDO as the latter have been reported to influence temperatures, the structure of the water column, upwelling dynamics in the SBB, and thus also nutrient availability and primary production [*Mantua et al.,* 1997; *Chavez et al.,* 2002]. Frequency analyses of the Niño 3.4 (1856-2006 AD) and PDO (1900-2005 AD) indices revealed both highly significant (>99%-χ^2 false-alarm level) periods at 5.6-5.8 years. A ~5.7 yr cycle has been reported in various other records and seems to be rooted in ENSO forcing [*Felis et al.,* 2000], it is evidently widespread in polar to tropical areas [*Felis et al.,* 2000; *Jevrejeva et al.,* 2004; *Felis et al.,* 2004; *Cronin et al.,* 2002] and may influence atmospheric indices such as the North Atlantic Oscillation (NAO) [*Felis et al.,* 2000]. A 5.7 yr cycle is also present in our 1849-1987 AD sedimentary TEX_{86} record, although its amplitude does not exceed the 80%- χ^2 false-alarm level. The lack of any highly significant cycles in the sedimentary TEX_{86} record of the SBB is most likely due to the strong decoupling between TEX_{86} and the temperature at any fixed depth interval.

The TEX_{86} signal in the SBB sedimentary record might also be complicated by fluctuating strengths of the California and Davidson currents, changing wind patterns, intermittent upwelling, and the tidal regime. The sedimentary input received by the SBB depocenter may include allochthonous material that is transported from nearby areas by currents, as well as tidally re-suspended sediment [*Berger et al.,* 2004]. However, the reported multi-annual tidal variability is dominated by the lunar nodal cycle of 18.3 years, a cycle which we do not find in our TEX_{86} record. In addition, our frequency analysis shows no

cycles that can be associated with those found for varve thickness or TOC records [*Zhao et al.,* 2000*; Berger et al.,* 2004], although all records use spatially compatible data from the same or similar sediment cores. This suggests that the variations observed in our TEX_{86} record are likely not caused by tidally-induced resuspension but by a complex array of varying depths of GDGT production and environmental factors such as upwelling.

5.5. Conclusions

TEX_{86} analyses of sediment trap samples reveal that temperatures inferred from this proxy do not reflect SST but predominantly sub-surface temperatures (below 100 m) in the SBB. They also indicate that either the Crenarchaeota change depth habitat or that the relative contributions of surface and deep-water signals change during times of upwelling when TEX_{86} reflects shallower water temperatures. Analyses of TEX_{86} from a time series of varved sediment intervals from the depocenter of the SBB also show lower than expected TEX_{86} values, suggesting a sub-surface signal over the last 150 yrs from varying water depths with time. Like in the sediment traps, these changes are likely caused by changes in Crenarchaeota depth habitat or varying depth origin of the TEX_{86} signal as influenced by environmental factors. Thus, in contrast to TEX_{86} signals from other marine areas, TEX_{86} in the SBB cannot be used to trace changes in surface temperature. Therefore, care must be exercised when applying TEX_{86} in regions where environmental conditions lead to a crenarchaeotal GDGT signal that is derived from various depths rather than predominantly from the upper part (<100) of the water column.

Acknowledgements

We thank Gesine Mollenhauer and David Field for helpful comments, and Norel Rimbu and Wolf Berger for assistance with the interpretation of the 5.7 year cycle. David Valentine and Alex Sessions granted access to BASIN 2004 box cores. This project was supported by NWO-ALW (Project no. 152911), by EU project 6C (Contract no. EVK2-2001-00179 - 6C), and by National Science Foundation grants OCE 9807745 to A.S and OCE 0315234 to R.T.

\

References

Berger, W. H., A. Schimmelmann, and C. B. Lange (2004), Tidal cycles in the sediments of Santa Barbara Basin, *Geology*, *32*, 329-332.

Biondi, F., C. B. Lange, M. K. Hughes, and W. H. Berger (1997), Inter-decadal signals during the last millennium (AD 1117-1992) in the varve record of Santa Barbara basin, California, *Geophys. Res. Lett.*, *24*, 193-196.

Black, D. E., R. C. Thunell, and E. J. Tappa (2001), Planktonic foraminiferal response to the 1997-1998 El Niño: A sediment-trap record from the Santa Barbara Basin, *Geology*, *29*, 1075-1078.

Chavez, F. P., J. T. Pennington, C. G. Castro, J. P. Ryan, R. P. Michisaki, B. Schlining, P. Walz, K. R. Buck, A. McFadyen, and C. A. Collins (2002), Biological and chemical consequences of the 1997-1998 El Niño in central California waters, *Progr. Oceangr.*, *54*, 205-232.

Cronin, T. M., G. S. Dwyer, S. B. Schwede, C. D. Vann, and H. Dowsett (2002), Climate variability from the Florida Bay sedimentary record: possible teleconnections to ENSO, PNA and CNP, *Clim. Res.*, *19*, 233-245.

Felis, T., G. Lohmann, H. Kuhnert, S. J. Lorenz, D. Scholz, J. Pätzold, S. A. Al-Rousan, and S. M. Al-Moghrabi (2004), Increased seasonality in Middle East temperatures during the last interglacial period, *Nature*, *429*, 164-168.

Felis, T., J. Pätzold, Y. Loya, M. Fine, A. H. Nawar, and G. Wefer (2000), A coral oxygen isotope record from the northern Red Sea documenting NAO, ENSO, and North Pacific teleconnections on Middle East climate variability since the year 1750, *Paleoceanography*, *15*, 679-694.

Field, D. B., and T. R. Baumgartner (2000), A 900 year stable isotope record of interdecadal and centennial change from the California Current, *Paleoceanography*, *15*, 695-708.

Field, D. B., T. R. Baumgartner, C. D. Charles, V. Ferreira-Bartrina, and M. D. Ohman (2006), Planktonic foraminifera of the California Current reflect 20th-century warming, *Science*, *311*, 63-66.

Hardee, M., and R. Thunell (2006), Calibration of the alkenone $U^{K'}_{37}$ proxy in the Santa Barbara Basin using multiple oceanographic datasets, *Eos*, in press.

Herbert, T. D., J. D. Schuffert, D. Thomas, C. Lange, A. Weinheimer, A. Peleo-Alampay, and J. C. Herguera (1998), Depth and seasonality of alkenone production along the California margin inferred from a core top transect, *Paleoceanography*, *13*, 263-271.

Herndl, G. J., T. Reinthaler, E. Teira, H. van Aken, C. Veth, A. Pernthaler, and J. Pernthaler (2005), Contribution of Archaea to total prokaryotic production in the deep Atlantic Ocean, *Appl. Environ. Microbiol.*, *71*, 2303-2309.

Hoefs, M. J. L., S. Schouten, J. W. deLeeuw, L. L. King, S. G. Wakeham, and J. S. S. Damste (1997), Ether lipids of planktonic archaea in the marine water column, Appl.Environ.Microbiol., 63, 3090-3095.

Hopmans, E. C., S. Schouten, R. D. Pancost, M. T. J. van der Meer, and J. S. Sinninghe Damsté (2000), Analysis of intact tetraether lipids in archaeal cell material and sediments by high performance liquid chromatography/atmospheric pressure chemical ionization mass spectrometry, *Rapid Comm. Mass Spectrom.*, *14*, 585-589.

Huguet, C., J. E. Cartes, J. S. Sinninghe Damsté, and S. Schouten (2006a), Marine crenarchaeotal membrane lipids in decapods: Implications for the TEX_{86} paleothermometer, *Geochem. Geophys. Geosyst.*, *7,* Q11010, doi:10.1029/2006GC001305.

Huguet, C., E. C. Hopmans, W. Febo-Ayala, D. H. Thompson, J. S. Sinninghe Damsté, and S. Schouten (2006b). An improved method to determine the absolute abundance of glycerol dibiphytanyl glycerol tetraether lipids. *Org. Geochem., 37*, 1036-1041.

Jevrejeva, S., J. C. Moore, and A. Grinsted (2004), Oceanic and atmospheric transport of multiyear El Niño-Southern Oscillation (ENSO) signatures to the polar regions, *Geophys. Res. Lett.*, *31*. doi:10.1029/2004GL020871.

Kaplan, A., M. A. Cane, Y. Kushnir, A. C. Clement, M. B. Blumenthal, and B. Rajagopalan (1998), Analyses of global sea surface temperature 1856-1991, *J. Geophy. Res. Oceans*, *103*, 18567-18589.

Karner, M. B., E. F. DeLong, and D. M. Karl (2001), Archaeal dominance in the mesopelagic zone of the Pacific Ocean, *Nature*, *409*, 507-510.

Kennedy, J. A., and S. C. Brassell (1992), Molecular records of twentieth-century El Niño events in laminated sediments from the Santa Barbara basin, *Nature*, *357*, 62-64.

Könneke, M., A. E. Bernhard, J. R. de la Torre, C. B. Walker, J. B. Waterbury, and D. A. Stahl (2005), Isolation of an autotrophic ammonia-oxidizing marine archaeon, *Nature*, *437*, 543-546.

Lynn, R.J., C.A. Collins, A. W. Mantyla, F. B. Schwing, T. Baumgartner, T. L. Hayward, T. Murphree, K. M. Sakuma, J.Garcia, K. H. Hyrenbach, A. Shanke and M.J. Tegner (1998), The state of the California current, 1997-1998: Transition to El Niño conditions, *CalCOFI Rep., 39*, 25-49.

Mantua, N. J., S. R. Hare, Y. Zhang, J. M. Wallace, and R. C. Francis (1997), A Pacific interdecadal climate oscillation with impacts on salmon production, *Bull. Amer. Met. Soc.*, *78*, 1069-1079.

Massana, R., E. F. DeLong, and C. Pedrós-Alió (2000), A few cosmopolitan phylotypes dominate planktonic archaeal assemblages in widely different oceanic provinces, *Appl. Environ. Microbiol.*, *66*, 1777-1787.

Murray, A. E., A. Blakis, R. Massana, S. Strawzewski, U. Passow, A. Alldredge, and E. F. DeLong (1999), A time series assessment of planktonic archaeal variability in the Santa Barbara Channel, *Aquat. Microbiol. Ecol.*, *20*, 129-145.

Pak, D.K., Lea, D.W., and Kennett, J.P., (2004).Seasonal and interannual variations in Santa Barbara Basin water temperatures observed in sediment trap foraminiferal Mg/Ca, *Geochem. Geophys. Geosyst*., *5,* doi:10.1029/2004GC000760.

Pearson, A., A. P. McNichol, B. C. Benitez-Nelson, J. M. Hayes, and T. I. Eglinton (2001), Origins of lipid biomarkers in Santa Monica Basin surface sediment: A case study using compound-specific $D^{14}C$ analysis, *Geochim. Cosmochim. Acta*, *65*, 3123-3127.

Powers, L. A., T. C. Johnson, J. P. Werne, I. S. Castañeda, E. Hopmans, J. S. Sinninghe Damsté, and S. Schouten (2005), Large temperature variability in the southern African tropics since the Last Glacial Maximum, *Geophys. Res. Lett.*, *32*, L08706-10.1029/2004GL022014.

Quinn, W. H. (1999), Climate variation in southern California over the past 2,000 years based on the El Niño Southern Oscillation, In Rose, M.R. and Wigand, P.E., editors, *Proceedings of the Southern California Climate Symposium 25 October 1991, Trends and Extremes of the Past 2000 Years, Los Angeles: Natural History Museum of Los Angeles County, Technical Reports 11*, 213-238.

Reimers, C. E., C. B. Lange, M. Tabak, and J. M. Bernhard (1990), Seasonal spillover and varve formation in the Santa Barbara Basin, California, *Limnol. Oceanogr.*, *35*, 1577-1585.

Schimmelmann, A., C. B. Lange, and W. H. Berger (1990), Climatically controlled marker layers in Santa Barbara Basin sediments and fine-scale core-to-core correlation, *Limnol. Oceanogr.*, *35*, 165-173.

Schimmelmann, A., and C. B. Lange (1996), Tales of 1001 varves: a review of Santa Barbara Basin sediment studies. In: (A.E.S. Kemp, ed.), *Palaeoclimatology and Palaeoceanography from Laminated Sediments*. Geological Society (of London), Special Publication No. *116*, pp. 121-141.

Schimmelmann, A., C. B. Lange, E. B. Roark, and B. L. Ingram (2006), Resources for paleoceanographic and paleoclimatic analysis: A 6,700-year stratigraphy and regional reservoir-age (ΔR) record based on varve counting and ^{14}C-AMS dating for the Santa Barbara Basin, offshore California, USA. *J. Sed. Res., 76*, 73-79.

Schulz, M. and M. Mudelsee, (2002), REDFIT: estimating red-noise spectra directly from unevenly spaced paleoclimatic time series. *Comp. Geoscien., 28*, 421-426.

Schwing, F. B., T. L. Hayward, K. M. Sakuma, T. Murphree, A. S. Mascarenas, S. I. L. Castillo, A. W. Mantyla, S. L. Cummings, F. P. Chavez, K. Baltz, and D. G. Ainley (1997), The state of the California Current, 1996-1997: Mixed signals from the tropics, *California Cooperative Oceanic Fisheries Investigations Reports*, *38*, 22-47.

Schouten, S., E. C. Hopmans, E. Schefuß, and J. S. Sinninghe Damsté (2002), Distributional variations in marine crenarchaeotal membrane lipids: a new tool for reconstructing ancient sea water temperatures?, *Earth Planet. Sci. Lett.*, *204*, 265-274.

Schouten, S., E. C. Hopmans, and J. S. Sinninghe Damsté (2004), The effect of maturity and depositional redox conditions on archaeal tetraether lipid palaeothermometry, *Org. Geochem.*, *35*, 567-571.

Simpson, J. S (1992), Response of the Southern California current system to the mid-latitude Northa Pacific costal warming events of 1982-1983 and 1940-1941, *Fish. Ocean., 1(1)*, 57-79.

Smith, T. M., and R. W. Reynolds (2003), Extended reconstruction of global sea surface temperatures based on COADS data (1854-1997), *J. Climate*, *16*, 1495-1510.

Smith, T. M., and R. W. Reynolds (2004), Improved extended reconstruction of SST (1854-1997), *J. Climate*, *17*, 2466-2477.

Thunell, R. (1998), Particle fluxes in a coastal upwelling zone: Sediment trap results from Santa Barbara Basin, California, *Deep-Sea Res., 45*, 1863-1884.

Thunell, R., E. Tappa, C. Pride, and E. Kincaid (1999), Sea-surface temperature anomalies associated with the 1997-1998 El Nino recorded in the oxygen isotope composition of planktonic foraminifera, *Geology*, *27*, 843-846.

Thunell, R. C., E. Tappa, and D. M. Anderson (1995), Sediment fluxes and varve formation in Santa-Barbara Basin, offshore California, *Geology*, *23*, 1083-1086.

Weinheimer, A. L., J. P. Kennett, and D. R. Cayan (1999), Recent increase in surface-water stability during warming off California as recorded in marine sediments, *Geology*, *27*, 1019-1022.

Wuchter, C., B. Abbas, M. J. L. Coolen, L. Herfort, J. van Bleijswijk, P. Timmers, M. Strous, E. Teira, G. J. Herndl, J. J. Middelburg, S. Schouten, and J. S. Sinninghe Damsté (2006a), Archaeal nitrification in the ocean, *PNAS*, *103*, 12317-12322.

Wuchter C., S. Schouten, S. G. Wakeham, and J. S. Sinninghe Damsté (2006b), Archaeal tetraether membrane lipid fluxes in the northeastern Pacific and the Arabian Sea: Implications for TEX_{86} paleothermometry. *Paleoceanography*, *21,* PA4208-1-PA4208-9.

Wuchter, C., S. Schouten, S. G. Wakeham, and J. S. Sinninghe Damsté (2005), Temporal and spatial variation in tetraether membrane lipids of marine Crenarchaeota in particulate organic matter: Implications for TEX_{86} paleothermometry, *Paleoceanography*, *20,* doi:10.1029/2004PA001110

Wuchter, C., S. Schouten, M. J. L. Coolen, and J. S. Sinninghe Damsté (2004), Temperature-dependent variation in the distribution of tetraether membrane lipids of marine Crenarchaeota: Implications for TEX_{86} paleothermometry, *Paleoceanography*, *19 (4)*, doi:10.1029/2004PA001041.

Zhao, M., G. Eglinton, G. Read, and A. Schimmelmann (2000), An alkenone ($U_{37}^{K'}$) quasi-annual sea surface temperature record (A.D. 1440 to 1940) using varved sediments from the Santa Barbara Basin. *Org. Geochem.*, *31*, 903-917

Chapter 6

Selective preservation of soil-derived glycerol dialkyl glycerol tetraether lipids in oxidized marine sediments

Carme Huguet, Gert J. de Lange, Jung Hyun Kim, Jaap S. Sinninghe Damsté, Stefan Schouten

Manuscript in preparation

Abstract

Burial of organic carbon (OC) in marine sediments is one of the major sinks for carbon and most of this burial takes place on the continental margins. Terrestrial organic matter (OM) is selectively preserved in (sub)oxic environments compared to marine OM but it is unclear if this is due to intrinsic chemical resilience of the terrestrial OM, or because the mineral matrix protects it from degradation. To test this we analyzed bulk organic carbon (OC), long-chain alkenones and glycerol dialkyl glycerol tetraethers (GDGTs) of oxidized and un-oxidized layers of a selection of organic-rich turbidites deposited at the Madeira Abyssal Plain (MAP). These distal, fine-grained, turbidites contain OM that first accumulated on the shelf and subsequently was redeposited in the abyssal plain. These turbidites are relatively homogenous and when exposed to bottom water oxygen this leads to an oxidation front progressing downward until the next turbidite unit is deposited. As a consequence of this oxidation, concentrations of OC, GDGTs and alkenones were reduced by one or two orders of magnitude in the oxidized upper parts of the turbidites compared to the un-oxidized lower parts, indicating substantial degradation. We also evaluated the effect of oxic degradation on two GDGTs proxies, the TEX_{86} and the BIT index. The TEX_{86} values remained unchanged upon oxidation in some turbidites but in other turbidites showed substantial changes with either increasing or decreasing values in the oxidized parts. In contrast, BIT indices were always substantially higher in the oxidized parts versus un-oxidized parts of the turbidites. The shifts in BIT and TEX_{86} indices can be explained by a strong relative increase in soil-derived GDGTs compared to the marine-derived GDGTs as a result of oxic degradation. This selective preservation of soil-derived lipids with chemical structures that are nearly identical to those of their marine counterpart suggests that the mineral matrix to which soil organic matter is attached enhanced its preservation.

6.1. Introduction

Burial of organic carbon (OC) in marine sediments is one of the major sinks for carbon on geological time with important effects on the global carbon cycle and atmospheric CO_2 levels. A large part of the OC burial takes place on continental margins [*Hedges and Keil,* 1995]. At these locations both marine and terrestrial OC, the latter mainly transported by rivers, are deposited. During deposition, this OC is substantially degraded, especially under oxic or sub-oxic conditions. However, terrestrial OC is, in general, better preserved compared to marine organic matter [e.g. *Cowie et al.,* 1998; *Hoefs et al.,* 1998a; *Burdige,* 2005]. For example, studies on turbidite sediments from the Madeira abyssal plain (MAP) reported that only 40% of the terrestrial OC was degraded while as much as 90% of the marine OC was degraded [*Prahl et al.,* 1997].

Different hypotheses have been suggested to explain the differential degradation between marine and terrestrial forms of organic carbon. Compared to marine organic compounds, certain terrestrial organic molecules such as plant waxes and lignins are relatively difficult to degrade by microbes and thus have a greater preservation potential [e.g. *de Leeuw and Largeau,* 1993]. Also, terrestrial OC is subjected to extensive oxic degradation before reaching the continental margins and therefore the terrestrial OC finally deposited would be intrinsically more resilient to degradation than marine OC (see *Hedges and Keil,* [1995] for review). Alternatively, the physicochemical packaging within the sedimentary matrix could be different for the terrestrial and marine OC [*Keil et al.,* 1994] and make the OC less accessible for microbial degradation (bio-availability). In marine sediments, much of the preserved OC is either absorbed to mineral surfaces or enclosed in particle aggregates [*Keil et al.,* 1994; *Hedges and Oades,* 1997] and more than 90% of the total organic matter in marine sediments can not be physically separated from its mineral matrix [*Hedges and Keil,* 1995]. The so-called sorptive preservation is related to the mineral surface area, with clay-size particles having a relatively higher percentage of OC [*Hedges and Keil,* 1995]. A combination of both intrinsic resilience and matrix protection has also been suggested as leading to enhanced preservation of terrestrial OC [*Prahl et al.,* 1997].

Besides having a general impact on OC preservation, oxic degradation may also affect the relative distribution of biomarker lipids. Studies of sediments deposited in the MAP [*Hoefs et al.,* 2002] and in the Arabian Sea [*Sinninghe Damsté et al.,* 2002] showed that post

depositional oxic degradation not only decreased the concentration of lipid biomarkers by several orders of magnitude, but also that the extent of the degradation was different for different compounds and thus may cause a severe bias in the biomarker distribution. An important effect of this bias is the impact it may have on organic paleoceanographic proxies such as $U^{K'}_{37}$, TEX_{86} and BIT. While some studies showed an effect of oxic degradation on alkenones and the $U^{K'}_{37}$ [*Hoefs et al.,* 1998a; *Gong and Hollander,* 1999] others only reported a decrease in alkenone abundances but no effect on the $U^{K'}_{37}$ ratio [*Prahl et al.,* 1989; *Prahl et al.,* 2003a]. On the other hand, a previous study comparing oxidized and un-oxidized cores in the Arabian Sea showed no significant differences in TEX_{86} [*Schouten et al.,* 2004]. However, the exposure time to oxygen in the latter study was relatively short compared to those in the MAP.

The MAP turbidites are an ideal site to study the effect of oxygen on OC and proxy biases as the organic matter in the sediment is relatively homogenous and oxygen diffusion into the sediment has created "oxidation fronts" which are easily identifiable [e.g. *de Lange,* 1998; *Cowie et al.,* 1998; *Hoefs et al.,* 1998a]. The MAP turbidite sediments were originally deposited on the anoxic African shelf and due to slope instability subsequently transported to the abyssal plain in a turbidity current and deposited as well mixed OC-rich turbidites in the oxic deep sea [*Cowie et al.,* 1995; *de Lange,* 1998; *Cowie et al.,* 1998; *Hoefs et al.,* 1998a]. The contact with the oxic bottom waters causes a "burn down" effect where the organic matter in the upper part of the turbidite is degraded by downward-diffusing oxygen while the lower part is left unaltered [*de Lange,* 1998]. This allows the study of the effect of oxygen degradation on the composition of OC. For example, it has been shown that oxic degradation is selective, with preferential preservation of terrestrial OC in the kerogen fraction [*Hoefs et al.,* 1998a]. Furthermore, as discussed above it has severe effects on the biomarker composition [*Hoefs et al.,* 1998b]. Thus, MAP turbidites are ideal material to study the long term mineralization processes that affect organic matter and proxies in both oxic and anoxic conditions [*de Lange,* 1998].

The aim of this study was to understand the effect that long term exposure of oxic degradation has on the abundance and composition of glycerol dialkyl glycerol tetraethers (GDGTs) and the GDGT-based proxies TEX_{86} and BIT index.

We compared the degree of degradation of GDGTs with those of OC and of long-chain alkenones and assessed the effects of oxic exposure on GDGT-based proxies.

6.2. Material and methods

6.2.1. Turbidite sediments

The Madeira Abyssal Plain has an average of 5400 m depth and covers an area of ~ 80000 km^2 at the bottom of the Canary Islands shelf [*Cowie et al.,* 1998]. The records in this area present meter-thick distal turbidites intercalated by cm-thin organic-matter poor marls [*Cowie et al.,* 1998]. The Pleistocene F-turbidite samples (see Table 1) are from core 90P22, which was recovered at 32ºN 03.0', 24ºW12.1' during the 1990 R/V Tyro cruise. The Pliocene/Miocene samples for this study (see Table 2) were collected on board the R/V JOIDES Resolution cruise, ODP Leg 157. The samples were stored in geochemical bags and were kept and transported dark and frozen from the ship to the laboratory [*de Lange,* 1998]. The five organic-rich turbidites used for this study are from different times of deposition: The F-turbidite emplacement took place ~127 Ka, whereas turbidites T2, T6, T10 and T13 (see table 2 for ODP codes) have emplacement times of up to 14 Ma. The F-turbidite was sampled in higher resolution (8 samples) while 3 or 4 samples were taken from turbidites T2, T6, T10 and T13**.**

6.2.2. TOC and $\delta^{13}C$ TOC

Total organic carbon content (TOC) and its stable isotope composition $\delta^{13}C_{org}$ were done on freeze-dried samples using Fisons 3100 Elemental analyzer coupled to an isotope ratio mass spectrometer (see *de Lange,* [1998] for details).

6.2.3. Lipid extraction

Freeze-dried sediment samples were extracted using an Accelerated Solvent Extractor 200 (ASE 200, DIONEX) with a mixture of dichloromethane (DCM) and methanol (MeOH) (9:1, vol:vol) at 100°C and $7.6 \cdot 10^6$ Pa. A known amount (1-2 µg) of C_{46} GDGT internal standard was added to the total extract to measure absolute GDGT abundances as described in [*Huguet et al.,* 2006]. An aliquot of each total extract was separated into an alkenone and a polar fraction, using a glass pipette column filled with activated alumina, and sequentially

eluting with hexane/DCM (1:1 vol:vol) and DCM/MeOH (1:1, vol:vol) yielding the alkenone and polar fraction, respectively.

6.2.4. Alkenone analysis

For quantification, an internal standard, a deuterated ante-iso C_{22} alkane, was added to the alkenone fraction. The alkenone fraction was saponified with 1 N KOH in 96:4 MeOH/H_2O for 1 h at 100°C. After saponification, the neutral fraction containing alkenones was obtained by partitioning into DCM and analyzed by capillary gas chromatography (GC) using an Agilent Technologies 6890 equipped with an auto injector and a flame ionisation detector (FID). A fused silica capillary column (50 m × 0.32 mm) coated with CP Sil 5 (film thickness 0.12 μm) was used with helium as carrier gas. The samples were dissolved in ethyl acetate and injected at 70°C. The oven was programmed to heat to 130°C at 20 °C/min and then at 4°C/min to 320°C at which it was held for 25 min. Alkenone analyses were performed at least three times. Peak areas of $C_{37:2}$ and $C_{37:3}$ alkenones were determined using the Atlas program.

6.2.5. GDGT analysis

The polar fraction was analyzed for GDGTs according to the procedure described by *Hopmans et al.* [2000]. GDGT abundances were calculated using the internal standard method as described by *Huguet et al.* [2006]. Analyses were performed in triplicate with an HP 1100 Series Liquid Chromatography-Mass Spectrometer (LC-MS) equipped with an auto-injector and ChemStation chromatography manager software. Separation was achieved on a Prevail Cyano column (2.1 x 150mm, 3μm; Alltech, Deerfield, Illinois, USA), maintained at 30°C. GDGTs were eluted isocratically first with hexane/isopropanol (99:1 %; vol:vol) for 5 min, then using a linear gradient up to 1.8 % vol of isopropanol over 45 min. Flow rate was 0.2 mL/min. After each analysis the column was cleaned by back flushing hexane/isopropanol (90:10; vol:vol) at 0.2 mL/min for 10 min. Detection was achieved using atmospheric pressure chemical ionization-mass spectrometry (APCI-MS) of the eluent using the following conditions; nebulizer pressure 60 psi, vaporizer temperature 400°C, N_2 drying gas flow 6 L/min at 200ºC, capillary voltage -3kV, corona 5 μA (~3.2kV).

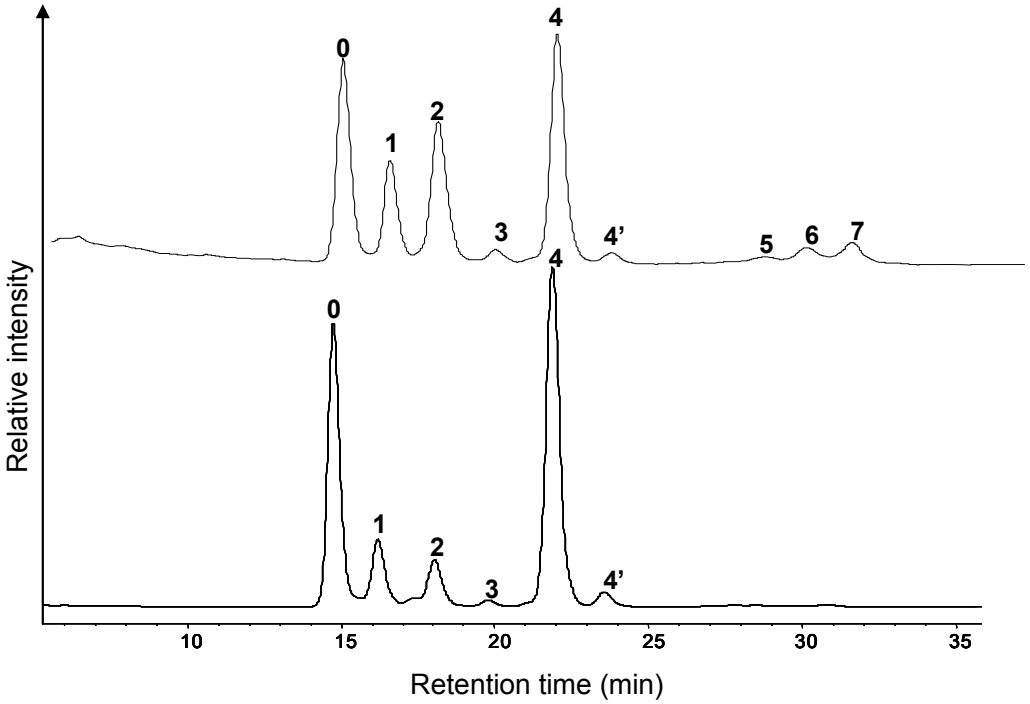

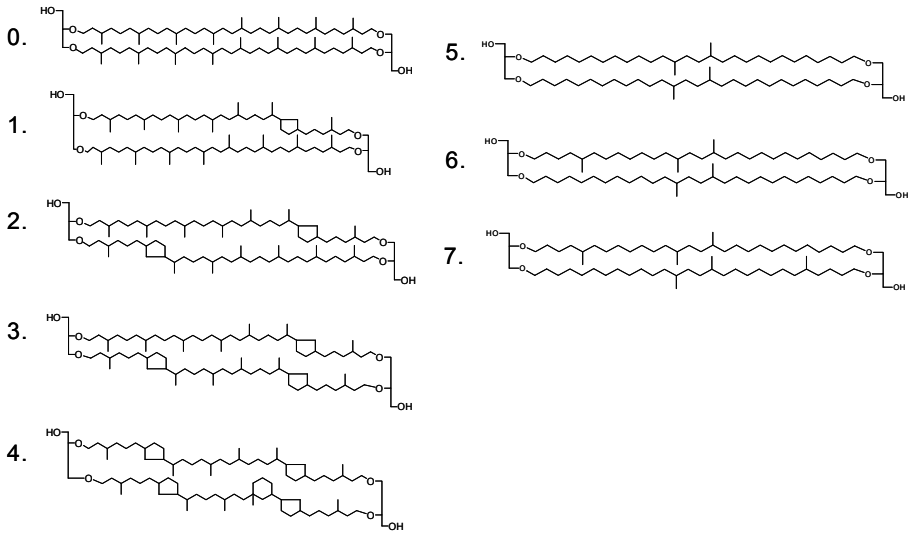

Figure 1. HPLC/MS base peak chromatograms of the F-turbidite oxidized sample at 1071 cm (upper panel) and un-oxidized sample at 1154 cm (lower panel). The numbers refer to structures of GDGTs shown below. The GDGTs on the left hand side (from 0-4') are isoprenoid GDGTs while branched GDGTs (5, 6 and 7) are in the right hand side.

Single Ion Monitoring (SIM) was used instead of full mass scanning because SIM increases the signal-to-noise-ratio and thus improves reproducibility [*Schouten et al* 2007]. SIM was set to scan the five $[M+H]^+$ ions of the GDGTs and the three $[M+H]^+$ ions of the branched tetraethers with a dwell time of 237 ms for each ion.

The TEX_{86} ratio was calculated based on the relative abundance of GDGTs as follows [*Schouten et al.,* 2002]:

$$TEX_{86} = \frac{GDGT\,2 + GDGT\,3 + GDGT\,4'}{GDGT\,1 + GDGT\,2 + GDGT\,3 + GDGT\,4'} \quad [1]$$

The numbers correspond to structures in Fig. 1. The TEX_{86} values relate to temperature according to the following empirical relationship [*Schouten et al.,* 2002]:

$$TEX_{86} = 0.015 \cdot T + 0.28 \quad [2]$$

The relative abundance of branched tetraethers (GDGT 5, 6 and 7) and crenarchaeol, GDGT 4, (Fig.1) were used to calculate the BIT index as follows [*Hopmans et al.,* 2004]:

$$BIT = \frac{[GDGT\,5 + GDGT\,6 + GDGT\,7]}{[GDGT\,5 + GDGT\,6 + GDGT\,7 + GDGT\,4]} \quad [3]$$

6.3. Results

6.3.1. TOC and $\delta^{13}C$ TOC

The division between the oxidized and un-oxidized part of the turbidites was initially established visually and then confirmed by the large changes in TOC and $\delta^{13}C_{TOC}$ [*Prahl et al.,* 1989; *de Lange,* 1992; *de Lange,* 1998] (Figs. 2 and 3). In the F-turbidite the TOC ranges from 0.2 to 0.9 wt % (Fig. 2a, Table 1) and shows similar values for the un-oxidized portion (0.9±0.04 wt %) while the TOC decreases sharply in the oxidized area (grey area in Fig. 2) in agreement with previous observations. The $\delta^{13}C_{TOC}$ shows a shift towards more negative values, from -20.3 ‰ in the un-oxidized part to ca. -23 ‰ in the oxidized part (Fig. 2b).

In the T2, T6, T10 and T13 turbidites the TOC content ranges from 0.16 to 1.6 wt % (Fig. 3a, Table 2), showing consistently higher values for the un-oxidized part and lower values for the oxidized upper part (grey area in Fig. 3) in agreement with the F-turbidite results. The $\delta^{13}C_{TOC}$ shows a shift towards more negative values, and ranges from -19 ‰ in the un-oxidized part to -22 ‰ in the oxidized part (Fig. 3b).

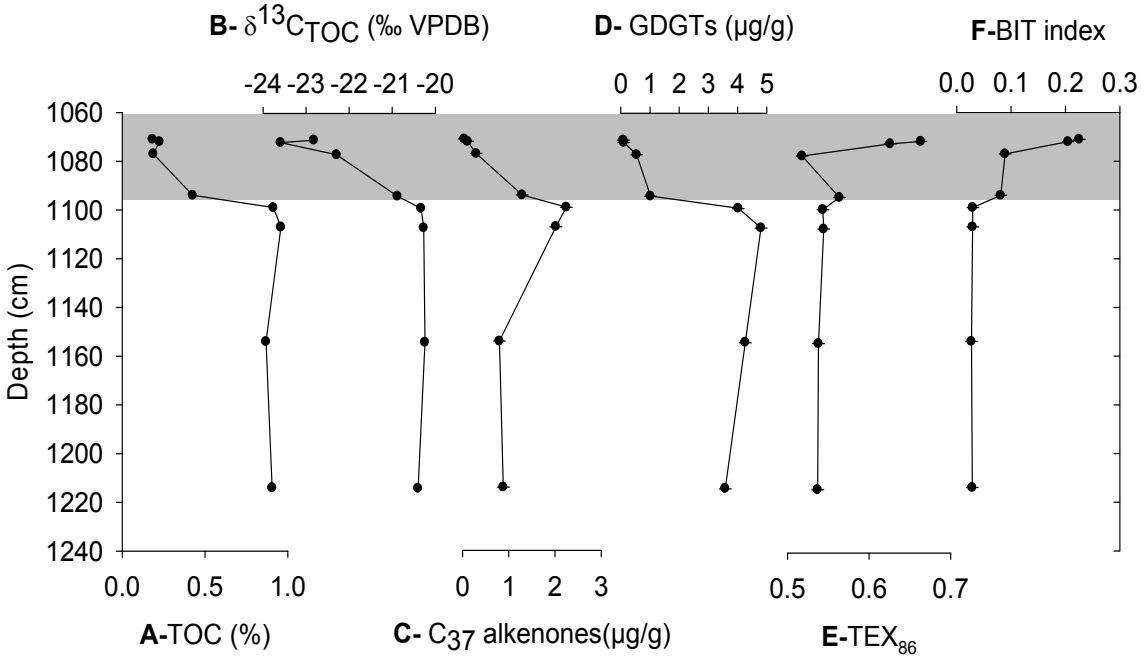

Figure 2. Profiles of A) TOC, B) $\delta^{13}C_{TOC}$, C) C_{37} alkenones abundance, D) GDGTs abundance, E) TEX_{86} and F) BIT index across the oxidation front in the F-turbidite. The oxidized part of the turbidite is indicated by the grey area.

Core code	Depth (cm)	Interval (cm)	TOC (wt%)	GDGTs (µg/g)	C_{37} alkenone (µg/g)
90P22-2	1071	0.5	0.18	0.09	0.04
90P22-2	1072	0.7	0.23	0.10	0.11
90P22-2	1077	1	0.19	0.54	0.30
90P22-2	1094	2	0.43	1.02	1.29
90P22-2	1099	1	0.91	4.02	2.25
90P22-2	1107	1	0.96	4.80	2.02
90P22-2	1154	1	0.87	4.26	0.80
90P22-2	1214	1	0.91	3.58	0.88

Table 1. Percentage of TOC (wt %) and concentrations of GDGTs and C_{37} alkenones in the F-turbidite with depth. Grey rows indicate oxidized samples.

6.3.2. Long -chain alkenones

In general, concentrations of C_{37} alkenones decrease sharply from the un-oxidized to the oxidized parts in the turbidites (Figs. 2 and 3). For the F-turbidite C_{37} alkenone abundances range between 0.04 and 2.3 µg/g with the highest value at 1100 cm depth (Fig. 2c, Table 1) and lowest values in the upper-most portion of the oxidized part (1071 cm depth). For turbidites T2, T6, T10 and T13 the C_{37} alkenone abundances range between 0.09 and 7.3 µg/g with the lowest concentrations in the oxidized part (Fig. 3c, Table 2).

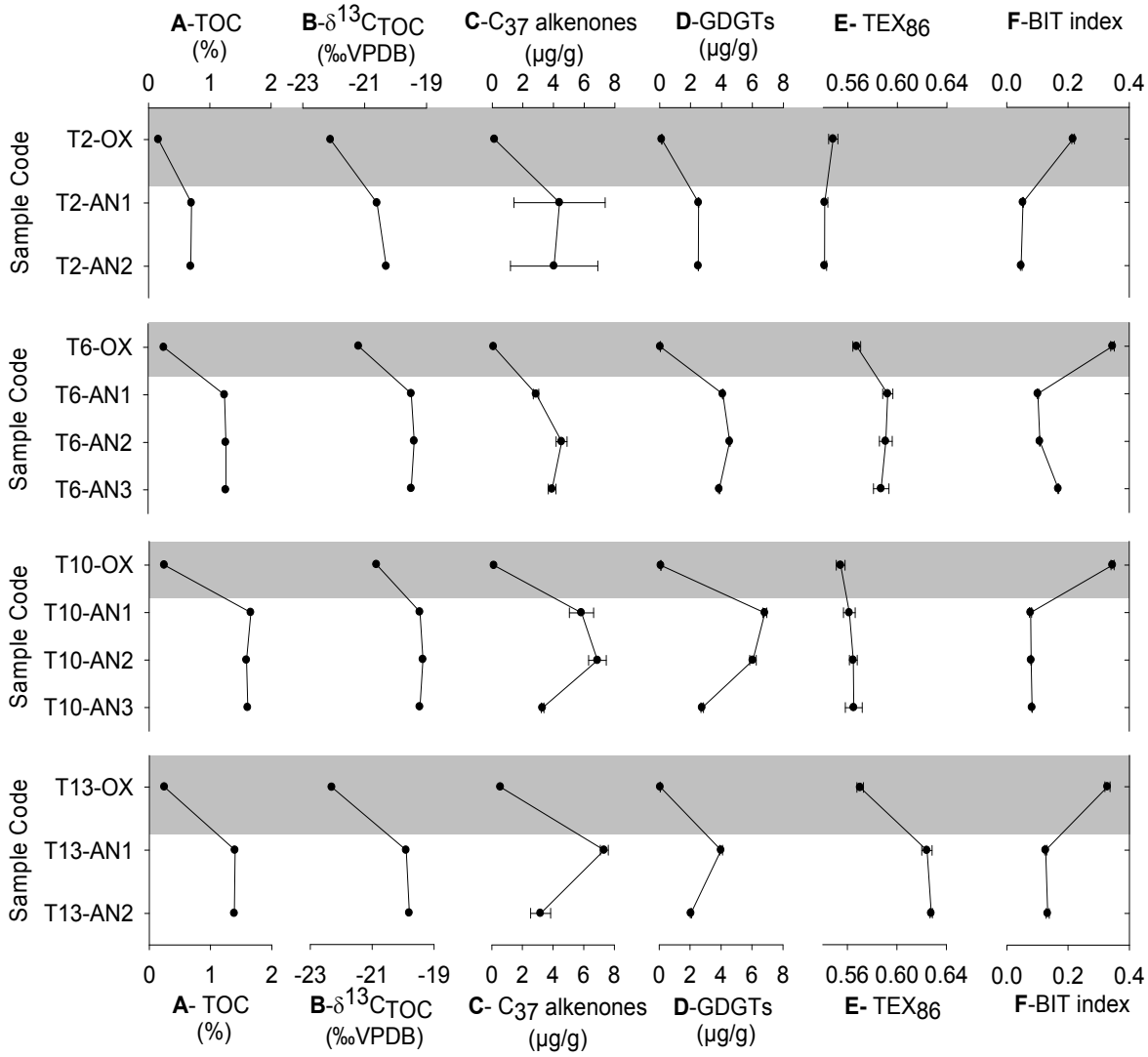

Figure 3. Profiles of A) TOC, B) $\delta^{13}C_{TOC}$, C) C_{37} alkenones abundance, D) GDGTs abundance, E) TEX_{86} and F) BIT index across the oxidation front in the T2, T6, T10 and T13 turbidites. The oxidized parts of the turbidites are indicated by the grey areas.

ODP code	Interval (cm)	Sample Code	TOC (wt%)	GDGTs (µg/g)	C_{37} alkenones (µg/g)
COW/951A/7H/6/71-77	6	T2-OX	0.16	0.14	0.16
COW/951A/7H/6/88-93	5	T2-AN1	0.70	2.52	4.40
COW/951A/7H/6/103-112	9	T2-AN2	0.69	2.50	4.04
COW/951A/25X/3/73-79	6	T6-OX	0.26	0.05	0.09
COW/951A/25X/3/96-104	8	T6-AN1	1.25	4.09	2.86
COW/951A/25X/4/42-50	8	T6-AN2	1.27	4.53	4.53
COW/951A/25X/4/108-117	9	T6-AN3	1.27	3.85	3.91
COW/952A/15H/1/6-14	8	T10-OX	0.25	0.08	0.12
COW/952A/15H/1/67-72	5	T10-AN1	1.66	6.80	5.83
COW/952A/15H/2/59-67	8	T10-AN2	1.59	6.03	6.87
COW/952A/15H/3/18-26	8	T10-AN3	1.61	2.75	3.29
COW/952A/27X/4/44-50	6	T13-OX	0.25	0.08	0.57
COW/952A/27X/4/61-71	10	T13-AN1	1.40	4.01	7.34
COW/952A/27X/4/82-92	10	T13-AN2	1.39	2.06	3.19

Table 2. Percentage of TOC (wt %) and concentrations of GDGTs and C_{37} alkenones in the T2, T6, T10 and T13 turbidites with depth. Grey rows indicate oxidized samples.

6.3.3. GDGTs

The total GDGT abundances in the F-turbidite substantially decrease from ca. 5 µg/g in the un-oxidized part to 0.1 µg/g in the upper oxidized part (Fig. 2d, Table 1). The other four turbidites show similar trends with total GDGT abundances ranging between ca. 7 and 0.05 µg/g with the lowest values always corresponding to the oxidized part of the turbidite (Fig. 3d, Table 2). Significant changes in TEX_{86} are observed in some turbidites. The largest difference is found in the F-turbidite where the lowest TEX_{86} value is 0.54±0.004 in the un-oxidized part and is up to a 0.66±0.001 in the oxidized part (Fig. 2e). The other four turbidites have different patterns with T2 and T10 turbidites showing no significant differences in TEX_{86} values whilst the T6 and especially the T13 turbidite show a significant change from higher TEX_{86} in the un-oxidized part of 0.59±0.005 and 0.63±0.003, respectively, to lower TEX_{86} in the oxidized part of 0.57±0.003, in both cases (Fig. 3e). These changes in TEX86 values correspond in case of the F-turbidite to an increase in reconstructed SST of ca. 10ºC and in the case of the T6 and T13 turbidites to a decrease of ca. 6ºC when using equation [2].

The BIT index showed in all instances an increase from the un-oxidized to the oxidized part of the turbidites. In the F-turbidite, BIT values change from 0.03 in the un-oxidized to 0.23 in the oxidized part (Fig. 2f). T2, T6 T10 and T13 turbidites also show strong changes with values in the un-oxidized area as low as 0.05 increasing up to 0.35 in the oxidized parts (Fig. 3f).

Depth (cm)	TOC (%)	C_{37} alkenone (%)	Total GDGTs (%)	GDGT-0 (%)	GDGT-1 (%)	GDGT-2 (%)	GDGT-3 (%)	GDGT-4 (%)	GDGT-4' (%)	GDGT-5 (%)	GDGT-6 (%)	GDGT-7 (%)
1071	20	2	2	2	3	7	5	2	2	7	29	24
1072	25	7	2	2	3	5	4	2	2	10	25	27
1077	21	20	13	14	13	13	11	12	9	19	70	58
1094	47	87	24	23	23	25	26	24	28	65	70	90

Table 3. Preservation factor of TOC, C_{37} alkenones and total GDGTs as well as different GDGT isomers in the F-turbidite with depth. The preservation factor for each turbidite was calculated as the relative percentage normalized on the average concentration of that compound in the un-oxidized part of the turbidite.

Sample Code	TOC (%)	C37 alkenones (%)	Total GDGTs (%)	GDGT-0 (%)	GDGT-1 (%)	GDGT-2 (%)	GDGT-3 (%)	GDGT-4 (%)	GDGT-4' (%)	GDGT-5 (%)	GDGT-6 (%)	GDGT-7 (%)
T2-OX	23	4	6	5.3	5.2	5.2	5.8	4.9	5.7	24.5	21.0	33.0
T6-OX	21	2	1	1.0	1.1	0.8	0.9	0.8	2.4	3.0	4.3	3.9
T10-OX	15	2	2	1.5	1.5	1.5	1.3	1.2	1.4	6.3	6.4	8.9
T13-OX	18	8	2	3.4	2.4	2.5	1.4	1.7	1.2	7.2	4.4	5.4

Table 4. Preservation factor of TOC, C_{37} alkenones and total GDGTs as well as different GDGT isomers in the T2, T6, T10 and T13. The preservation factor for each turbidite was calculated as the relative percentage normalized on the average concentration of that compound in the un-oxidized part of the turbidite.

6.4. Discussion

6.4.1. Selective degradation of OC

It is clear from our results that both GDGTs and C_{37} alkenones show a strong decline in concentration in the oxidized part of the turbidites and are thus severely degraded upon long-term exposure to oxygen. This is in agreement with previous studies that showed that both alkenones [*Prahl et al.,* 1989; *Hoefs et al.,* 1998a; *Hoefs et al.,* 1998b; *Gong and Hollander,* 1999; *Prahl et al.,* 2003b] and GDGTs [*Sinninghe Damsté et al.,* 2002; *Schouten et al.,* 2004] are degraded under (sub)oxic conditions. We calculated a preservation factor to establish the relative degree of preservation of the different compounds in the oxidized part of the turbidites (Tables, 3 and 4). The preservation factor for each compound in the oxidized samples was calculated as a relative percentage of the average compound concentration in the unoxidized part [cf. *Hoefs et al.*, 2002]. The degree of degradation of both GDGTs and C_{37} alkenones is more extensive than the general OC decline as, e.g., 20% of the original TOC is still present in the upper sample of the oxidized part of the F-turbidite whereas only 2% of the GDGTs and C_{37} alkenones are still present in that sample (Tables 3). In the case of the T2, T6, T10 and T13 turbidites the TOC declines down to 15-23% while the GDGTs and C_{37} alkenones preservation range from 1 to 8% (Table 4). In general there seems to be no large difference between the relative preservation of total GDGTs and C_{37} alkenones (Table 4), suggesting that GDGTs and C_{37} alkenones are degraded to a similar extent. It should be noted that, unlike the TOC profiles, GDGTs and C_{37} alkenone concentrations vary to some extent in the un-oxidized part (Table 1 and 2) of the turbidites suggesting that they are perhaps not as homogeneous as previously thought. Nonetheless, both the calculated preservation factor (Tables 3 and 4) and the degradation profiles (Figs, 2 and 3) show a strong effect of oxic degradation on GDGTs and C_{37} alkenones indicating that long-term exposure to oxygen will strongly reduce the concentration of both types of biomarkers.

In general, alkenones, exclusively of marine origin, and total GDGTs, of mixed terrestrial and marine origin, show similar preservation factors. However, calculation of the preservation factor of individual GDGT isomers shows that there is a differential preservation of GDGTs with some isoprenoid GDGT are substantially more degraded, especially when compared to the branched GDGT 5, GDGT 6 and GDGT 7.

For the F-turbidite only 2 % of the original GDGT 0, GDGT 4 and GDGT 4' concentration is left in the upper oxidized part (Table 3). In contrast, ca. 24-29% of the branched GDGT 6 and GDGT 7 is left in the uppermost section of the oxidized part, which represents an even higher preservation than that of TOC (Table 3). For the T2, T6, T10 and T13 turbidites the same trends are observed (Table 4), with GDGT 5, GDGT 6 and GDGT 7 always showing the highest degree of preservation (Table 4). These differential preservations are also reflected in the BIT index which shows a large increase upon oxic degradation (Figs. 2 and 3). Thus, it is clear that the terrestrially derived branched GDGTs are much better preserved than most isoprenoid GDGTs such as crenarchaeol which are predominantly of marine origin.

There may be several reasons for the enhanced preservation of branched GDGTs. Different biomarkers can have different preservation potentials depending on their chemical structure [*de Leeuw and Largeau,* 1993; *Hoefs et al.,* 2002; *Sinninghe Damsté et al.,* 2002], and thus branched GDGTs could be chemically more resistant against degradation than isoprenoid GDGTs. However, some of the isoprenoid GDGTs are better preserved than others in each turbidite (Tables 3 and 4), and this cannot be caused by intrinsic chemical resilience. This suggests that intrinsic chemical resilience may not be the main reason why branched are better preserved than isoprenoid GDGTs. Furthermore, it is difficult to envisage why polar lipids with branched carbon skeletons should be degraded slower than isoprenoid carbon skeletons as degradation is like to start at the functionalized glycerol moiety. Finally, in general it has been observed that branched alkyl chains are more easily degradable than isoprenoid chains [*Peters et al.* 2005]. The results can be better explained by the different origins of the branched GDGTs and isoprenoid GDGTs, i.e. soil derived matter versus marine derived matter. Analysis of a collection of globally distributed soils revealed that, though in low concentration, isoprenoid GDGTs are also present in most soils and this results in terrestrial BIT indices sometimes as low as 0.5 [*Weijers et al.,* 2006]. Thus, a better preservation of terrestrial matter would also result in a better preservation of some isoprenoid GDGT isomers that are present in small quantities in the original NW African soils and would influence the TEX_{86} and BIT values as is observed in our results (Figs. 2 and 3). Depending on the relative distribution of the isoprenoid GDGTs in soils and those in the marine environment the TEX_{86} may either increase or decrease, explaining the different behaviour of the TEX_{86} in the different turbidites.

Thus, it seems that GDGTs derived from soil organic matter are much better preserved than isoprenoid GDGTs which are mainly synthesized in the marine environment. The preferential preservation of terrestrial versus marine organic organic compounds, and of OC in general, has been observed before [e.g. *Hoefs et al.,* 1998a; *Sinninghe Damsté et al.,* 2002; *Burdige,* 2005]. However, up to now it was not possible to assess if this preferential preservation was due to the chemical structure of the terrestrial organic matter, or because the mineral matrix protects it from degradation. The enhanced preservation of soil-derived isoprenoid GDGTs which are chemically nearly identical to that of their marine counterpart suggests that the mineral matrix to which soil organic matter is attached enhanced their preservation.

6.4.2 Impact of selective degradation on the TEX_{86} and BIT proxies

Our results indicate large changes in TEX_{86} values upon long term exposure to oxygen showing a different response depending on the turbidite analyzed and can lead to temperature biases of up to 10ºC. While in the F-turbidite the TEX_{86} increases after degradation, TEX_{86} values in the T6 and T13 turbidites show a decrease and in the T2 and T10 turbidites no significant changes are observed. In view of the discussion above, these results can be readily explained by an imprint of terrestrial GDGTs on the TEX_{86} values. Depending on the environment TEX_{86} values of isoprenoid GDGTs in soils can be substantially higher or lower than those in marine sediments [*Weijers et al.,* 2006]. In the un-oxidized sediment the contribution of terrestrial GDGTs is relatively minor as evidenced by the low BIT values and the contribution of isoprenoid GDGTs from soils to the total isoprenoids GDGTs will be negligible. Consequently, the TEX_{86} value is based on marine derived GDGTs. In the oxidized part, the TEX_{86} value is also substantially influenced by the isoprenoid GDGTs derived from the continent. Thus, the effect of oxic degradation on the TEX_{86} will depend on the composition of isoprenoidal GDGTs derived from the continent in the original turbidite sediment compared to that in the marine environment and our results suggest that this may vary substantially. If TEX_{86} values on the continent are higher than those in the marine environment then oxic degradation will lead to an increase in TEX_{86} values and *vice versa*. Therefore, the TEX_{86} proxy should be used with care in sediments which have been severely degraded by oxygen exposure.

However, the simultaneous measurement of the BIT index could be a tool in deciphering the impact of oxygen degradation on the TEX_{86} as large changes in TEX_{86} due to oxic degradation are always accompanied by concomitant large changes in the BIT index (see Figs. 2 and 3). Thus, in paleoclimatic records where a strong correlation is observed between the TEX_{86} and BIT index, care should be taken.

6.5. Conclusions

Our study of the Madeira abyssal plain turbidites reveals a sharp decrease in the abundance of both GDGTs and alkenones upon long term oxygen exposure. Branched GDGTs derived from the continent are degraded to a much lesser extent than isoprenoid GDGTs derived from the marine environment. This is likely due to the selective preservation of terrestrial organic matter due to mineral matrix protection. As a consequence of this BIT values increase and TEX_{86} values either decrease or increase upon long time oxygen exposure up to one order of magnitude and 10ºC, respectively. The degree and direction of change in TEX_{86} will depend on the isoprenoid GDGTs derived from the continent present in the original sediment. This suggests that care has to be taken when analyzing both TEX_{86} and BIT in cores which have been deposited under prolonged oxic conditions.

Acknowledgements

This project was supported by NWO-ALW (Project nr. 152911) ALW/NWO is thanked for their financial contribution to core 90P22 recovery and ODP 157 sampling; G. Nobbe is thanked for analytical support.

References

Burdige, D. J. (2005), Burial of terrestrial organic matter in marine sediments: A re-assessment, *Glob. Biogeochem. Cycles*, *19,* GB4011, doi:10.1029/2004GB002368.

Cowie, G. L., S. Calvert, G. J. de Lange, R. G. Keil, and J. Hedges (1998), Extents and implications of organic matter alterations at oxidation fronts in turbidites from the Madeira Abyssal Plain, *Proc.ODP,Sci.Results*, *157*, 581-589.

Cowie, G. L., J. I. Hedges, F. G. Prahl, and G. J. de Lange (1995), Elemental and Major Biochemical-Changes Across on Oxidation Front in A Relict Turbidite - An Oxygen Effect, *Geochim. Cosmochim. Acta*, *59*, 33-46.

de Lange, G. J. (1992), Distribution of Exchangeable, Fixed, Organic and Total Nitrogen in Interbedded Turbiditic Pelagic Sediments of the Madeira Abyssal-Plain, Eastern North-Atlantic, *Mar. Geol.*, *109*, 95-114.

de Lange, G. J. (1998), Oxic vs.anoxic diagenetic alteration of Turbiditic sediments in the Madeira Abyssal Plain, Eastern North Atlantic, *Proc.ODP, Sci. Results*, *157*, 573-580.

de Leeuw, J. W. and C. Largeau (1993), A review of macromolecular organic compounds that comprise living organisms and their role in kerogen, coal and petroleum formation., *Org.Geochem.*, 23-63.

Gong, C. and D. J. Hollander (1999), Evidence for differential degradation of alkenones under contrasting bottom water oxygen conditions: Implications for paleotemperature reconstruction, *Geochim. Cosmochim. Acta*, *63*, 405-411.

Hedges, J. I. and R. G. Keil (1995), Sedimentary Organic-Matter Preservation - An Assessment and Speculative Synthesis, *Mar.Chem.*, *49*, 81-115.

Hedges, J. I. and J. M. Oades (1997), Comparative organic geochemistries of soils and marine sediments, *Org. Geochem.*, *27*, 319-361.

Hoefs, M. J. L., W. I. C. Rijpstra, and J. S. Sinninghe Damsté (2002), The influence of oxic degradation on the sedimentary biomarker record I: Evidence from Madeira Abyssal Plain turbidites, *Geochim. Cosmochim. Acta*, *66*, 2719-2735.

Hoefs, M. J. L., J. S. Sinninghe Damsté, G. J. de Lange, and J. W. de Leeuw, Changes in kerogen composition across an oxidation front in Madeira Abyssal Plain turbidites as revealed by pyrolysis GC-MS, in *Proceedings of the Ocean Drilling Program, Scientific Results*, edited by P. P. E. Weaver, H.-U. Schmincke, J. V. Firth, and W. Duffield, pp. 591-607, 1998a.

Hoefs, M. J. L., G. J. M. Versteegh, W. I. C. Rijpstra, J. W. de Leeuw, and J. S. Sinninghe Damsté (1998b), Postdepositional oxic degradation of alkenones: Implications for the measurement of palaeo sea surface temperatures, *Paleoceanography*, *13*, 42-49.

Hopmans, E. C., S. Schouten, R. D. Pancost, M. T. J. Van der Meer, and J. S. Sinninghe Damsté (2000), Analysis of intact tetraether lipids in archaeal cell material and sediments by high performance liquid chromatography/atmospheric pressure chemical ionization mass spectrometry, *Rapid Comm. Mass Spectrom*, *14*, 585-589.

Hopmans, E. C., J. W. H. Weijers, E. Schefuss, L. Herfort, J. S. Sinninghe Damsté, and S. Schouten (2004), A novel proxy for terrestrial organic matter in sediments based on branched and isoprenoid tetraether lipids, *Earth Planet. Sci. Lett.*, *224*, 107-116.

Huguet, C., E. C. Hopmans, W. Febo-Ayala, D. H. Thompson, J. S. Sinninghe Damsté, and S. Schouten (2006), An improved method to determine the absolute abundance of glycerol dibiphytanyl glycerol tetraether lipids, *Org. Geochem.*, *37*, 1036-1041.

Keil, R. G., D. B. Montluçon, F. G. Prahl, and J. I. Hedges (1994), Sorptive preservation of labile organic matter in marine-sediments, *Nature*, *370*, 549-552.

Peters, K. E., C. C. Walters and J. M. Moldowan, The biomarker guide 2nd. Ed. *Vol. 2. Biomarkers and isotopes in petroleum exploration and earth history.* Cambridge University press, ISBN 0 521 83762 6, 2005.

Prahl, F. G., G. L. Cowie, G. J. de Lange, and M. A. Sparrow (2003a), Selective organic matter preservation in "burn-down" turbidites on the Madeira Abyssal Plain, *Paleoceanography*, *18 (2)*, 1052, doi:10.1029/2002PA000853.

Prahl, F. G., G. J. de Lange, S. Scholten, and G. L. Cowie (1997), A case of post-depositional aerobic degradation of terrestrial organic matter in turbidite deposits from the Madeira Abyssal Plain, *Org. Geochem.*, *27*, 141-152.

Prahl, F. G., L. A. Muehlhausen, and M. Lyle (1989), An organic geochemical assessment of oceanographic conditions at MANOP site C over the past 26,000 years., *Paleoceanography*, *4*, 495-510.

Prahl, F. G., G. V. Wolfe, and M. A. Sparrow (2003b), Physiological impacts on alkenone paleothermometry, *Paleoceanography*, *18*, (2), 1025, doi:10.1029/2002PA000803.

Schouten, S., E. C. Hopmans, E. Schefuss, and J. S. Sinninghe Damsté (2002), Distributional variations in marine crenarchaeotal membrane lipids: a new tool for reconstructing ancient sea water temperatures?, *Earth Planet. Sci. Lett.*, *204*, 265-274.

Schouten, S., E. C. Hopmans, and J. S. Sinninghe Damsté (2004), The effect of maturity and depositional redox conditions on archaeal tetraether lipid paleothermometry, *Org. Geochem.*, *35*, 567-571.

Schouten, S., C. Huguet, E.C. Hopmans, M. V.M. Kienhuis and J. S. Sinninghe Damsté (2007), Improved analytical methodology and constraints on analysis of the TEX86 paleothermometer by high performance liquid chromatography/atmospheric pressure chemical ionization-mass spectrometry. *Analy. Chem.* doi:10.1021/ac062339v

Sinninghe Damsté, J. S., W. I. C. Rijpstra, and G. J. Reichart (2002), The influence of oxic degradation on the sedimentary biomarker record II. Evidence from Arabian Sea sediments, *Geochim.Cosmochim. Acta*, *66*, 2737-2754.

Weijers, J. W. H., S. Schouten, O. C. Spaargaren, and J. S. Sinninghe Damsté (2006), Occurrence and distribution of tetraether membrane lipids in soils: Implications for the use of the TEX_{86} proxy and the BIT index, *Org. Geochem.*, *37*, 1680-1693.

Chapter 7

Twentieth century proxy records of temperature and soil organic matter input in the Drammensfjord, southern Norway

Carme Huguet, Rienk H. Smittenberg, Wim Boer, Jaap S. Sinninghe Damsté and Stefan Schouten

Organic Geochemistry in press

Abstract

The Drammensfjord, in Southern Norway, is an enclosed anoxic basin with a laminated sedimentary record. The fjord is a transition area between the marine and terrestrial environments and thus its sedimentary archive contains information on both environments. In order to reconstruct recent environmental changes in Southern Norway, two sediment cores covering the last 90 years, were analyzed. We used the Branched versus Isoprenoid Tetraether (BIT) index as an indicator of terrestrial organic mater input and compared it to the stable carbon isotopic composition of total organic carbon ($\delta^{13}C_{TOC}$). The $\delta^{13}C_{TOC}$ and BIT index show opposing trends, with $\delta^{13}C_{TOC}$ indicating an increase in terrestrial input while the BIT index suggests a decrease towards the present. This contradiction is probably due to the different sources reflected by $\delta^{13}C_{TOC}$ (vegetation, soil and anthropogenic input) and the BIT index (only soil organic matter input). In addition, an increase in the recycling of respired CO_2 within the fjord's water column could have depleted the $\delta^{13}C_{TOC}$ of the marine component towards more negative values thus seemingly indicating an increase in terrestrial input whilst the BIT index could have been affected by a reduction of riverine input and/or an increase in archaeal biomass production. The TetraEther indeX of lipids with 86 carbons (TEX_{86}) was determined as a proxy for past water surface temperatures. While some of the signal could be coming from the chemocline our results suggest that TEX_{86} indicates surface (upper 25m) temperatures. Moreover, TEX_{86} temperature patterns seem to follow variations in the historical record of averaged spring to fall Oslo air temperature suggesting the signal is produced during this period. Therefore, TEX_{86} temperature records of fjord sediment cores can potentially be a useful tool in reconstructing past variations of coastal climates.

7.1. Introduction

Fjords are the result of marine inundation of glacially eroded valleys and are diverse and unique coastal ecosystems. Fjords are often stratified, for at least large parts of the year, due to riverine fresh water in the surface layer that floats atop denser marine bottom waters and the presence of a shallow sill between the deeper waters inside and outside the fjord. As fjords are transition areas between rivers and coastal seas the terrestrial input is usually relatively high. This, coupled to the sheltered location, the prevalence of anoxic or sub-oxic conditions and sedimentation rates of more than 0.5 mm per year [*Mikalsen et al.,* 2001], often makes fjords an ideal area to obtain sediment cores for high-resolution studies [cf. *Smittenberg et al.* 2005]. Both large-scale and local climatic variability affect fjords [*Mikalsen et al.,* 2001] and these changes will be registered in the sedimentary record of the fjord, which functions as a high-resolution archive. A variety of parameters such as terrestrial input or temperature can be estimated from fjord records [e.g. *Alve*, 1991; *Mikalsen et al.,* 2001; *Filipsson and Nordberg*, 2004; *Smittenberg et al.*, 2005; *van Breugel et al.*, 2005a]. For example, previous studies in western Norwegian fjords have used $\delta^{18}O$ of foraminifera to study past sea surface temperatures (SSTs) and compared those to the North Atlantic Oscillation index (NAO) and instrumental records [*Mikalsen et al.*, 2001; *Kristensen et al*., 2004]. In both cases a strong correlation between reconstructed SST, instrumental records and NAO was found.

Determination of marine and terrestrial organic matter input in coastal environments is essential to understand the global carbon budget because a large part of the organic matter is buried there [*Wagner and Dupont* 1999 and references therein; *Hedges and Keil*, 1995]. For this reason a variety of proxies such as the C/N ratio, the carbon isotopic composition of organic carbon $\delta^{13}C_{OC}$ and terrestrial biomarkers such as *n*-alkanes are used [*Wagner and Dupont,* 1999]. However, the use of these proxies is often complicated because they are typically influenced by more than one parameter [see *Wagner and Dupont*, 1999 and *Pancost and Boot*, 2004 for reviews]. Recently a new proxy, the Branched versus Isoprenoid Tetraether (BIT) index [*Hopmans et al.*, 2004] was introduced, which, together with the above methods, can help to trace the origin of organic matter (OM) in marine sediments. This proxy uses the ratio of branched glycerol dialkyl glycerol tetraethers (GDGTs) derived from anaerobic bacteria of terrestrial origin (GDGTs 5, 6, 7; Fig. 1) [*Weijers et al.,* 2006b] and

crenarchaeol (GDGT 4; Fig.1), a GDGT synthesized by group I Crenarchaeota [*Sinninghe Damsté et al.*, 2002]. The anaerobic bacteria which synthesize the branched GDGTs are mainly found in soils and peat bogs [*Weijers et al.,* 2006a] and their lipids are subsequently transported to coastal areas via rivers [*Hopmans et al.,* 2004; *Herfort et al.,* 2006; *Kim et al.,* 2006]. In contrast, marine Group I Crenarchaeota, and thus crenarchaeol, have been found in a wide variety of aquatic environments and are distributed throughout the water column but usually more abundant in the upper hundred meters.

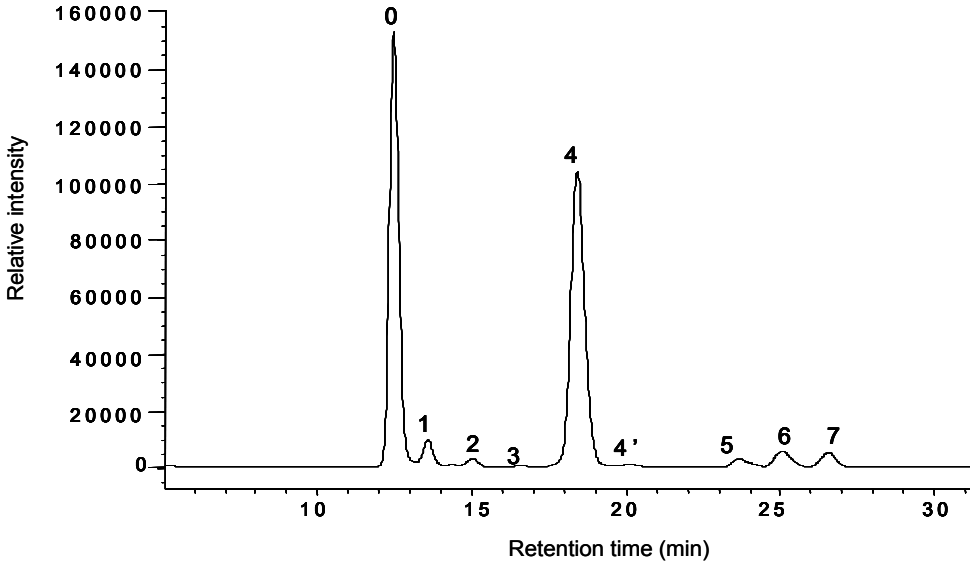

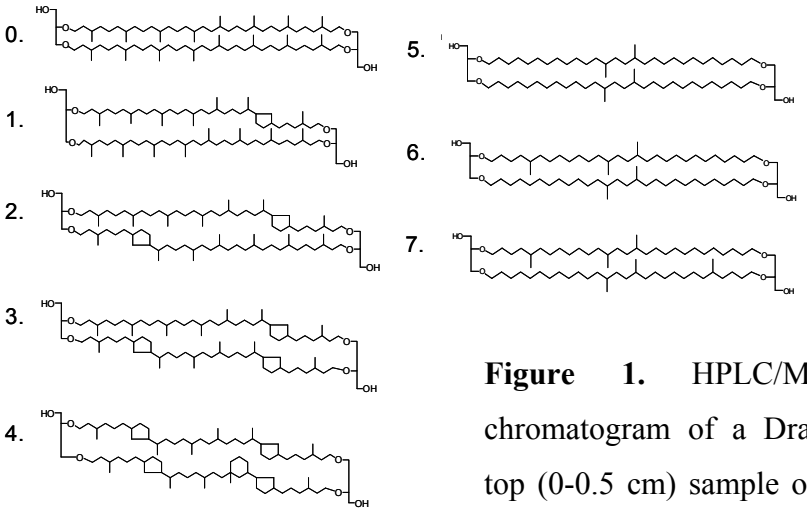

Figure 1. HPLC/MS base peak chromatogram of a Drammensfjord core top (0-0.5 cm) sample of core D2-C. The numbers refer to structures of GDGT shown below.

However, low abundances of crenarchaeol have also been found in soils [*Weijers et al.,* 2006b], lakes [*Powers et al.,* 2004] and rivers [*Herfort et al.,* 2006] although this does not seem to affect the use of the BIT index to a large degree [*Kim et al.,* 2006]. The BIT index can be used to assess the relative fluvial input of terrestrial organic mater in marine environments and ranges from 0-1 with zero referring to pure marine OM and 1 indicating pure terrestrial OM [*Hopmans et al.,* 2004].

Group I non-thermophilic Crenarchaeota biosynthesize isoprenoid GDGTs with a varying number of cyclopentyl moieties (GDGTs 0-4'; Fig.1). The distribution of isoprenoid GDGTs 0-4'of Crenarchaeota has been found to change according to temperature [*Schouten et al.,* 2002; *Wuchter et al.,* 2004]. Thus by determining the distribution of isoprenoid GDGTs, quantified with the TEX_{86}, present in sediments, the temperature at which Crenarchaeota were living can be reconstructed forming the basis of a new SST proxy, [cf. *Schouten et al.,* 2002]. Experiments with Crenarchaeota enrichment cultures and particulate OM studies have shown that this proxy is strongly correlated with temperature and is not dependent on salinity or nutrient concentration [*Wuchter et al.,* 2004; *Wuchter et al.,* 2005].

In this study we analysed the two proxies based on the distribution of GDGTs, BIT and TEX_{86}, to reconstruct both past terrestrial input and water temperatures in the Drammensfjord, Southern Norway (Fig. 2), a silled basin with anoxic bottom waters. The Drammen river feeds the Drammensfjord [*Alve*, 1990] creating a brackish surface layer and, thereby, a distinct salinity stratification, resulting in euxinic bottom water conditions in the basin. In addition, the Drammen river brings a large volume of particulate matter that is deposited in the fjord. The Drammensfjord has been subject to strong human impact especially during the last century, when domestic and agricultural waste increased drastically [*Alve*, 1991] (Fig. 3). These environmental changes and anthropogenic impacts have been recorded in the sedimentary record [*Alve,* 1995; *Smittenberg et al.,* 2005]. While previous work in the Drammensfjord provided information on various biomarkers on a centennial time scale [*Smittenberg et al.,* 2005], in this study we focus on the last century in quasi annual resolution, thereby allowing comparison with instrumental records.

7.2. Material and Methods

7.2.1. Sampling area

The Drammensfjord is a hyposaline (salinity < 32) silled basin with a length of 20 km and a width of 1.6-3 km. (Fig. 2) [*Alve,* 1991]. The Drammen river that enters at the head of the fjord creates a surface brackish water layer (salinity 1-10) on top of the saline bottom waters (salinity 31) below 40 m water depth [*Alve,* 1990].When the cores were taken the chemocline was at 40 m depth (Fig. 2) but this may change both seasonally and annually.

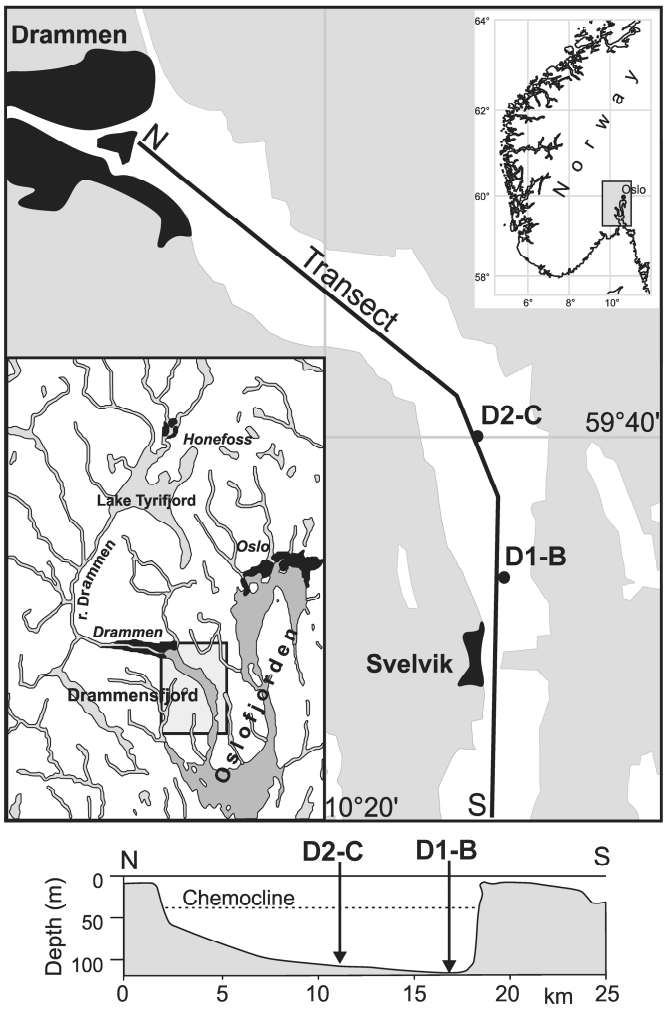

Figure 2. Map and lateral profile of Drammensfjord (modified from Smittenberg et al., 2005). The location of the two sediment cores is indicated.

The annually averaged fresh water supply is 290 $m^3 \cdot s^{-1}$. Since 1910 the river water regulations caused a smoothing of the annual fresh water supply and a shift of the main water input from winter to summer [*Alve*, 1991]. The Drammensfjord is separated from the larger Oslofjord by a sill at Svelvik (Fig. 2), which prevents the exchange of bottom waters with the open ocean. This together with degradation of OM leads to euxinic conditions in the bottom waters [*Alve*, 1991]. Oxygen depletion was first detected in 1899, and the presence of H_2S was first reported in 1933 [*Smittenberg et al.,* 2005]. Incursions of oceanic waters occur currently once every 3-5 years, mainly between November and May [*Alve*, 1995]. The sediment is deposited in a laminated structure as the anoxic bottom waters prevent infaunal activity.

7.2.2. Sediment cores

Two standard box cores (300 mm diameter, 550 mm depth) were collected with RV 'Pelagia' on 29 October 1999. Core D2-C was taken in the centre of the Drammensfjord (59°40'N 10°24'E) and Core D1-B was taken 3 km south at 59º38'N 10º26'E (Fig. 2). In both box cores, sub-cores of 70 mm in diameter were recovered, cut into 0.5 cm slices and subsequently stored frozen at -20°C. Samples were freeze dried prior to geochemical analysis. Core D2-C was analysed for total organic carbon (TOC), $\delta^{13}C$ of TOC ($\delta^{13}CTOC$) and GDGTs whilst core D1-B was analysed for GDGTs only.

7.2.3. Sediment core dating

Core D1-B was analyzed and dated previously using the specific activities of ^{137}Cs and ^{210}Pb [see *Zegers et al.*, 2003 for details]. Core D2-C was analyzed using the same ^{210}Pb method. ^{210}Pb data were decay corrected to the sampling date. Mass AR were derived with the ^{210}Pb CF/CS-model [*Appleby and Oldfield*, 1992] using a cumulative mass depth to correct for compaction. The model was then used to plot the data.

7.2.4. Bulk parameters

The TOC contents and $\delta^{13}C_{TOC}$ of total organic carbon of sediment core D2-C were determined by elemental analysis (EA)/isotope-ratio-monitoring mass spectrometry (EA/irmMS). EA/irmMS analyses were performed on decalcified (by reaction with 1 N HCl for 18 h) sediments using a Carlo Erba Flash elemental analyzer coupled to a Thermofinnigan

Delta^{PLUS} irmMS system. The total organic carbon content was determined using external standards with known carbon content. Stable carbon isotope ratios were determined using lab standards calibrated on NBS-22 oil (IAEA) [*Coplen et al.*, 2006] and reported in Vienna Pee Dee Belemnite (VPDB) notation.On average the samples were measured at least in duplicate and mostly in triplicate and the analytical error was on average 0.3% for the TOC contents and 0.16‰ for the $\delta^{13}C_{TOC}$ (Fig. 3).

7.2.5. GDGT analysis

Freeze-dried sediment samples of ca. 0.1g were extracted using an Accelerated Solvent Extractor (ASE 200, DIONEX) with a mixture of dichloromethane (DCM) and methanol (MeOH) (9:1; vol:vol) at 100°C and $7.6 \cdot 10^6$ Pa. An aliquot of each total extract was divided into an apolar and a polar fraction, using a glass pipette column filled with activated alumina, and sequentially eluting with hexane/DCM (9:1; vol:vol) and DCM/MeOH (1:1; vol:vol), respectively. Polar fractions were analyzed for GDGTs according to the procedure described by *Hopmans et al.* [2000]. Analyses were performed in triplicate with an HP 1100 Series Liquid Chromatography-Mass Spectrometer (LC-MS) equipped with an auto-injector and ChemStation chromatography manager software. Separation was achieved on a Prevail Cyano column (2.1 x 150 mm, 3 µm; Alltech, Deerfield, Illinois, USA), maintained at 30°C. GDGTs were eluted isocratically first with hexane/isopropanol (99:1; % vol:vol) for 5 min, then using a linear gradient up to 1.8 % vol of isopropanol over 45 min. Flow rate was 0.2 mL min^{-1}. After each analysis the column was cleaned by back flushing hexane/propanol (90:10; vol:vol) at 0.2 mL min^{-1} for 10 min. Detection was achieved using atmospheric pressure chemical ionization-mass spectrometry (APCI-MS) of the eluent using the following conditions; nebulizer pressure 60 psi, vaporizer temperature 400°C, N_2 drying gas flow 6 L min^{-1} at 200ºC, capillary voltage -3 kV, corona 5 µA (~3.2 kV). Single Ion Monitoring (SIM) was used instead of full mass scanning because SIM increases the signal-to-noise-ratio and thus improves reproducibility [*Schouten et al.* 2007]. SIM was set to scan the five $[M+H]^+$ ions of the isoprenoid GDGTs and the three $[M+H]^+$ ions of the branched GDGTs with a dwell time of 237 ms for each ion.

The TEX_{86} ratio was calculated based on the relative abundance of GDGTs as follows [*Schouten et al*., 2002]:

$$TEX_{86} = \frac{GDGT\,2 + GDGT\,3 + GDGT\,4'}{GDGT\,1 + GDGT\,2 + GDGT\,3 + GDGT\,4'} \quad [1]$$

The numbers correspond to structures in Fig. 1.The TEX_{86} values relate to temperature according to the following empirical relationship [*Schouten et al.*, 2002]:

$$TEX_{86} = 0.015 \cdot T + 0.28 \quad [2]$$

The branched GDGTs (GDGT 5, 6 and 7) and crenarchaeol (GDGT 4; Fig.1) were used to measure the BIT index as follows [*Hopmans et al.*, 2004]:

$$BIT = \frac{[GDGT\,5 + GDGT\,6 + GDGT\,7]}{[GDGT\,5 + GDGT\,6 + GDGT\,7 + GDGT\,4]} \quad [3]$$

where the numbers correspond to structures in Fig. 1.

An aliquot of an Arabian Sea sediment extract was measured every 10 samples to assess the analytical reproducibility. The resulting mean TEX_{86} value for 15 repeat analyses was 0.68 with a standard deviation of ±0.034, corresponding to 26.6 ± 0.5°C according to equation [2]. The BIT value of this sample was 0.02 with a standard deviation of ±0.003. TEX_{86} were measured at least three times for each sample and the standard deviation of the TEX_{86} was on average ±0.02 which according to equation [2] correspond to ±0.7ºC. The BIT samples were measured only once, thus we assume a constant analytical error of ±0.003 as calculated from the Arabian Sea sample.

7.3. Results

7.3.1. Bulk parameters

The age models of both cores are based on ^{210}Pb measurements and were fitted to a constant accumulation rate model [*Appleby and Oldfield*, 1992]. The accumulation rates (AR) of sediment of core D1-B is 750 and D2-C is 850 $g \cdot m^{-2} \cdot yr^{-1}$, in agreement with previous studies in the Drammensfjord that reported values of 500-1000 $g \cdot m^{-2} \cdot yr^{-1}$ between 1000 and 1940 [*Smittenberg et al.*, 2005].

The TOC values of the sediments recovered with core D2-C are usually around 3% with peak values of 5% in sediments deposited from 1945 to 1950 and ca. 6% in those deposited from 1965 to 1970 and in 1989 (Fig. 3a). These TOC values compared well with the 2-4.5 % TOC values reported previously for Drammensfjord sediments [*Alve,* 1990; *Alve*, 1991].

The organic carbon AR ranges between 20 and 60 $g \cdot m^{-2} \cdot yr^{-1}$ (Fig. 4a). It is relatively constant from 1923 to 1942 and it shows an increase from ca. 20 to 45 $g \cdot m^{-2} \cdot yr^{-1}$ towards 1945, then it decreases to ca. 25 $g \cdot m^{-2} \cdot yr^{-1}$ until 1951. The main increase in organic carbon AR starts in 1951 and reaches its peak value of 50 $g \cdot m^{-2} \cdot yr^{-1}$ in 1965, then the AR decreases to ca. 25 until 1980 and remains around 20 $g \cdot m^{-2} \cdot yr^{-1}$until 1989 when there is a peak of 55 $g \cdot m^{-2} \cdot yr^{-1}$ (Fig. 4a). Finally there is a small peak in organic carbon AR between 1993 and 1997 (Fig. 4a).

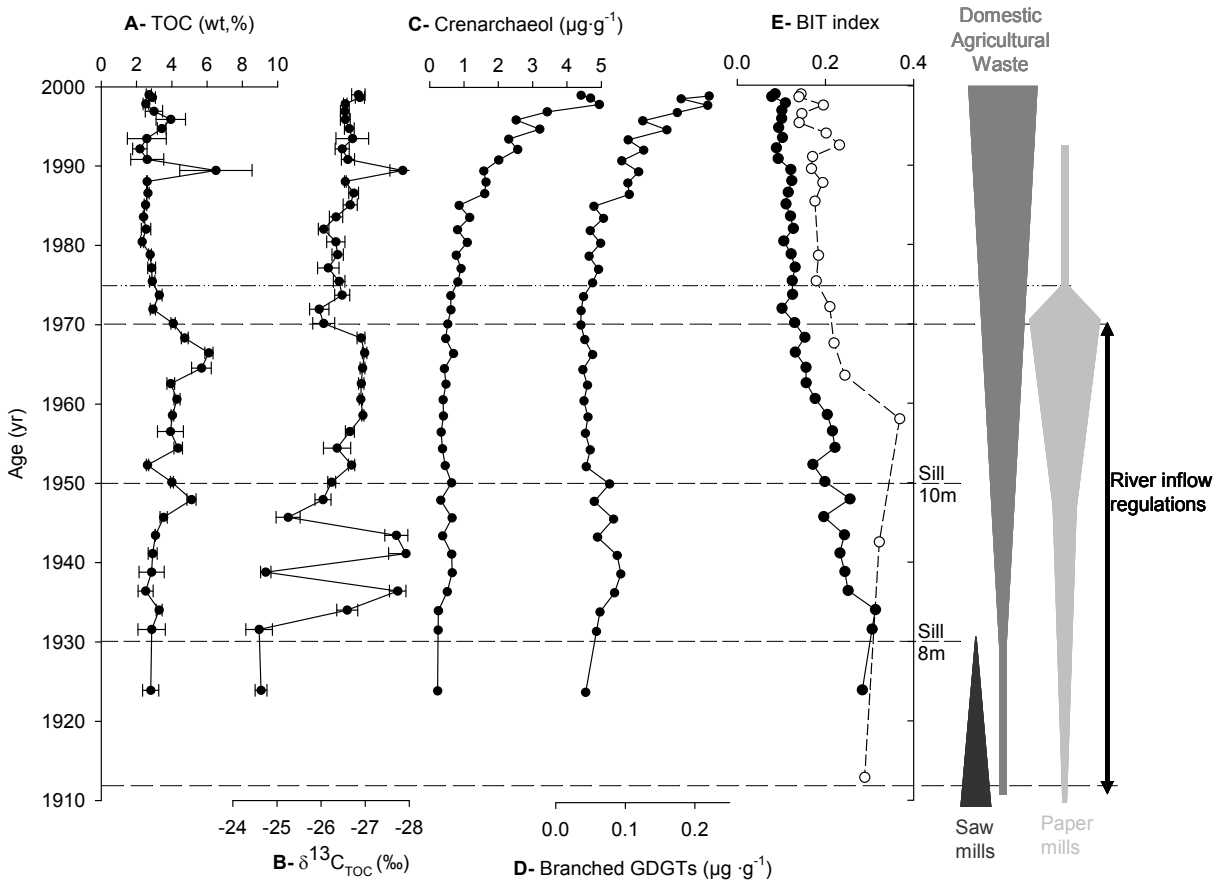

Figure 3. Bulk and GDGT data for core D2-C (filled circles) and D1-B (empty circles), (a) TOC (wt, %), (b) $\delta^{13}C_{TOC}$ (‰), (c) crenarchaeol (GDGT-4) concentration ($\mu g \cdot g^{-1}$), (d) branched GDGT concentration ($\mu g \cdot g^{-1}$) and (e) BIT index. Anthropogenic activities with a potential environmental impact on the fjord are plotted in the right hand side (adapted from *Alve* [1991]).

The $\delta^{13}C_{TOC}$ ranges from -24.6 to -27.9‰. The less ^{13}C-depleted values (-24.6‰) are recorded in the oldest sediments deposited between 1923 and 1930 (Fig. 3b). There are subsequently two negative spikes in $\delta^{13}C_{TOC}$, one in the late 1930s and another in the late 1940s (Fig. 3b). Then, $\delta^{13}C_{TOC}$ values decrease to their more ^{13}C-depleted value of -26.9‰ in 1954 and then remain around this value until 1965 when there is an increase of 1‰. From 1970 to 1999 the $\delta^{13}C_{TOC}$ values show a slight depletion in ^{13}C from -26.3‰ to -26.8‰ with the exception of the point at 1989 which shows a value of -27.9‰ (Fig. 3b).

7.3.2. GDGT concentrations and accumulation rates

GDGT analysis of the two cores reveals the presence of GDGTs 0-7 with GDGT-0 and GDGT-4 (crenarchaeol) showing the highest concetrations (Fig.1). Total GDGT concentration in core D2-C ranged from 0.5 to 11 $\mu g \cdot g^{-1}$. Concentrations of crenarchaeol in core D2-C ranges from 0.2 to 5 $\mu g \cdot g^{-1}$and show in general an increase towards the surface (Fig. 3c). The branched GDGTs (GDGTs 5, 6 and 7; Fig.1) range in concentration from 0.04 to 0.25 $\mu g \cdot g^{-1}$and their concentration profile strongly resembles that of crenarchaeol (cf. Figs. 3c and 3d). However, the concentration of branched GDGTs shows a larger increase from 1923 up to 1940 before it decreases until 1950 and show quite constant values of 0.05 $\mu g \cdot g^{-1}$ between 1950 and 1980 after which it increases to 5 $\mu g \cdot g^{-1}$ towards the surface (Fig. 3c and d). The crenarchaeol AR ranges between 0.2 and 4.2 $mg \cdot m^{-2} \cdot yr^{-1}$ showing relatively constant values between 1920 and 1990 and then increase by 2 $mg \cdot m^{-2} \cdot yr^{-1}$ from 1990-2000 (Fig. 4b). The AR of branched GDGTs varies between 0.04 and 0.2 $mg \cdot m^{-2} \cdot yr^{-1}$ and shows a pattern similar to that of crenarchaeol AR. However, the branched GDGTs AR also shows three minor peaks, one between 1930 and 1940, one in 1945 and one around 1950 (Fig. 4c).

7.3.3. BIT index and TEX_{86}

The BIT index ranges from 0.08 to 0.31 in core D2-C and from 0.11 to 0.37 in core D1-B (Fig. 3e) which compares well with BIT indices previously reported for coastal and lacustrine environments [*Hopmans et al.,* 2004]. Both cores show the same trend with decreasing BIT values up core. However, core D2-C shows a decrease of values from 1923 to 1999 while core D1-B indicates an increase from 1912 to 1958 and then a decrease towards 1999 (Fig. 3e).

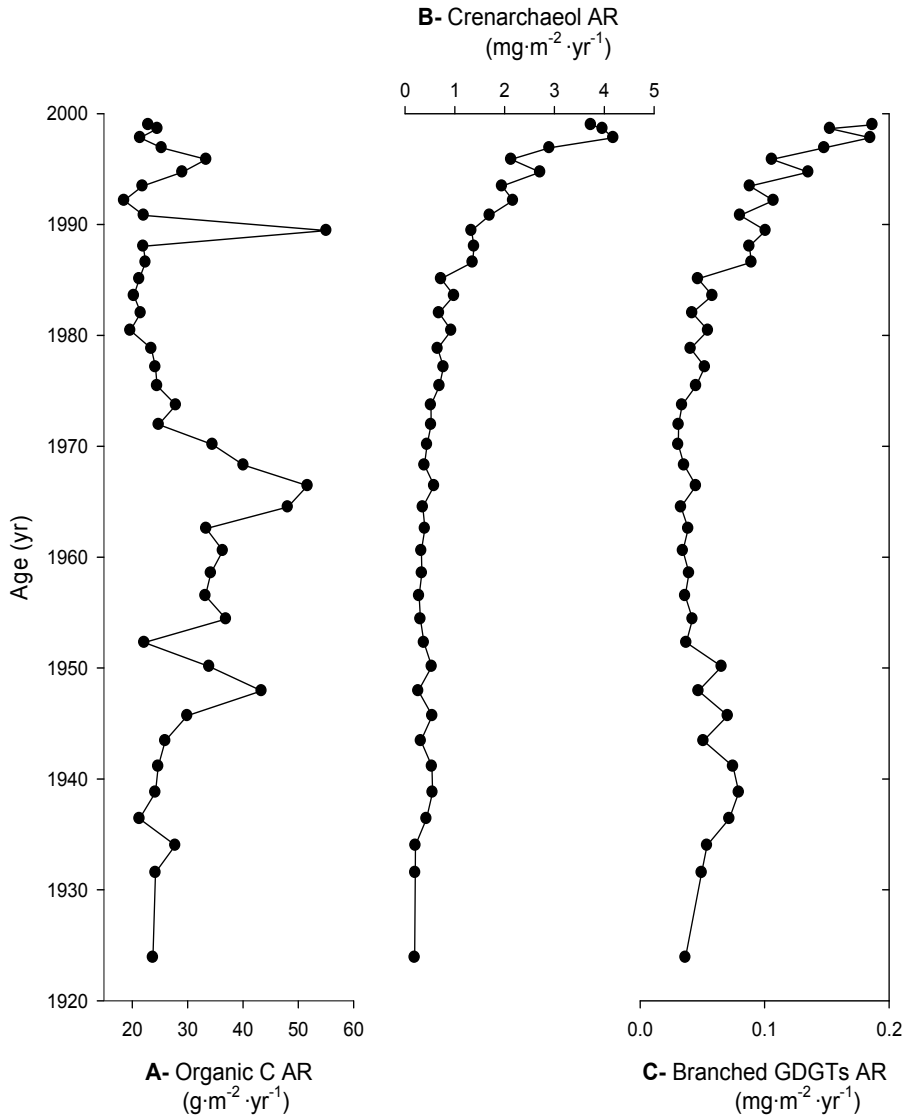

Figure. 4. Accumulations rates of (a) organic carbon ($g \cdot m^{-2} \cdot yr^{-1}$), (b) crenarchaeol ($mg \cdot m^{-2} \cdot yr^{-1}$) and (c) branched GDGTs ($mg \cdot m^{-2} \cdot yr^{-1}$) in core D2-C.

TEX_{86}-derived temperatures range between 8.2 and 12.6 Cº in core D2-C and between 8.2 and 10.5 Cº in core D1-B (Fig. 5). Both TEX_{86} records show a similar pattern although core D1-B has a lower resolution than D2-C especially between 1910 and 1960. The standard deviation intervals for each point are plotted for both cores (grey filled areas, Fig. 5) and show in general a good overlap between the two cores. TEX_{86} temperatures show two main peaks one between 1960 and 1972, and the other between 1972 and 1990 with some minor peaks between 1930 and 1940 and in 1952. TEX_{86} temperatures decrease from 1990 to 1999 (Fig. 5).

7.4. Discussion

7.4.1. Contribution of terrestrial organic matter to the fjord

The $\delta^{13}C_{TOC}$ of around -26‰ found in most of the Drammensfjord sediments is close to the average $\delta^{13}C$ of terrestrial OM (-27‰), [*Deines*, 1980; *Tyson*, 1995], suggesting that the sedimentary OM is primarily of terrigenous origin in the Drammensfjord, in agreement with conclusions from *Smittenberg et al.* [2005]. In contrast, the average BIT index of 0.2 suggests a relatively low terrestrial input and shows intermediate values when compared to other coastal environments [*Hopmans et al.*, 2004]. Similar results were observed in the south North Sea with BIT values ranging from 0.02 to 0.26 [*Herfort et al.*, 2006], but BIT values between 0.7 and 0.9 have been reported for particulate OM in rivers in the Mediterranean [*Kim et al.,* 2006] and for sediments from another Norwegian fjord [*Hopmans et al.*, 2004]. . Thus, BIT indices between 0.08-0.37 are unexpectedly low as the fjord is directly fed by the river Drammen which has a relatively large catchment area (Fig. 2) and a high river influx [*Öztürk*, 1995].

Besides seemingly contrasting indications for the relative amount of terrestrial OM in Drammensfjord, the $\delta^{13}C_{TOC}$ and BIT index trends are also different (Fig. 3). While the BIT index shows a gradual change towards more marine values in 1999, the $\delta^{13}C_{TOC}$ data seems to indicate an increase in ^{13}C-depleted terrestrial versus marine OM up core (Fig. 3). The relatively low BIT values could be explained if the relative amount of terrigenous OM would decrease from the head to the mouth of the fjord. However, the BIT values of core D1-B, in a more southern location than D2-C (Fig. 1) are slightly higher, suggesting that this can not explain the low BIT values. More likely, therefore, is that there is a relatively high input of crenarchaeol, either from production in the fjord by marine Crenarchaeota, or upstream in the extensive lake system (Fig. 2) by fresh water Crenarchaeota [cf. *Powers et al.*, 2004]. In both cases there would be a high crenarchaeol input which would result in a low BIT index. However, the difference in the source between the branched GDGTs and total terrestrial OM has to be taken into consideration as well. Branched GDGTs are only transported by rivers [*Hopmans et al.,* 2004; *Herfort et al.,* 2006; *Kim et al.,* 2006] and are primarily derived from soil OM [*Weijers et al.,* 2006b], while $\delta^{13}C_{TOC}$ is affected by the total terrestrial organic carbon input, i.e. including both soil organic matter and terrestrial vegetation.

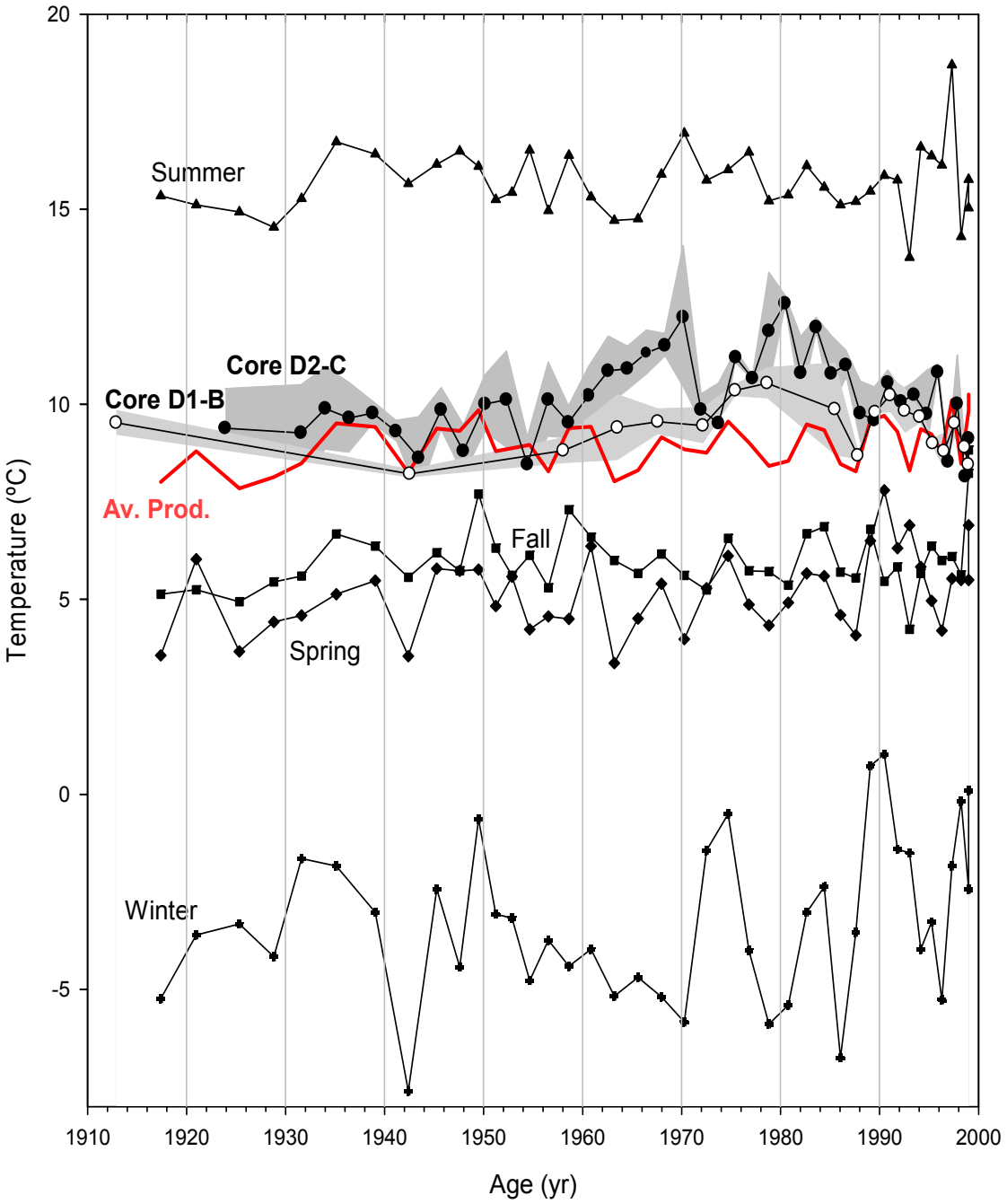

Figure 5. TEX_{86}-calculated temperatures obtained from core D2-C (filled circles) and D1-B (empty circles) compared to averaged seasonal air temperatures in Oslo for Summer (June-August), Fall (October-November), Spring (March-May) and Winter (December-February) (http://met.no/met/vanlig_var/temp.html). Average temperatures of the productive season (Av. Prod; spring, summer and fall) are plotted in red. The grey filled areas indicate the standard deviation for the TEX_{86} temperatures.

Thus, if there is a large contribution of this latter source and only a minor contribution of soil OM, this could explain the apparent discrepancy between $\delta^{13}C_{TOC}$ and the BIT index. Indeed, there has been a large input of wood and paper from industrial sources in Drammensfjord over the last century [*Alve,* 1991; Fig. 3], which will strongly contribute to the $\delta^{13}C_{TOC}$ signal and not to the BIT index. Finally, the $\delta^{13}C_{TOC}$ could be affected by a change in the isotopic composition of marine OM through recycling of respired CO_2. Decaying OM will yield ^{13}C-depleted CO_2 which can be re-used by phytoplankton, thus influencing the isotopic composition of marine OM towards more negative values [e.g. *Deevey et al.*, 1963; *Küspert*, 1982; *Wachniew and Rozanski*, 1997]. High amounts of ^{13}C-depleted CO_2 have been observed previously in lakes and fjords where there were anoxic bottom waters and where $\delta^{13}C_{TOC}$ was relatively depleted in ^{13}C [*van Breugel et al.*, 2005b]. Indeed, *Smittenberg et al.* [2005] found relatively ^{13}C-depleted crenarchaeol, suggesting that recycling of CO_2 may take place in the Drammensfjord. Thus, the relatively ^{13}C-depleted values of TOC in Drammensfjord may be partly due to relatively ^{13}C-depleted fjord OM rather than high contributions of ^{13}C-depleted terrestrial OM. These factors make it difficult to interpret the $\delta^{13}C_{TOC}$ sedimentary record.

The GDGT ARs show relatively constant values between 1923 and 1980, although the branched GDGTs AR show a small increase between 1923 and 1952. The decrease in the BIT index between 1930 and 1970 is thus mainly caused by a decrease in the AR of the branched GDGTs pointing to a relative reduction of the branched GDGTs input (Fig. 4 b and c). The latter would be related to the changes in the riverine input after the strong regulation of the river inflow since 1910 [*Bradshaw et al.,* 1991] with a reduction in floods and hence less wash out of branched GDGTs from soils into the riverine system.

The strongest increase in the ARs of both crenarchaeol and branched GDGTs is between 1980 and 1999. As the Drammensfjord is an anoxic basin and the OC AR does not show the same trend in the upper part of the sediment core (Fig. 4a) this trend seem at first sight unlikely to have been caused by diagenetic processes. However, in general, biomarkers degrade faster than bulk OM [*Hoefs et al.*, 2002]. This may be even more likely in this case since most of the bulk OM seems to be of terrestrial origin (e.g. wood) which is more resilient towards degradation than aquatic OM. Thus, the decreasing ARs of both types of GDGTs (Fig. 4) down to 1923 likely suggest anaerobic mineralization in surface sediments, as has been observed for the many biomarkers in the euxinic Black Sea [*Sun and Wakeham*, 1994].

Alternatively but less likely, the increased ARs in the top sediment may indicate that there is an increased production of both soil bacteria and crenarchaeota. The former could be related to the changes in the riverine input after the strong regulation of the river inflow since 1910 [*Bradshaw et al.*, 1991]. The latter may have been due to an increase in agricultural and urban waste in the Drammensfjord [*Alve*, 1991]. This increase in waste would in turn increase the nutrient input such as ammonia into the fjord and result in higher productivity of Crenarchaeota as part of these microbes are using ammonia as an energy source [*Könneke et al.,* 2005; *Wuchter et al*., 2006a]. This enhanced nutrient input would also stimulate phytoplankton productivity in general and not necessarily be reflected in the TOC deposition as the largest increases in TOC seem to be associated to the period of high paper mill activity (Fig. 3) and is probably a direct reflection of waste dumped in the river by the paper industry.

7.4.2. TEX_{86} temperature record

The TEX_{86} paleothermometer has been applied in marine [*Huguet et al.*, 2006] and lake [*Powers et al.*, 2005] sediment cores but never before in a transition environment like the Drammensfjord and thus our record is unique in this aspect. In principle the TEX_{86} estimates in the Drammensfjord could be compromised by high input of terrestrial GDGTs [*Weijers et al*., 2006b]. However, BIT values are in general relatively low (<0.3; Fig. 3) and there is no apparent correlation between TEX_{86} and BIT index (r^2=0.1). Thus, it seems that the TEX_{86} temperature record is not affected by terrestrial input to a substantial degree.

TEX_{86}-derived values (8.2-12.6ºC) fall in the middle of the average surface temperature range reported for the Drammensfjord (1-24ºC) [*Alve*, 1995]. As there is, to the best of our knowledge, no long term in-situ water temperatures record available for the Drammensfjord, we compared our TEX_{86} results with a historical monthly air temperature record from a weather station in nearby Oslo as a proxy for the historical changes in surface temperatures of the fjord. Unlike our D1-B core, Oslo air temperature data have an annual resolution and for this reason a variable running average smoothing was applied to the mean annual Oslo air temperature data to match the TEX_{86} temperature temporal resolution in the D1-B core (Fig. 4). The same smoothing was applied to Oslo air monthly temperatures, and the resulting values were then averaged for summer (June-August), fall (October-November), spring (March-May) and winter (December-February) and also for the productive season, i.e. spring,

summer and autumn when predominantly light and, to some degree, temperature are sufficiently high to stimulate phytoplankton growth (Fig. 5). We assume that air temperature changes will be reflected in surface water temperatures and that there is a relatively small offset due to both air water temperature equilibration and age model error. The comparison shows that TEX_{86}-derived temperatures fall between summer and spring/fall air values (Fig. 5) and that they are close to the calculated average air temperature of these three seasons, i.e. the productive season (red line Fig. 5). This suggests that the Crenarchaeota in Drammensfjord are possibly active during the spring/fall period and not during winter. In other areas high Crenarchaeota abundances have actually been noted in winter [*Murray et al.*, 1999; *Wuchter et al.*, 2006b] as then the Crenarchaeota do not need to compete for ammonia with the phytoplankton. The reason why this is different for the Drammensfjord may be the continuous high nutrient supply in the Drammensfjord throughout the year [*Alve*, 1995]. With a plentiful nutrient supply there is no need to compete with the phytoplankton for nutrients and other factors like the low winter temperatures in the area may become more limiting in archaeal productivity. Alternatively as the food web activity is greatly reduced in the Drammensfjord during the winter months this may lead to a decline in the export of GDGTs from the upper part in the water column to the sediment surface [cf. *Wuchter et al.,* 2005].

We should also consider the possibility that the TEX_{86} signal is not derived from the surface waters but from deeper in the water column. Crenarchaeota have been shown to be abundant at strong chemoclines such as in the Black Sea [*Coolen et al.* 2007] and this may lead to colder TEX_{86} temperatures than expected [*Menzel et al.,* 2006]. As the Drammensfjord has a permanent and strong chemocline, it is possible that the Crenarchaeota are living deeper in the water column at the chemocline. The chemocline depth at the time of coring was 40 m (Fig. 1) and according to *Alve* [1991; 1995] temperatures below 25 m remained around 6ºC between 1982 and 1988 in contrast to surface temperatures which ranged from 1 to 24ºC. Thus, if Crenarchaeota were only living in the chemocline we would expect no substantial changes in the TEX_{86} temperatures during this period. This is not the case as temperatures do not only change between 1982 and 1988 but are considerably higher than 6ºC (Fig.5). This leads us to conclude that at least part of the TEX_{86} signal is coming from surface waters (above 25 m). A shift in the position of the chemocline could also have resulted in the observed changes in the $TEX_{86,}$ however, in general TEX_{86} follows, within the uncertainty of

the age model, Oslo air temperature changes through time making this possibility less likely. This fitting is particularly remarkable when comparing TEX_{86} values to average air temperature for the productive season (in red, Fig. 5). This suggests a connection between atmospheric temperatures and water temperatures in the fjord. However, the 1970 and 1980 peaks in TEX_{86} temperatures are not present in the averaged productive season Oslo air temperature record. This might be the result of local factors affecting the water temperature in the fjord. It could also be the result of a shift towards higher summer production by Crenarchaeota, as while the 1970 and 1980 peaks are not present in the averaged productive season Oslo air record they are apparent in the summer Oslo air temperature record (Fig. 5).

7.5. Conclusions

The $\delta^{13}C_{TOC}$ and BIT index give contrasting results regarding the relative contribution of terrestrial OM in Drammensfjord. This is likely due to the different types of terrestrial OM recorded by these proxies, i.e. soil OM by the BIT index and vegetation and soil and vegetation OM by $\delta^{13}C_{TOC}$. Furthermore, there are uncertainties with the marine end-member value of $\delta^{13}C_{TOC}$ which can be affected by recycling of respired CO_2 within the water column of the stratified fjord. This illustrates that proxies to measure the relative contributions of the organic carbon in sediments must be used with great caution and that the use of multiple proxies is essential and complementary. The application of the TEX_{86} in this marine-terrestrial transition area yielded temperatures which are similar to the average of spring to fall (productive season) air temperatures in Oslo. This suggests that Crenarchaeota production mainly takes place during this period. Moreover TEX_{86} temperatures correlate relatively well to annual Oslo air temperature between spring and fall thus indicating a seasonal signal. Therefore, the TEX_{86} may be a suitable temperature proxy to use in transition coastal areas to estimate past temperatures.

Acknowledgements

The authors thank the crew of R/V Pelagia from the Netherlands Institute for Sea Research for their assistance in obtaining the sediment cores. Martin van der Zeijden is thanked for his assistance with TOC and $\delta^{13}C_{TOC}$ measurements.This project was supported by grants from NWO-ALW to SS and JSSD (projects. 152911 and 850.20.006, respectively). The two reviewers Dr. Andrew Revill and Dr. Mark Yunker are thanked for their constructive comments.

Reference List

Alve, E., Variations in estuarine foraminiferal biofacies with diminishing oxygen conditions in Drammensfjord, SE Norway., in Palaeoecology, biostrasratigraphy, palaeoceanography, and taxonomy of agglutinated foraminifera, edited by C. Hemleben, C.Scott D.B., M. Kaminski, and W. Kuhnt, pp. 661-694, Kluwer Academic Publishers, *Dordrecht*, 1990.

Alve, E. (1991), Foraminifera, climatic change, and pollution: a study of late Holocene sediments in Drammensfjord, southeast Norway, *The Holocene*, *1,* 243-261.

Alve, E. (1995), Benthic foraminiferal distribution and recolonization of formerly anoxic environments in Drammensfjord, southern Norway, *Mar.Micropaleontol*., *25*, 169-186.

Appleby, P.G., Oldfield, F., (1992), Application of lead-210 to sedimentation studies, in: Ivanovich, M., Harmon, R.S. (Eds.), Uranium series Disequilibrium, *Applications to Earth, Marine and Environmental sciences*, Clarendon Press, Oxford, pp 731-778.

Bradshaw, S. A., S. C. M. O'Hara, E. D. S. Corner, and G. Eglinton (1991), Effects on dietary lipids of the marine bivalve Scrobicularia plana feeding in different modes, *J.Mar.Biol.Ass.U.K.*, *71*, 635-653.

Coolen, M. J., B. Abbas, J. van Bleiswijk, E.C. Hopmans, M.M.M.Kuypers, S. G. Wakeham and J. S. Sinninghe Damsté (2007), Putative ammonia-oxidizing Crenarchaeota in suboxic waters of the Black Sea: a basin-wide ecological study using 16S ribosomal and functional genes and membrane lipids, *Environ. Microbiol.* doi:10.1111/j.1462-2920.2006.01227

Coplen, T. B., W. A. Brand, M. Gehre, M. Gröning, H. A. J. Meijer, B. Toman, and R. M. Verkouteren (2006), New guidelines for d13C measurements, *Anal.Chem., 78*, 2439-2441.

Deevey, E. S., N. Nakai, and M. Stuiver (1963), Fractionation of sulfur and carbon isotopes in a meromictic lake, *Science, 139*, 407-408.

Deines, P., The isotopic composition of reduced organic carbon, in *Handbook of environmental isotope geochemistry*, edited by P. Fritz and J. Ch. Fontes, pp. 329-406, Elsevier Scientific Publishing Company, Amsterdam-Oxford-New York, 1980.

Filipsson, H. L. and K. Nordberg (2004), Climate variations, an overlooked factor influencing the recent marine environment. An example from Gullmar Fjord, Sweden, illustrated by benthic foraminifera and hydrographic data, *Estuaries, 27*, 867-881.

Hedges, J. I. and R. G. Keil (1995), Sedimentary Organic-Matter Preservation - An Assessment and Speculative Synthesis, *Mar.Chem., 49*, 81-115.

Herfort, L., S. Schouten, J. P. Boon, M. Woltering, M. Baas, J. W. H. Weijers, and J. S. Sinninghe Damsté (2006), Characterization of transport and deposition of terrestrial organic matter in the southern North Sea using the BIT index, *L&O. 51*, 2196-2205.

Hoefs, M. J. L., W. I. C. Rijpstra, and J. S. Sinninghe Damsté (2002), The influence of oxic degradation on the sedimentary biomarker record I: Evidence from Madeira Abyssal Plain turbidites, *Geochim. Cosmochim. Acta, 66*, 2719-2735.

Hopmans, E. C., S. Schouten, R. D. Pancost, M. T. J. Van der Meer, and J. S. Sinninghe Damsté (2000), Analysis of intact tetraether lipids in archaeal cell material and sediments by high performance liquid chromatography/atmospheric pressure chemical ionization mass spectrometry, *Rap. Comm. Mass Spectrom., 14*, 585-589.

Hopmans, E. C., J. W. H. Weijers, E. Schefuss, L. Herfort, J. S. Sinninghe. Damsté, and S. Schouten (2004), A novel proxy for terrestrial organic matter in sediments based on branched and isoprenoid tetraether lipids, *Earth and Planetary Science Letters*, 224, 107-116.

Huguet, C., J. H. Kim, J. S. Sinninghe Damsté, and S. Schouten (2006b), Reconstruction of sea surface temperature variations in the Arabian Sea over the last 23 kyr using organic proxies (TEX_{86} and $U^{K'}_{37}$), *Paleoceanography*, *21,* doi:10.1029/2005PA001215.

Kim, J.-H., S. Schouten, R. Buscail, W. Ludwig, J. Bonnin, J. S. Sinninghe Damsté, and F. Bourrin (2006), Origin and distribution of terrestrial organic matter in the NW Mediterranean (Gulf of Lions): Exploring the newly developed BIT index, *Geochem.Geophy.Geosy*., 7, 1-20.

Könneke, M., A. E. Bernhard, J. R. de la Torre, C. B. Walker, j. B. Waterbury, and D. A. Stahl (2005), Isolation of an autotrophic ammonia-oxidizing marine archaeon, *Nature, 437*, 543-546.

Kristensen, D. K., H. P. Sejrup, H. Haflidason, I. M. Berstad, and G. Mikalsen (2004), Eight-hundred-year temperature variability from the Norwegian continental margin and the North Atlantic thermohaline circulation, Paleoceanography, 19.

Küspert, W., Environmental changes during oil shale deposition as deduced from stable isotope ratios, in *Cyclic and Event Stratification*, edited by G. Einsele and A. Seilacher, pp. 482-501, Springer, Heidelberg, 1982.

Menzel, D., E. C. Hopmans, S. Schouten, and J. S. Sinninghe Damsté (2006), Membrane tetraether lipids of planktonic Crenarchaeota in Pliocene sapropels of the eastern Mediterranean Sea, *Palaeogeography Palaeoclimatology Palaeoecology*, 239, 1-15.

Mikalsen, G., H. P. Sejrup, and I. Aarseth (2001), Late-Holocene changes in ocean circulation and climate: foraminiferal and isotopic evidence from Sulafjord, western Norway, *Holocene, 11*, 437-446.

Murray, A. E., A. Blakis, R. Massana, S. Strawzewski, U. Passow, A. Alldredge, and E. F. DeLong (1999), A time series assessment of planktonic archaeal variability in the Santa Barbara Channel, *Aquat.Microb.Ecol., 20*, 129-145.

Öztürk, M. (1995), Trends of trace metal (Mn, Fe, Co, Ni, Cu, Zn, Cd and Pb) distributions at the oxic-anoxic interface and in sulfidic water of the Drammensfjord, *Mar.Chem., 48*, 329-342.

Pancost, R. D. and C. S. Boot (2004), The palaeoclimatic utility of terrestrial biomarkers in marine sediments, *Mar.Chem., 92*, 239-261.

Powers, L. A., T. C. Johnson, J. P. Werne, I. S. Castañeda, E. Hopmans, J. S. Sinninghe Damsté, and S. Schouten (2005), Large temperature variability in the southern African tropics since the Last Glacial Maximum, *Geophys.Res.Lett., 32*, L08706-10.1029/2004GL022014.

Powers, L. A., J. P. Werne, T. C. Johnson, E. C. Hopmans, J. S. Sinninghe Damsté, and S. Schouten (2004), Crenarchaeotal membrane lipids in lake sediments: A new paleotemperature proxy for continental paleoclimate reconstruction?, *Geology, 32*, 613-616.

Schouten, S., E. C. Hopmans, E. Schefuss, and J. S. S. Damste (2002), Distributional variations in marine crenarchaeotal membrane lipids: a new tool for reconstructing ancient sea water temperatures?, *Earth and Planetary Science Letters*, 204, 265-274.

Schouten, S., C. Huguet, E.C. Hopmans, M. V.M. Kienhuis and J. S. Sinninghe Damsté (2007), Improved analytical methodology and constraints on analysis of the TEX86 paleothermometer by high performance liquid chromatography/atmospheric pressure chemical ionization-mass spectrometry. *Anal. Chem.* doi:10.1021/ac062339v

Sinninghe Damsté, J. S., S. Schouten, E. C. Hopmans, A. C. T. van Duin, and J. A. J. Geenevasen (2002), Crenarchaeol: the characteristic core glycerol dibiphytanyl glycerol tetraether membrane lipid of cosmopolitan pelagic crenarchaeota, *J.Lipid Res.*, *43*, 1641-1651.

Smittenberg, R. H., M. Baas, M. J. Green, E. C. Hopmans, S. Schouten, and J. S. Sinninghe Damsté (2005), Pre- and post-industrial environmental changes as revealed by the biogeochemical sedimentary record of Drammensfjord, Norway, *Mar.Geol., 214*, 177-200.

Sun, M. Y. and S. G. Wakeham (1994), Molecular Evidence for Degradation and Preservation of Organic-Matter in the Anoxic Black-Sea Basin, *Geochim. Cosmochim.Acta, 58*, 3395-3406.

Tyson, R. V., (1995) Distribution of the palynomorph group: phytoplankton subgroup, Chlorococcale algae. 16.1 Botryococcus, in *Sedimentary organic matter, organic facies and palynofacies*, edited by R. V. Tyson, pp. 309-317, Chapman & Hall, London.

van Breugel, Y., S. Schouten, M. Paetzel, R. Nordeide, and J. S. Sinninghe Damsté (2005a), The impact of recycling of organic carbon on the stable carbon isotopic composition of dissolved inorganic carbon in a stratified marine system (Kyllaren fjord, Norway), *Org.Geochem., 36*, 1163-1173.

van Breugel, Y., S. Schouten, M. Paetzel, J. Ossebaar, and J. S. Sinninghe Damsté (2005b), Reconstruction of delta d13C of chemocline CO2 (aq) in past oceans and lakes using the d13C of fossil isorenieratene, *Earth.Planet.Sci.Lett., 235*, 421-434.

Wachniew, P. and K. Rozanski (1997), Carbon budget of a mid-latitude, groundwater-controlled lake: Isotopic evidence for the importance of dissolved inorganic carbon recycling, *Geochim.Cosmochim.Acta*, 61, 2453-2465.

Wagner, T. and L. M. Dupont (1999), Terrestrial organic matter in marine sediments: analytical approaches and eolian-marine records in the central Equatorial Atlantic, in Use of proxies in *Paleoceanography: Examples from the South Atlantic*, edited by G. Fischer and G. Wefer, pp. 547-574, Springer-Verlag, Berlin-Heidelberg.

Weijers, J. W. H., S. Schouten, E. C. Hopmans, J. A. J. Geenevasen, O. R. P. David, J. M. Coleman, R. D. Pancost, and J. S. Sinninghe Damste (2006a), Membrane lipids of mesophilic anaerobic bacteria thriving in peats have typical archaeal traits, *Environ. Microbiol. 8*, 648-657.

Weijers, J. W. H., S. Schouten, O. C. Spaargaren, and J. S. Sinninghe Damsté (2006b), Occurrence and distribution of tetraether membrane lipids in soils: Implications for the use of the TEX86 proxy and the BIT index, *Org.Geochem. 37,* 1680-1693.

Wuchter, C., B. Abbas, M. J. L. Coolen, L. Herfort, J. van Bleijswijk, P. Timmers, M. Strous, E. Teira, G. J. Herndl, J. J. Middelburg, S. Schouten, and J. S. Sinninghe Damsté (2006a), Archaeal nitrification in the ocean, *PNAS, 103*, 12317-12322.

Wuchter, C., S. Schouten, M. J. L. Coolen, and J. S. Sinninghe Damsté (2004), Temperature-dependent variation in the distribution of tetraether membrane lipids of marine Crenarchaeota: Implications for TEX86 paleothermometry, *Paleoceanography, 19(4)*, doi:10.1029/2004PA001041

Wuchter, C., S. Schouten, S. G. Wakeham, and J. S. Sinninghe Damsté (2005), Temporal and spatial variation in tetraether membrane lipids of marine Crenarchaeota in particulate organic matter: Implications for TEX86 paleothermometry, *Paleoceanography, 20,* doi:10.1029/2004PA001110

Wuchter, C., S. Schouten, S. G. Wakeham, and J. S. Sinninghe Damsté (2006b), Archaeal tetraether membrane lipid fluxes in the northeastern Pacific and the Arabian Sea: Implications for TEX_{86} paleothermometry, *Paleoceanography, 21*, PA4208-1-PA4208-9.

Zegers, B. N., W. E. Lewis, K. Booij, R. H. Smittenberg, W. Boer, J. de Boer, and J. P. Boon (2003), Levels of polybrominated diphenyl ether flame retardants in sediment cores from Western Europe, *Environ.Sci.Technol., 37*, 3803-3807.

Chapter 8

Reconstruction of sea surface temperature variations in the Arabian Sea over the last 23 kyr using organic proxies (TEX_{86} and $U^{K'}_{37}$).

Carme Huguet, Jung-Hyun Kim, Jaap S. Sinninghe Damsté and Stefan Schouten

Published in *Paleoceanography,* **21,** doi:10.1029/2005PA001215 (2006)

Abstract

Two sediment cores from the western Arabian Sea, NIOP905 and 74KL were analyzed to determine sea surface temperature (SST) variations over the last 23 kyr. Two organic molecular SST proxies were used, the well established $U^{K'}_{37}$ based on long-chain unsaturated ketones synthesized by haptophyte algae, and the newly proposed TEX_{86} derived from the membrane lipids of Crenarchaeota. Comparison of NIOP905 and 74KL core top data with present day SST (0-10 m) values, indicate that both proxies yield temperatures similar to local annual mean SSTs. However, TEX_{86} and $U^{K'}_{37}$ SST downcore records derived from the same cores differ in magnitude and phasing. The alkenone SST record of NIOP905 shows small changes in SST (~0.5°C) over the last 23 kyr while that of core 74KL shows a ~2°C increase from the Last Glacial Maximum (LGM; 23-19 cal kyr BP) through the Holocene (the last 11.5 cal kyr BP) synchronous with changes in the northern hemisphere. In contrast, the TEX_{86} records of both cores show a large increase in SST from 22-23°C in the LGM to 28-30°C during Termination I (19-11.5 cal kyr BP), decreasing to present day annual means of ~26°C. A cold phase between 14.5 and 12 cal kyr BP that may correspond to the Antarctic Cold Reversal is also observed. This implies a southern hemisphere control on tropical SST reconstructed by the TEX_{86}, possibly related to SW monsoon. Our results suggest that the application of both TEX_{86} and $U^{K'}_{37}$ give different but complementary information on SST developments in past marine environments.

8.1. Introduction

Evidence of large-magnitude and rapid climate changes on millennial timescales (e.g., Dansgaard-Oeschger events, Heinrich Events) that characterized the last glaciation during the Late Pleistocene have been provided by ice core records [e.g *Grootes and Stuiver,* 1997; *Jouzel et al.,* 2003] as well as by continental and marine sediment records [e.g., *Schulz et al*., 1998; *Wang et al.*, 2001]. To better understand such abrupt millennial-scale climate changes, their consequences, and their underlying mechanisms, it is essential to construct SST records at a high temporal resolution.

Several geochemical proxies are used for SST reconstruction, the most common being $\delta^{18}O$ and Mg/Ca ratios of planktic foraminifera [*Chave,* 1954; *Emiliani,* 1955; *Nurnberg et al.*, 1996] and the $U_{37}^{K'}$ index of long-chain unsaturated ketones synthesized by haptophyte algae [*Brassell et al.,* 1986]. Reconstruction of SST with these proxies is, however, associated with a number of problems. The use of planktic foraminifera $\delta^{18}O$ for SST reconstruction is complicated by several uncertainties related to the formation and preservation of shells as well as the carbonate ion concentration, the $\delta^{18}O$ and the salinity of the original seawater [*Spero et al.,* 1997; *Wefer et al.,* 1999; *Lea,* 2003]. The Mg/Ca ratio [*Elderfield and Ganssen*, 2000] is less affected by these factors, except by species-dependent vital effects and shell dissolution [*Wefer et al.,* 1999; *Lea,* 2003]. The $U_{37}^{K'}$ index is often considered more robust, as the values are not directly controlled by sea-water chemistry and, hence, assumptions concerning this are not needed. Furthermore, global surveys of surface sediments and particulate organic matter reveal a strong and identical correlation between the $U_{37}^{K'}$ and SST (reviewed by *Herbert* [2003]). However, the biochemical function of alkenones is still unknown and the $U_{37}^{K'}$ may be affected by changes in the species composition through time and also by oxic degradation [*Herbert,* 2003].

Recently, *Schouten et al.* [2002] introduced a new SST proxy, the TEX_{86} based on the relative distribution of glycerol dibiphytanyl glycerol tetraethers (GDGTs), which are membrane lipids produced by non-thermophilic Crenarchaeota. These organisms are ubiquitous and abundant in seawater [*Hoefs et al.,* 1997; *Massana et al.,* 2000; *Karner et al.,* 2001] and large lakes [*Powers et al*., 2005].

Marine crenarchaeota biosynthesize different GDGTs with a varying number of cyclopentane rings according to temperature [*Wuchter et al*., 2004]. Therefore, by measuring the relative amounts of GDGTs present in sediments, the temperature at which Crenarchaeota were living can be reconstructed. Experiments with an enrichment culture, containing a single archaeal species falling in the phylogenetic cluster of the marine crenarchaeota, showed that TEX_{86} is linearly correlated with temperature and that changes in salinity and nutrients do not substantially affect the TEX_{86} [*Wuchter et al*., 2004]. Particulate organic matter analysis revealed that the TEX_{86} correlates well with surface water temperatures (depths <100m) and that the signal in the deeper water layers and surface sediments is primarily derived from these upper 100 meters [*Wuchter et al*., 2005]. This suggests that the signal from the surface waters is efficiently transported to the sediment probably by grazing [*Wakeham et al., 2003*]. Indeed, recent studies of sediment trap material showed that the TEX_{86} signal at different depths in sediment particles is derived from the upper layer of the water column [*Wuchter et al., 2006*]. This new organic geochemical proxy also seems to be unaffected by water redox conditions [*Schouten et al.,* 2004]. However, a number of factors such as the ecology and physiology of crenarchaeota in different oceanic provinces and its effect on the $TEX_{86,}$ need to be further constrained. But, there are already some developments in those fields, for example, a species of marine Crenarchaeota was recently isolated and shown to be an autotrophic ammonium-oxidizer [*Könneke et al., 2005*] in agreement with previous observations [*Wuchter et al., 2004*]. This could explain observed seasonal distributions of marine Crenarchaeota in surface waters, i.e their high abundance during times of low phytoplankton productivity and high nutrients [cf *Wuchter et al., 2005* and references therein]. However, to what extent this influences their depth habitat, their seasonality in low and high nutrient environments and how widespread this metabolism is remains unknown. Recently, it has also become clear that GDGTs such as those occurring in marine Crenarchaeota are present in terrestrial organic matter albeit in much lower abundances [*Hopmans et al., 2004; Weijers et al., 2004*]. Thus, at sites which receive high amounts of terrestrial organic matter, the TEX_{86} could potentially be biased. Nevertheless, despite these limitations, the TEX_{86} proxy may be a useful tool to reconstruct SSTs.

Here, for the first time, we applied the TEX_{86} to Quarternary marine sediment cores and investigated its potential as a tool in multi proxy paleoceanography and paleoclimate studies

in comparison with the $U_{37}^{K'}$. The western Arabian Sea (Fig. 1) was selected for this study as it is an area where organic-rich sediments are deposited with high accumulation rates, allowing the recovery of continuous high-resolution records with sufficient amounts of organic matter. Furthermore, previous low-resolution $U_{37}^{K'}$ records from this area revealed quite contrasting differences between LGM and Holocene SSTs varying between 0.3°C and 3°C [*Sonzogni et al*., 1998]. Our approach based on two lipid biomarker proxies, $U_{37}^{K'}$ and TEX_{86}, provides detailed information on SST variations in the western Arabian Sea over the last 23 kyr and the impact of the Arabian Sea monsoonal climate system on SST records.

8.2. Material and Methods

8.2.1. Modern atmospheric and oceanographic setting

The western Arabian Sea is predominantly influenced by monsoon climate related annual cycles driven by the pressure gradient that exists between Tibet plateau and the South Indian Ocean [*Rixen et al.,* 2000]. The annual cycle can be divided into four phases; (a) the northeast (NE) monsoon from December to March; (b) the summer intermonsoon from March to June; (c) the southwest (SW) monsoon from June to September; and (d) the fall intermonsoon from September to December [*Wakeham et al.,* 2002] (Table 2). The differential pressure results in southwesterly winds during the SW monsoon and in northeasterly winds during the NE monsoon [*Rixen et al.,* 2000; *Andruleit et al.,* 2000; *Bush,* 2002]. The SW monsoon induces strong upwelling of nutrient rich, cool waters that leads to lower SST (Fig. 1), higher productivity, an intense oxygen minimum zone and a high particle flux [*Wakeham et al.,* 2002]. The NE monsoon causes a deepening of the mixed layer and no upwelling, resulting in relatively higher SST (Fig. 1) and only a small increase in production and particle flux [*Wakeham et al.,* 2002].

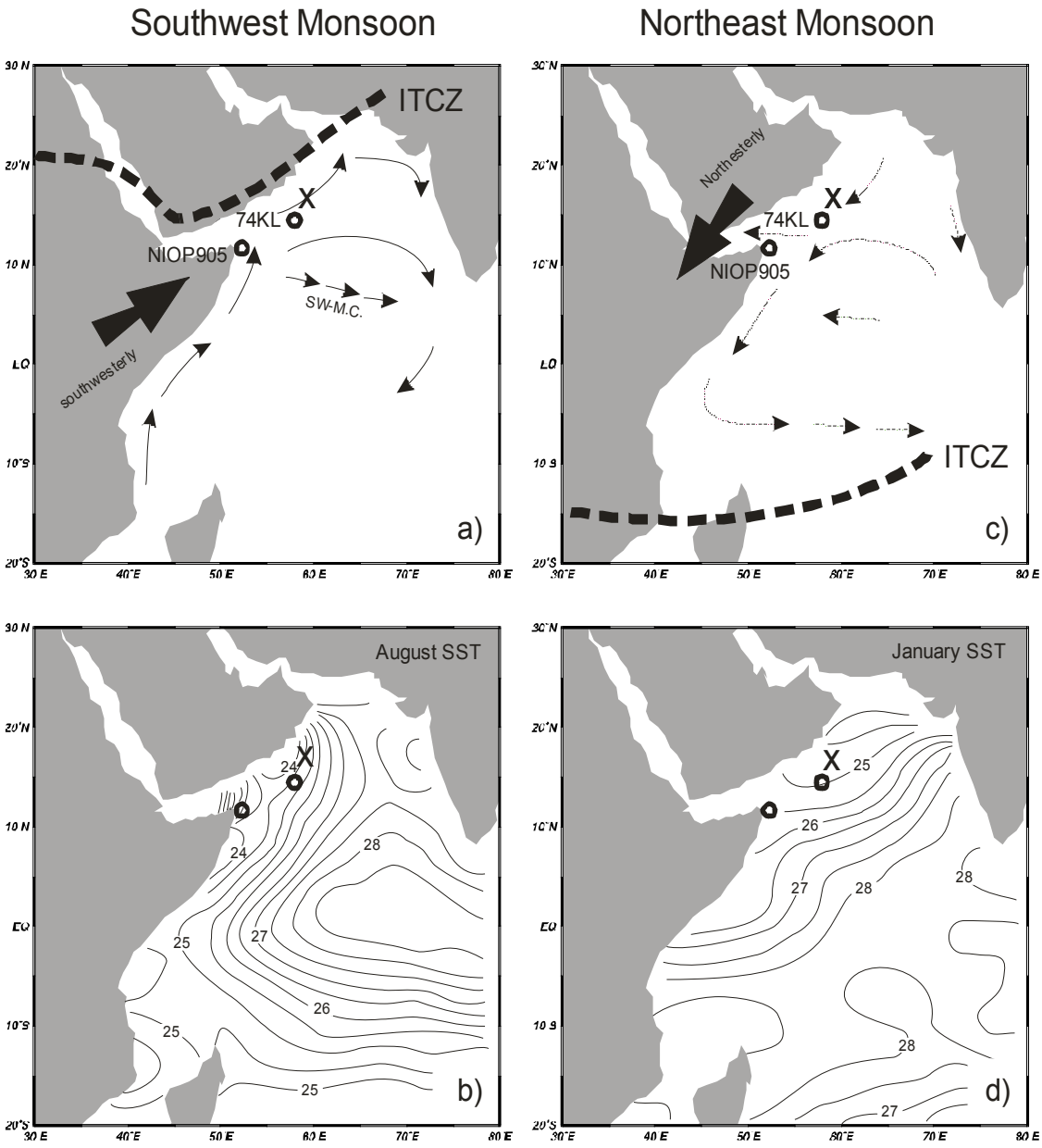

Figure 1. Map of study area showing core locations (open circles), sediment trap location of *Wakeham et al.* [2002] and *Wuchter et al.* [2006] (cross) ITCZ positions, and prevalent wind directions during the SW monsoon and the NE monsoon. (a) Sea surface circulation pattern during the SW monsoon. (b) August SST distribution pattern [Levitus and Boyer, 1994]. (c) Sea surface circulation pattern during the NE monsoon. (d) January SST distribution pattern [Levitus and Boyer, 1994]. Core NIOP905 (10° 47'N, 51° 56'E) was taken in the Somalia Basin, under the Socotra upwelling. Core 74 KL (14° 19.26'N, 57°20.82'E) taken off the Oman coast.

8.2.2. Sample collection and stratigraphy

Two sediment cores (NIOP905 and 74KL) from the western Arabian Sea were investigated in this study. Core NIOP905 (10°47'N, 51°56'E) was taken in the Socotra upwelling cell of the Somalia Basin (Fig. 1), ca. 80 km off the coast of Somalia and at 1567 m water depth. Core 74KL (14°19'N, 57°20'E) was obtained from the East Sheba Ridge, 1000 m above the turbidity plain of the Indus fan, 300 km south of the Arabian continental margin (Fig. 1). Core NIOP905 was sampled at 2 to 5 cm intervals and core 74KL at 2.5 cm intervals. Both cores have been studied previously in detail for the $\delta^{18}O$ of foraminifera [*Sirocko et al.*, 1993; *Ivanova,* 2000; *Jung et al*., 2002; *Ivanochko*, 2005a] and, in case of NIOP905, trace elements [*Ivanochko*, 2005a].

The age models of cores NIOP905 and 74KL were established by nineteen accelerator mass spectrometry (AMS) ^{14}C dates from mixed planktic foraminifera and thirteen AMS ^{14}C determinations on *Globigerinoides ruber*, respectively (Table 1) which were published previously [*Sirocko et al.*, 1993; *Ivanova,* 2000; *Jung et al*., 2002; *Ivanochko*, 2005a]. We employed a correction for the regional ^{14}C reservoir age (ΔR = the deviation from the surface ocean average of 400 years) of 190 ±25 years for the western Arabian Sea [*Southon et al.,* 2002], although the ΔR in the Arabian Sea can vary substantially through time as demonstrated by *Staubwasser et al.* [2002]. However, the age model based on the varying ΔR of *Staubwasser et al.* [2002] from the eastern Arabian Sea (not shown) does not affect the conclusions made in this study. Continuous time scales for both cores were obtained by linear interpolations between the age control points after converting the ^{14}C ages into calendar years (years before 1950) using the latest version of the radiocarbon-calendar year calibration software CALIB 5.0.1 [*Stuiver et al.,* 2005]. The average temporal resolution is ~200 years for NIOP905 and ~300 years for core 74KL.

8.2.3. Lipid extraction

For core NIOP905, freeze-dried and homogenized sediment samples were ultrasonically extracted with MeOH, MeOH/DCM (1:1;v/v) and finally with DCM. The supernatants were collected and after evaporating the solvents, the extracts were dried over a sodium sulfate column.

Sediment core	Depth in core [cm]	Uncorrected AMS ^{14}C ages [yr BP]	Analytical error (± 1-σ) [yrs]	ΔR^b [yrs]	ΔR error [yrs]	Calibrated calendar ages (2-σ ranges) [cal yr BP]	Calibrated calendar ages (1-σ ranges) [cal yr BP]	Mean calibrated calendar ages used for the age models [cal yr BP]	Reference for original AMS ^{14}C data
NIOP 905	20	1410	n.a.	190	±25	664-890	691-820	755.5	Ivanova, 2000
	40	2420	n.a.	190	±25	1692-1972	1760-1905	1832.5	Ivanova, 2000
	80	4050	n.a.	190	±25	3656-3977	3728-3894	3811.0	Ivanova, 2000
	120	5410	n.a.	190	±25	5458-5703	5520-5645	5582.5	Ivanova, 2000
	167-167.5[a]	6653	50	190	±25	6812-7135	6874-7042	6958.0	Jung *et al.*, 2002
	183-183.5[a]	7125	50	190	±25	7332-7552	7398-7501	7449.5	Jung *et al.*, 2002
	200	7620	45	190	±25	7776-7997	7839-7944	7891.5	Ivanova, 2000
	249.5-251[a]	8620	50	190	±25	8892-9240	8972-9117	9044.5	Jung *et al.*, 2002
	291 -291.5[a]	9748	50	190	±25	10261-10538	10355-10505	10430.0	Jung *et al.*, 2002
	313.75	10371	47	190	±25	11101-11256	11146-11214	11180.0	Ivanochko, 2005b
	320	10500	n.a.	190	±25	11174-11433	11210-11346	11278.0	Ivanova, 2000
	340	11100	n.a.	190	±25	12236-12709	12434-12632	12533.0	Ivanova, 2000
	360	12000	n.a.	190	±25	13162-13383	13215-13314	13264.5	Ivanova, 2000
	361.25	12131	62	190	±25	13247-13556	13297-13431	13364.0	Ivanochko, 2005b
	376.25	12895	52	190	±25	14002-14602	14044-14287	14165.5	Ivanochko, 2005b
	391.25	13975	55	190	±25	15518-6300	15688-16067	15877.5	Ivanochko, 2005b
	400	14190	n.a.	190	±25	15811-16593	15978-16366	16172.0	Ivanova, 2000
	411.25	14701	61	190	±25	16385-17197	16620-17029	16824.5	Ivanochko, 2005b
	480.25	20580	114	190	±25	23598-24298	23778-24109	23943.5	Ivanochko, 2005b
74KL	7.5	1230	60	190	±25	509-711	553-656	604.5	Sirocko *et al.*, 1993
	35	3350	100	190	±25	2736-3229	2825-3096	2960.5	Sirocko *et al.*, 1993
	55	5540	90	190	±25	5539-5922	5623-5832	5727.5	Sirocko *et al.*, 1993
	70	7850	90	190	±25	7941-8320	8004-8213	8108.5	Sirocko *et al.*, 1993
	80	8700	120	190	±25	8831-9440	8989-9298	9143.5	Sirocko *et al.*, 1993
	97.5	10580	120	190	±25	11177-11927	11245-11670	11457.5	Sirocko *et al.*, 1993
	115	11780	130	190	±25	12881-13285	12962-13189	13075.5	Sirocko *et al.*, 1993
	127.5	13060	150	190	±25	14049-15064	14220-14816	14518.0	Sirocko *et al.*, 1993
	142.5	14200	170	190	±25	15617-16763	15889-16471	16180.0	Sirocko *et al.*, 1993
	160	15880	170	190	±25	18096-18896	18501-18855	18678.0	Sirocko *et al.*, 1993
	165	16260	170	190	±25	18668-19244	18781-19033	18907.0	Sirocko *et al.*, 1993
	180	17130	180	190	±25	19344-20072	19509-19846	19677.5	Sirocko *et al.*, 1993
	197.5	20580	260	190	±25	22990-24594	23590-24288	23939.0	Sirocko *et al.*, 1993

[a]Mean values were used for the age model.

[b]The regional reservoir age (ΔR) for the western Arabian Sea was used according to Southon *et al.* [2002].

n.a. Analytical errors are not available for these data. Therefore, we assumed ±50 years for the analytical determination.

Table 1. Age control points for sediment cores NIOP905 and 74KL

An aliquot of the total lipid extract was used to analyze the alkenones for determination of the $U_{37}^{K'}$ ratio. The total extract was derivatized with diazomethane and BSTFA/pyridine. The derivatized total extract was analyzed by gas chromatography (GC) and gas chromatography/mass spectrometry to quantify alkenones. For GDGT analysis an aliquot of the total lipid extract was fractionated into apolar and polar fractions using a small column with activated alumina and using hexane/DCM (9:1;v/v) and DCM/MeOH (1:1;v/v) as eluents, respectively. The polar fractions were analyzed for GDGTs.

For core 74KL, the samples were extracted in a similar way than NIOP905. Subsequently, the total extracts were separated into DCM and MeOH/DCM (1:1;v/v) fractions, using a silica gel cartridge (Varian Bond Elute; 1 cc per 100 mg). The DCM fraction was saponified at 80°C for 2 h with 300 µl of 0.1 M KOH in 90:10 MeOH/H_2O. The neutral fraction containing the alkenones was obtained by partitioning into hexane. The MeOH/DCM (1:1;v/v) fraction was used for GDGT analysis.

8.2.4. Alkenone analysis and $U_{37}^{K'}$ *SST*

Peak areas of $C_{37:2}$ and $C_{37:3}$ alkenones were determined by GC analysis [cf Kim et al., 2004]. The alkenone unsaturation index $U_{37}^{K'}$ was calculated from $U_{37}^{K'} = (C_{37:2})/(C_{37:2} + C_{37:3})$, where $C_{37:2}$ and $C_{37:3}$ are the di- and tri-unsaturated C_{37} methyl alkenones [Prahl and Wakeham, 1987]. The $U_{37}^{K'}$ values were converted into temperature values applying the global core-top calibration ($U_{37}^{K'} = 0.033 \times T + 0.044$) of Müller et al. [1998].

8.2.5. GDGT analysis and TEX_{86} *SST*

For cores NIOP905 and 74KL, the polar fractions (DCM/MeOH, 1:1; v/v) were analyzed for GDGTs according to the procedure described by *Hopmans et al.,* [2000]. Aliquots of polar fractions blown down under a stream of nitrogen, re-dissolved in hexane/propanol (99:1;v/v), and filtered through 0.45 µm PTFE filters. The samples were analyzed with an HP (Palo Alto, CA, USA) 1100 series LC-MS equipped with an auto-injector and Chemstation chromatography manager software. Separation was achieved on a Prevail Cyano column (2.1 x 150mm, 3µm; Alltech, Deerfield, Illinois, USA), maintained at 30°C. The GDGTs were eluted using a changing mixture of (A) hexane and (B) propanol as

follows, 99 A:1 B for 5 min, then a linear gradient to 1.8 B in 45 min. Detection was achieved using atmospheric pressure chemical ionization-mass spectrometry of the eluent. Single Ion Monitoring (SIM) was used as it gives better reproducibility than full mass scanning by reducing the signal to noise ratio. The SIM method was set to scan the 5 $[M^+]$+H ions of the GDGTs with a dwell time of 237 ms for each ion. All TEX_{86} analyses were performed at least in duplicate.

The TEX_{86} ratio (TEX_{86}= ($GDGT_2$+$GDGT_3$+Crenarchaeol-isomer)/($GDGT_1$+ $GDGT_2$+$GDGT_3$+Crenarchaeol-isomer)) was calculated based on the relative abundance of GDGTs and converted into temperature values applying the calibration (TEX_{86}=0.015×T+0.028) of *Schouten et al*. [2002].

8.2.6. Analytical reproducibility

To determine the analytical reproducibility of the $U_{37}^{K'}$ and TEX_{86} SST values, a set of 12 sub-samples from a large homogenized batch of sediment from GeoB 1707-1 (recovered during METEOR cruise M20/2 at 1232 m near the Angola coast in the Atlantic Ocean; 19°41'S, 10°39'E) were extracted independently and measured at regular intervals during the analysis of the 74KL sample series. The standard deviation of the $U_{37}^{K'}$ and TEX_{86} SST analysis of these sub-samples was 0.2°C (±1σ) and 0.4°C (±1σ), respectively.

8.3. Results

8.3.1 Core NIOP905

The $U_{37}^{K'}$ SST range for NIOP905 is fairly narrow and varies between 25.0 and 26.5°C for the time interval between 23 and 0 cal kyr BP. This is in contrast to the $\delta^{18}O$ record of *G. ruber* [*Jung et al.,* 2001] which shows a gradual decrease during Termination I (Fig. 2a). $U_{37}^{K'}$ SST during the LGM (23-19 cal kyr BP) was 25.5°C with only a small, relatively abrupt increase in SST during the glacial-interglacial transition between 18 to 16 cal kyr BP of ~0.5°C (Fig. 2b). After this rise, the NIOP905 record shows a small drop in $U_{37}^{K'}$ SST of ~0.5°C between 16 and 14 cal kyr BP and a rise of ~0.5°C between 14 and 12.5 cal kyr BP.

This is followed by a decrease of ~0.7°C between 12 and 10.5 cal kyr BP. Then SST stabilized around 25.7°C until 5 cal kyr BP and then rose to the core top value of 26.3°C.

The TEX_{86} record for NIOP905 is quite different from the $U^{K'}_{37}$ SST record and the $\delta^{18}O$ record. TEX_{86} SST values for the studied interval of 23-0 cal kyr BP range from 22 to ca. 30°C with a few data points above 30°C (Fig. 2c). TEX_{86} SST is ~22.5°C during the LGM (23-19 cal kyr BP) and increased to 29°C between 18 and 16 cal kyr BP. This ~6°C increase is significant compared to the analytical error of 0.4°C. After the rapid warming of SST between 18 and 16 cal kyr BP there was a substantial lowering of SST from ~26°C between 16 and 14 cal kyr BP (Fig. 2c). After this cooling, the TEX_{86} SST increased again by up to 5°C to a maximum of 31°C at 12 cal kyr BP before rapid cooling of ~3°C until 11 cal kyr BP. An additional SST spike of ~3°C is noticeable at around 10.5 cal kyr BP and SST then slowly decreased from 27°C at 10 cal kyr BP to the present day core top value of 25.7°C.

8.3.2. Core 74KL

The $U^{K'}_{37}$ SST range for 74KL is larger than for NIOP905 and varies from 24.8 to 27.3°C between 23 and 0 cal kyr BP (Fig. 3b). SST during the LGM (23-19 cal kyr BP) was again 25°C as with NIOP905 but the increase in SST during Termination I was larger (~1.5°C) and more gradual in 74KL and was synchronous with the decrease in $\delta^{18}O$ values of *G. ruber* (Fig. 3a and 3b). After Termination I $U^{K'}_{37}$ SST increased slightly up to the core top value of 27.3°C.

The TEX_{86} record at 74KL is again quite different from $U^{K'}_{37}$ SST record, but closely resembles the pattern evident in the TEX_{86} record from core NIOP905. TEX_{86} SST values for 74KL have a somewhat smaller range than in NIOP905 and vary between 24 and 30°C (Fig. 3c). LGM SSTs for 74KL (~24°C) were slightly higher than at NIOP905 (~22.5°C). TEX_{86} SST values then rapidly increased to ~30°C between 18 and 16 cal kyr BP followed by a drop in SST down to 26°C between 16 and 14 cal kyr BP. SST then rapidly increased again to 29°C at 12.5 cal kyr BP followed by a rapid drop to 27.5°C. SST then slowly decreased to the core top value of 26.4°C.

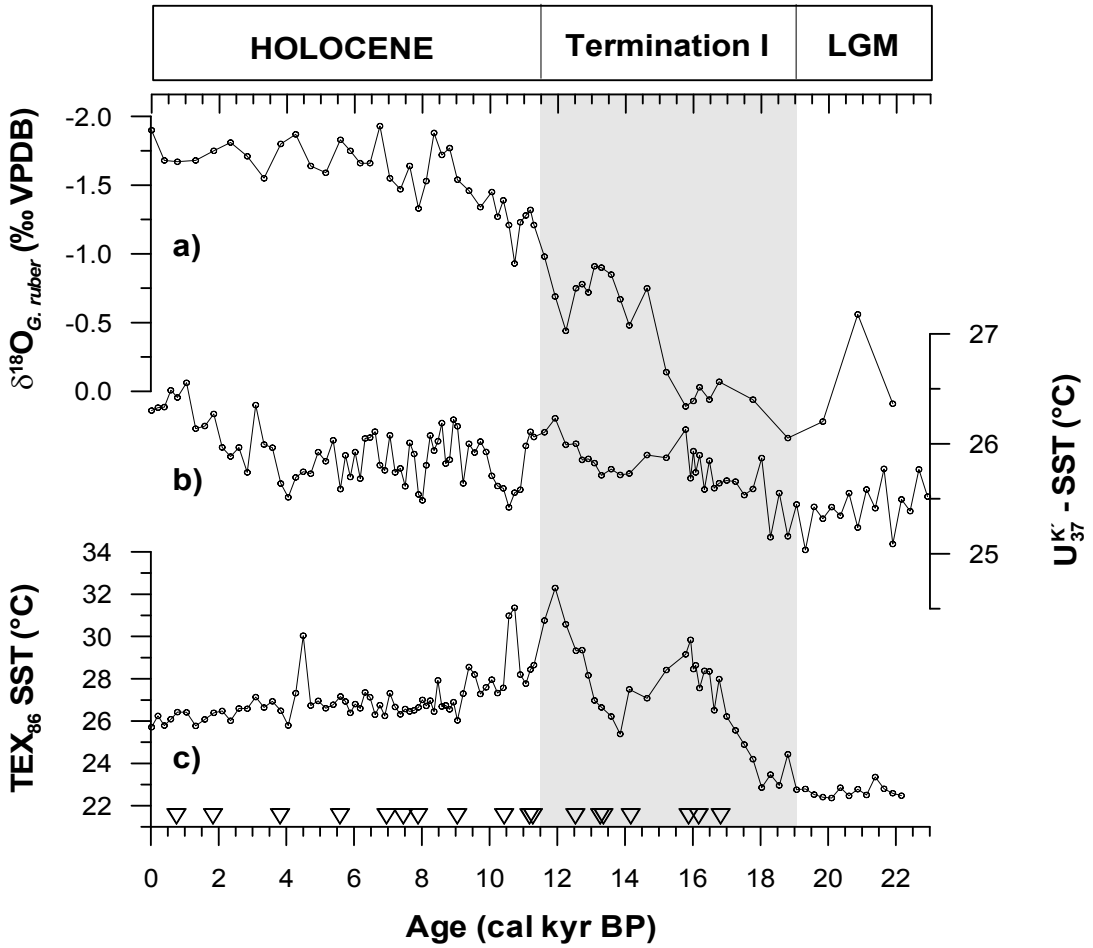

Figure 2. Time series of (a) stable $\delta^{18}O$ record of the planktic foraminifera *G. ruber* [from *Jung et al.*, 2001] and (b) $U^{K'}_{37}$ and (c) TEX_{86} SST records for core NIOP905, plotted against calendar ages. Open triangles on lower axis show age control points. Broad grey bar indicates the time interval for Termination I.

8.4. Discussion

8.4.1 Comparison of core tops and present day SSTs

One way of establishing the origin of the reconstructed SST of proxies is to compare core top reconstructed SSTs (0-2.5 cm depth representing the last ~300 years) with those of annual mean and seasonal mean SST (0-10 m depth). For NIOP905 the TEX_{86} and the $U^{K'}_{37}$ give a core top SSTs of 25.7 and 26.3°C, respectively.

Considering the analytical error of 0.4°C and 0.2°C, respectively, these results correspond well with present day annual mean SST of 26.0°C (Table 2). Similarly, at site 74KL both TEX_{86} and $U_{37}^{K'}$ SST, with core top values of 26.4°C and 27.3°C, respectively, correspond well with present day annual mean SST of 26.8°C.

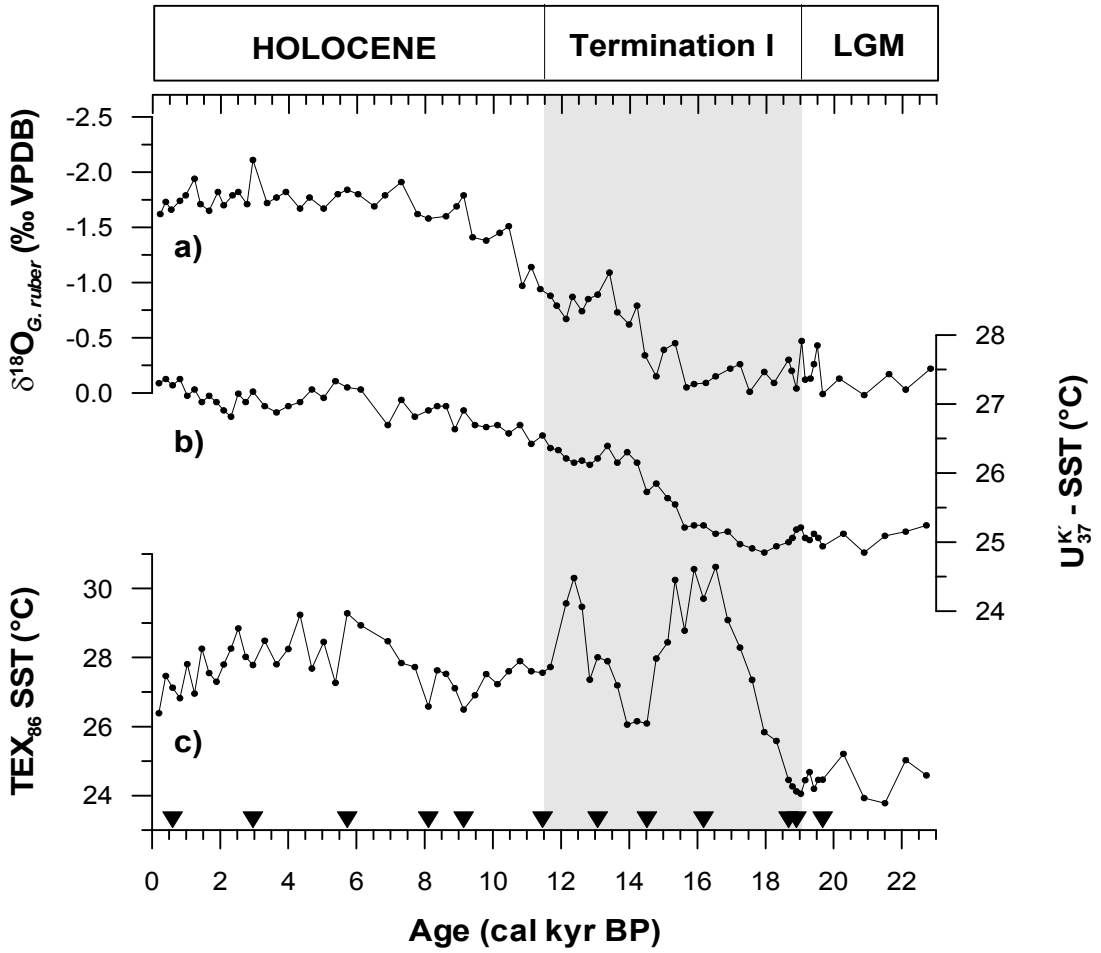

Figure 3. Time series of (a) stable $\delta^{18}O$ record of the planktic foraminifera *G. ruber* [Sirocko *et al*., 1993] and (b) $U_{37}^{K'}$ and (c) TEX_{86} SST records for core 74KL, plotted against calendar ages. Solid black triangles on lower axis show age control points. Broad grey bar indicates the time interval for Termination I.

Although both proxies seem to record annual mean SSTs, it has been reported that both Crenarchaeota [*Massana et al.,* 1998; *Murray et al.,* 1999; *Wuchter et al*., 2005a] and haptophyte algae [*e.g. Bac et al.,* 2003] vary considerably in abundance during the annual cycle. In the Arabian Sea primary production is strongly associated with upwelling dynamics and monsoonal cycles (Fig. 1). This most likely determines the annual cycle of the abundance of organisms that produce the biomarkers on which the SST proxies are based. Trap studies in the coastal and central Arabian Sea show that more than 50% of the particle flux to the sediments occurs during the SW monsoon and to a lesser extent (~25%) during the NE monsoon [*Prahl et al.,* 2000; *Wakeham et al.,* 2002]. *Wakeham et al*. [2002] described a distinct succession in phytoplankton biomarker fluxes. During the early SW monsoon the biomarker flux is dominated by C_{30}-diol and C_{30}-ketols from *Proboscia* diatoms [*Sinninghe Damsté et al.*, 2003]. This is followed by maximum fluxes of alkenones, and diatom and dinoflagellate sterols. At the end of the upwelling season the flux of 25:3 highly branched isoprenoid produced by *Rhizosolenoid* diatoms increase substantially. These findings are in good agreement with results from other sediment trap studies in central Arabian Sea area, where a sharp peak in the flux of alkenones was measured in the middle of the SW monsoon as well as a minor peak during the NE monsoon [*Prahl et al.,* 2000]. Taken together these studies indicate that sedimentary alkenones are mainly derived from alkenones produced during the SW monsoon and, to a lesser extent, during the NE monsoon. A recent study on the same sediment trap material from the *Wakeham et al.* [2002] in the Arabian Sea, showed that fluxes of GDGT material in a location near 74KL (Fig. 1) were also highest during the SW monsoon and to a lesser degree in the NE monsoon [*Wuchter et al.*, 2006]. However, GDGT fluxes only moderately increased during both monsoon periods compared to the intermonsoon periods (ca. 3 times). In contrast, the fluxes of alkenones were substantially higher (ca. 9 times) during monsoon periods than in intermonsoon periods. *Wuchter et al.,* [2006] suggested that this is because the relative abundance of Crenarchaeota during upwelling is lower than outside the upwelling period, while the opposite is observed for phytoplankton abundance. This is in agreement with previous studies which showed a negative correlation between Crenarchaeota and phytoplankton abundance [*Massana et al.,* 1998; *Murray et al.,* 1999; *Wuchter et al,* 2005]. Based on the above considerations, $U^{K'}_{37}$ SST values in the

present-day Arabian Sea should correspond to the SST prevalent during the SW monsoon, while the crenarchaeotal TEX_{86} is also influenced by SST from periods outside the SW monsoon and, thus, perhaps reflects a more annual mean signal.

Phase	Month	Site NIOP905		Site 74KL	
		Monthly mean temp. [°C]	**Seasonal mean temp.** [°C]	**Monthly mean temp.** [°C]	**Seasonal mean temp.** [°C]
Northeast monsoon	December	26.4		26.0	
	January	25.9		25.4	
	February	25.8	26.0	25.1	25.5
Summer intermonsoon	March	26.9		26.7	
	April	28.7		28.8	
	May	28.6	28.2	29.7	28.4
Southwest monsoon	June	26.1		28.7	
	July	23.3		25.7	
	August	22.7		24.8	
	September	23.8	24.0	25.4	26.2
Fall intermonsoon	October	26.9		27.5	
	November	27.2	27.1	27.2	27.4
Annual mean:		26.0		26.8	
Alkenone flux weighted mean[a]:		24.6		25.9	
GDGT flux weighted mean[b]:		26.0		26.8	
$U^{K'}_{37}$ **core top[c]**		25.7		26.6	
$U^{K'}_{37}$ **core top[d]**		25.9		27.3	
$U^{K'}_{37}$ **core top[e]**		26.3		27.3	
TEX_{86} core top		25.7		26.4	

[a]Calculated using flux data of Prahl et [2000] and mean monthly SST

[b]Calculated using flux data of Wuchter et al. [2005b] and mean monthly SST

[c]According to the calibration of Prahl *et al*. [1988]: T [°C] = ($U^{K'}_{37}$ -0.039)/0.034

[d]According to the calibration of Sonzogni *et al*. [1997]: T [°C] = ($U^{K'}_{37}$ -0.317)/0.023

[e]According to the calibration of Müller *et al*. [1998]: T [°C] = ($U^{K'}_{37}$ -0.033)/0.04

Table 2. Mean monthly sea surface temperature (0-10 m) data corresponding to core sites [World Ocean Atlas 1998, On-line version at www.nodc.noaa.gov/OC5/WOA98F], calculated flux weighted TEX_{86} and $U^{K'}_{37}$ SST and core top TEX_{86} and $U^{K'}_{37}$ SST values for NIOP905 and 74KL.

Based on the sediment trap studies reported we can estimate the flux weighted annual SST for alkenones and GDGTs, i.e. the annual mean SST corrected for the times of the largest fluxes of these components, by combining alkenone and GDGT flux data from the central Arabian Sea [*Prahl et al.,* 2000; *Wakeham et al.,* 2002; *Wuchter et al*., 2006] and monthly average SST (Table 2). The flux weighted annual SST for alkenones is 1.4°C lower than $U^{K'}_{37}$ SST core top value for NIOP905 but only 0.8°C lower than core top $U^{K'}_{37}$ SST at 74KL (Table 2). The comparison of core top values to monthly mean SSTs (Table 2) suggests that the $U^{K'}_{37}$ is not recording the upwelling of cold water between June and September. During the SW monsoon, the Arabian Sea shows substantially lower SSTs, especially at NIOP905 where SSTs are up to 3°C lower than annual mean SST (Table 2). Hence, it seems that the pulses in alkenone production during upwelling seasons do not have a substantial effect on the temperature signal recorded by $U^{K'}_{37}$ in the sediment. It should be noted, however, that most sediment trap studies cover just one cycle at one specific location and that interannual variability in production could be of importance [*Herbert,* 2003]. Furthermore, it is important to take into account that the core top (0-2.5 cm) represents an integrated SST signal of up to 300 years. Finally, the SST estimate from $U^{K'}_{37}$ analysis will also depend on the calibration used and can vary by up to 0.7°C (Table 2). However, other studies in the Arabian Sea show similar results, in that the flux of alkenones to the sediment is seasonal, yet an annual mean SST is recorded in the sediment core tops [*Doose-Rolinski et al.,* 2001; *Rosell-Melé et al.,* 2004]. A similar calculation for GDGT flux-weighted TEX_{86} SST yields 26.0°C and 26.8°C for NIOP905 and 74KL, respectively (Table 2). These values are identical to the actual annual mean SST and are within analytical error of the core top TEX_{86} value. The flux weighted TEX_{86} SST is higher than the flux-weighted $U^{K'}_{37}$ SST in agreement with the relatively higher fluxes of alkenones compared to GDGT during the SW monsoon. This suggests that the TEX_{86} is recording annual mean SST although, based on the above considerations for the $U^{K'}_{37}$, we can not exclude that certain seasonal periods may have a substantial influence on the TEX_{86}.

We can thus not rule out that there is a seasonal component in our SST proxies, even though this is not apparent from our core top results. It is also possible that the seasonal signal

was stronger during certain periods of time, e.g. during the LGM, which may explain why the proxies show different behavior in our sedimentary record (see below).

8.4.2 Comparison of SST proxy records

The $U_{37}^{K'}$ records of the two cores differ in both timing and magnitude of SST variations during deglaciation but both record relatively small variations in SST of <3°C. Remarkably, $U_{37}^{K'}$ SSTs reconstructed for the LGM for both sites are very similar at 25°C but the rise in SST during Termination I was much larger at 74 KL (2°C) than at NIOP905 (0.5°C). This is in agreement with previous results of *Sonzogni et al.* [1998] who showed that the $U_{37}^{K'}$ SST rising during Termination I is only 0.3°C for NIOP 905 but 1-3°C at other sites in the Indian Ocean. The reasons for the different $U_{37}^{K'}$ records of the two sites are unclear but based on the study of *Sozogni et al.* [1998] the unusual $U_{37}^{K'}$ record at NIOP905 seems to be a local feature. After Termination I, $U_{37}^{K'}$ SST in both records vary by <1°C suggesting relatively stable conditions. Remarkably, the $U_{37}^{K'}$ record at 74KL is roughly similar in phase to changes in $\delta^{18}O$ record, which contains a substantial SST component, in contrast to the $U_{37}^{K'}$ record at NIOP905 which is dissimilar to the $\delta^{18}O$ record. However, it should be noted that comparison of $U_{37}^{K'}$ record and $\delta^{18}O$ record should be done with caution as SST is not the only factor determining $\delta^{18}O$ (e.g. $\delta^{18}O$ of sea water, salinity) and, despite being analysed in the same sediment layer, could represent SST of different ages [cf. *Ohkouchi et al.*, 2002]

Both 74KL and NIOP905 cores gave similar TEX_{86} SST records, taking into account the errors in TEX_{86} analysis and the age models. However, they are quite different from the $U_{37}^{K'}$ records at both sites show substantially larger variability in SST. For example, SSTs rose by 4-6°C during Termination I with a pronounced cooling between 15.5and 12 cal kyr BP whilst $U_{37}^{K'}$ SST rose fairly smoothly by only 0.5-1.5°C. The trends in the TEX_{86} SST records are also different from those in $\delta^{18}O$ records, e.g. they show a more gradual trend from LGM to Holocene and no pronounced cooling between 15.5-12 cal kyr BP. However, comparison between the TEX_{86} record and $\delta^{18}O$ record are hampered by the same problems as discussed for the $U_{37}^{K'}$ record and $\delta^{18}O$ record. In contrast, the differences between the two organic SST

proxy records, TEX_{86} and $U^{K'}_{37}$, are unlikely to be caused by sea water composition changes and are more likely to be caused by the different response of the proxy-producing organisms to changes in climatic conditions such as monsoon and upwelling intensity, as has been documented for this area [e.g. *Ivanochko et al.*, 2005b]. Thus, both proxies probably do not record annual mean SST but are strongly influenced by seasonal SSTs. Below we attempt to explain the impact of this component on LGM SST reconstruction, and the phasing of SST changes.

8.4.3 LGM SST reconstructions

Large discrepancies exist in estimates of tropical LGM temperatures [*Mix et al.,* 2001]. These discrepancies are dependent on the method used to estimate LGM temperatures. Transfer function values of distributions of planktic foraminifera show small SST changes for the glacial-interglacial transition, e.g. the CLIMAP project reconstruction suggests SSTs of 2°C lower for the LGM in the Arabian Sea [*CLIMAP*, 1981]. *Mix et al*.[2001] suggested that CLIMAP might have underestimated ice-age cooling in the tropics, and that SST could have cooled almost 3ºC. $U^{K'}_{37}$ studies in the Arabian Sea and Indian Ocean show differences between the LGM and present day SST of 1.5 to 2.5°C [*Bard et al.,* 1997; *Sonzogni et al.,* 1998; *Schulte and Müller,* 2001; *Rosell-Melé et al.,* 2004]. Analyses of Mg/Ca ratios of planktic foraminifera at tropical areas in the equatorial Atlantic and Pacific show a 2.5-3°C cooler SST during the LGM [*Hastings et al.,* 1998; *Lea et al.,* 2000] while a recent summary suggested 2-3.5°C lower SSTs in tropical areas during the LGM [*Barker et al.,* 2005, and references cited therein],. Sr/Ca ratios in corals indicate up to 5°C difference in SST between the LGM and the present [*Guilderson et al.,* 1994]. Reconstructions of SST in the western Arabian Sea using artificial neural networks based on quantitative analysis of planktonic foraminifera suggests LGM SST 2°C below Holocene values [*Naidu and Malmgren,* 2005], in agreement with predictions based on atmosphere-ocean models [Mix et al. 2001, an references therein]. Some modeling results also suggest relatively cool temperatures in the tropics with LGM SST values ca. 4°C lower than Holocene SST values for the Arabian Sea [*Toracinta et al.,* 2004]. In general, proxy data suggest LGM SSTs between 1.5-5°C lower than present-day values, suggesting that Arabian Sea LGM temperatures were between 21.5 and 24.5°C.

The proxy records in this study also reveal a difference, i.e. SSTs estimated for the LGM are ~23°C with TEX_{86} and ~25°C with the $U^{K'}_{37}$. Thus, the temperature increase from the LGM to present day is 0.5-1.5°C when measured with $U^{K'}_{37}$, and 3-4°C when we use the TEX_{86}. The LGM SST values reconstructed with TEX_{86} are slightly lower than other LGM estimates (see above). However, LGM SST TEX_{86} estimates are still well within the range measured by other proxies in the tropical area. Furthermore, preliminary measurements of Mg/Ca ratio of planktic foraminifera in the NIOP905 core suggest that calcification temperatures were up to 3°C lower during the LGM compared to the late Holocene (*Anand et al., personal communication*). This is in good agreement with the TEX_{86} proxy estimates of glacial-interglacial SST changes in the Arabian Sea.

On the other hand, $U^{K'}_{37}$ SSTs in both cores indicate that the LGM was only 0.5-1.5°C cooler than present day and suggest LGM SSTs of 25°C. These temperatures are somewhat higher than SST estimates based on inorganic proxies and the TEX_{86}. Several studies show that in general alkenone-based SSTs give smaller changes from the LGM to the Holocene in tropical and subtropical areas compared to other proxies such as Sr/Ca or $\delta^{18}O$ [*Rosell-Melé et al.,* 2004; *Toracinta et al.,* 2004] for reasons which are presently unclear. Thus, it seems that the LGM TEX_{86} SST estimates are somewhat lower than estimates using other proxies and modeling results while our $U^{K'}_{37}$ LGM SST estimates are somewhat higher.

The strong control of primary production in the area by upwelling may explain why alkenone-based glacial SSTs are substantially higher than those based on the TEX_{86}. A decrease in the upwelling intensity has been documented for the Arabian Sea during the LGM [*e.g. Naidu and Malmgren,* 2005] and the Ba/Al record from NIOP905, a measure for marine productivity, shows lower ratios during the LGM and at the beginning of Termination I [*Ivanochko et al*., 2005a] suggesting lower productivity. It is reasonable to assume that these large changes could affect the seasonal abundance of the organisms living in the upwelling region. A decrease in the intensity of the SW monsoon during the LGM would indeed affect the depth of alkenone production, increase the stratification of surface waters and reduce production. All those changes would affect the alkenone temperature signal [*Mix et al.,* 2000, *Prahl et al.,* 2003] and could, likewise, affect the production and flux of crenarchaeotal GDGTs during the annual cycle. It has been suggested that the monsoon dynamics might have

been different during the LGM with a very weak SW monsoon and relatively strong NE monsoon resulting in a shift in alkenone production to the winter months in the Arabian Sea [*Higginson et al.,* 2004]. This would result in relatively higher SSTs during the LGM as temperatures during the SW monsoon are lower than during the NE monsoon (Table 2). The idea of a seasonal shift in alkenone production has indeed been used to explain the relatively warm glacial SST measured by $U_{37}^{K'}$ in the subtropical North Atlantic [*Chapman et al.,* 1996]. If this also occurred at our study sites then the $U_{37}^{K'}$ glacial SSTs values may be reflecting preferentially NE monsoon SST during the LGM. This is in contrast to the present day situation in which the alkenones seem to record annual mean temperature. Possibly, such changes in monsoon strength were of lesser importance for the TEX_{86} SST record as the seasonal abundance of Crenarchaeota is probably not so tied to upwelling dynamics and the relative GDGT flux increase during monsoon periods is lower than for the alkenones [*Wuchter et al*., 2006]. Alternatively, the location of strong upwelling sites, such as those at NIOP905 and 74KL, may have shifted through changes in ocean circulation during the last 23 kyr and in this way have affected the dynamics of the organic proxies.

8.4.4 Phasing of SST records during Termination I

Comparison of the TEX_{86} SST records with ice core records reflecting temperature from Antarctica (δD EPICA Dome C; Fig 4f) [*Jouzel et al.,* 2003] and Greenland ($\delta^{18}O$ GISP2; Fig 4a) [*Dansgaard et al.,* 1993] shows that the increase in TEX_{86} SST from the LGM to the Early Holocene is in phase with the southern hemisphere warming, suggesting that this proxy is primarily forced by southern hemisphere climate (Fig. 4). The TEX_{86} SST records also show a cooling during Termination I in phase with the Antarctic Cold Reversal, which has been noted exclusively in the southern hemisphere [*Stenni et al.,* 2001] (Fig. 4). The $U_{37}^{K'}$ SSTs at 74KL lag Antarctic records and resemble more the Arctic ice record (Fig. 4) while $U_{37}^{K'}$ SST record at NIOP905 does not show much variation at all and perhaps only slightly resembles the Antarctica record (Fig. 4).

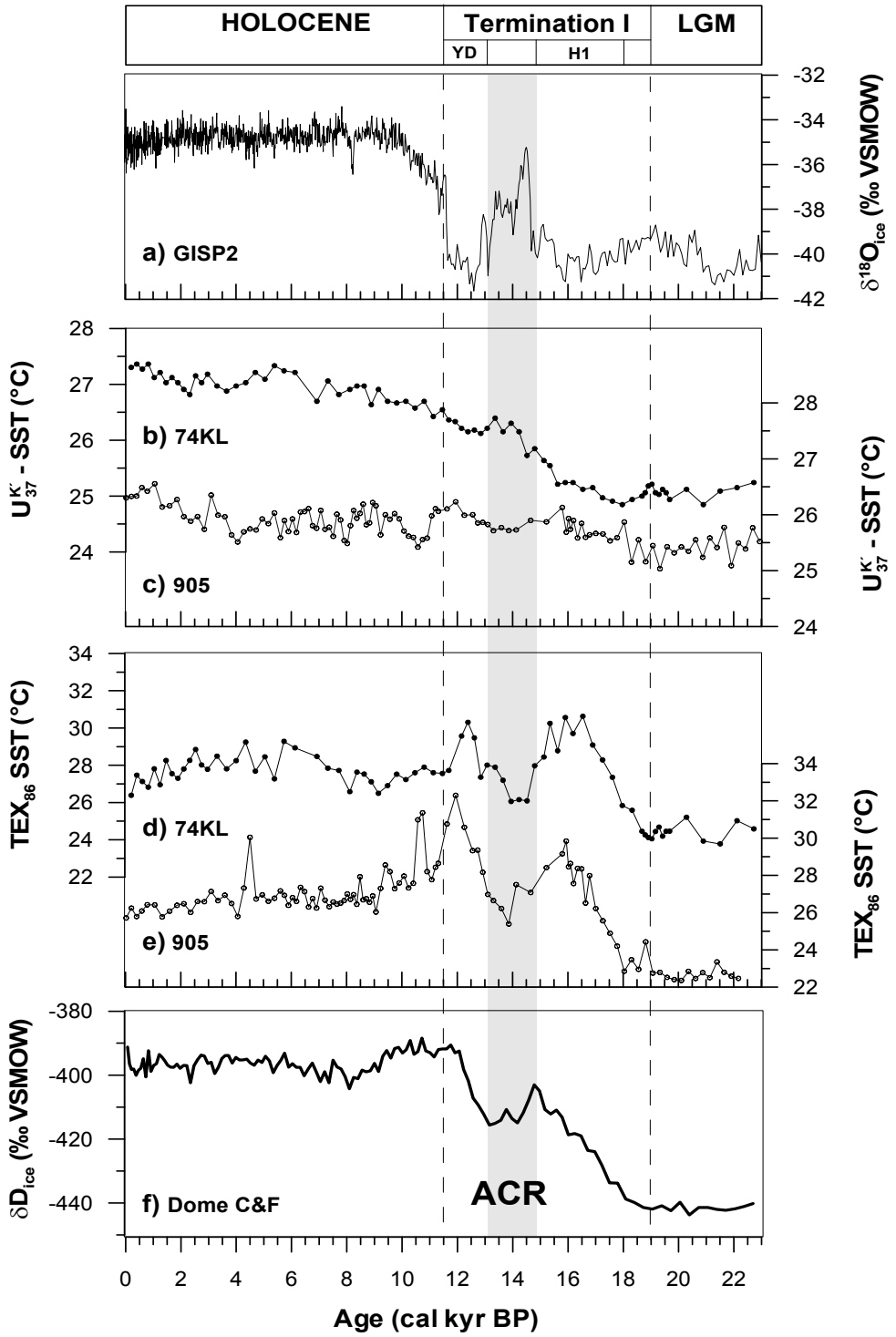

Figure 4. Comparison of SST records from the western Arabian Sea with ice core isotope records from Greenland and Antarctic. (a) GISP2 $\delta^{18}O$ record from Greenland [*Dansgaard et al.*, 1993], (b) $U^{K'}_{37}$ SST for 74KL, (c) $U^{K'}_{37}$ SST for NIOP 905, (d) TEX_{86}SST from 74KL, (e) TEX_{86} SST from NIOP 905, and (f) δD from Dome C in Antarctica [*Jouzel et al*. 2003].

In addition, the $U^{K'}_{37}$ SST record at 74KL shows a small drop in SST in phase with the Younger Dryas in the northern hemisphere. Previous studies in the Arabian Sea area show that the $U^{K'}_{37}$ records from the Oman and Pakistan Margins are also predominantly affected by northern hemisphere climate dynamics [*Schulte and Müller,* 2001; *Doose-Rolinski et al.,* 2001; *Higginson et al.,* 2004]. The reason why the $U^{K'}_{37}$ SST record at NIOP905 is not reflecting northern hemisphere dynamics is unclear. It should be noted that the NIOP 905 $U^{K'}_{37}$ record is very different from other $U^{K'}_{37}$ records in the area [*Sonzogni et al*., 1998], suggesting that local features may have overwritten the global change in SST.

The question thus remains why we detect southern hemisphere dynamics with the TEX_{86} proxy, even at 74KL, and not with the $U^{K'}_{37}$ proxy. This may only be explained if the TEX_{86} proxy is more influenced by the SW monsoon, when the southern hemisphere dynamics dominate the area, even when this was substantially reduced during the LGM and Termination I. In contrast, the $U^{K'}_{37}$ may be more influenced by the NE monsoon during this time, as suggested previously [*Higginson et al*., 2004] and therefore records northern hemisphere climate. To the best of our knowledge SST records of tropical oceans have not revealed, until now, a dominant southern hemisphere component making it difficult to speculate what the mechanism behind the control on the TEX_{86} SST is.

8.4.5 Holocene SST reconstructions

Similar to the ice core records no large short-term changes in SST are observed during the Late Holocene in either the TEX_{86} and $U^{K'}_{37}$ SST records. However, both TEX_{86} and $U^{K'}_{37}$ values for NIOP905 and 74KL show relatively consistent opposing SST trends during the Holocene. While the TEX_{86} values show a slight decrease in SST from Termination I to present day values, the $U^{K'}_{37}$ record indicates a small increase in SST in this time period. Using artificial neural networks analysis of the distributions of planktic foraminifera, *Naidu and Malmgren* [2005] show a cooling trend in the Arabian Sea in the Holocene, which is more pronounced in boreal winter than in boreal summer. This cooling trend is also observed in the western Pacific, eastern Atlantic and western Mediterranean as well as in the Arabian Sea [*Naidu and Malmgren,* 2005, and references cited therein]. In contrast, $U^{K'}_{37}$ SST records

over the last 7 kyr have shown a general warming in the tropics [*Kim et al.,* 2004]. A data-model comparison study based on globally distributed $U^{K'}_{37}$ SST records and transient ensemble climate simulations suggests that the Holocene warming in the tropics is due to an orbitally-driven insolation increase during the boreal winter (December-January-February) in the low-latitudes [*Lorenz et al*., 2006]. The apparent discrepancy between TEX_{86} SST records and $U^{K'}_{37}$ SST records is most likely caused by the fact that SST proxies are not consistently recording annual mean SST but seasonal SST.

8.5. Conclusions

$U^{K'}_{37}$ and TEX_{86} SST records from two sites in the Arabian Sea revealed different temperature variations over the last 23 kyr for each proxy. TEX_{86} SST records were similar at two sampling sites in the Arabian Sea over the last glacial-interglacial cycle and they are in phase with temperature changes recorded in Antarctica ice core records. This suggests that the TEX_{86} records of SST in the area are mainly controlled by the southern hemisphere climate dynamics during the SW monsoon. $U^{K'}_{37}$ SST records from the same cores are different in magnitude of change and differ also in phase, and are party in phase with northern hemisphere climate dynamics during the NE monsoon. This is likely due to different growing seasons of the biomarker source organisms, and to a change in the upwelling dynamics and monsoon strengths between the LGM and the Holocene. Our results suggest that if the impact of seasonality on the different organic proxies can be better constrained, then complementary information on SST can be obtained by this multiproxy approach.

Acknowledgements

We would like to thank Martijn Woltering and Annemiek Vos van Avezaathe for analytical support, Lydie Herfort and Gert Jan Reichart for useful comments and Ellen Hopmans for assistance with the HPLC/MS, Tjeerd van Weering, Erica Koning and Geert Jan Brummer for providing access to the NIOP905 core and Frank Sirocko for the 74KL sediment samples. Andreas Lückge, Joe Werne and two anonymous reviewers are thanked for constructive comments on earlier drafts of this paper. This project was supported by NWO-ALW (Project nr. 152911) and by the EU project 6C (Contract no. EVK2-2001-00179-6C).

Reference

Andruleit, H. A., U. Von Rad, A. Bruns, and V. Ittekkot (2000) Coccolithophore fluxes from sediment traps in the northeastern Arabian Sea off Pakistan, *Mar. Micropaleontol.*, *38*, 285-308.

Bac, M. G., K. R. Buck, F. P. Chavez, and S. C. Brassell (2003) Seasonal variation in alkenones, bulk suspended POM, plankton and temperature in Monterey Bay, California: implications for carbon cycling and climate assessment, *Org. Geochem.*, *34*, 837-855.

Bard, E., F. Rostek, and C. Sonzogni (1997) Interhemispheric synchrony of the last deglaciation inferred from alkenone palaeothermometry, *Nature*, *385*, 707-710.

Barker, S., I. Cacho, H. Benway, and K. Tachikawa, Planktonic foraminiferal Mg/Ca as a proxy for past oceanic temperatures: a methodological overview and data compilation for the Last Glacial Maximum, *Quart.Sci. Rev.*, *24*, 821-834, 2005.

Brassell, S. C., G. Eglinton, I. T. Marlowe, U. Pflaumann, and M. Sarnthein (1986). Molecular stratigraphy: A new tool for climatic assessment*, Nature, 320*, 129-133.

Bush, A. B. G. (2002) A comparison of simulated monsoon circulations and snow accumulation in Asia during the mid-Holocene and at the Last Glacial Maximum, *Glob. Plan. Change*, *32*, 331-347.

Chapman, M. R., N. J. Shackleton, M. Zhao, and G. Eglinton (1996) Faunal and alkenone reconstructions of subtropical North Atlantic surface hydrography and paleotemperature over the last 28 kyr, *Paleoceanography*, *11*, 343-357.

Chave, K. E. (1954) Aspects of the Biogeochemistry of magnesium.1.Calcareous marine organisms, *J. Geol.*, *62,* 266-283.

CLIMAP Project Members (1981) Seasonal reconstructions of the Earth's surface at the last glacial maximum, *Geolog. Soc. Am. Map Chart Ser.*, MC-36.

Dansgaard, W., S. J. Johnsen, H. B. Clausen, D. DahlJensen, N. S. Gundestrup, C. U. Hammer, C. S. Hvidberg, J. P. Steffensen, A. E. Sveinbjornsdottir, J. Jouzel, and G. Bond (1993) Evidence for general instability of past climate from a 250-Kyr ice-core record, *Nature*, *364*, 218-220.

Doose-Rolinski, H., U. Rogalla, G. Scheeder, A. Lückge, and U. Von Rad (2001) High-resolution temperature and evaporation changes during the late Holocene in the northeastern Arabian Sea, *Paleoceanography*, *16*, 358-367.

Emiliani, C. (1955) Pleistocene Temperatures*, J. Geol., 63*, 538-578.

Elderfield H. and G. Ganssen (2000) Past temperature and $\delta^{18}O$ of surface ocean waters inferred from foraminiferal Mg/Ca ratios. *Nature, 405*, 442-445.

Grootes, P. M. and M. Stuiver (1997) Oxygen 18/16 variability in Greenland snow and ice with 10^3- to 10^5-year time resolution, *J Geophys. Res.-Oceans*, *102*, 26455-26470.

Guilderson, T. P., R. G. Fairbanks, and J. L. Rubenstone (1994) Tropical temperature variations since 20,000 years ago: modulating interhemispheric climate change, *Science*, 263, 663-665.

Hastings, D. W., A. D. Russell, and S. R. Emerson (1998) Foraminiferal magnesium in *Globeriginoides sacculifer* as a paleotemperature proxy, *Paleoceanography*, *13*, 161-169.

Herbert, T. D. (2003) Alkenone paleotemperature determinations, in: *Treatise on Geochemistry vol. 6: The Ocean and Marine Geochemistry*, edited by H. D. Holland and Turekian.K.K., pp. 391-432, Elsevier-Pergamon, Oxford.

Higginson, M. J., M. A. Altabet, L. Wincze, T. D. Herbert and D. W. Murray, (2004) A solar (irradiance) trigger for millennial-scale abrupt changes in the southwest monsoon?, *Paleoceanography*, 19, doi:10.1029/2004PA001031.

Hoefs, M. J. L., S. Schouten, J. W. de Leeuw, L. L. King, S. G. Wakeham, and J. S. Sinninghe Damsté (1997) Ether lipids of planktonic archaea in the marine water column, *Appl. Environ. Microbiol.*, *63*, 3090-3095.

Hopmans, E. C., S. Schouten, R. D. Pancost, M. T. J. Van der Meer, and J. S. Sinninghe Damsté (2000) Analysis of intact tetraether lipids in archaeal cell material and sediments by high performance liquid chromatography/atmospheric pressure chemical ionization mass spectrometry, *Rap. Comm. Mass Spectrom.*, *14*, 585-589.

Ivanochko, T.S., R.S. Ganesham, G.J. Brummer, G. Ganssen, S.J.A. Jung, S. G. Moreton and D. Kroon (2005a) Variations in tropical convection as an amplifier of global climate change at the millennial scale, *Earth Plan. Sci. Lett., 235*, 302-314.

Ivanochko, T. S. (2005b) Sub-orbital scale variations in the intensity of the Arabian Sea monsoon, PhD thesis, University of Edinburgh, Edinburgh, 230 pp.

Ivanovana, E. (2000) Late Quaternary monsoon history and paleoproductivity of the western Arabian Sea, Free University, Amsterdam, 172 pp.

Jouzel, J., F. Vimeux, N. Caillon, G. Delaygue, G. Hoffmann, V. Masson-Delmotte, and F. Parrenin (2003) Magnitude of isotope/temperature scaling for interpretation of central Antarctic ice cores, *J. Geophys. Res.-Atmospheres*, *108*, doi:10.1029/2002JD002677.

Jung, S.J.A., G.M. Ganssen, and G.R. Davies (2001) Multidecadal variation in the early Holocene outflow of Red Sea Water into the Arabian Sea, *Paleoceanography*, *16*, 658-668.

Jung, S. J. A., G. R. Davies, G. Ganssen, and D. Kroon (2002) Decadal-centennial scale monsoon variations in the Arabian Sea during the Early Holocene, *Geochem. Geophys. Geosys.*, *3*, doi:10.1029/2002GC000348.

Karner, M. B., E. F. DeLong, and D. M. Karl (2001) Archaeal dominance in the mesopelagic zone of the Pacific Ocean, *Nature*, *409*, 507-510.

Kim, J.-H., R. R. Schneider, P. J. Müller, and G. Wefer (2002) Interhemispheric comparison of deglacial sea-surface temperature patterns in Atlantic eastern boundary currents, *Earth Planet. Sci. Lett.*, *194*, 383-393.

Kim, J.H., N. Rimbu, S.J. Lorenz, G. Lohmann, S.I. Nam, S. Schouten, C. Ruhlemann and R.R. Schneider (2004) North Pacific and North Atlantic sea-surface temperature variability during the Holocene. *Quat Sci. Rev*., *23*, 2141-2154.

Könneke, M., A.E., Bernhard, J.R. de la Torre, C.B. Walker, J.B. Waterbury, and D.A. Stahl,D.A. (2005) Isolation of an autotrophic ammonia-oxidizing marine archaeon. *Nature* 237, 543-546.

Lea, D. W. (2003) Elemental and isotopic proxies of past ocean temperatures, in *Treatise on Geochemistry. Vol 6: The Ocean and Marine Geochemistry*, edited by H. D. Holland and Turekian.K.K., pp. 365-390, Elsevier-Pergamon, Oxford.

Lea, D. W., D. K. Pak, and H. J. Spero (2000) Climate impact of late Quaternary equatorial Pacific sea surface temperature variations, *Science*, *289*, 1719-1724.

Levitus, S. and T. P. Boyer (1994). World Ocean Atlas 1994, Volume 4: Temperature, NOAA ATLAS NESDIS 4, 117 pp.

Lorenz, J. S., J.H. Kim, N. Rimbu, R. R. Schneider, and G. Lohmann (2006) Orbitally-driven insolation forcing on Holocene climate trends: evidence from alkenone data and climate modeling. *Paleoceanography*, *21*, 10.1029/2005PA001152.

Massana, R., E. F. DeLong, and C. Pedrós-Alió (2000) A few cosmopolitan phylotypes dominate planktonic archaeal assemblages in widely different oceanic provinces, *Appl. Environ. Microbiol.*, *66*, 1777-1787.

Massana, R., L. T. Taylor, A. E. Murray, K. Y. Wu, W. H. Jeffrey, and E. F. DeLong (1998) Vertical distribution and temporal variation of marine planktonic archaea in the Gerlache Strait, Antarctica, during early spring, *Limnol. Oceanogr.*, *4*3, 607-617.

Mix, A. C., E. Bard, G. Eglinton, L. D. Keigwin, A. C. Ravelo, and Y. Rosenthal (2000) Alkenones and multiproxy strategies in paleoceanographic studies, *Geochem. Geophys. Geosys.*, *1*, 2000GC000056.

Mix, A. C., E. Bard, and R. Schneider (2001) Environmental processes of the ice age: land, oceans, glaciers (EPILOG), *Quat. Sci. Rev*., 20, 627-657.

Müller, P., G. Kirst, G. Ruhland, I. von Storch, and A. Rosell-Melé (1998) Calibration of the alkenone paleotemperature index $U^{K'}_{37}$ based on core-tops from the eastern South Atlantic and the global ocean (60'N-60'S), *Geochim. Cosmochim. Acta, 62*, 1757-1772.

Murray, A. E., A. Blakis, R. Massana, S. Strawzewski, U. Passow, A. Alldredge, and E. F. DeLong (1999) A time series assessment of planktonic archaeal variability in the Santa Barbara Channel, *Aquat. Microb. Ecol.*, *20*, 129-145.

Naidu P.D. and B.A. Malmgren (2005) Seasonal sea surface temperature contrast between the Holocene and last glacial period in the western Arabian Sea (Ocean Drilling Project Site 723A): Modulated by monsoon upwelling *Paleoceanography*, 20, doi:10.1029/2004PA001078.

Nurnberg, D, J. Bijma, and C. Hemleben (1996) Assessing the reliability of Magnesium in foraminiferal calcite as a proxy for water mass temperatures, *Geochim. Cosmochim. Acta*, *60*, 803-814.

Ohkouchi, N., T. I. Eglinton, L. D. Keigwin, and J. M. Hayes (2002) Spatial and temporal offsets between proxy records in a sediment drift, *Science*, 298, 1224-1227.

Powers, L. A., T. C. Johnson, J. P. Werne, I. S. Castañeda, E. Hopmans, J. S. Sinninghe Damsté, and S. Schouten (2005) Large temperature variability in the southern African tropics since the Last Glacial Maximum, *Geophys. Res. Lett., 32*, doi:10.1029/2004GL022014.

Prahl, F. G. and S. G. Wakeham (1987) Calibration of unsaturation patterns in long-chain ketone compositions for paleotemperature assessment, *Nature*, *330*, 367-369.

Prahl, F. G., J. Dymond, and M. A. Sparrow (2000) Annual biomarker record for export production in the central Arabian Sea, *Deep-Sea Res. II, 47*, 1581-1604.

Prahl, F.G., G.V. Wolfe and M.A. Sparrow (2003) Physiological impacts on alkenone paleothermometry, *Paleoceanography, 18.* doi:10.1029/2002PA000803.

Rosell-Melé, A., E. Bard, K. C. Emeis, B. Grieger, C. Hewitt, P. J. Müller, and R. R. Schneider (2004) Sea surface temperature anomalies in the oceans at the LGM estimated from the alkenone-$U_{37}^{K'}$ index: comparison with GCMs, *Geophys. Res. Lett.*, *31*, doi:10.1029/2003GL018151.

Rixen, T., V. Ittekkot, B. Haake-Gaye, P. Schäfer (2000) The influence of the SW monsoon on the deep-sea organic carbon cycle in the Holocene, *Deep-Sea Res. II, 47,* 2629-2651.

Schouten, S., E. C. Hopmans, E. Schefuss, and J. S. Sinninghe Damsté (2002) Distributional variations in marine crenarchaeotal membrane lipids: a new tool for reconstructing ancient sea water temperatures?, *Earth. Planet. Sc. Lett.*, *204*, 265-274.

Schouten, S., E. C. Hopmans, and J. S. Sinninghe Damsté (2004) The effect of maturity and depositional redox conditions on archaeal tetraether lipid paleothermometry, *Org. Geochem.*, *35*, 567-571.

Schulte, S. and P. J. Müller (2001) Variations of sea surface temperature and primary productivity during Heinrich and Dansgaard-Oescher events in the northeastern Arabian Sea, *Geo-Mar. Lett.*, *21*, 168-175.

Schulz, H., U. von Rad, and H. Erlenkeuser (1998) Correlation between Arabian Sea and Greenland climate oscillations of the past 110,000 years, *Nature, 393*, 54-57.

Sinninghe Damsté, J. S, S. Rampen, W.I.C. Rijpstra, B. Abbas, G. Muyzer and S. Schouten (2003) A diatomaceous origin for long-chain diols and mid-chain hydroxy methyl alkanoates widely occurring in Quaternary marine sediments: Indicators for high-nutrient conditions, *Geochim. Cosmochim. Acta, 67*, 1339-1348.

Sirocko, F., M. Sarnthein, H. Erlenkeuser, H. Lange, M. Arnold, and J. C. Duplessy (1993) Century-scale events in monsoonal climate over the past 24,000 Years, *Nature*, *364*, 322-324.

Sonzogni, C., E. Bard, F. Rostek, R. Lafont, A. Rosell-Melé and G. Eglinton (1997) Core-top calibration of the alkenone index vs sea surface temperature in the Indian Ocean, *Deep Sea Res. II*, *44*, 1445-1460.

Sonzogni, C., E. Bard, and F. Rostek (1998) Tropical sea-surface temperature during the last glacial period: a view based on alkenones in Indian Ocean sediments, *Quat. Sci. Rev.*, *17*, 1185-1201.

Southon, J., M. Kashgarian, M. Fontugne, B. Metivier, and W. W. S. Yim (2002) Marine reservoir corrections for the Indian Ocean and southeast Asia*, Radiocarbon, 44*, 167-180.

Spero, H. J., J. Bijma, D. W. Lea, and B. E. Bemis (1997) Effect of seawater carbonate concentration on foraminiferal carbon and oxygen isotopes, *Nature*, *390*, 497-500.

Staubwasser, M., F. Sirocko, P.M. Grootes, and H. Erlenkeuser (2002). South Asian monsoon climate change and radiocarbon in the Arabian Sea during early and mid Holocene, *Paleoceanography*, *17*, PA1063.

Stenni, B., V. Masson-Delmotte, S. Johnsen, J. Jouzel, A. Longinelli, E. Monnin, R. Röthlisberger, and E. Selmo (2001) An oceanic cold reversal during the last deglaciation, *Science*, *293*, 2074-2077.

Stuiver, M., P. J. Reimer, and R. W. Reimer (2005) CALIB 5.0 [WWW program and documentation at http://calib.qub.ac.uk/calib/].

Toracinta, E. R., R. J. Oglesby, and D. H. Bromwich (2004) Atmospheric response to modified CLIMAP ocean boundary conditions during the Last Glacial Maximum, *J. Clim.*, *17*, 504-522.

Wakeham, S. G., M. L. Peterson, J. I. Hedges, and C. Lee (2002) Lipid biomarker fluxes in the Arabian Sea: with a comparison to the equatorial Pacific Ocean, *Deep-Sea Res.II*, *49*, 2265-2301.

Wang, Y. J., H. Cheng, R. L. Edwards, Z. S. An, J. Y. Wu, C.C. Shen, and J. A. Dorale (2001) A high-resolution absolute-dated Late Pleistocene monsoon record from Hulu Cave, China, *Science*, *294*, 2345-2348.

Wefer, G., W. H. Berger, J. Bijma, and G. Fisher (1999) Clues to ocean history: a brief overview of proxies, in *The use of proxies in palaeoceanography: Examples from the South Atlantic*, edited by G. Fisher and G. Wefer, pp. 1-68, Springer-verlag, Berlin.

Weijers, J.W.H. S. Schouten, M. van den Linden, B. van Geel, and J.S. Sinninghe Damsté (2004) Water table related variations in the abundance of intact archaeal membrane lipids in a Swedish peat bog, *FEMS Microbiol. Lett.*, 239, 51-56.

World Ocean Atlas 1998 On-line version at www.nodc.noaa.gov/ OC5/WOA98F/, *National Oceanographic Data Center Internal Report 16,* Silver Spring.

Wuchter, C., S. Schouten, M. J. L. Coolen, and J. S. Sinninghe Damsté (2004) Temperature-dependent variation in the distribution of tetraether membrane lipids of marine Crenarchaeota: Implications for TEX_{86} paleothermometry, *Paleoceanography*, *19*, doi: 10.1029/2004PA001041.

Wuchter C., S. Schouten, S.G. Wakeham and J.S. Sinninghe Damsté (2005) Temporal and spatial variation in tetraether membrane lipids of marine Crenarchaeota in particulate organic matter: Implications for TEX_{86} paleothermometry, *Paleoceanography*, 20. doi:10.1029/2004PA001110.

Wuchter C., S. Schouten, S. G. Wakeham and J. S. Sinninghe Damsté (2006) Archaeal tetraether membrane lipid fluxes in the northeastern Pacific and Arabian sea: Implications for TEX_{86} paleothermometry, *Paleoceanography*, 21, doi:10.1029/2006PA42078.

Chapter 9

Abrupt sea surface temperature variations in the western Mediterranean during Marine Isotope Stages 6 and 7 as revealed by the $U^{k'}_{37}$ and TEX_{86} paleothermometers

Carme Huguet, Belen Martrat, Joan O, Grimalt, Jaap S. Sinninghe Damsté and Stefan Schouten

Manuscript in preparation

Abstract

In the Northern hemisphere, large-magnitude and rapid climate changes on millennial timescales (e.g., Dansgaard/Oeschger events and Heinrich events) characterized the last climate cycle, i.e. the past 130 ky. A recent study in the Alboran Sea (western Mediterranean, core ODP-977A) revealed that the sea surface temperature (SST) derived from the alkenone index ($U^{k'}_{37}$) also displays stadial-interstadial changes over the penultimate climate cycle, i.e. from 244 to 130 ky BP. To independently confirm these observations we applied the TEX_{86} proxy in the same core. The TEX_{86} temperature record shows similar stadial-interstadial patterns as those observed with the $U^{k'}_{37}$. However, the amplitude of the variations estimated by the two proxies are different during the penultimate glacial or marine isotope stage (MIS) 6 (190-130 cal. ky BP) compared to the preceding interglacial or MIS 7 (244-190 cal. ky BP). During MIS 7 there is a good correspondence in absolute temperature estimates between the two proxies. However during MIS 6 the TEX_{86} shows much larger temperature changes compared to the $U^{k'}_{37}$. We hypothesize that this may be caused by changes in the season in which the haptophytes and Crenarchaeota are blooming and/or variations in the depth habitat of Crenarchaeota. As the climate forcing differs between glacials and interglacials, a change in seasonal patterns and/or depth habitat can be expected when changing from the inter-glacial MIS 7 to glacial MIS 6, which would have a strong and differential effect on the TEX_{86} and $U^{k'}_{37}$ proxies. To fully understand the factor(s) causing the difference between the two proxies during MIS 6, further work is needed to establish the effects of seasonality and depth habitat on both proxies in the Alboran Sea.

9.1. Introduction

Northern hemisphere climate variations include some large and rapid climate changes on millennial timescales [i.e. Dansgaard/Oeschger (D/O) oscillations and the Heinrich events (HEs)] and longer term variations such as the glacial-interglacial changes described by the marine isotope stages (MISs). The MISs are alternating cold and warm periods in Earth's climate deduced from oxygen isotope data of benthic foraminifera and have time scales on the order of 100 ky [*Martinson et al.,* 1987]. The D/O events are rapid temperature changes (<1 ky) inferred from ice cores [*Dansgaard et al.,* 1993; *Grootes and Stuiver,* 1997] and the HEs are associated with catastrophic iceberg discharges and southern migrations of the Arctic front and their effects in marine sediment records [*Heinrich,* 1988]. These events took place during the last climate cycle, but similar rapid changes have also been found in older periods [*McManus et al.,* 1999; *Martrat et al.,* 2004].

The impact of the millennial scale northern hemisphere climate variability in the Alboran Sea, western Mediterranean has been extensively documented [e.g. *Cacho et al.,* 1999; *Cacho et al.,* 2000; *Cacho et al.,* 2001; *Moreno et al.,* 2004; *Martrat et al.,* 2004] (Fig. 1). This latitudinal teleconnection is thought to be controlled by both cold Atlantic waters and wind patterns inducing rapid changes in the Mediterranean thermohaline circulation, and seem to be independent from direct iceberg discharges [*Cacho et al.,* 1999; *Moreno et al.,* 2004] (Fig. 1b). Past changes in the thermohaline circulation could be caused by the extension of polar waters reaching a more southern position than previously thought leading to an influx of polar water through the Gibraltar Strait [*Cacho et al.,* 1999]. High frequency changes in the westerly wind patterns could account for the variability in deep-water ventilation in the western Mediterranean [*Moreno et al.,* 2004].

Previous studies in the Alboran sea showed a good correspondence between sea surface temperature (SST) proxy data and northern hemisphere climatic changes reconstructed from the GISP 2 ice-core, revealing that SST changes are related to both glacial-interglacial transitions and D/O or HE events [*Cacho et al.,* 2000; *Cacho et al.,* 2002]. However, little is known from the penultimate glacial as the deepest sections of the Greenland ice cores that cover the penultimate glacial are distorted by basal deformation [*Grootes and Stuiver,* 1997]. To provide a better understanding of the millennial scale variation over the penultimate glacial, *Martrat et al.* [2004] constructed a high-resolution alkenone SST record from a core

in the Alboran Sea spanning the past 250 ky. This record indicated that during MIS 6 there were SST changes reflecting stadial-interstadial patterns but of lower magnitude than those of MIS 3 and that the most prominent events occurred during MIS 7. They also reported abrupt SST changes which were referred to warming or cooling episodes that happened at a rate equal to or faster than the SST variation over the last deglaciation (i.e., an average warming of 2.6ºC/ky in core ODP-977A) [*Martrat et al.,* 2004]. However, confirmation of these trends using other temperature proxies was lacking.

We applied another molecular SST proxy to provide an independent record to the previously reported SST $U^{k'}_{37}$ one. We used the TEX_{86} proxy, which is based on the relative distribution of glycerol dibiphytanyl glycerol tetraethers (GDGTs; Schouten at al. [2002]) as it has provided complementary information to the $U^{k'}_{37}$ in previous studies [e.g. *Huguet et al.* 2006]. The TEX_{86} record in this study was obtained from the same sediment samples as those used to construct the $U^{k'}_{37}$ record [*Martrat et al.,* 2004].

9.2. Material and Methods

9.2.1. Study area

The Alboran Sea (western Mediterranean) is a transition area between the Atlantic and the Mediterranean and, therefore, any changes in either the Atlantic or Mediterranean will be reflected in the water column structure, temperature gradient and nutrient distribution. The Alboran Sea is also influenced by the surrounding land masses through fluvial and aeolian inputs coming from North Africa and the southern Iberian peninsula, although the riverine input is low and irregular [*Fabres et al.,* 2002]. Strong winds result in wind-driven upwelling resulting in high surface production [*Garcia-Gorriz and Carr,* 1999]. There is a stable gyre structure composed of a western Alboran gyre (WAG) and the eastern Alboran gyre (EAG) (Fig. 1a). The area presents a complex water column structure with deep Mediterranean and surface Atlantic water masses (Fig. 1b). The water column in the Alboran sea has a surface layer of inflowing Atlantic sea water (0-300m), an intermediate layer formed by out-flowing Levantine intermediate water (LAW) (300-600m) which is formed in eastern Mediterranean and a deep water mass (>600m) consisting of western Mediterranean deep water (WMDW) [*Fabres et al.,* 2002].

The area is also characterised by local turbulence caused by the water exchange and coastal upwelling caused by the gyres which result in very high primary productivity of up to 200 g $C \cdot m^{-2} \cdot y^{-1}$ [*Fabres et al.,* 2002]. The highest primary productivity takes place in coastal areas and at the periphery of the WAG [*Garcia-Gorriz and Carr,* 1999].·At present, SST in the area ranges between 14ºC in February and 25ºC in August with a phytoplankton bloom period from November to March and lowest primary production from May to September [*Garcia-Gorriz and Carr,* 1999].

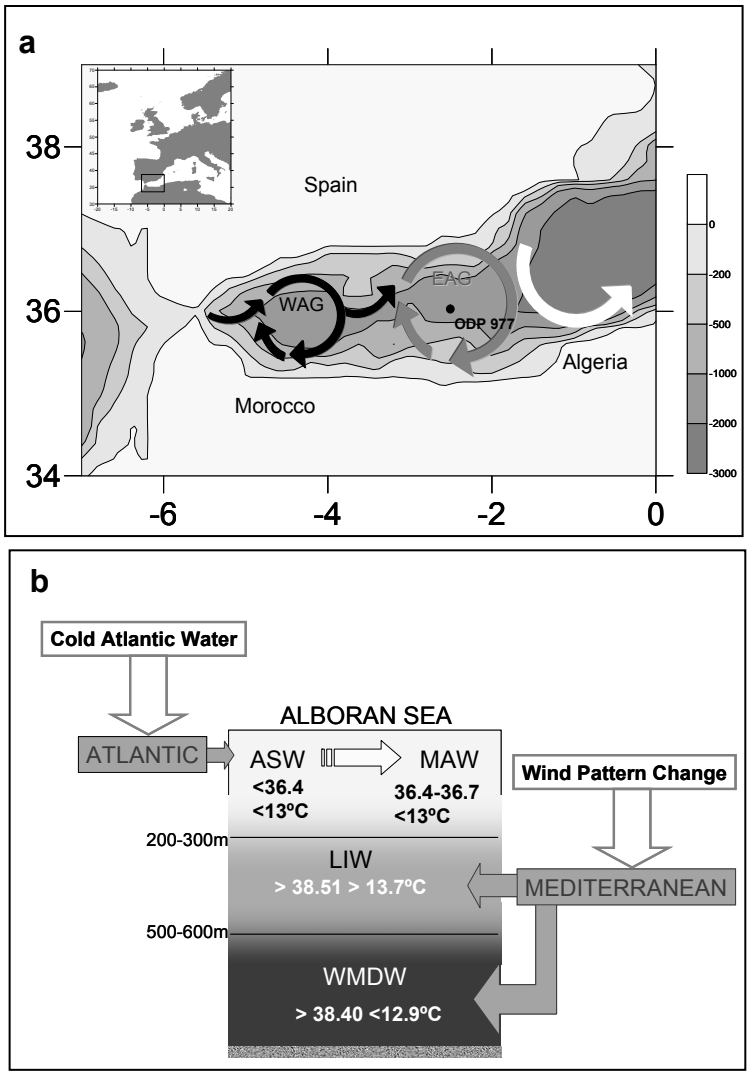

Figure 1. a) Map of the study area showing the core location and the two stable gyres in the area, the Western Alboran gyre (WAG) and the Eastern Alboran gyre (EAG); **b)** Water column structure with the different water masses, Atlantic surface water (ASW), Modified Atlantic water (MAW), Levantine intermediate water (LIW) and western Mediterranean deep water (WMDW), average temperatures and salinities are indicated (adapted from [*Fabres et al.,* 2002]).

9.2.2. Sampling strategy

Core ODP-977A (36º1.907'N, 1º57.3198W') was retrieved from the eastern sub-basin of the Alboran sea during leg 161 of the Ocean Drilling Program in 1996 [*Comas et al.,* 1996] (Fig. 1a). In the previous study by *Martrat et al.* [2004], the analysis of the 40m spanning ODP-977A core permitted the high-resolution reconstruction of the climatic history along the past 250 ky, using stable isotopes (n=794 samples) and sea surface temperature derived from the alkenone index (n=655 samples) with an average time resolution of 386±131 years. In this study, covering MISs 6 and 7, the average temporal resolution remains comparable at centennial scale throughout the whole period studied (244-145 cal. ky BP; n=199 samples). The age model of the investigated interval of the core was constructed by comparing the $\delta^{18}O$ profile of *G. bulloides* with thirteen defined orbital tuned isotopic events assuming constant sedimentation rates between control points (see *Martrat et al.,* [2004] for details).

9.2.3. GDGT analysis

Freeze-dried sediment samples were extracted using an Accelerated Solvent Extractor 200 (ASE 200, DIONEX) with a mixture of dichloromethane (DCM) and methanol (MeOH) (9:1; vol:vol) at 100°C and $7.6 \cdot 10^6$ Pa. An aliquot of each total extract was divided into a ketone and a polar fraction, using a glass pipette column filled with activated alumina, and sequentially eluting with hexane/DCM (1:1; vol:vol) and DCM/MeOH (1:1; vol:vol), respectively.

The polar fraction was analyzed for GDGTs according to the procedure described by [*Hopmans et al.,* 2000] and [*Schouten et al.* 2007]. Analyses were performed in triplicate with an HP 1100 Series Liquid Chromatography-Mass Spectrometer (LC-MS) equipped with an auto-injector and ChemStation chromatography manager software. Separation was achieved on a Prevail Cyano column (2.1 x 150mm, 3µm; Alltech, Deerfield, Illinois, USA), maintained at 30°C. GDGTs were eluted isocratically first with hexane/isopropanol (99:1 % ;vol:vol) for 5 min, then using a linear gradient up to 1.8 % vol of isopropanol over 45 min. Flow rate was 0.2 mL/min. After each analysis the column was cleaned by back flushing hexane/isopropanol (90:10; vol:vol) at 0.2 mL/min for 10 min. Detection was achieved using atmospheric pressure chemical ionization-mass spectrometry (APCI-MS) of the eluent with the following conditions; nebulizer pressure 60 psi, vaporizer temperature 400°C, N_2 drying gas flow 6 L/min at 200ºC, capillary voltage -3kV, corona 5µA (~3.2kV). Single Ion

Monitoring (SIM) was used instead of full mass scanning because SIM increases the signal-to-noise-ratio and thus improves reproducibility [*Schouten et al.* 2007]. SIM was set to scan the five $[M+H]^+$ ions of the GDGTs and the three $[M+H]^+$ ions of the branched tetraethers with a dwell time of 237 ms for each ion. The TEX_{86} ratio was calculated according to *Schouten et al.* [2002]. The TEX_{86} values relate to temperature according to the following empirical relationship [*Schouten et al.,* 2002]:

$$TEX_{86} = 0.015 \cdot T + 0.28 \quad [1]$$

The BIT index was calculated according to *Hopmans et al.* [2004]. Samples were run in triplicate and the average standard deviation for TEX_{86} was 0.004 or 0.3 ºC, whilst the average standard deviation for BIT index was 0.01.

9.3. Results

The TEX_{86} ranged between 0.36 and 0.65 or 5.5 and 24.8ºC when translated to temperature using the temperature calibration of *Schouten et al.* [2002] (Fig. 2a). The average TEX_{86} value was lower in the glacial MIS 6 (14.4ºC) than during the interglacial MIS 7 (18.2ºC). TEX_{86}-derived temperatures in MIS 6 show great variability and corresponded well with known cold events (stadials, vertical numbers in Fig. 2c) and warm events (interstadials; horizontal number in Fig. 2c) previously reported for this core by *Martrat et al.* [2004]. During MIS 7 temperatures were more stable with only six stadials and interstadials. Most of the changes in TEX_{86} temperatures were synchronous with the ones previously reported using the $U^{k'}_{37}$ palaeothermometer [*Martrat et al.,* 2004] (Figs. 2a and c).

We also measured the BIT index which is a relative ratio of marine-derived crenarchaeol versus terrestrially-derived branched tetraether lipids [*Hopmans et al.*, 2004] and it is used to estimate riverine input of terrestrial organic matter. The BIT values ranged between 0.01 and 0.17 indicating only a small input of riverine terrestrial organic matter [cf. [*Hopmans et al.,* 2004; *Weijers et al.,* 2006]), consistent with the absence of a large river system in the area. The average BIT values were nearly identical for MIS 6 (0.05) and MIS 7 (0.06). There were six peaks in BIT record of up to 0.15 during MIS 6 (149.9, 153.6, 166.7, 176.6, 181.4 and 184.5 cal. ky BP) (Fig. 2b).

During MIS 7 a small increase of this index is observed between 191 and 194 cal. ky BP and 223 and 230 cal. ky BP with a smaller peak at 238 cal. ky BP.

9.4. Discussion

The Alboran Sea area is strongly influenced by the surrounding land masses [*Fabres et al.,* 2002] and, thus, large amounts of terrestrial organic matter may be present in the sediment which can compromise the TEX_{86} temperature estimates [*Weijers et al.,* 2006]. However, BIT values are always low (<0.2) and there is no correlation between TEX_{86} and BIT index (Fig. 3a). This is in agreement with the idea that BIT is reflecting fluvial input which is known to be relatively small in the Alboran Sea [*Fabres et al.,* 2002]. Therefore, the TEX_{86} record can be interpreted with confidence as reflecting a marine temperature signal.

The trends in TEX_{86} temperatures are consistent with both the $\delta^{18}O$ record of planktonic foraminifera *G. bulloides* and $U^{k'}_{37}$ temperatures (Figs. 2c-e), suggesting that the TEX_{86} proxy reflects temperature changes in the Alboran Sea. The changes in temperatures are nearly always synchronous between TEX_{86}, $U^{k'}_{37}$ and $\delta^{18}O$ suggesting no temporal offset due to dissimilar sedimentation processes between archaea, coccolithophores and foraminifera in agreement with previous observations in the Alboran Sea [*Martrat et al.,* 2004] but in contrast to results from radiocarbon studies in other areas [e.g. *Ohkouchi et al.,* 2002; *Mollenhauer et al.,* 2005]. But most importantly, the TEX_{86} record confirms the presence of stadial-interstadial episodes during MIS 6 and MIS 7 and also corroborates that these periods were less stable than previously thought.

However, while the patterns in temperature change are the same, the absolute temperature ranges are different for the two molecular proxies. The TEX_{86} varies over a 15ºC range, which is considerably larger than the 11.5ºC range of the $U^{k'}_{37}$. While TEX_{86}-derived temperatures are similar to those derived with the $U^{k'}_{37}$ during MIS 7 they show a much wider range during MIS 6, i.e. during MIS 6 TEX_{86} temperatures are higher than $U^{k'}_{37}$ temperatures during interstadials and lower during stadials (Figs. 2 and 3).

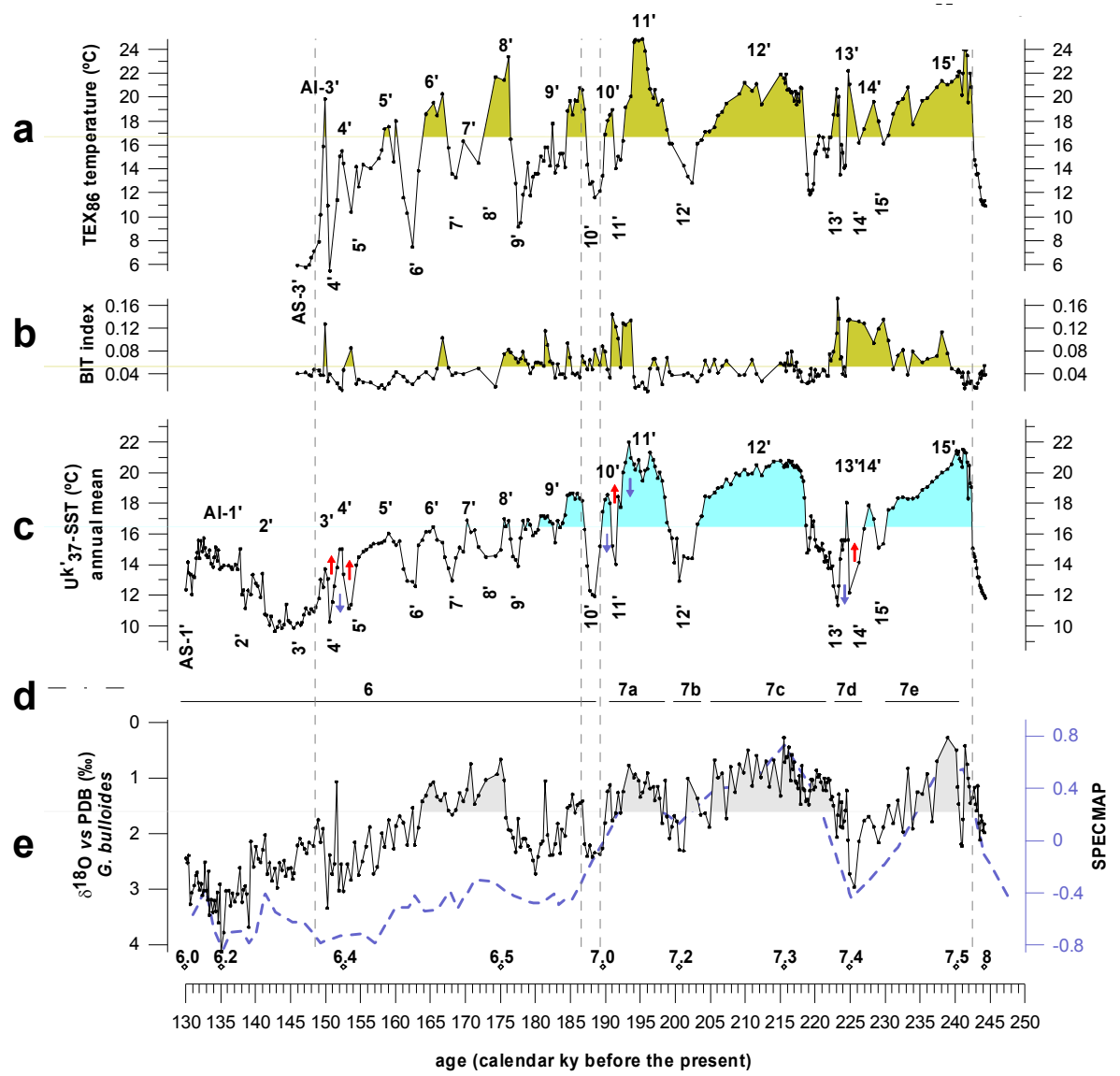

Figure. 2. Palaeoenvironmental records over MIS 6 and MIS 7 in ODP-977A: **a**) TEX_{86} temperature record **b**) BIT index record, **c**) $U^{k'}_{37}$-SST record. This record show fifteen warm (AI-1′ to 15′) and fifteen cold (AS-1′ to 15′) spells and abrupt changes were defined as warming (red arrows) or cooling (blue arrows) episodes that happened at rate equal to or faster than the SST variation over the last deglaciation [(2.6ºC/ky) [*Martrat et al.,* 2004].; **d)** Glacial (6) and interglacial (7) marine isotope stages (MISs); **e)** $\delta^{18}O$ of *Globigerina bulloides* [*Martrat et al.,* 2004] compared with the SPECMAP standard isotope curve, which is shown by the dotted line [*Martinson et al.,* 1987]. Diamonds show some of the control points used for the age model. Values above average are indicated by the filled areas.

This phenomenon can be best illustrated by cross correlating the TEX_{86} record with the $U^{k'}_{37}$ record for MIS 6 and MIS 7 separately (Figs. 3b-d). The degree of correlation between $U^{k'}_{37}$ and TEX_{86} is similar during the interglacial (r^2=0.56) and the glacial period (r^2=0.52) but the slope of the correlation differs substantially, 0.89 for MIS 7 and 1.35 during MIS 6 (Fig. 3). Thus, a change of 1°C in the $U^{k'}_{37}$ record is reflected as a ~1.4°C change in the TEX_{86} temperature record in MIS 6 and a ~0.9°C change during MIS 7.

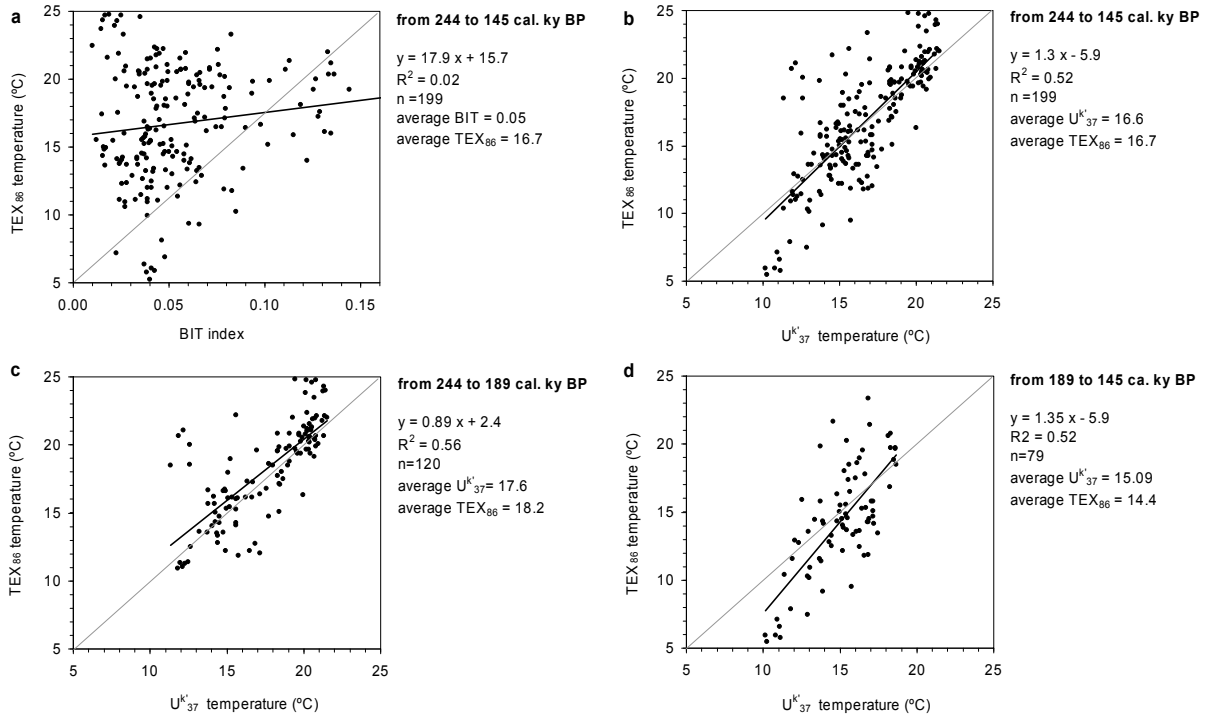

Figure. 3. a) Correlation between TEX_{86} temperatures and the BIT index for the whole period studied (244-145 cal. ky BP) and correlations between $U^{k'}_{37}$ and TEX_{86} temperatures for different time spans: **b)** from 244 to 145 cal. ky BP; **c)** from 244 to 189 cal. ky BP (MIS 7); **d)** from 189 to 145 cal. ky BP (most of MIS 6). Fitted linear equations, the R^2 values, number of data points used (n) and average values are indicated. The 1:1 correlation is indicated by the grey line.

The remarkable agreement between TEX_{86} and $U^{k'}_{37}$ temperatures during MIS 7 suggests that the organisms producing the lipids on which these proxies are based are reflecting temperatures of the same season and similar depth (<100m). In the Alboran Sea two main regimes occur; the fall to winter bloom (November-March) and the non-bloom period (May to September) [*Garcia-Gorriz and Carr,* 1999]. Thus, it seems likely that haptophytes would be growing mainly in fall-winter in the study area and thus, presently, $U^{k'}_{37}$ may preferentially record winter temperatures in the area. Present temperatures in the bloom period (November-March) are on average 16-17ºC [*Garcia-Gorriz and Carr*, 1999] which is similar to the average $U^{k'}_{37}$ values for the interglacial MIS 7 of 17.6ºC. The similar average TEX_{86} temperature for MIS 7 (18.2ºC) suggests that Crenarchaeota also may have thrived in fall-winter. Unfortunately, it is not known what the seasonal abundance of Crenarchaeota is in the Alboran Sea and this hypothesis cannot be tested at present.

During MIS 6, TEX_{86} and $U^{k'}_{37}$ behave differently with TEX_{86} temperatures being higher than $U^{k'}_{37}$ temperatures during interstadials and lower during stadials. There may be two reasons for this differential response of the TEX_{86} and $U^{k'}_{37}$: seasonality and/or depths habitats. Possibly, the Crenarchaeota shifted to a different season, i.e. from fall-winter during MIS 7 to spring-summer during MIS 6. However, this difference in seasonality can only explain why TEX_{86} during interstadials shows higher SSTs than $U^{k'}_{37}$ (Fig. 3b). It does not explain why in stadials TEX_{86}-reconstructed SSTs are substantially lower than those based on the $U^{k'}_{37}$ unless during stadials Crenarchaeota and haptophytes are blooming in opposite seasons, i.e. fall-winter for Crenarchaeota and spring-summer for haptophyte algae.

Alternatively, the TEX_{86} proxy signal could be derived from a different depth than the $U^{k'}_{37}$ during MIS 6 in contrast to what seems to be the case for MIS 7. As haptophytes are light dependent they are constrained to surface waters (<100 m). Indeed, the maximum abundances of alkenones range from 30-100m in the western Mediterranean [*Ternois et al.,* 1997; *Sicre et al.,* 1999; *Bentaleb et al.,* 1999]. However, as Crenarchaetoa are chemoautotrophs, they are not light dependent and can thrive deeper in the water column as has been shown in numerous studies [e.g *Massana et al.,* 1998; *Murray et al.,* 1999; *Karner et al.,* 2001; *Herndl. et al.*, 2005]. However, previous studies have shown that the TEX_{86} correlates well with surface water temperatures (depths <100m) and that the signal in the deeper water layers and sediments is primarily derived from these surface waters [*Wuchter et*

al., 2005; *Huguet et al.* 2006], which also seems to be the case for the interglacial MIS 7. However, recent evidence suggests that sometimes TEX_{86} reflects subsurface temperatures rather than SST [*Huguet et al.* 2007, in press]. Currently, there is not a strong temperature gradient in the water column (Fig. 1b) [*Fabres et al.,* 2002] and thus the difference in depth habitat between haptophytes and Crenarchaeota would have a fairly small effect (<1ºC), which could also explain the good correspondence between TEX_{86} and $U^{k'}_{37}$ during MIS 7. However, during glacial MIS 6 there could have been a much larger temperature gradient with depth. Indeed, a multiproxy study in the Alboran Sea revealed that the Atlantic-Mediterranean temperature gradient was larger during glacial periods (~4ºC) than during the Holocene (1-2ºC) [*Cacho et al.,* 2001], suggesting a steeper temperature gradient between Atlantic and Mediterranean water masses during cold periods. This is supported by other studies in the area that indicated a change in the ventilation of the Alboran sea during glacial stages which will have resulted in change of the water column structure and temperature gradient and the occurrence of colder, more oxygenated deep water masses during stadials [*Cacho et al.,* 2002; *Moreno et al.,* 2004]. Therefore, at times of abrupt climate change and likely nutrient reorganisation and stratification [*Moreno et al.,* 2004], Crenarchaeota could be moving to deeper, colder waters such as the LIW or WMDW (Fig. 1b) and thus reflect colder water temperatures than the $U^{k'}_{37}$, especially during the glacial MIS 6. However, while this may explain the colder TEX_{86} values during stadials it does not explain the warmer values during interstadials. Thus, at present, no single hypothesis can fully explain the difference observed between $U^{k'}_{37}$ and TEX_{86} during MIS 6 but a combination of both seasonality and depth changes could explain both the higher and lower TEX_{86} values during stadial and interstadial episodes, respectively. To fully understand our results further work in the Alboran Sea is necessary to establish both the seasonality and depth distribution of Crenarchaeota and haptophyte algae, especially during glacial periods.

9.5. Conclusions

The TEX_{86} record of the Alboran Sea shows very similar trends to the $U^{k'}_{37}$ and confirms the previously inferred stadial and interstadial episodes detected with the $U^{k'}_{37}$. The absolute temperature estimates of TEX_{86} and $U^{k'}_{37}$ agree well during MIS 7 but there is substantial difference between the two proxies in temperature range during MIS 6 with TEX_{86} showing more extreme temperature variations compared to the $U^{k'}_{37}$. We propose two hypotheses to explain the differences between the two proxies during MIS 6 i.e. a change in the growth season or depth distribution of the Crenarchaeota. A shift of Crenarchaeota seasonality towards summer could explain the warmer TEX_{86} interstadial temperatures. During stadials Crenarchaeota could be moving deeper in the water column while haptophytes would remain in the surface water. A combination of these two processes could potentially explain both the higher and lower TEX_{86} values during stadial and interstadials during MIS 6. However a better constrain of the seasonality and depth distribution of Crenarchaeota and haptophyte algae is needed to resolve that issue.

Acknowledgements

This project was supported by NWO-ALW (Project nr. 152911)

References

Bentaleb, I., J. O. Grimalt, F. Vidussi, J. C. Marty, V. Martin, M. Denis, C. Hatté, and M. Fontugne (1999), The C_{37} alkenone record of seawater temperature during seasonal thermocline stratification, *Mar.Chem.*, *64*, 301-313.

Cacho, I., J. O. Grimalt, M. Canals, L. Sbaffi, N. J. Shackleton, J. Schonfeld, and R. Zahn (2001), Variability of the western Mediterranean Sea surface temperature during the last 25,000 years and its connection with the Northern Hemisphere climatic changes, *Paleoceanography*, *16*, 40-52.

Cacho, I., J. O. Grimalt, C. Pelejero, M. Canals, F. J. Sierro, J. A. Flores, and N. Shackleton (1999), Dansgaard-Oeschger and heinrich event imprints in Alboran Sea paleotemperatures, *Paleoceanography*, *14*, 698-705.

Cacho, I., J. O. Grimalt, F. J. Sierro, N. Shackleton, and M. Canals (2000), Evidence for enhanced Mediterranean thermohaline circulation during rapid climatic coolings, *Earth Planet. Sci. Lett*, *183*, 417-429.

Cacho, I., F. Sierro, N. J. Shackleton, H. Elderfield, and J. Grimalt (2002), Reconstructing Alboran Sea hydrography during the last organic rich layer formation, *Geochim. Cosmochim. Acta*, *66*, A115.

Comas M. C., Zahn R., Klaus A. et al., (1996). Site 977. Proceedings of the Ocean Drilling Program, in : *Initial Reports, College Station, TX (Ocean Drilling Program), volume 161*, 299-353

Dansgaard, W., S. J. Johnsen, H. B. Clausen, D. Dahljensen, N. S. Gundestrup, C. U. Hammer, C. S. Hvidberg, J. P. Steffensen, A. E. Sveinbjornsdottir, J. Jouzel, and G. Bond (1993), Evidence for General Instability of Past Climate from A 250-Kyr Ice-Core Record, *Nature*, *364*, 218-220.

Fabres, J., A. Calafat, A. Sanchez-Vidal, M. Canals, and S. Heussner (2002), Composition and spatio-temporal variability of particle fluxes in the western Alboran Gyre, Mediterranean Sea, *J. Mar. Sys.*, *33*, 431-456.

Garcia-Gorriz, E. and M. E. Carr (1999), The climatological annual cycle of satellite-derived phytoplankton pigments in the Alboran Sea, *Geophys. Res. Lett.*, *26*, 2985-2988.

Grootes, P. M. and M. Stuiver (1997), Oxygen 18/16 variability in Greenland snow and ice with 10^{-3} to 10^{5}year time resolution, *J. Geophys. Res.-Oceans*, *102*, 26455-26470.

Heinrich, H. (1988), Origin and Consequences of Cyclic Ice Rafting in the Northeast Atlantic-Ocean During the Past 130,000 Years, *Quat. Res.*, *29*, 142-152.

Herndl, G. J., T. Reinthaler, E. Teira, H. van Aken, C. Veth, A. Pernthaler, and J. Pernthaler (2005), Contribution of Archaea to total prokaryotic production in the deep Atlantic Ocean, *Appl. Environ. Microbiol.*, 71, 2303-2309.

Hopmans, E. C., S. Schouten, R. D. Pancost, M. T. J. Van der Meer, and J. S. Sinninghe Damsté (2000), Analysis of intact tetraether lipids in archaeal cell material and sediments by high performance liquid

chromatography/atmospheric pressure chemical ionization mass spectrometry, *Rap. Commun. Mass Spectr.*, *14*, 585-589.

Hopmans, E. C., J. W. H. Weijers, E. Schefuss, L. Herfort, J. S. Sinninghe Damsté, and S. Schouten (2004), A novel proxy for terrestrial organic matter in sediments based on branched and isoprenoid tetraether lipids, *Earth Planet. Sci. Lett*, *224*, 107-116.

Huguet, C., J-H. Kim, J. S. Sinninghe Damsté, S. Schouten, (2006). Reconstruction of sea surface temperature variations in the Arabian Sea over the last 23 kyr using organic proxies (TEX_{86} and $U^{K'}_{37}$). *Paleoceanography* 21 doi:10.1029/2005PA001215

Karner, M. B., E. F. DeLong, and D. M. Karl (2001), Archaeal dominance in the mesopelagic zone of the Pacific Ocean, *Nature*, *409*, 507-510.

Könneke, M., A. E. Bernhard, J. R. de la Torre, C. B. Walker, J. B. Waterbury, and D. A. Stahl (2005), Isolation of an autotrophic ammonia-oxidizing marine archaeon, *Nature*, *437*, 543-546.

Martinson, D. G., N. G. Pisias, J. D. Hays, J. Imbrie, T. C. Moore, and N. J. Shackleton (1987), Age Dating and the Orbital Theory of the Ice Ages - Development of A High-Resolution-0 to 300,000-Year Chronostratigraphy, *Quat. Res.*, *27*, 1-29.

Martrat, B., J. O. Grimalt, C. Lopez-Martinez, I. Cacho, F. J. Sierro, J. A. Flores, R. Zahn, M. Canals, J. H. Curtis, and D. A. Hodell (2004), Abrupt temperature changes in the Western Mediterranean over the past 250,000 years, *Science*, *306*, 1762-1765.

Massana, R., L. T. Taylor, A. E. Murray, K. Y. Wu, W. H. Jeffrey, and E. F. DeLong (1998), Vertical distribution and temporal variation of marine planktonic archaea in the Gerlache Strait, Antarctica, during early spring, *Limnol. Oceanogr.*, *43*, 607-617.

McManus, J. F., D. W. Oppo, and J. L. Cullen (1999), A 0.5-million-year record of millennial-scale climate variability in the North Atlantic, *Science*, *283*, 971-975.

Mollenhauer, G., M. Kienast, F. Lamy, H. Meggers, R. R. Schneider, J. M. Hayes, and T. I. Eglinton (2005), An evaluation of ^{14}C age relationships between co-occurring foraminifera, alkenones, and total organic carbon in continental margin sediments, *Paleoceanography*, *20*, PA1016 10.1029/2004PA001103

Moreno, A., I. Cacho, M. Canals, J. O. Grimalt, and A. Sanchez-Vidal (2004), Millennial-scale variability in the productivity signal from the Alboran Sea record, Western Mediterranean Sea, *Palaeogeography Palaeoclimatology Palaeoecology*, *211*, 205-219.

Murray, A. E., A. Blakis, R. Massana, S. Strawzewski, U. Passow, A. Alldredge, and E. F. DeLong (1999), A time series assessment of planktonic archaeal variability in the Santa Barbara Channel, *Aquat.Microb.Ecol.*, *20*, 129-145.

Ohkouchi, N., T. I. Eglinton, L. D. Keigwin, and J. M. Hayes (2002), Spatial and temporal offsets between proxy records in a sediment drift, *Science*, *298*, 1224-1227.

Schouten, S., E. C. Hopmans, E. Schefuss, and J. S. Sinninghe Damsté (2002), Distributional variations in marine crenarchaeotal membrane lipids: a new tool for reconstructing ancient sea water temperatures?, *Earth Planet. Sci. Lett*, *204*, 265-274.

Schouten, S., C. Huguet, E.C. Hopmans, M. V.M. Kienhuis and J. S. Sinninghe Damsté (2007), Improved analytical methodology and constraints on analysis of the TEX86 paleothermometer by high performance liquid chromatography/atmospheric pressure chemical ionization-mass spectrometry. *Analy. Chem*. doi:10.1021/ac062339v

Sicre, M. A., Y. Ternois, J. C. Miquel, and J. C. Marty (1999), Alkenones in the Northwestern Mediterranean sea: interannual variability and vertical transfer, *Geophys.Res.Lett.*, *26*, 1735-1738.

Ternois, Y., M. A. Sicre, A. Boireau, M. H. Conte, and G. Eglinton (1997), Evaluation of long-chain alkenones as paleo-temperature indicators in the Mediterranean Sea, *Deep-Sea Res. Part I-Oceanographic Research Papers*, *44*, 271-286.

Weijers, J. W. H., S. Schouten, O. C. Spaargaren, and J. S. Sinninghe Damsté (2006), Occurrence and distribution of tetraether membrane lipids in soils: Implications for the use of the TEX_{86} proxy and the BIT index, *Org. Geochem.*, *37*, 1680-1693.

Wuchter, C., S. Schouten, S. G. Wakeham, and J. S. Sinninghe Damsté (2005), Temporal and spatial variation in tetraether membrane lipids of marine Crenarchaeota in particulate organic matter: Implications for TEX_{86} paleothermometry, *Paleoceanography*, *20,* doi:10.1029/2004PA001110.

Summary

Determination of past sea surface temperature (SST) is of primary importance for the reconstruction of natural climatic changes, modelling of climate and reconstruction of ocean circulation. A number of geochemical proxies for SST reconstruction are currently used but their application are associated with several uncertainties and thus there is a need .for new SST proxies to complement presently used proxies. Recently, a new SST proxy was introduced, the TetraEther indeX of lipids with 86 carbons (TEX_{86}), which is based on temperature-related changes that occur in the composition of creanarchaeotal membrane lipids. The membranes of Crenarchaeota are composed of glycerol dibiphytanyl glycerol tetraethers (GDGTs) and changes in the relative abundance of these lipids allow them to adjust their membrane fluidity as a response to fluctuations in water temperature. An empirical correlation between TEX_{86} values of sediment core tops from a wide variety of geographical locations and annual mean SST has been used to calibrate the TEX_{86} proxy. The main objective of the work described in this thesis was to improve, validate and apply the TEX_{86} proxy. To do this we focused on a) the analytical aspects of the TEX_{86}, b) the transport of GDGTs to the sediment and the influence of diagenesis and c) the application of the proxy in various settings.

Regarding the analytical aspects, a comparison of different extraction techniques revealed no significant differences in TEX_{86} values. Comparison of TEX_{86} analysis using different mass spectrometry techniques, i.e. Single Ion Mode (SIM) and mass scanning detection, showed that SIM is up to two orders of magnitude more sensitive. The detection limit of the GDGTs was also established and shown to be 0.05 ng GDGTs injected on-column. Application of SIM improved the analytical reproducibility to 0.3ºC. Thus, the TEX_{86} can now be measured with a much better accuracy than was previously possible. A new synthetic internal GDGT standard was used which greatly improved the accuracy of GDGT abundance measurements. With this method the standard deviation in the determination of the abundance was only 5% compared to 43% when using an external standard. This increases the potential of GDGTs in (paleo)ecological studies substantially.

The transport and diagenesis of GDGTs were also subject of study as they are essential in understanding and applying the TEX_{86} as palaeothermometer.

Although several studies have established that Crenarchaeota are distributed throughout the water column, previous studies have shown that TEX_{86} values of particulate organic matter, sediment traps and sediment core tops are better correlated with SST (depth <100 m) than with deeper water temperatures. However, Crenarchaeotal cells do not have sufficient density to sink to the sediment after cell death and this would prevent the TEX_{86} signal from reaching the sediment surface. To investigate this, GDGTs were analysed in stomachs and intestines of crustacean decapods, which are key element of most pelagic food webs. This study revealed the presence of GDGTs in both stomachs and, in lower amounts, in the intestines showing uptake of GDGTs by decapods. This, together with pigment analysis, suggests that both passive (by sinking particles) and active (by organism migration) transport mechanism can explain, at least in part, the transport of GDGTs from surface waters to the sediment. GDGT abundances are significantly lower in intestines, but TEX_{86}-derived temperatures are not significantly different between stomachs and intestines (<1°C), suggesting that TEX_{86} values are not altered during gut transit. In contrast to these results, a study using sediment traps and a sediment core covering the last 150 years in the Santa Barbara Basin revealed that TEX_{86} values were always substantially lower than sea surface temperatures (SST), indicating a sub-surface origin, likely between 100-150 m. This could be related to the depth origin of the TEX_{86} signal and be ultimately controlled by the phytoplankton surface community and water column dynamics. This result highlights the importance of performing calibration studies using sediment traps and core tops before applying the TEX_{86} temperature proxy in a given study area.

To investigate the effect of degradation by long term exposure to oxygen we analyzed GDGTs abundance, TEX_{86} and Branched versus Isoprenoid Tetraether index (BIT) in several Madeira Abyssal Plain turbidites across an oxidation front. A decrease by several orders of magnitude in the concentrations of GDGTs was found and also substantial shifts in the BIT and TEX_{86}. The shifts are interpreted to be caused by a strong relative increase in soil-derived GDGTs relative to the marine-derived GDGTs. This selective preservation of soil-derived lipids which are chemically nearly identical to that of their marine counterpart strongly suggests that the mineral matrix to which soil organic matter is attached enhanced its preservation. This indicates that care has to be taken when analyzing TEX_{86} in sediments which have been exposed to oxygen for a long time.

Finally the application of the TEX_{86} to a range of environments and time resolutions in combination with other SST proxies allowed the validation of the TEX_{86} proxy as a paleothermometer. Analysis of two cores in the Drammensfjord, Norway, with a centennial time scale at an almost annual resolution, suggested that TEX_{86} recorded surface (upper 25m) temperatures. Moreover, TEX_{86} temperature patterns followed variations in the historical record of averaged spring to fall Oslo air temperature relatively closely, suggesting the signal is produced during this period. Therefore, TEX_{86} temperature records of fjord sediment cores can potentially be a useful tool in reconstructing past variations of coastal climates. We also compared the TEX_{86} and $U^{K'}_{37}$ index derived form long-chain alkenones from haptophyte algae during the last glacial-interglacial transition in two cores in the Arabian Sea. TEX_{86} SST records were similar at the two sites over the last glacial-interglacial cycle and were in phase with temperature changes recorded in Antarctica ice core records. This suggests that the TEX_{86} records of SST in the area are mainly controlled by the southern hemisphere climate dynamics during the SW monsoon. $U^{K'}_{37}$ SST records from the same cores are different in magnitude of change and differ also in phase, and are partly in phase with northern hemisphere climate dynamics during the NE monsoon. This is likely due to different growing seasons of the biomarker source organisms, and to a change in the upwelling dynamics and monsoon strengths between the LGM and the Holocene.

In the oldest sediments analysed, TEX_{86} was applied to a sediment core spanning the Marine Isotope Stadials (MIS) 6 and 7 in the Western Mediterranean. A recent study in the Alboran Sea (Western Mediterranean, core ODP-977A) revealed that alkenone records not only show temperature trends similar to $\delta^{18}O$ records of *G. bulloides*, but also stadial-interstadial temperature changes during the penultimate climate cycle (from 244 to 130 cal. ky BP). To independently confirm these abrupt changes, we applied the TEX_{86} proxy to reconstruct SST using the same sediment core. The TEX_{86} indicated similar stadial-interstadial temperature changes as detected with the $U^{K'}_{37}$, thus providing independent evidence for rapid temperature changes. However, the two proxies behaved differently during glacial marine isotopic stage (MIS-6) and interglacial MIS-7. During MIS-7 there is good correspondence in absolute SST estimates between the two proxies, but in MIS-6 the TEX_{86} showed much larger temperature changes compared to the $U^{K'}_{37}$. We hypothesize that this may

be caused by changes in the season in which the haptophytes and Crenarchaeota are blooming and/or variations in the depth habitat of Crenarchaeota. As the climate forcing differs between glacials and interglacials, a change in seasonal patterns and/or depth habitat can be expected which could have a strong and differential effect on the TEX_{86} and $U^{k'}_{37}$ proxies.

In summary, the results described in this thesis resulted in a substantial improvement of the analytical aspects of TEX_{86}, resulting in a better reproducibility in measuring this proxy. The origin and transport of the GDGT signal was also studied and shown to be mediated by both passive and active transport mechanisms. This work also provided essential information about constraints and pitfalls of the proxy such as its varying depth origin and the effects of long-term oxic degradation. Finally, the proxy was validated through core measurements and comparison with other proxies. This thesis shows that TEX_{86} is a useful SST proxy which can provide complementary information to other SST proxies.

Samenvatting

Het bepalen van vroegere oppervlakte zeewatertemperaturen (OZT) is van groot belang voor de reconstructie van natuurlijke klimaatveranderingen en de oceaancirculatie in het verleden. Deze informatie is op haar beurt weer van belang om klimaatmodellen, die onder andere gebruikt worden om het toekomstige klimaat te voorspellen, te testen. Een aantal geochemische proxies voor de reconstructie van OZT zijn op dit moment beschikbaar maar aan hun toepassing kleeft een aantal onzekerheden. Nieuwe proxies voor OZT zijn dus noodzakelijk om de momenteel beschikbare proxies te complementeren. Recentelijk is een nieuwe OZT proxy geïntroduceerd; de TetraEther indeX van lipiden met 86 koolstofatomen (TEX_{86}), gebaseerd op temperatuurgerelateerde veranderingen in de samenstelling van membraanlipiden van pelagische Crenarchaeota, een groep micro-organismen die binnen het domein van de archaea vallen. De membranen van Crenarchaeota zijn samengesteld uit glycerol dibiphytanyl glycerol tetraethers (GDGTs) en veranderingen in de relatieve hoeveelheden van deze lipiden maken het mogelijk de membraanfluïditeit aan te passen aan veranderingen in watertemperatuur. Een empirische correlatie tussen TEX_{86} in oppervlaktesedimenten van geografisch verschillende herkomst en OZT is gebruikt voor de calibratie van deze proxy. Het belangrijkste doel van het werk beschreven in dit proefschrift was het verbeteren, valideren en toepassen van de TEX_{86} proxy. Daartoe werden 1) analytische aspecten van de TEX_{86}, 2) het transport van GDGTs naar het sediment en de invloed van diagenese en 3) de toepassing van de proxy in verschillende milieus bestudeerd.

Betreffende de analytische aspecten liet een vergelijking tussen verschillende extractietechnieken zien dat er geen significante verschillen in TEX_{86} zijn. Vergelijking van verschillende massaspectrometrische detectietechnieken [Single Ion Monitoring (SIM) en detectie door middel van massa scanning], liet zien dat de SIM methode tot twee ordes van grootte gevoeliger is. De detectielimiet van de GDGT analyse werd bepaald op 5 pg GDGTs on-column geïnjecteerd. Toepassing van de SIM methode verbeterde ook de analytische reproduceerbaarheid van de TEX_{86} tot 0.3ºC, een aanzienlijke verbetering ten opzichte van de eerder toegepaste methode. Het gebruik van een nieuwe synthetische GDGT interne standaard verbeterde de kwantificering van GDGTs aanzienlijk:

met deze methode was de standaarddeviatie slechts 5% terwijl bij gebruik van een bepaling met een externe standaard een standaarddeviatie van 43% werd behaald. Deze verbetering maakt het potentiële gebruik van GDGTs in (paleo)ecologische studies veel groter.

Ook het transport van GDGTs van de waterkolom naar het sediment en mogelijke effecten van diagenese in het sediment werden onderzocht, omdat een goed begrip van deze processen essentieel is voor een correcte toepassing van de TEX_{86} palaeothermometer. Hoewel verschillende studies hebben laten zien dat Crenarchaeota voorkomen in de gehele waterkolom, heeft ander onderzoek aangetoond dat de TEX_{86} van gesuspendeerd organisch materiaal, sedimentvallen en oppervlaktesedimenten beter correleren met OZT (diepte <100m) dan met de temperatuur van het diepere water. De kleine cellen van Crenarchaeota hebben echter niet een voldoende hoge dichtheid om na de celdood te bezinken naar het sediment waardoor het TEX_{86} signaal de zeebodem niet zou kunnen bereiken. Om dit nader te bestuderen werden GDGTs geanalyseerd in de maag en darmen van decapoda (tienpotigen), die een sleutelrol vervullen in de pelagische voedselketen. Deze studie liet zien dat GDGTs aanwezig zijn in zowel de maag als in de darmen, zij het in lagere hoeveelheden. Dit toonde aan dat GDGTs opgenomen worden door kreeftachtigen. Samen met pigmentanalyse suggereerde dit dat zowel passief (via zinkende deeltjes) als actief (via migratie van organismen) transport kan verklaren waarom GDGTs uit oppervlaktewater preferent getransporteerd worden naar het sediment. Hoewel de GDGT concentraties significant lager zijn in de darmen, waren de TEX_{86}-waarden niet significant verschillend tussen de maag en darmen. Dit suggereerde dat de TEX_{86} niet veranderde tijdens degradatie in de maag.

Een studie van sedimentvallen en een sedimentkern afgezet in de laatste 150 jaar in het Santa Barbara Basin liet zien dat de berekende TEX_{86} temperaturen altijd substantieel lager waren dan de gemeten OZT, en meer overeenkwamen met de temperatuur van diepere wateren, rond de 100-150 m. Dit komt waarschijnlijk door een diepere oorsprong van het TEX_{86} signaal die ook nog eens variabel is door de dynamiek van de waterkolom. Dit resultaat onderstreept het belang van het verrichten van calibratiestudies door middel van sedimentvallen en oppervlaktesedimenten voordat de TEX_{86} proxy toegepast kan worden in palaeoklimaatreconstructies.

Om het effect van degradatie door lange-termijn blootstelling aan zuurstof vast te stellen werden GDGT concentraties, de TEX_{86} en de Branched versus Isoprenoid Tetraether

index (BIT) geanalyseerd in een aantal Madeira Abyssal Plain turbidieten over een oxidatiefront. GDGT concentraties waren ordes van grootte lager in de geoxideerde turbidietlagen. Er werden ook substantiële veranderingen gevonden in de BIT and TEX_{86}. Deze veranderingen worden veroorzaakt door een relatieve toename van GDGTs afkomstig uit bodems ten opzichte van GDGTs afkomstig uit het mariene milieu. Deze selectieve preservatie van lipiden afkomstig van bodems en die chemisch gezien vrijwel identiek zijn aan die afkomstig uit het mariene milieu suggereerde dat de minerale matrix waarmee het organische bodemmateriaal geassocieerd is de preserveringskansen sterk doet toenemen. Dit geeft ook aan dat men voorzichtig moet zijn met de analyses van TEX_{86} in sedimenten die langdurig zijn blootgesteld aan zuurstof.

Tenslotte werd de TEX_{86} toegepast in verschillende milieus en met verschillende tijdsresolutie in combinatie met andere OZT proxies om de TEX_{86} proxy verder te valideren als paleothermometer. De analyse van twee kernen uit Drammensfjord, Noorwegen, afgezet in de laatste eeuw en bemonsterd met een jaarlijkse tijdsresolutie suggereerde dat de TEX_{86} de OZT (< 25 m) weergaf. Bovendien co-varieerden de TEX_{86} temperatuurvariaties met de historische variaties in de gemiddelde lente-herfst luchttemperatuur in Oslo. Dit suggereerde dat het TEX_{86} signaal in deze tijdsperiode werd geproduceerd. TEX_{86} temperatuur profielen van fjordsedimenten kunnen dus potentieel nuttig zijn voor de reconstructie van vroegere variaties in kustklimaten. Door middel van analyse van twee boorkernen uit de Arabische Zee werden temperatuurschattingen van de laatste glaciaal-interglaciaal overgang verkregen en met behulp van de TEX_{86} vergeleken met die verkregen met behulp van de $U^{K'}_{37}$ index. De $U^{K'}_{37}$ index is gebaseerd op de samenstelling van alkenonen afkomstig van haptofyte algen. De met de TEX_{86} verkregen OZT profielen waren zeer goed vergelijkbaar in de twee kernen over de laatste glaciaal-interglaciaal cyclus en in fase met temperatuurveranderingen geregistreerd in Antarctische ijskernen. Dit suggereerde dat de met de TEX_{86} gereconstrueerde OZT in dit gebied voornamelijk bepaald werden door klimaatveranderingen op het zuidelijk halfrond gedurende de zuidwest passaat. OZT profielen op basis van de $U^{K'}_{37}$ van dezelfde boorkernen verschilden in de mate van temperatuurveranderingen en ook in fase, en zijn gedeeltelijk in fase met klimaatveranderingen op het noordelijk halfrond. De verschillen in temperatuursignalen geregistreerd met de TEX_{86} en de $U^{K'}_{37}$ index worden waarschijnlijk veroorzaakt door verschillen in het groeiseizoen van de organismen die de biomarkers

produceerden en door veranderingen in de upwellingdynamiek en sterkte van de passaatwinden tussen het laatste glaciaal en het Holoceen.

De TEX_{86} methode werd ook toegepast op een boorkern uit de Westelijke Middellandse Zee die sedimenten afgezet tijdens de Mariene Isotoop Stadia (MIS) 6 en 7 bevatte. Een recente studie aan deze kern liet zien dat OZT profielen die gebaseerd zijn op distributies van alkenonen niet alleen temperatuurveranderingen lieten zien die vergelijkbaar zijn met die gebaseerd op $\delta^{18}O$ waarden van de foraminifeer *G. bulloides*, maar ook stadiaal-interstadiaal temperatuurveranderingen gedurende de op één na laatste klimaatcyclus (van 244 tot 130 cal. ky BP). Ter vergelijking werd de TEX_{86} proxy toegepast op dezelfde sedimentkern om OZT te reconstrueren. Het TEX_{86} profiel liet stadiaal-interstadiaal temperatuurveranderingen zoals eerder gedetecteerd met behulp van de $U^{K'}_{37}$ zien en leverde dus onafhankelijk bewijs voor snelle temperatuurveranderingen. De twee proxies gedroegen zich echter verschillend tijdens het glaciale MIS-6 en het interglaciale MIS-7. Gedurende MIS-7 was er een goede overeenkomst tussen de absolute OZT-schattingen van de twee proxies maar gedurende MIS-6 waren temperatuurvariaties gereconstrueerd met de TEX_{86} veel groter dan die gereconstrueerd met de $U^{K'}_{37}$ index. Dit wordt mogelijk veroorzaakt door de verandering in het seizoen waarin de haptofyten en de Crenarchaeota groeiden of door variaties in de diepte van het water waarin de Crenarchaeota leefden. Omdat het regionale klimaat en milieu verschillend waren tussen glacialen en interglacialen kunnen er verschillen worden verwacht in seizoenspatronen en leefdiepte wat een sterk effect kan hebben op de temperaturen gereconstrueerd met de TEX_{86} en $U^{k'}_{37}$ proxies.

Samenvattend kan gesteld worden dat de resultaten beschreven in dit proefschrift geleid hebben tot een substantiële verbetering in de analyse van de TEX_{86}. Dit heeft heeft geresulteerd in een verbeterde reproduceerbaarheid in de bepaling van deze proxy. De oorsprong en het transport van het GDGT signaal werd ook bestudeerd waaruit bleek dat zowel actieve als passieve transportmechanismen een rol spelen. Deze studie gaf ook essentiële informatie over de beperkingen van de proxy zoals de variërende diepteoorsprong en de effecten van langdurige blootstelling aan zuurstof. Tenslotte werd de proxy gevalideerd door metingen aan sedimentkernen en vergelijking met andere proxies. Dit proefschrift laat zien dat de TEX_{86} een nuttige OZT proxy is die additionele informatie kan geven ten opzichte van andere OZT proxies.

Resum

Determinar la temperatura superficial del mar (SST) és essencial per a reconstruir el canvi climàtic natural versus l'antropogènic, modelar el clima i reconstruir la circulació oceànica. Tot i que existeixen diverses SST proxies, totes presenten incerteses, per aquesta raó son necessaries noves proxies per a complementar els resultats existents. Una nova SST proxy basada en els canvis en la composició lipídica de les membranas dels Crenarchaeota, la TetraEther indeX of lipids with 86 carbons (TEX_{86}) has sigut introduïda recentment. Les membranes dels Crenarchaeota estan formades per glycerol dibiphytanyl glycerol tetraethers (GDGTs), i els canvis en l'abundancia relativa d'aquests lipids permet a aquests organismes adaptar la fluidesa de la membrana a fluctuacions en la temperatura de l' aigua on viuen. La TEX_{86} ha sigut calibrada amb una correlació empírica entre els valors de TEX_{86} d'una gran vairetat d'arees geogràfiques amb la SST mitja anual. L'objectiu principal d'aquesta tesis era millorar, validar i aplicar la TEX_{86}. Per aquesta rao la tesi es centra en a) aspectes analítics de la TEX_{86}, b) el transport de GDGTs als sediments i la influència de la diagènesi i c) l'aplicació de la proxi a diverses arees d'estudi.

En relació als aspectes analítics no s'observen diferències significatives a l'usar tècniques d'extracció diferents. Pero quan s'analitza la TEX_{86} utilitzant diferents tècniques d'espectrometria de masses com: Single Ion Mode (SIM) i Mass Scanning Detection (MSD), els resultats indiquen que la tècnica SIM es dos ordres de magnitut més sensitiva. Els experiments també han permes establir el limit de detecció a 0.05 ng de GDGTs injectats en columna. L'aplicació de la tècnica SIM ha millorat la reproducibilitat de les mesures de TEX_{86} amb un error de només 0.3ºC. Gràcies a aquestes millores la TEX_{86} pot ser mesurada molt més acuradament que abans. La precisió de la mesura de les abundancies absolutes de GDGTs també ha sigut millorada degut a la introducció d'un standard sintètic a la mostra. Amb aquest nou mètode, la desviació estándar en la determinacio d'abundancies de GDGTs ha millorat fins al 5% respecte al 43% amb l'estándar extern. Incrementant així el potencial d'us de GDGTs en estudis (paleo)ecològics.

El transpor i la diagènesi de GDGTs també és essencial per a entendre i aplicar la TEX_{86}. Tot i que hi ha evidència de que les Crenacheotes poden viure a tota la columna d'aigua, estudis previs indiquen que els valors de TEX_{86} de particules orgàniques i sediments de superficie estan més ben correlacionades amb SST (profunditats <100m) que amb temperatures a més gran profunditat. Però les cel·lules de Crenachota son massa petites (< 1 μm) per a sedimentar després de morir i això evitaria que el senyal de la TEX_{86} arribés al sediment. Per tal d'investigar això, estomacs i intestins de decapodes (elements clau en moltes xarxes tròfiques pelàgiques) foren analitzats per establir la presència de GDGTs. El nostre estudi revela la presència de GDGTs a estomacs i en menor quantitat a intestines, indicant que els decapods ingereixen GDGTs. Aquests resultants en combinació amb anàlisis de pigments sugereixen que el transport de GDGTs de la superficie als sediments pot ocorrer tant per mecanismes passius (sedimentació de partícules) com actius (migració). El més rellevant és que tot i que l'abundància de GDGTs està significativament reduida als intestins, no hi ha una diferència significativa (<1ºC) entre TEX_{86} a estomacs i intestins, sugerint que el transit a través del sistema digestiu no altera els valors de TEX_{86}. Contrastant aquests resultats, un estudi usant trampes de sediment i sediment cores cobrint els ultims 150 anys a la Santa Barbara Basin ha revelat que els valors de TEX_{86} es trobaven sempre per sota de les SST, indicant per tant un origen sub-superficial, segurament entre 100 i 150m. Això podria estar relacionat amb la profunditat d'origen de la senyal de TEX_{86} i podria estar controlat per la communitat planctònica superficial i per la dinàmica de la columna d'aigua. Aquests resultats posen de manifest la importància de realitzar estudis de calibració usant trampes de sediment i sediments superficials abans d'aplicar la TEX_{86} a qualsevol area d' estudi.

Per tal d'investigar els efectes de la degradació deguda a una exposició a llarg termini a l'oxigen, vem analitzar l'abundància de GDGTs així com, TEX_{86} i Branched versus Isoprenoid Tetraether index (BIT) a diverses turbites de la Madeira Abyssal Plain al llarg d'un front d'oxidació. Els resultats indiquen una reducció en l'abundància de GDGTs que resulta en canvis substancials en TEX_{86} i BIT. Nosaltres postulem que els canvis son deguts a un increment realtiu dels GDGTs d'origen terrestre versus els d'origen marí. Aquesta conservació selective de GDGTs terrestres amb una estructura química quasi idèntica als d'origen marí sugereix que és la matriu mineral la que protegeix els GDGTs terrestres. Això

indica que cal tenir cura quan s'aplica la TEX_{86} a sediments que hagin estat exposats a oxygen durant llargs periòdes de temps.

Gràcies a l'aplicació de la TEX_{86} a diferents arees amb diferents resolucions temporals i en combinació amb altres proxies, aquesta tesis valida la TEX_{86} com a paleotermometre. Dos cores del Drammensfjord, Noruega, analitzats amb una resolució quasi-anual cobrint els ultims 100 anys suggereix que la TEX_{86} reflexa temperatures superficials (0-25 m). Ademés les temperatures calculades amb la TEX_{86} segueixen bastant accuradament canvis en el record històric de temperatures mitjanes de l' aire a Oslo, concretament entre primavera i tardó indicant que el senyal es produeix en aquest periode. En conclusió sembla que mesurar la temperatura amb la TEX_{86} a sediments de fjords pot ser una eina important per a reconstruir variacions climàtiques a zones costaneres. També hem comparat la TEX_{86} and l'index $U_{37}^{K'}$ (que es deriva de les alkenones de cadena llarga de les algues haptophytes) durant l'última transició glacial-interglacial en dos cores al mar d'Arabia. Les temperatures calculades amb la TEX_{86} eren iguals als dos cores. A mes a més els canvis observats durant l'últim cicle glacial-interglacial estaven en fase amb els canvis trobats a cores de gel de l' Antartida. Aquests resultats indiquen que els canvis de la TEX_{86} en aquesta àrea estan principalment controlats pel clima de l'hemisferi sud durant el SW monzó. En canvi temperatures mesurades amb la $U_{37}^{K'}$ indiquen no només diferents magnituds a les measurades amb TEX_{86}, sinó que semblen estar en fase amb l'hemisferi nort durant el NE monzó. Segurament aquestes diferències son degudes a que els organismes que sintetizen els compostos utilitzats en les dues proxies creixen en diferents estacions de l'any, combinat amb un canvi en la dinàmica del monsó i l'upwelling local entre el LGM i l'Holocè.

El sediment més antic analitzat en aquesta tesi es d'un core que cobreix els Marine Isotope Stadials (MIS) 6 and 7 al mar d' Alboran, Mediterrani oest. Un estudi recent en aquesta zona (core ODP-977A) revela que les alkenones no només presenten tendencies de temperatura similars a la $\delta^{18}O$ de *G. bulloides*, sinó també canvis de temperatura entre stadials interstadials durant el penultim cicle climàtic (from 244 to 130 cal. ky BP). Per tal de confirmar aquests canvis de forma independent, la TEX_{86} es va aplicar al mateix sediment core i els resultants indicaren canvis similars durant stadials interstadials. De tota manera les dues proxies presenten una millor correlacio durant MIS-7 que durant MIS-6. Durant MIS-6

la TEX_{86} indica uns canvis de temperatura molt més accentuats que els de la $U^{K'}_{37}$, per aquesta raó presentem la hipotesi que aquestes diferències es poden explicar per un canvi en la estació de creixement de les haptophytes i Crenarchaeotes i/o variacions en la profunditat de l'habitat de les Crenarchaeotes. Com que el clima és diferent durant glacials i interglacials, un canvi en la dinàmica estacional i/o la profunditat es bastant probable i en qualsevol dels casos això tindria un efecte diferent en les dues proxies.

En resum, els resulstats d'aquesta tesi esdevenen una millora substancial dels aspects analytics de la TEX_{86}, millorant en torn la precisió de la determinació de la proxi. L'origen i transport de GDGTs també s'ha estudiat i sembla que pot ser mediat tant per mecanismes passius com actius. El treball d' aquesta tesis també ha sigut essencial per a determiner els límits d'aplicació i problemes associats a l'us de la TEX_{86}, com els canvis de profunditat o la degradació òxica a llarg termini. Finalment l'us de la proxi en diferents arees, i en conjunt amb alters proxies ha permes de validar la TEX_{86}. Aquesta tesi il·lustra que la TEX_{86} pot ésser una bona mesura de SST i que pot aportar informació complementària a les altres proxies.

Acknowledgements

I want to thank Dr. Micheo, Dr. Cabezos, R. Gomez, N. Grifoll, M. Reina, J. Garcia, B. Madden, P. Shnabel and many more that helped me in many ways, because the boat can not float without water.

My four years of doctorate have been made lighter, shorter and so much more enjoyable by many people at the NIOZ which usually go unnoticed, that is why I would like to thank all the people in the cleaning, reception, administration and personnel departments. Especially I want to acknowledge Joke Mulder who made my dealing with Netherlands bureaucracy that much smoother. Also I would like to thank the IT department for rescues during the journey, and all the others that were there to lend a hand at crucial moments.

I would like to thank all the MBTers for so many things, from lunch discussions to seminars, to much needed help in and out of work. Not to forget many kilos of cream delivered by countless birthday cakes and other celebrations, dank u wel!

Special thanks go to, Lydie Herfort mercy, thank you Jung-Hyun Kim, danke Cornelia Wuchter, Astrid Forster and Andrea Jaeschke for graphs, fruitful discussion, corrections and generally bearing with me. Not to forget taking care of me, and of course for all the delicious dinners and bottles of wine we shared. I could not have made it without you and I can not thank you enough, I know it was not always easy.

I would like to thank Michiel Kienhuis for useful comments and computer rescue, but also Dutch translations, administrative dealings recipe swapping and for general mood improvement (Gracias).

To Marianne Baas for teaching me how to work in a chemical lab and turning me into a budding geochemist which is not without merit with my biological background and genetic clumsiness. Also to Jort Ossebaar, Sebastian Rampen (keep smiling) and Martijn Woltering for assistance in the lab and out of it too.

Thank you also Ellen Hopmans for teaching me how to use an HPLC/MS, and helping me in so many other occasions (I still remember those 100 samples that you helped me pick up from the floor on my first HPLC-MS measuring day). Thanks are also given to Wim Boer for lead 210 analysis and Eilke Berghuis for pigment analysis.

I would also like to thank all the people that gave me samples and made this thesis not only possible but so much better, thus, thank you very much Frank Sirocko, Jung-Hyun Kim, Gert J. de Lange, Rienk H. Smittenberg, Joan Cartes, Belen Martrat, Joan Grimalt, Arndt Schimmelmann and Karin Zonneveld.

Thanks are also due to Lluís Camarero for making me realize how much was still to be learnt in science and how enjoyable the journey could be. Also to Pere Abelló who opened a door back to biology for me and has had tons of patience holding it open for me since. Joan Cartes is also thanked for helping me keep in touch with Spanish science and for taking such a gamble with me. Special thanks go to Joan Grimalt who gave me a very good advice about my career which I intend to follow.

And of course I would like to thank Stefan Schouten specially as after my confession in the interview that I did not know any analytical chemistry, paleocenaography or statistics he still gave me the job and then went on to put up with me for four years. Thank you for the many answer to my many questions for the speed of light corrections and for never loosing faith in the data even when I had given up. Thanks are also due to Jaap Sinninghe Damsté for project supervision and article corrections as well as data discussion. I would also like to thank both of them for letting me do things my own way and only interfering when strictly necessary and teaching me a lot of things on the way.

And last but not least, one must not forget the hand that feeds one, thus thanks go to the NWO-ALW (Project nr. 152911) as it allowed me, for the first time, to make money out of my passion for science.

Curriculum Vitae

Carme Huguet Micheo was born the 11th of October 1976 in Barcelona, Spain. After finishing 4 years of pure science high school she went on to pursue a Bachelors degree in Biology at the Universitat Autonoma de Barcelona, Spain. She specialised in systems ecology and after obtaining an Erasmus grant, she spent the last year of her degree in St. Andrews University, Scotland were she specialised in marine ecology and biology. In St. Andrews she did a project on "Diatom distribution along the shore in the Eden Estuary" under the supervision of Dr. Patterson**.** After finishing her Bachelors degree in 1999 she went on to study a master in Oceanography at the University of Southampton, UK. During her masters she specialized in deep-sea marine ecology and did a project on "Distribution of Decapod crustaceans in the Continental Slope and Abyssal Plain" under the supervision of Dr. Billett. In 2000 she returned to Spain were she taught English and worked voluntarily first at the Universitat de Barcelona (EMERGE Europen program) and then in the CMIMA oceanographic institute in Barcelona. The Study of high mountain lake basin soils in the Pyrenees within the EMERGE Europen program, supervised by Dr. Camarero was finished in 2001 and an article was published in Biogeochemistry in 2007. From 2001 to the present she has been collaborating with Dr. Abelló and Dr. Cartes at the CMIMA in Barcelona and so far two articles were published, one at the Journal of sea research in 2003, and one at Deep-Sea Research I in 2007. From April 2003 to April 2007 she completed her PhD studies at the Royal NIOZ under the supervision of Dr. Schouten and Dr. Sinninghe-Damsté. Currently she is a postdoctoral research associate at the University of Washington in Seattle.

Scientific Assessment committee

Prof. Dr. J.W. de Leeuw
Royal Netherlands Institute for Sea Research, Marine Biogeochemistry and Toxicology, P.O. Box 59,1790 AB Den Burg (Texel), The Netherlands
And
Faculty of Geosciences, Utrecht University, P.O. Box 80.021, 3508 TA Utrecht, The Netherlands

Prof. Dr. G. J. de Lange
Faculty of Geosciences, Utrecht University, P.O. Box 80.021, 3508 TA Utrecht, The Netherlands

Prof. Dr. J. O. Grimalt
Department of Environmental Chemistry, Institut d' Investigacions Quimiques i Ambientals de Barcelona, Consell Superior d'Investigacions Cientifiques (CSIC) 08034 Barcelona, Spain.

Prof. Dr. J. Volkman
CSIRO Marine Research, Castray Esplanade, Hobart, Tasmania, Australia.